

申报	系列：教师系列教学
	科研并重型
	专业：植物学
	职称：教授

业绩成果材料

（申报人的业绩成果材料包括论文、科研项目、获奖以及其他成果等）

单 位（二级单位） 林学与风景园林学院

姓 名 刘林川

材料核对人：

单位盖章：

核对时间：

华南农业大学制

目 录

一、教学研究业绩

1.教学研究项目：基于创新能力培养的《林木细胞生物学》 课程教学方法改革与实践立项通知	1
2.教改论文：利用拟南芥生长素转运突变体开展细胞生物学 教学探索与实践	7
3.编写教材：高等院校教材《植物生理学》	17
4.编写教材：十三五规划教材《科技文献检索与利用》	21
5.编写教材：十四五规划教材《科技文献检索与利用》	25

二、科研项目

1.主持 2017 国家自然科学基金(青年)项目的立项通知	29
2.主持 2020 国家自然科学基金(面上)项目的立项通知	42
3.主持 2024 国家自然科学基金(面上)项目的立项通知	56
4.主持 2022 广东自然科学基金(面上)项目的立项通知	71
5.主参 2018 国家自然科学基金(重点)项目证明	82
6.主参 2019 广东省林业科技创新专项资金项目证明	82
7.主参 2019 广东省教育厅青年项目证明	82
8.主参 2019 广州市科技计划项目证明	82

三、论文、著作等

1.检索证明	83
2.发表本专业论文情况	
2.1 A temperature-sensitive misfolded bri1-301 receptor requires its kinase activity to promote growth	92
2.2 PAWH1 and PAWH2 are plant-specific components of an Arabidopsis endoplasmic reticulum-associated degradation complex	108
2.3 Communications between the Endoplasmic Reticulum and other organelles during abiotic stress response in plants	126

2.4 A predominant role of AtEDEMI in catalyzing a rate-limiting demannosylation step of an Arabidopsis Endoplasmic Reticulum associated degradation process	141
2.5 Mechanisms of Endoplasmic Reticulum protein homeostasis in plants	159
2.6 Post-translational regulation of BRI1-EMS suppressor 1 and Brassinazole-Resistant 1	176

四、其他业绩

1.指导创新创业训练项目	
1.1 2023 大学生创新创业训练计划项目证明	184
2.个人荣誉	
2.1 2019 华南农业大学“优秀共产党员”证书	187
2.2 2021 华南农业大学“优秀共产党员”证书	188
2.3 2021 林学与风景园林学院“优秀班主任”证书	189
2.4 2023 科睿唯安“全球高被引科学家”证书	190
3.学术兼职	
3.1 《植物生理学报》第 12 届编委聘书	191
3.2 国家林业和草原局院校教材建设专家聘书.....	193

华南农业大学文件

华南农教〔2023〕68号

关于公布华南农业大学 2023 年度 校级教改项目和质量工程项目立项的通知

各学院、部处、各单位：

根据《广东省教育厅关于开展 2023 年度广东省本科高校教学质量与教学改革工程项目申报推荐工作的通知》和学校《关于开展 2023 年度本科教学质量与教学改革工程项目申报工作的通知》要求，为进一步推进学校教学改革，建设一流本科教育，提升人才培养质量，学校组织开展了 2023 年度校级本科教学质量与教学改革工程项目遴选工作。

经项目负责人申请、所在单位遴选推荐、学校组织专家评审和公示无异议等程序，确定“高阶思维视域下《种子生物学》‘四维融合’混合式教学模式改革与实践”等122个项目立项为2023年度校级教学改革项目，具体名单见附件1；确定“绿色与智能

精准纳米农药实验室”等47个项目立项为2023年度校级质量工程项目，具体名单见附件2。

请各项目负责人按照项目建设任务及要求，及时开展各项工作，加快推进学校人才培养改革，并力争取得高水平的教学成果。各单位要切实履行项目建设主体责任，加强对项目建设的督促、指导，以确保项目能如期高质量完成建设任务。

特此通知。

- 附件： 1. 华南农业大学 2023 年校级教改项目立项名单
2. 华南农业大学 2023 年校级质量工程项目立项名单

华南农业大学

2023 年 12 月 13 日

（联系人：孙齐胜、孙 航，电 话：85288020、85280052）

公开方式：主动公开

华南农业大学党政办公室

2023 年 12 月 25 日印发

华南农业大学2023年校级教改项目立项名单

序号	项目编号	项目类别	项目名称	项目负责人	项目负责人单位
1	JG2023001	重点项目	高阶思维视域下《种子生物学》“四维融合”混合式教学模式改革与实践	周玉亮	农学院
2	JG2023002	重点项目	新林科视域下森林培育学知识图谱课程建设与教学模式创新	邱权	林学与风景园林学院
3	JG2023003	重点项目	一流专业建设背景下风景园林规划设计课程教学改革研究	陈崇贤	林学与风景园林学院
4	JG2023004	重点项目	一流农科高校基础实验课程思政教学一体化改革与实践——以大学物理实验课程为例	劳媚媚	基础实验与实践训练中心
5	JG2023005	重点项目	双一流高校“科-教-思”融合培养学生高阶思维的实验教学改革研究——以遗传学实验为例	李楠	基础实验与实践训练中心
6	JG2023006	重点项目	工程结构设计软件课程的“融合+分层”教学	李文雄	水利与土木工程学院
7	JG2023007	重点项目	基于竞赛和创新方法提升大学生创新能力的实证研究	易欣	材料与能源学院
8	JG2023008	重点项目	基于创新创业能力培养的“赛教融合”《养羊学》课程改革与实践	柳广斌	动物科学学院
9	JG2023009	重点项目	人工智能赋能生态化大学英语混合教学改革研究	苏君	外国语学院
10	JG2023010	重点项目	基于创新能力培养的《电路实验》教学改革研究与实践	王建华	电子工程学院 (人工智能学院)
11	JG2023011	重点项目	新时代高校思政课“问题链”教学模式研究——聚焦《习近平新时代中国特色社会主义思想概论》课程	何艳玲	马克思主义学院
12	JG2023012	重点项目	三产融合理论在《茶叶生物化学》中的应用	张钰乾	园艺学院
13	JG2023013	重点项目	工程认证背景下基于知识图谱的新工科一流专业建设和提升的研究与实践	王金凤	数学与信息学院、软件学院
14	JG2023014	重点项目	融合数据分析思维和学科交叉的《线性代数》课程教学创新与实践	张伟峰	数学与信息学院、软件学院
15	JG2023015	重点项目	基于创新能力培养的统计学专业数据分析类实验课程改革探索与实践	周燕	数学与信息学院、软件学院
16	JG2023016	招标项目	基于知识图谱的农业院校课程思政建设探索——以公共数学基础课为例	张娜	数学与信息学院、软件学院
17	JG2023017	重点项目	基于新兽医人才培养的《分子生物学》课程改革与实践探索	沈永义	兽医学院
18	JG2023018	重点项目	思政视角下《国际金融》课程教学改革与实践	周超	经济管理学院
19	JG2023019	重点项目	新农科背景下基于“数字标本”的智慧植保实验体系研究与实践	李云锋	植物保护学院
20	JG2023020	重点项目	低碳农业背景下基于一特两驱教学模式的环境土壤学课程体系构建	林庆祺	资源环境学院
21	JG2023021	重点项目	“双一流”建设视野下安全教育模式嵌入环境化学实验室课程体系的实践与优化	高婷	资源环境学院
22	JG2023022	重点项目	“三台协同，以美育人”——以课程教学为基础的高校舞蹈美育建设研究与实践	郑琳喆	艺术学院
23	JG2023023	重点项目	劳动教育融入设计类专业课程路径探索——以《纤维艺术造型设计》课程为例	林汉聪	艺术学院
24	JG2023024	招标项目	人工智能背景下的新文科艺术专业人才培养研究与创新：以动画专业为例	王柯	艺术学院
25	JG2023025	重点项目	“新农科”背景下《植物学》课程教学改革创新研究与实践	白玫	生命科学学院
26	JG2023026	重点项目	基于真人图书馆的“就业创业+思政”融合课程体系改革研究——以法学专业为例	李玮舜	人文与法学院
27	JG2023027	重点项目	生成式人工智能背景下公共管理类课程教学模式创新研究与实践	张小娟	公共管理学院
28	JG2023028	重点项目	基于课程思政融合及项目驱动教学创新方法的研究与实践	孔莲芳	工程学院
29	JG2023029	招标项目	工程教育认证背景下的教学过程评价体系研究——以《区块链原理与技术》课程为例	肖媚燕	数学与信息学院、软件学院
30	JG2023030	招标项目	面向乡村振兴的农业高校传媒类新文科人才培养研究	胡辉	艺术学院
31	JG2023031	重点项目	以教育数字化转型为契机的《林木遗传育种学》混合式教学创新研究	李培	林学与风景园林学院
32	JG2023032	重点项目	国际合作办学背景下建成环境历史课的中外融合与创新	李晓雪	林学与风景园林学院
33	JG2023033	重点项目	“双碳”背景下《包装材料学》课程教学改革与实践	刘涛	食品学院
34	JG2023034	重点项目	构建《遗传学》课程思政教学体系的探索与实践	刘自强	农学院
35	JG2023035	重点项目	基于数据挖掘的土木工程专业人才培养方案优化研究	张巍	水利与土木工程学院
36	JG2023036	重点项目	以培养创新人才为导向的《分析化学实验》教学改革与实践	熊亚红	材料与能源学院
37	JG2023037	重点项目	课程思政引领的《药剂学实验》线上线下混合式教学探究与实践	胡洋	材料与能源学院

38	JG2023038	重点项目	课程链模式下农林院校学生用外语讲中国农耕文化故事能力的培养	秦建华	外国语学院
39	JG2023039	重点项目	基于人工智能技术的大学物理课程思政教学研究与实践	徐初东	电子工程学院(人工智能学院)
40	JG2023040	重点项目	“大思政课”视域下高校思政课实践教学 协同育人创新模式研究与实践	林晓燕	马克思主义学院
41	JG2023041	重点项目	基于文本挖掘的课程思政元素挖掘研究--以应用统计学为例	张建桃	数学与信息学院、软件学院
42	JG2023042	重点项目	新农科背景下《动物解剖与组织胚胎学》课程思政改革创新	马勇江	兽医学院
43	JG2023043	重点项目	学科交叉融合的植物检疫学线上线下一体化教学实践	何晓芳	植物保护学院
44	JG2023044	重点项目	测绘地理信息类专业“学赛研”三位一体实践教学改革研究	刘惠明	资源环境学院
45	JG2023045	重点项目	新农科建设背景下高校图书馆开展中华优秀传统文化教育的探索与实践	黎小妮	图书馆
46	JG2023046	重点项目	大学生创新创业训练计划培育机制改革及育人实效提升研究——以华南农业大学为例	萧润正	党委学生工作部(党委研究生工作部)
47	JG2023047	重点项目	以赋能乡村振兴为导向的一流动画专业优化提升建设的探索和实践	涂先智	艺术学院
48	JG2023048	重点项目	面向工程教育认证的农业院校车辆工程人才培养探索	郭嘉明	工程学院
49	JG2023049	一般项目	面向社会服务的风景园林规划设计类课程教学改革与实践	汤辉	林学与风景园林学院
50	JG2023050	一般项目	基于创新能力培养的《林木细胞生物学》课程教学方法改革与实践	刘林川	林学与风景园林学院
51	JG2023051	一般项目	乡村振兴背景下规划专业人才软技能培养体系研究	王凌	林学与风景园林学院
52	JG2023052	一般项目	“食品仪器分析”线上线下混合式 一流课程的建设与实践	陈运娇	食品学院
53	JG2023053	一般项目	课程思政与“五育并举”融合发展的高校足球课程改革与实践研究	陈存志	体育教学研究部
54	JG2023054	一般项目	思政引导的体育课程内容体系改革与实践--以瑜伽课为例	何灵捷	体育教学研究部
55	JG2023055	一般项目	新农科背景下的《遗传学》教学改革与实践	汪文毅	农学院
56	JG2023056	一般项目	“双一流”背景下基于信息技术的实验室安全教育平台优化建设	陈志民	基础实验与实践训练中心
57	JG2023057	一般项目	理论力学多平台混合教学线上线下一体化设计与实践	刘新红	水利与土木工程学院
58	JG2023058	一般项目	《饲料科学》线上线下一体化混合教学设计探究	朱勇文	动物科学学院
59	JG2023059	一般项目	新农科背景下基于“双元制”教学设计的《蚕桑概论》课程改革与实践	杨婉莹	动物科学学院
60	JG2023060	一般项目	多模态话语分析理论下《跨文化交际》课程中中国文化对外传播路径研究	杜龙鼎	外国语学院
61	JG2023061	一般项目	人工智能赋能英语语言技能课程教学创新实践研究	李飞武	外国语学院
62	JG2023062	一般项目	基于研究性教学的大学物理实验课程思政实践教学探索	杨小红	电子工程学院(人工智能学院)
63	JG2023063	一般项目	高校思政课问题式教学的探索研究——以“思想道德与法治”课程为例	刘智娴	马克思主义学院
64	JG2023064	一般项目	《果蔬栽培学》课程思政设计与实践	苏钻贤	园艺学院
65	JG2023065	一般项目	《园艺种质资源与分类》实验教学内容体系优化的研究与实践	张志珂	园艺学院
66	JG2023066	一般项目	“真人+数字人”的智能教学模式探索与实践--以《数据结构》课程为例	梁云	数学与信息学院、软件学院
67	JG2023067	一般项目	数字化背景下《大学生心理健康教育》课程思政建设与实践	严颖	数学与信息学院、软件学院
68	JG2023068	一般项目	基于创新型人才培养目标对《海洋环境化学》的教学改革研究	公晗	海洋学院
69	JG2023069	一般项目	“四微一体”课堂教学实践与应用-以“水产品质量安全控制”课程为例	周爱国	海洋学院
70	JG2023070	一般项目	数智时代《财务管理》课程教学改革研究	周小春	经济管理学院
71	JG2023071	一般项目	虚-实二维教学模式在环境监测实践课程中的应用	郑芊	资源环境学院
72	JG2023072	一般项目	能源动力类专业课程产教协同育人模式探索与实践	魏国强	生物质工程研究院
73	JG2023073	一般项目	心理资本视域下心理健康课程改革探索	林媛	党委学生工作部(党委研究生工作部)
74	JG2023074	一般项目	轻咨询 融入高校心理健康教育课程的实践路径研究 ——以必修课《大学生心理健康教育》为例	刘桂娥	党委学生工作部(党委研究生工作部)
75	JG2023075	一般项目	基于可持续创新人才培养的《首饰镶嵌工艺》教学改革与实践	潘子广	艺术学院
76	JG2023076	一般项目	“声动岭南”——音乐与表演专业中的新媒体技术创新教学项目研究与实践	冯逸章	艺术学院
77	JG2023077	一般项目	人工智能技术背景下影像艺术课程的内容改革：以乡村影像为例	程蔚新	艺术学院

78	JG2023078	一般项目	《植物学实验》“课程思政”的探索与实践	梁祥修	生命科学学院
79	JG2023079	一般项目	聚焦SCAU特色的遗传学课程思政建设的维度研究与实践	郑少燕	生命科学学院
80	JG2023080	一般项目	教育数字化转型背景下微课赋能古代文学教学应用研究	李桂芹	人文与法学学院
81	JG2023081	一般项目	领军人才培养目标下的《人类行为与社会环境》教学改革与实践	林诚彦	公共管理学院
82	JG2023082	一般项目	行政管理专业法学类课程思政教学改革研究与实践——以《行政法》为例	宋丽娟	公共管理学院
83	JG2023083	一般项目	融合“新工科”视野的工业设计专业--交互设计课程跨学科融合与实践创新	李莎莎	工程学院
84	JG2023084	一般项目	以知识图谱的构建赋能信号类课程的OBE理念教学模式探索	徐梅宣	电子工程学院(人工智能学院)
85	JG2023085	青年项目	基于工程教育认证的食品科学与工程一流专业人才培养实践教学体系重构	黎攀	食品学院
86	JG2023086	青年项目	基于“新工科”背景的《畜产食品工艺学》多模式教学探索与实践	艾民珉	食品学院
87	JG2023087	青年项目	传感检测类课程的混合式教学创新与实践	冯婉媚	电子工程学院(人工智能学院)
88	JG2023088	青年项目	优秀传统文化融入“马克思主义基本原理”课程的路径研究	刘海成	马克思主义学院
89	JG2023089	青年项目	案例教学法在《习近平新时代中国特色社会主义思想概论》课程的创新与运用	朱露	马克思主义学院
90	JG2023090	青年项目	“大历史观”引领《中国近现代史纲要》研究与实践	李征	马克思主义学院
91	JG2023091	青年项目	基于“SPOC+Seminar”的《形势与政策》教学模式改革与实践	聂锐	马克思主义学院
92	JG2023092	青年项目	数字化兽医病例库的构建及其在OBE教学模式下的《兽医临床诊断学》教学中的探索与实践	廖建昭	兽医学院
93	JG2023093	青年项目	新文科背景下本科生《产业经济学》课程体系建设与教学改革路径优化	赵纯凯	经济管理学院
94	JG2023094	青年项目	教育数字化背景下高校管理会计课程改革探析	张京心	经济管理学院
95	JG2023095	青年项目	高校史学理论教学的多元化模式研究——以《史学概论》为例	赖泽冰	人文与法学学院
96	JG2023096	自筹项目	树立文化自信的城市建设史与规划史课程思政探索与实践	王婷	林学与风景园林学院
97	JG2023097	自筹项目	深化产教融合校企合作的育人模式探索与实践--以华南农业大学为例	解加米	林学与风景园林学院
98	JG2023098	自筹项目	以学生为中心的城乡规划专业基础美术课程混合式教学模式探索与实践	吴宝娜	林学与风景园林学院
99	JG2023099	自筹项目	高校体育课程思政教学质量评价指标体系构建研究	姚业戴	体育教学研究部
100	JG2023100	自筹项目	基于翻转课堂的管理通识训练课程混合式教学模式的探索与实践	谢佳佳	基础实验与实践训练中心
101	JG2023101	自筹项目	探究式教学模式在绿色建筑设计与节能技术课程中的实践	崔艳琦	水利与土木工程学院
102	JG2023102	自筹项目	新农科背景下《基因工程原理》线上线下教学一体化教学设计与实践	孙媛	动物科学学院
103	JG2023103	自筹项目	语言智能时代非英语专业学生翻译能力提升路径创新研究	李志英	外国语学院
104	JG2023104	自筹项目	大学英语四级词汇教学改革与实践：比较文 化的视角	黄海翔	外国语学院
105	JG2023105	自筹项目	农业院校统计学专业创新创业教育的研究与实践	徐小红	数学与信息学院、软件学院
106	JG2023106	自筹项目	基于知识图谱的《计算机组成原理》课程智慧化教学研究与实践	杨磊	数学与信息学院、软件学院
107	JG2023107	自筹项目	管理类本科创新创业实践教学生态圈构建	毛小娟	数学与信息学院、软件学院
108	JG2023108	自筹项目	基于新农人创新能力培养的“四位一体”教学方法研究与实践	郭永龙	兽医学院
109	JG2023109	自筹项目	以价值引领、学科融合、全面育人为目标的公选课混合式教学模式探究——以《奇妙的动物》课程为例	曾芳	海洋学院
110	JG2023110	自筹项目	“百千万工程”背景下高校“三大课堂”融合培育爱农兴农人才的教学体系研究与实践	陈洋	经济管理学院
111	JG2023111	自筹项目	双一流建设背景下丁颖班本科人才培养机制深化研究	陈建平	植物保护学院
112	JG2023112	自筹项目	工程测量学实践、实验教学内容体系改革和整体优化	林观土	资源环境学院
113	JG2023113	自筹项目	基于虚拟仿真平台的《测量学》虚实融合的混合式实验教学改革	于红波	资源环境学院
114	JG2023114	自筹项目	多元信息素养教育中线上线下教学一体化研究	刘汉忠	图书馆
115	JG2023115	自筹项目	学科交叉在生物学中的教学实践——以课程《细胞的语言》建设为研究案例	胡宇飞	生命科学学院
116	JG2023116	自筹项目	历史建筑档案在文化遗产研学中的教育教学功能开发策略研究	谢君	文博馆(档案馆、华南农业博物馆)
117	JG2023117	自筹项目	教与评：新文科背景下思政教育融入“中国史学史”课堂教学的探索与实践	翟麦玲	人文与法学学院

118	JG2023118	自筹项目	课程思政背景下国际法专业教学模式创新与实践研究	官隆清	人文与法学院
119	JG2023119	自筹项目	后疫情时代《大学生心理健康教育》课程教学质量提升研究	石如彬	公共管理学院
120	JG2023120	自筹项目	新文科背景下本科生就业能力评价及提升策略研究——以土地资源管理专业为例	朱庆莹	公共管理学院
121	JG2023121	自筹项目	基于工程实践的工程热力学与传热学课程混合教学设计研究与实践	张烨	工程学院
122	JG2023122	自筹项目	融合AIGC建设工业设计创新性实验课程的研究与实践	曾志雄	工程学院

生物学杂志

JOURNAL OF BIOLOGY

ISSN 2095-1736

CN 34-1081/Q



第 6 期

2024 年 12 月

第 41 卷 总第 242 期

太空射线对微生物基因组照射引发其突变

图片设计: 张雅馨



合肥市科学技术协会 主办
生物学杂志社 出版

编委会

顾

问

刘新垣 刘德培 赵国屏 蒋作君 盛志刚 宋礼华

主任委员

蔡敬民

常务副主任委员

柏劲松

副主任委员

孙周通 肖卫华 肖亚中 吴克 张欣 程功

委

员

丁建华 马三梅 马小飞 王晶 王玉炯 王冬梅 王储炎 太光平(英国) 仓春蕾 方泽民
石先阳 卢向阳 田云 田素娟 付爱根 冯涛 司怀军 成永旭 成家杨(美国) 朱宏
朱万龙 朱国旗 刘柱 刘洋 刘普 刘臻 刘占英 刘延峰 刘雪梅 关锋 祁克宗
李祝 李文奇 李文雅 李忠虎 李忠秋 李度昀(韩国) 李鸿钧 李鸿彬 杨杨 杨春英
杨铁林 吴杭 吴子健 吴甘霖 吴坚平 吴家文 余龙江 张智 张巍 张大伟 张小平
张子丁 张红玉 张建丽 张保卫 张美玲 张贵锋 张洪斌 张部昌 张海军 陆勇军 陈乃富
陈士超 陈天虎 陈春丽 陈善元 茆灿泉 范国平(美国) 林宏辉 金腾川(美国) 周勉
周文广 周旭明 郑华宝 孟德龙 赵文 赵长明 赵立青 赵志刚 胡维平 段瑞君 信丰学
侯昕 姚银安 聂桓 徐岩 徐振林 徐索文 徐维平 高峰 郭新红 涂健 黄青
黄升海 康翠洁 章文明 梁士楚 董毅 曾润颖 阙显照 谭明乾 潘皎 潘志明 霍丹群
霍毅欣 戴传超 Hermann FRISTER(德国) Anuj CHAUHAN(美国)

主管单位:安徽省科学技术协会

主办单位:合肥市科学技术协会

出版单位:生物学杂志社

编辑单位:《生物学杂志》编辑部

社长:葛玲

编辑部副主任:邓宇

文字编辑:李延璐 童梦玲

美术编辑:葛玲

英文编辑:金杰

网络编辑:费东

电话:0551-62673629/62635632

电子信箱:swxzz@163.com

网址:www.swxzz.com

QQ号码:1557931860

地址:安徽省合肥市花园街83号合肥大厦9楼

邮政编码:230001

印刷单位:安徽省快马印务有限责任公司

邮发代号:26-50

总发行:合肥市邮政局

订购处:全国各地邮政局(所)

定价:15.00元/册

ISSN 2095-1736

CN 34-1081/Q



目 次

特约综述

空间微生物研究及生物工程应用 孙丽超, 赵鹏卓, 胡伟, 霍毅欣(1)

研究报告

UHRF1 在人乳腺癌细胞中调控基因差异表达的鉴定及分析 宫春雪, 董钦才, 刘莹, 曹诚(12)

抑制 GS 活性增强放疗诱导的胶质瘤细胞铁死亡 卢益军, 周臣, 钱俊超(20)

儿茶素减轻小鼠肺泡巨噬细胞炎症反应的作用及机制研究 陈淑珍, 许秋凤, 王皇斌, 黄莎莎, 黄丽端, 熊闯(26)

不同浓度的四环素对秀丽隐杆线虫肠道菌群中抗生素抗性基因扩散效率的影响
..... 宣艳梅, 张颖, 李顺顺, 高泽萍, 黄涛, 孙庆业, 周国伟(31)

重组蔗糖异构酶在枯草芽孢杆菌中的表达及发酵优化 姜晨, 吴昕瞳, 陈慧玲, 刘乐, 张谦, 李宪臻, 郭小宇(39)

云南省地生兰根内微生物多样性分析 吴峰婧琳, 陈健鑫, 杨娅琳, 姬靖捷, 张东华, 马焕成, 伍建榕(47)

水分胁迫下德兰臭草对内生真菌感染的生理响应 张梦梦, 王传哲, 何嘉坤, 施宠(56)

KXF6501 特基拉芽孢杆菌发酵液处理采后蓝莓果实的代谢组分析 杨阔, 刘地, 伍建榕, 邓佳, 王芳(62)

西伯利亚鲟(*Acipenser baerii*) *IFN- γ* 基因克隆、原核表达和单克隆抗体制备 田照辉(69)

柴达木盆地小黑麦与豌豆混播饲草农艺性状和营养品质差异分析 马文艳, 曹东, 刘宝龙, 王东霞(74)

疏花水柏枝在四川岷江的地理分布新纪录 高刚, 陈绪言, 李义航, 唐静(82)

中国茄科一新归化种——绿果龙葵 宋文丹, 马占仓, 潘成南, 南占元, 阎平(84)

汞胁迫对高原牧草生理特征的影响 赵明德, 王瑾, 李晓晓(87)

综述与专论

植物干细胞前沿研究:从基础理论到应用 陈柳, 张吉祥, 陈春丽(92)

BDNF 对中枢神经系统疾病作用的研究进展 宋雪晴, 孙雅伦, 周丽芳, 王松华, 孟玮(96)

技术方法

基于高光谱技术的重金属污染蛤仔快速无损鉴别 刘忠艳, 杨俊杰, 乔沐溪, 刘瑶(104)

教学研究

“医产教研融合”在检验诊断学研究生培养模式的探究 周强, 王琴, 叶乃芳, 张浩, 刘周, 姚杰(111)

DNA 条形码技术在植物分类学实验课程中的教学设计与实践 周亚东, 杨过, 管毕财(116)

多元化育人目标下生命科学导论教学创新改革与实践 李军林, 魏宁, 张宇, 付爱根, 石张燕, 崔继红, 陈富林, 张亚妮, 关锋(121)

利用拟南芥生长素转运突变体开展细胞生物学教学探索与实践 刘林川, 毛娟, 王永飞, 马三梅(126)

Contents

INVITED REVIEW

Space microbiology and its bioengineering applications SUN Lichao, ZHAO Pengzhuo, HU Wei, HUO Yixin(1)

STUDY REPORTS

Identification and analysis of differential expression genes regulated by UHRF1 in breast cancer cells
..... GONG Chunxue, DONG Qincai, LIU Xuan, CAO Cheng(12)

Inhibition of glutamine synthetase in glioma cells enhances radiotherapy-induced ferroptosis LU Yijun, ZHOU Chen, QIAN Junchao(20)

Study on the anti-inflammatory effect and mechanism of catechin on mouse alveolar macrophages
..... CHEN Shuzhen, XU Qinfeng, WANG Huangbin, HUANG Shasha, HUANG Liduan, XIONG Min(26)

Antibiotic-resistant genes dissemination in the intestinal flora of *Canorhabditis elegans* in response to antibiotic pressure
..... DA Yanmei, ZHANG Ying, LI Shunshun, GAO Zeping, HUANG Tao, SUN Qingye, ZHOU Guowei(31)

Expression and fermentation optimization of recombinant sucrose isomerase in *Bacillus subtilis*
..... JIANG Chen, WU Xintong, CHEN Huiling, LIU Le, ZHANG Qian, LI Xianzhen, GUO Xiaoyu(39)

Analysis of microbial diversity in the roots of terrestrial orchids in Yunnan Province
..... WU Fengjinglin, CHEN Jianxin, YANG Yalin, JI Jingjie, ZHANG Donghua, MA Huancheng, WU Jianrong(47)

Physiological responses of *Melica transsilvanica* to endophytic fungi infection under conditions of water stress
..... ZHANG Mengmeng, WANG Chuanzhe, HE Jiakun, SHI Chong(56)

Metabolomic analysis of postharvest blueberry fruits treated by *Bacillus tequilensis* KXF6501 fermentation
..... YANG Kuo, LIU Di, WU Jianrong, DENG Jia, WANG Fang(62)

Cloning, prokaryotic expression and monoclonal antibody preparation of *IFN- γ* of *Acipenser baerii* TIAN Zhaohui(69)

Analysis on difference of agronomic characters and nutritional quality of mixed sowing for triticale and pea in the Qaidam Basin
..... MA Wenyan, CAO Dong, LIU Baolong, WANG Dongxia(74)

New distribution record of the *Myricaria laxiflora* in Minjiang River of Sichuan Province GAO Gang, CHEN Xuyan, LI Yihang, TANG Jing(82)

Solanum nudiabaccatum Bitter. a newly naturalized species of Solanaceae in China
..... SONG Wendan, MA Zhancang, PAN Chengnan, NAN Zhanyuan, YAN Ping(84)

Effects of mercury stress on physiological characteristics of forage grass in plateau ZHAO Mingde, WANG Jin, LI Xiaoxiao(87)

REVIEWS AND TREATISES

Frontier research of plant stem cells: from basic theory to application CHEN Liu, ZHANG Jixiang, CHEN Chunli(92)

Research progress on the effects of BDNF on central nervous system diseases
..... SONG Xueqing, SUN Yalun, ZHOU Lifang, WANG Songhua, MENG Wei(96)

TECHNIQUES AND METHODS

Rapid non-destructive identification of heavy metal contaminated clams based on hyperspectral technology
..... LIU Zhongyan, YANG Junjie, QIAO Muxi, LIU Yao(104)

TEACHING RESEARCH

Exploration of "integration of medicine, industry, education and research" in the training model of master's student in laboratory medicine
..... ZHOU Qiang, WANG Qin, YE Naifang, ZHANG Hao, LIU Zhou, YAO Jie(111)

Teaching design and practice of DNA barcode technology in plant taxonomy experimental course ZHOU Yadong, YANG Guo, GUAN Bicai(116)

Innovative reform and practice of introduction to life sciences under the goal of diverse talents education
..... LI Junlin, WEI Ning, ZHANG Yu, FU Aigen, SHI Zhangyan, CUI Jihong, CHEN Fulin, ZHANG Yani, GUAN Feng(121)

Exploration and practice in cell biology teaching by using *Arabidopsis thaliana* auxin transport mutants
..... LIU Linchuan, MAO Juan, WANG Yongfei, MA Sanmei(126)

doi:10.3969/j.issn.2095-1736.2024.06.126

利用拟南芥生长素转运突变体开展细胞生物学 教学探索与实践

刘林川¹, 毛娟¹, 王永飞², 马三梅²

(1. 华南农业大学 林学与风景园林学院 亚热带农业资源保护与利用国家重点实验室, 广州 510642;

2. 暨南大学 生命科学技术学院, 广州 510632)

摘要 课程以拟南芥生长素转运突变体为材料,探索利用模式植物开展细胞生物学教学与实践。通过讨论式教学,结合表型观察分析与亚细胞定位等实验,使学生深入理解膜蛋白结构与功能之间的联系,认识到物质跨膜运输对植物生长发育的重要性。在培养学习兴趣的同时,加强学生对细胞生物学及相关学科知识的深入理解和综合运用,提高他们的思维能力和科研能力。为培养适应学科交叉融合的创新型人才奠定基础。

关键词 细胞生物学; 细胞膜; 转运蛋白; 跨膜运输; 生长素; 教学设计

中图分类号 G642;Q943.2

文献标识码 C

文章编号 2095-1736(2024)06-0126-05

Exploration and practice in cell biology teaching by using *Arabidopsis thaliana* auxin transport mutants

LIU Linchuan¹, MAO Juan¹, WANG Yongfei², MA Sanmei²

(1. State Key Laboratory for Conservation and Utilization of Subtropical Agro-Bioresources, College of Forestry and Landscape Architecture, South China Agricultural University, Guangzhou 510642, China;

2. College of Life Science and Technology, Jinan University, Guangzhou 510632, China)

Abstract In our study, we investigated the use of auxin transport mutants of *Arabidopsis thaliana* as a model for teaching cell biology. Through discussion-based teaching methods, phenotypic observation and analysis, and subcellular localization experiments, students can gain a deep understanding of the relationship between membrane protein structure and their functions, emphasizing the significance of transmembrane transport in plant growth and development. In addition to fostering students' interest, this course promotes a comprehensive understanding and application of knowledge in cell biology and related fields, thereby enhancing critical thinking and scientific research skills. Taken together, our teaching approach cultivates innovative individuals capable of thriving in interdisciplinary collaborations.

Keywords cell biology; cell membrane; transporter; transmembrane transport; auxin; teaching design

细胞生物学是生物和农林科学相关专业本科生的核心课程,是今后开展生命科学相关研究的必备基础。细胞生物学主要从不同层面研究细胞的结构与功能,揭示细胞的基本生命活动规律,目前已成为生命科学领域发展最迅速、交叉性最强的学科之一。在近30年

中,有十余项诺贝尔奖出自该研究领域^[1]。

由于该学科课程理论性强、知识点多且内容抽象,特别是在教学内容中涉及遗传学、生物化学和分子生物学等其他学科知识,学生对相关概念和研究方法的掌握较为困难,从而难以建立完整的细胞生物学学科

收稿日期:2024-07-15;最后修回日期:2024-09-19

基金项目:国家自然科学基金项目(31970187);华南农业大学教学改革项目(JG2023050);暨南大学研究生教育教学成果培育项目(2023YPY009和2024YPY009)

作者简介:刘林川,博士,教授,研究方向为植物激素信号转导,E-mail:lcliu@scau.edu.cn

通信作者:马三梅,博士,副教授,研究方向为植物生殖生物学,E-mail:msmwdw@163.com

知识体系。

拟南芥是植物科学研究中被广泛使用的模式植物,因其基因组小、生长周期短以及便于遗传转化等特点,广泛应用于植物基因功能和细胞生长发育研究。目前,通过突变体库和基因编辑手段能够获得基因敲除突变体,为拟南芥功能基因组的研究奠定了基础^[2]。

为了使学生更好地学习和掌握细胞生物学基本知识,灵活运用相关理论和方法解决实际问题,本课程以“十二五”普通高等教育本科国家级规划教材《细胞生物学》(第5版)章节内容为基础,利用拟南芥生长素转运突变体和相关转基因材料设计教学内容并开展实验,旨在将植物科学研究的前沿引入细胞生物学课堂。

通过“知识讲解-观察分析-互动交流-理解运用”4个模块开展教学活动,最终达到知识的融会贯通和学以致用。经过连续4年的教学实践和效果评价,学生能够灵活掌握细胞生物学课程中的重点和难点,激发了学生的学习兴趣,培养了学生多学科交叉融合的创新能力。

1 教学背景介绍

细胞质膜和物质的跨膜运输是细胞生物学课程的重点,也是培养学生建立细胞结构决定细胞功能逻辑思维的基础。传统的细胞生物学课堂主要借助模式图对理论知识进行讲授式教学,学生较难从抽象的概念中建立起细胞质膜结构和功能、物质跨膜转运和个体生长发育之间的联系。

生长素是一种重要的植物激素,参与植物生长发育各个阶段的调节^[3]。生长素的跨膜转运影响了其在不同组织部位的分布,对植物器官的形成与发育极为重要。植物细胞膜上存在不同类型的生长素转运蛋白,分别介导生长素在细胞中的输入和输出^[4]。P-糖蛋白1(P-glycoprotein 1, PGP1)和P-糖蛋白19(PGP19)是拟南芥质膜定位的ABC转运蛋白(ATP-binding cassette transporter),负责将生长素从细胞内转运至细胞外^[5]。生长素通过细胞与细胞间运输,在植物体内形成浓度梯度和局部浓度差异,从而调控植物的生长发育过程。

在拟南芥 *pgp1* *pgp19* 突变体中,由于细胞向质膜外转运生长素的功能出现异常,导致拟南芥植株出现矮化和生长发育缺陷的表型^[6]。通过选取拟南芥生长素转运蛋白突变体开展实验,学生可以直观地观察植株表型的变化,充分认识生长素跨膜运输对植物生长发育的重要性,为深入理解细胞质膜和转运蛋白的生

物学功能奠定基础。

同时,为了使學生掌握细胞生物学常用的研究方法,可以借助生长素转运蛋白与绿色荧光蛋白(green fluorescent protein, GFP)融合的转基因植株开展实验,观察生长素转运蛋白在根中的分布情况。促使学生在学习荧光显微镜使用的同时,掌握亚细胞定位分析的原理与相关实验技能,为今后开展相关科研工作奠定基础。

此外,在该教学设计中可以有效融入课程思政内容。生长素是最早被发现和研究的植物激素。100多年前英国科学家达尔文对金丝雀蓟草(*Phalaris canariensis*)幼苗向光性现象的观察,以及随后半个多世纪众多科学家对生长素本质和作用方式的猜想与实验验证,是兴趣驱使研究探索,建立科学假说并用科学实验加以证明形成科学理论的典型案例^[7],体现了科学家们严谨的科学态度和创新的科学精神。同时,绿色荧光蛋白的发现和应用为生命科学的发展带来了革命性的影响,也提供了多方面的科学启示,包括对偶然性科学发现的关注、持之以恒的探索精神和跨学科的交叉合作等,这些都是取得重要科研成果极为关键的因素。

因此,选取拟南芥生长素转运突变体开展细胞生物学教学与实验对深入认识细胞生物学学科,培养学生的科学思维和科学素养具有非常重要的意义。

2 教学方案实施

2.1 理论课教学

在理论课教学过程中,围绕课程教学内容对教材中重要知识点开展深层次学习,设计相关问题进行互动式讨论,循序渐进地引导学生从理论知识的认识和理解逐渐过渡到对科学研究中实际问题的思考和解决。首先,启发学生从细胞质膜的组成和结构上认识细胞膜的功能,重点关注膜蛋白在细胞物质跨膜运输和信息传递中的作用。在此基础上,与学生回顾细胞中物质跨膜运输的主要方式和特点,重点讲授载体蛋白介导的细胞主动运输原理和过程。ABC转运蛋白是细胞中一类典型的通过水解ATP实现物质主动运输的载体蛋白,普遍存在于动物、植物和微生物细胞中。由于该家族蛋白中一些成员参与了动植物生长发育调控过程,并与许多遗传疾病和肿瘤耐药性有关,因此,成为细胞生物学领域研究的热点^[8]。

为了深入学习ABC转运蛋白的结构和功能特点,借助生长素转运的实例进行讲解。生长素主要在植物生长旺盛的部位合成,但它需要在不同组织中发挥作

用,植物是如何实现这一过程的?在提出科学问题后,鼓励学生积极思考,通过查阅文献资料了解有关生长素的背景知识。经过自主学习和互动讨论,学生能够掌握生长素在植物体内的分布依赖于不同细胞间的转运,为后续实验课上学习和观察生长素转运蛋白亚细胞定位奠定基础。最后,提出生长素转运蛋白定位于细胞膜并发挥作用,然而它的合成却发生在细胞质中。那么,生长素转运蛋白是通过哪些途径和机制被运输到细胞膜上的?这为后续章节学习蛋白质的分泌途径和囊泡转运奠定了基础。

2.2 实验课教学

PGP1 和 PGP19 是拟南芥 ABC 转运蛋白家族中 ABCB 亚族成员,主要负责将生长素从细胞内转运至细胞外。向学生提出问题:这两个蛋白在结构上有什么特点使其具备生长素转运的功能?如果编码这两个蛋白的基因发生突变,会对植物产生什么样的不利影响?同时,启发学生思考用什么样的方法能够观察到 PGP1 或 PGP19 在细胞中的分布和定位。

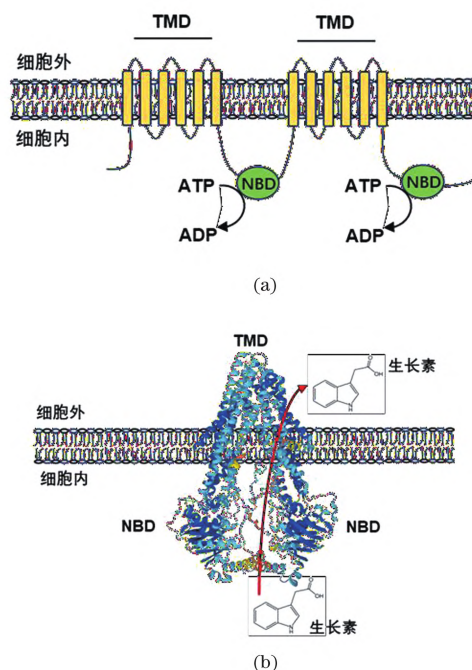
围绕以上问题,安排了实验内容:以 PGP1 蛋白为例,讲解和演示利用 PowerPoint 或 Illustrator 软件绘制蛋白质结构域示意图,学习利用 AlphaFold 进行蛋白质三维结构预测。观察分析生长素转运突变体 *pgp1* *pgp19* 的表型,与学生讨论 PGP1 和 PGP19 在植物生长发育中的重要功能。以 PGP1 和 PGP19 融合绿色荧光蛋白表达的转基因拟南芥为材料,开展生长素转运蛋白亚细胞定位的观察。

2.2.1 生长素转运蛋白模式图的绘制与三维结构预测

模式图是细胞局部形态结构的直观展示。为了让学生认识细胞膜上转运蛋白的结构特点,进一步巩固和理解教材中的理论知识,以生长素转运蛋白 PGP1 为例,讲授和演示蛋白模式图的绘制方法。PGP1 具有 12 次跨膜结构,包含核苷酸结合结构域 (nucleotide binding domain, NBD) 和跨膜结构域 (transmembrane domain, TMD) 两部分。其中,NBD 负责 ATP 的结合和水解,为生长素的转运提供能量;而 TMD 则形成疏水通道,行使生长素转运的功能^[9]。利用学生较为熟悉的 Microsoft PowerPoint 软件中的绘图功能,分别绘制组成细胞膜的磷脂双分子层结构。在此基础上,绘制 PGP1 的跨膜结构域和核苷酸结合结构域,并在图中标记出转运蛋白对物质的转运依赖于 ATP 的水解[图 1(a)]。通过模式图绘制,学生们掌握 ABC 转运蛋白的结构特点。

为了让学生们更深入理解“结构决定功能”这一基本规律,采用人工智能方法来分析蛋白质结构,通过

AlphaFold 在线网站预测 PGP1 的三维空间结构^[10][图 1(b)]。学生在这一过程中能够学习到拟南芥蛋白质一级序列的获取方法,以及三维空间结构图的预测、分析和展示。为了巩固学习效果,课后布置作业让学生以 PGP19 为例自主进行模式图绘制和三维结构预测。通过这种教学模式,学生们学习了最新的分析方法,提高了他们的学习兴趣。



(a) PGP1 蛋白结构域示意图,黄色部分代表跨膜结构域(TMD),绿色部分代表核苷酸结合结构域(NBD);(b)利用 AlphaFold 在线网站预测 PGP1 蛋白的三维结构。

图 1 PGP1 蛋白模式图和结构预测

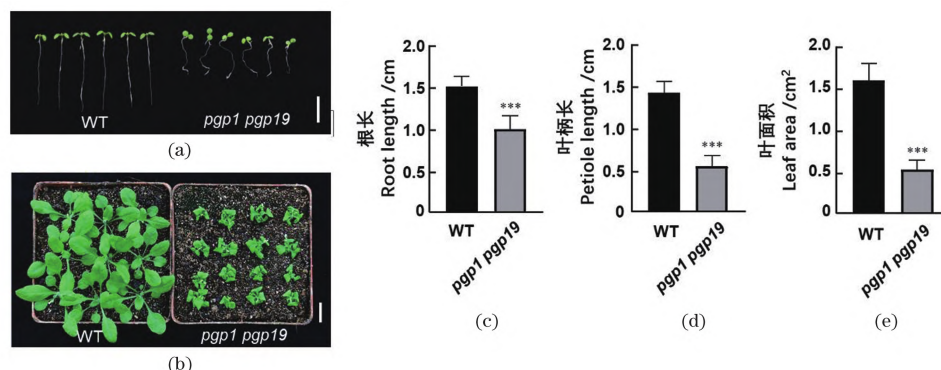
Figure 1 Schematic diagram and structure prediction of PGP1

2.2.2 生长素转运突变体表型观察与分析

为了进一步让学生了解生长素转运蛋白的功能重要性,分别选取生长 7 d 和 1 个月的野生型植株 (WT) 和 *pgp1* *pgp19* 突变体开展实验[图 2(a)和(b)]。首先学生观察拟南芥野生型与突变体植株之间的表型差异,学习利用 Image J 软件测量幼苗的根长、成熟期植株的叶柄长度和叶片大小等生长指标,并用 GraphPad Prism 软件进行作图和统计[图 2(c)~(e)],以掌握表型差异的量化分析方法。其次,与学生一起复习遗传学中有关突变体和基因突变的知识,启发学生从分子水平、细胞水平到个体发育水平等不同层面认识植株表型产生差异的原因。同时,回顾植物生理学中生长素在促进细胞伸长、细胞分裂和植物生长中的作用,让学生联想到根长和叶片大小的变化可能是由生长素的含量变化或分布差异所导

致。让学生思考和讨论生长素有别于其他植物激素最为重要的特点,帮助他们建立生长素转运蛋白功能与生长素在植物体内分布之间的联系。通过以上表型观察、分析与引导,学生不仅掌握了科学研究中

常用的统计方法,也很容易从分子机制的角度理解 *pgp1* *pgp19* 突变体的生长发育异常主要是由生长素转运蛋白功能缺陷所引起,导致生长素在拟南芥根、叶柄和叶片等部位的分布不均。



(a) 1/2MS 培养基中生长 10 d 的拟南芥野生型和 *pgp1* *pgp19* 突变体的表型;(b) 土壤中生长 30 d 拟南芥野生型和 *pgp1* *pgp19* 突变体的表型;(c) 1/2MS 培养基中生长 10 d 的拟南芥野生型和 *pgp1* *pgp19* 突变体根长的比较;(d) 土壤中生长 30 d 拟南芥野生型和 *pgp1* *pgp19* 突变体叶柄长度的比较;(e) 土壤中生长 30 d 拟南芥野生型和 *pgp1* *pgp19* 突变体叶片面积的比较。图中比例尺为 1 cm,***为 $P<0.001$ 。

图 2 生长素转运蛋白突变体 *pgp1* *pgp19* 的表型分析

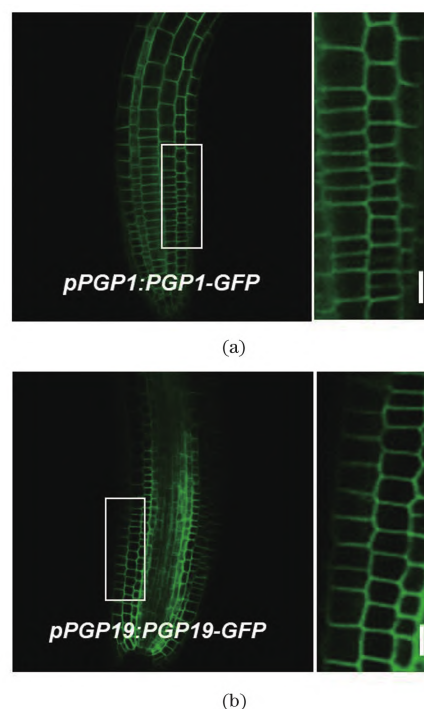
Figure 2 Phenotypic analysis of auxin transport mutant *pgp1* *pgp19*

2.2.3 生长素转运蛋白亚细胞定位预测与观察

蛋白质合成后需要运输到细胞的特定位置才能发挥作用。为准确直观地了解 PGP1 和 PGP19 的生物学功能,除对其进行蛋白质结构分析外,通常需要预测和观察其亚细胞定位,以判断其在细胞中发挥功能的主要场所。围绕这一教学目标,指导学生借助在线网站 TargetP-2.0 及蛋白序列信息对目的蛋白的亚细胞定位进行分析和预测。同时,讲授绿色荧光蛋白的发现历史、相关概念与发光原理,并学习如何通过融合表达目的蛋白和绿色荧光蛋白进行亚细胞定位观察。以在 1/2 MS 培养基上生长 5 d 的 *pPGP1*:*PGP1*-GFP 和 *pPGP19*:*PGP19*-GFP 拟南芥转基因幼苗为实验对象,在荧光显微镜下观察转基因植株根部的绿色荧光信号,从而明确 PGP1 和 PGP19 的亚细胞定位。由于转基因植株中 PGP1 和 PGP19 蛋白的 C 端分别融合了 GFP,因此,在 488 nm 激发光下,可以清晰观察到 PGP1-GFP 和 PGP19-GFP 的亚细胞定位。如图 3 所示,PGP1-GFP 和 PGP19-GFP 均定位于细胞膜。通过该实验,学生既能够学习和掌握荧光显微镜的使用,又能加深对绿色荧光蛋白在细胞生物学研究中应用的理解。这不仅使学生掌握了实验技能,还激发了他们的学习热情并开阔了视野。

3 课程实施效果与评价

在课程中融入学科前沿,将植物科学研究的热点



(a) *pPGP1*:*PGP1*-GFP 转基因拟南芥幼苗根中观察 PGP1-GFP 的亚细胞定位;(b) *pPGP19*:*PGP19*-GFP 转基因拟南芥幼苗根中观察 PGP19-GFP 的亚细胞定位;(a) 和 (b) 右侧荧光图分别为白色方框区域的放大图,图中标尺为 20 μm 。

图 3 PGP1 和 PGP19 的亚细胞定位观察

Figure 3 Subcellular localization of PGP1 and PGP19

内容与细胞生物学教学内容有机结合,有效激发了学生学习的主动性,显著提高了学生分析和解决实际问

题的能力。连续 4 年对参与创新性教学的学生进行了能力测验,主要围绕教学中的重要知识点和文献中的相关案例设置考查内容(表 1)。采用问答题和实验设计题替代名词解释和填空题等题型,避免了学生通过死记硬背的方式应对考试。考核增强了学生对知识的积累和灵活运用能力,促使学生由被动学习转变为主动探索式学习。通过理论课和实验课相结合的教学方式,有效提高了学生的学习效率和学习效果。与实施创新课程之前相比,学生的学习兴趣 and 考试成绩明显提高。

同时,围绕该课程内容制定了评价指标,利用匿名问卷调查的形式请学生对授课效果和教学质量进行了评价。在连续 4 个学年里,共收到 145 名学生的反馈结果。其中,97.0% 的学生认为本课程设计能够理论联系实际,反映了本学科最新的前沿进展,思考问题的深度得到了提升。96.5% 的学生认为本课程有助于培养他们多学科知识融会贯通的能力,提高了文献阅读效率。

此外,在学生反馈和教学过程中发现,细胞生物学中一些相关的知识点出现在教材的不同章节。如何将这些知识点串联起来讲授具有一定的难度。特别是在实际科研过程中,需要从整体上认识细胞的功能,这就需要借助相关案例,建立知识点之间的联系,以达到学以致用目的。因此,在科学研究过程中需要不断总结和挖掘教学素材,以满足以上教学要求。

表 1 教学中重要知识要点与考查内容

Table 1 The important knowledge points and examination content in teaching

对应章节 Chapter	知识要点 Knowledge point	考查内容 Examination content
细胞质膜	膜蛋白的类型 细胞质膜的基本功能	细胞膜的结构和功能完整性对细胞的生长和发育等活动有哪些重要影响? 举例说明常见的膜蛋白有哪些。
物质的跨膜运输	载体蛋白 主动运输 ABC 转运蛋白	载体蛋白具有哪些结构特征? ABC 转运蛋白为什么能够介导主动运输? 如何利用 AlphaFold 进行蛋白质三维结构预测?
蛋白质分选与膜运输	多次跨膜蛋白形成 转运蛋白与囊泡转运	转运蛋白如何合成并定位至细胞膜?
细胞生物学研究方法	模式生物 荧光显微镜 绿色荧光蛋白	拟南芥作为模式植物有哪些优点? 如何选取荧光显微镜的激发波长? 绿色荧光蛋白在细胞生物学研究中有哪些应用?

4 本教学设计和改革的创新点

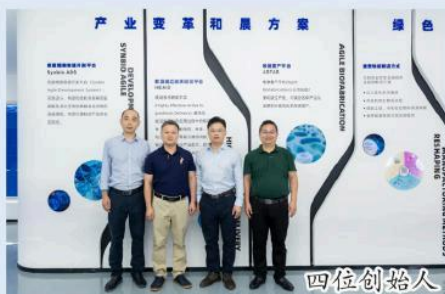
如何将科学研究前沿知识引入课堂教学,培养学生的学习和创新能力,是细胞生物学课程教学改革的重点,也是新时期国家创新人才培养的重要目标^[1]。通过创新性教学和实验设计,培养学生的自我探索能力,对学生的成长和成才具有非常重要的意义。

本课程围绕物质跨膜运输与转运蛋白功能开展创新性教学设计。一方面,由于该研究方向是生命科学领域的热点,许多人类重大疾病的发生以及动植物的生长发育均与转运蛋白的功能调节密切相关。另一方面,目前很少高校有条件开展这部分实验内容。在教学中,结合教师的科研方向,从科研中挖掘教学素材,创新性地利用生长素转运蛋白突变体进行教学设计,突出不同学科知识和技能的整合,促进了学生跨学科思考的能力。同时,这一过程也培养了学生的自主学习和创新素养,取得了良好的教学效果。

参考文献

- [1] 李佳,唐红,张琳,等.以诺贝尔奖为案例的细胞生物学课程思政教学探索[J].中国细胞生物学学报,2023,45(7):1075-1081.
- [2] 潘晓寒.模式植物基因功能突变数据库资源报告[J].江苏农业科学,2014,42(2):39-42.
- [3] 冯寒露,李超.生长素信号转导研究进展[J].生物技术通报,2018,34(7):24-30.
- [4] 资丽媛,林浴霞,傅若楠,等.植物激素转运研究进展[J].植物生理学报,2022,58(12):2238-2252.
- [5] CECCHETTI V, BRUNETTI P, NAPOLI N, et al. ABCB1 and ABCB19 auxin transporters have synergistic effects on early and late *Arabidopsis* anther development[J]. Journal of Integrative Plant Biology, 2015, 57(12): 1089-1098.
- [6] NOH B, MURPHY A S, SPALDING E P. Multidrug resistance-like genes of *Arabidopsis* required for auxin transport and auxin-mediated development[J]. The Plant Cell, 2001, 13(11): 2441-2454.
- [7] 饶猛兵.基于科学思维和科学探究视角下的科学史教学实践——以“植物生长素的发现”为例[J].生物学通报,2020,55(10):40-41.
- [8] DO T H T, MARTINOIA E, LEE Y. Functions of ABC transporters in plant growth and development[J]. Current Opinion in Plant Biology, 2018, 41: 32-38.
- [9] 刘艳青,赵永芳.ABC 转运蛋白结构与转运机制的研究进展[J].生命科学,2017,29(3):223-229.
- [10] JUMPER J, EVANS R, PRITZEL A, et al. Highly accurate protein structure prediction with AlphaFold[J]. Nature, 2021, 596(7873): 583-589.
- [11] 许星鸿,赖晓芳,姬南京,等.基于创新性人才培养的细胞生物学课程教学改革[J].科教导刊,2021(33):54-56.

合肥和晨生物科技有限公司



合肥和晨生物科技有限公司成立于2022年5月，是一家以合成生物学和前沿递送技术“双引擎”为驱动，打造生物活性原料、生物化工原料及应用方案一体化的生物制造企业。公司致力于通过高效微生物细胞工厂的构建与优化，实现美容与个护、营养与健康、可持续农业、生物基化学品等关键生物基原料的规模化生产与绿色制造。公司坚持打造“双引擎”生物制造体系，为客户提供一体化技术解决方案。纵向瞄准生物科技前沿，不断夯实核心技术，横向聚焦市场客户需求，加速技术应用落地。合成生物底盘细胞设计研究平台重点聚焦高附加值氨基酸及其衍生物的生物合成与产业化应用；前沿递送技术研究平台聚焦客户和终端消费者需求，以活性原料高效递送为核心，开发定制化功能活性原料、功效组合制剂技术和产品应用解决方案，助力客户提升产品差异化竞争优势。

公司核心团队来自天津科技大学、联合利华、杜邦等高校院所和企业，具有国际化视野、多学科交叉背景、复合型产业经验，能力涵盖菌种工程、发酵、提取、前沿递送技术、配方和渠道等全产业链。



采用生物制造方式生产的活性原料



公司产品美芯球



植物生理学

王永飞 马三梅 李宏业 主编



科学出版社

第 17 页

植物生理学

王永飞 马三梅 李宏业 主编

国务院侨务办公室立项

彭磷基外招生人才培养改革基金资助项目

国家西甜瓜产业技术体系资助项目

暨南大学教材资助项目

科学出版社

北京

内 容 简 介

本书依据植物生理学的学科性质,在力求全面地阐述基本概念、基础知识和基本理论的基础上,参考国际上近年来较通行教材的内容,按照“植物的生命活动大致可分为生长发育和形态建成、物质和能量转化、信息传递和信号转导等方面”的理念,将全书分成“生长发育和形态建成”“物质和能量转化”“信息传递和信号转导”共3篇12章。其中,生长发育和形态建成篇包括植物的生长生理与形态建成、生殖生理、成熟和衰老生理3章;物质和能量转化篇包括植物的生长物质、水分生理、矿质营养、光合作用、同化物的运输与分配、呼吸作用、次生代谢产物7章;信息传递和信号转导篇包括植物的信号转导和抗逆生理2章。为便于学生自学和复习,每章一开始就列出了本章的思维导图,并在章后提供了一些综合性的复习思考题。同时为授课教师准备了相应课件,供备课时参考。

本书作为高等院校植物生理学课程的教材,可供综合性大学、师范学院、农林院校的师生使用,也可供从事相关研究的科研人员使用和参考。

图书在版编目(CIP)数据

植物生理学/王永飞,马三梅,李宏业主编. —北京:科学出版社,2019.6
ISBN 978-7-03-061493-3

I. ①植… II. ①王… ②马… ③李… III. ①植物生理学—高等学校—教材 IV. ①Q945

中国版本图书馆CIP数据核字(2019)第110061号

责任编辑:席慧刘晶/责任校对:严娜

责任印制:张伟/封面设计:迷底书装

科学出版社 出版

北京东黄城根北街16号

邮政编码:100717

<http://www.sciencep.com>

北京虎彩文化传播有限公司 印刷

科学出版社发行 各地新华书店经销

*

2019年6月第 一 版 开本:787×1092 1/16

2019年6月第一次印刷 印张:18 1/4

字数:467 000

定价:59.00元

(如有印装质量问题,我社负责调换)

《植物生理学》编写委员会

主 编 王永飞 马三梅 李宏业

副 主 编 孙小武 屈红霞 王少奎 刘林川

编写人员 (按姓氏笔画排序)

马三梅 (暨南大学)

王 翔 (暨南大学)

王少奎 (华南农业大学)

王永飞 (暨南大学)

毛 娟 (华南农业大学)

刘林川 (华南农业大学)

孙小武 (湖南农业大学)

李万昌 (河南师范大学)

李宏业 (暨南大学)

何晓明 (广东省农业科学院)

张卓欣 (华南农业大学)

张荣京 (华南农业大学)

屈红霞 (中国科学院华南植物园)

胡建广 (广东省农业科学院)



普通高等教育“十三五”规划教材

科技文献检索与利用

(第二版)

马三梅 王永飞 孙小武 主编



科学出版社

普通高等教育“十三五”规划教材

科技文献检索与利用

(第二版)

马三梅 王永飞 孙小武 主编

国务院侨务办公室立项

彭磷基外招生人才培养改革基金资助

国家西甜瓜产业技术体系资助

暨南大学教材资助项目

科学出版社

北 京

内 容 简 介

本书围绕如何获取与利用科技文献这一主题,对检索、保存、利用科技文献的知识和技巧进行详细阐述,为培养学生“会查、会读、会想、会写”的能力奠定基础。全书共10章,对科技文献检索的基础知识、EndNote X6软件的使用、常用中文数据库的检索、常用英文数据库的检索、常用阅读器和APP及微信公众号的使用、硕士论文和博士论文及专利的检索、图像检索、如何利用文献、科技论文的写作、论文查重和SCI影响因子等内容进行介绍。附录部分以编者已发表的论文为例,向读者展示论文投稿和修改的全过程,并结合编者的亲身实践,对论文写作的技巧和思路进行介绍。附录中还列出了一些文献检索常用网址和《中国图书馆分类法》(第五版)简表等内容,便于读者参考和拓展学习。此外,书中提供相关内容的视频,授课教师可获赠教学课件一份。

本书可作为高等院校本科生和研究生科技文献检索与利用的教材,也可作为从事教学和科研等工作的人员进行文献检索的参考书。

图书在版编目(CIP)数据

科技文献检索与利用/马三梅,王永飞,孙小武主编. —2版. —北京:科学出版社,2019.1

普通高等教育“十三五”规划教材

ISBN 978-7-03-059243-9

I. ①科… II. ①马… ②王… ③孙… III. ①科技文献-文献检索与利用 IV. ①G254.97

中国版本图书馆CIP数据核字(2018)第250717号

责任编辑:席慧 张静秋 赵晓静 / 责任校对:王晓茜

责任印制:师艳茹 / 封面设计:蓝正设计

科学出版社 出版

北京东黄城根北街16号

邮政编码:100717

http://www.sciencep.com

文林印务有限公司 印刷

科学出版社发行 各地新华书店经销

*

2014年3月第 一 版 开本:720×1000 1/16

2019年1月第 二 版 印张:14 1/2

2019年1月第九次印刷 字数:300 000

定价:48.00 元

(如有印装质量问题,我社负责调换)

《科技文献检索与利用》(第二版)编写委员会

主 编 马三梅 王永飞 孙小武

副 主 编 张立杰 屈红霞 王少奎 刘林川

编写人员 (按姓氏笔画排序)

马三梅 (暨南大学)

王少奎 (华南农业大学)

王永飞 (暨南大学)

毛 娟 (华南农业大学)

刘林川 (华南农业大学)

孙小武 (湖南农业大学)

李 峰 (复旦大学)

李 蔚 (暨南大学)

李万昌 (河南师范大学)

李宏业 (暨南大学)

杨军英 (河南师范大学)

张立杰 (梧州学院)

屈红霞 (中国科学院华南植物园)

胡建广 (广东省农业科学院)

郭国庆 (暨南大学)



科学出版社“十四五”普通高等教育本科规划教材

新形态教材


科技文献检索与利用

(第三版)

SCIENTIFIC LITERATURE RETRIEVAL AND UTILIZATION
(Third Edition)

王永飞 马三梅 主编



 科学出版社

科学出版社“十四五”普通高等教育本科规划教材

科技文献检索与利用

(第三版)

王永飞 马三梅 主编

暨南大学本科教材资助项目

科学出版社

北 京

内 容 简 介

本书围绕“如何获取与利用科技文献”这一主题,对检索、保存、利用科技文献的知识和技巧进行了详细阐述,为培养学生的“会查、会读、会想、会写”能力奠定了基础。

全书共 10 章,按照科技文献检索的基本知识介绍—科技文献的检索—文献的利用—论文查重和引用情况检索的写作主线,对文献检索的基础知识、EndNote X9 软件的使用、常用中文数据库的检索、常用英文数据库的检索、常用 APP 和微信公众号的使用、硕士论文和博士论文及专利的检索、图像检索、如何利用文献、科技论文的写作,以及论文查重、SCI 影响因子及 CSCD 等内容进行了介绍。在附录部分列出了《论文的新意从何来》和《发表在〈生命的化学〉上几篇文章的写作思路》等论文,以编者发表的论文为例,让读者看到论文投稿和修改的全过程,并结合编者的亲身实践对论文写作的技巧和思路进行了介绍和展示,处处体现着“文章是改出来的”这一主题,为读者掌握科技文献检索与利用方法提供了实际指导。此外,在附录中还列出一些文献检索常用的网址和《中国图书馆分类法》(第五版)简表等内容,便于读者参考和拓展学习。

本书可以作为高等院校本科生和研究生科技文献检索与利用的教材,也可作为教学和科研人员进行文献检索与利用的参考书。

图书在版编目(CIP)数据

科技文献检索与利用/王永飞,马三梅主编. —3 版. —北京:科学出版社, 2023.3

科学出版社“十四五”普通高等教育本科规划教材

ISBN 978-7-03-074111-0

I. ①科… II. ①王… ②马… III. ①科技情报—情报检索—高等学校—教材 IV. ①G252.7

中国版本图书馆 CIP 数据核字(2022)第 232728 号

责任编辑:张静秋 赵萌萌 / 责任校对:严 娜

责任印制:张 伟 / 封面设计:无极书装

科 学 出 版 社 出 版

北京东黄城根北街 16 号

邮政编码:100717

<http://www.sciencep.com>

北京九州迅驰传媒文化有限公司 印刷

科学出版社发行 各地新华书店经销

2014 年 3 月第 一 版 开本: 720×1000 1/16

2023 年 3 月第 三 版 印张: 17 1/4

2023 年 3 月第十七次印刷 字数: 353 000

定价: 59.80 元

(如有印装质量问题,我社负责调换)

《科技文献检索与利用》(第三版)

编写委员会

主 编 王永飞 马三梅

副主编 屈红霞 王少奎 刘林川

参 编 (按姓氏笔画排序)

马三梅 (暨南大学)

王少奎 (华南农业大学)

王永飞 (暨南大学)

王冬梅 (南宁市林业局)

毛 娟 (华南农业大学)

刘林川 (华南农业大学)

屈红霞 (中国科学院华南植物园)

姜兆玉 (临沂大学)

黄 博 (广东药科大学)

关于国家自然科学基金资助项目批准及有关事项的通知

刘林川 先生/女士：

根据《国家自然科学基金条例》的规定和专家评审意见，国家自然科学基金委员会（以下简称自然科学基金委）决定批准资助您的申请项目。项目批准号：

31600996，项目名称：核苷酸单糖转运蛋白ROCK1/EBS8在拟南芥内质网蛋白质质量控制中的作用机制研究，直接费用：21.00万元，项目起止年月：2017年01月至2019年12月，有关项目的评审意见及修改意见附后。

请尽早登录科学基金网络信息系统（<https://isisn.nsfc.gov.cn>），获取《国家自然科学基金资助项目计划书》（以下简称计划书）并按要求填写。对于有修改意见的项目，请按修改意见及时调整计划书相关内容；如对修改意见有异议，须在计划书电子版报送截止日期前提出。**注意：请严格按照《国家自然科学基金资助项目资金管理办法》填写计划书的资金预算表，其中，劳务费、专家咨询费科目所列金额与申请书相比不得调增。**

计划书电子版通过科学基金网络信息系统（<https://isisn.nsfc.gov.cn>）上传，由依托单位审核后提交至自然科学基金委进行审核。审核未通过者，返回修改后再行提交；审核通过者，打印为计划书纸质版（一式两份，双面打印），由依托单位审核并加盖单位公章后报送至自然科学基金委项目材料接收工作组。计划书电子版和纸质版内容应当保证一致。

向自然科学基金委提交和报送计划书截止时间节点如下：

- 1、提交计划书电子版截止时间为**2016年9月11日16点**（视为计划书正式提交时间）；
- 2、提交计划书电子修改版截止时间为**2016年9月18日16点**；
- 3、报送计划书纸质版截止时间为**2016年9月26日16点**。

请按照以上规定及时提交计划书电子版，并报送计划书纸质版，未说明理由且逾期不报计划书者，视为自动放弃接受资助。

附件：项目评审意见及修改意见

国家自然科学基金委员会
生命科学部
2016年8月17日

附件：项目评审意见及修改意见表

项目批准号	31600996	项目负责人	刘林川	申请代码1	C060102
项目名称	核苷酸单糖转运蛋白ROCK1/EBS8在拟南芥内质网蛋白质质量控制中的作用机制研究				
资助类别	青年科学基金项目	亚类说明			
附注说明					
依托单位	中国科学院上海生命科学研究院				
直接费用	21.00 万元	起止年月	2017年01月 至 2019年12月		
<p>通讯评审意见：</p> <p><1>本项目采用生物化学手段，结合遗传学、分子生物学和细胞生物学技术，利用申请者实验室建立完善的遗传筛选和验证体系对 AtUtr1、AtUtr3和 ROCK1/EBS8 的功能进行深入研究。探讨核苷酸 单糖转运蛋白 ROCK1/EBS8 在拟南芥内质网蛋白质质量监控中的作用 方式和作用机制，对另外两个内质网定位的 NSTs 蛋白 AtUtr1和 和 AtUtr3 之间 的关系进行研究。</p> <p>申请者实验技能全面，发表多篇论文，所在课题组前期工作基础比较好，具有良好的公共平台设施和国际上先进的大型仪器设备，能够在细胞生物学、基因组学、生物信息学和蛋白质组学等领域开展深入的研究，项目组技术力量和硬件支持满足工作的需要,本项目的研究内容丰富详实，技术路线可行，经费预算合理，可以保证该项目的顺利完成。</p> <p><2>无论对于植物还是动物，蛋白质能够正确折叠对于其正常行使功能十分重要，因此蛋白质折叠控制机制的研究具有重要科学价值。该项目以模式植物拟南芥为材料，研究核苷酸单糖转运蛋白ROCK1/EBS8参与内质网蛋白质正确折叠、修饰等质量控制机制，以及与内质网定位的另外2个蛋白AtUtr1和AtUtr3的关系；研究内容创新性强，研究方案具体详细，其研究结果可为动物蛋白质功能相关研究提供参考。予以资助。</p> <p><3>本项目通过对拟南芥核苷酸单糖转运蛋白ROCK1/EBS8进行研究，利用申请人已有的鉴定体系，探索ROCK1/EBS8蛋白在内质网蛋白质质量控制中的作用机制，并分析其与另外两个内质网膜定位蛋白AtUtr1和AtUtr3之间的关系。拟解决的科学问题具有针对性，研究内容合适、总体方案合理，技术路线可行，具有较好的前期研究基础和实验条件。</p> <p>建议给予优先资助。</p> <p><4>本研究以模式植物拟南芥为材料,关注核苷酸单糖转运蛋白在内质网蛋白质质量控制中的作用. 该研究立意新颖,关注蛋白质质量工程中的控制因子. 研究内容丰富,研究路线可行性好. 研究者具备很好的科研积累,在相关领域开展了长期而优秀的工作,团队成员合理,相信可以圆满完成任务. 同意优先资助.</p> <p><5>课题申请者前期以拟南芥bri1-9突变体构建遗传学筛选模型，获得了参与内质网蛋白质质量控制的一个重要组分EBS8。申请人以此为基础，旨在进一步研究EBS8在内质网蛋白质质量控制中的作用机制，以及与拟南芥中已知NSTs蛋白之间的关系。此外，该筛选系统暗示EBS8可能参与植物逆境胁迫和抗病防御反应。该课题研究目标明确，方案可行，前期工作基础扎实，拟解决的科学问题新颖。</p> <p>建议优先资助。</p> <p>对研究方案的修改意见：</p> <p style="text-align: right;">生命科学部</p> <p style="text-align: right;">2016年8月17日</p>					



项目批准号	31600996
申请代码	C060102
归口管理部门	
依托单位代码	20003108B1308-2410



国家自然科学基金委员会 资助项目计划书

资助类别：青年科学基金项目

亚类说明：

附注说明：

项目名称：核苷酸单糖转运蛋白ROCK1/EBS8在拟南芥内质网蛋白质质量控制中的作用机制研究

直接费用：21万元 执行年限：2017.01-2019.12

负责人：刘林川

通讯地址：上海市松江区辰花公路3888号上海植物逆境生物学研究中心

邮政编码：201602 电话：021-57078263

电子邮件：liulinchuan@163.com

依托单位：中国科学院上海生命科学研究院

联系人：王江 电话：021-54920062

填表日期：2016年09月06日

国家自然科学基金委员会制



国家自然科学基金委员会资助项目计划书填报说明

- 一、项目负责人收到《关于国家自然科学基金资助项目批准及有关事项的通知》（以下简称《批准通知》）后，请认真阅读本填报说明，参照国家自然科学基金相关项目管理办法及《国家自然科学基金资助项目资金管理办法》（请查阅国家自然科学基金委员会官方网站首页“政策法规”-“管理办法”栏目），按《批准通知》的要求认真填写和提交《国家自然科学基金委员会资助项目计划书》（以下简称《计划书》）。
- 二、填写《计划书》时要求科学严谨、实事求是、表述清晰、准确。《计划书》经国家自然科学基金委员会相关项目管理部门审核批准后，将作为项目研究计划执行和检查、验收的依据。
- 三、《计划书》各部分填写要求如下：
 - （一）简表：由系统自动生成。
 - （二）摘要及关键词：各类获资助项目都必须填写中、英文摘要及关键词。
 - （三）项目组主要成员：计划书中列出姓名的项目组主要成员由系统自动生成，与申请书原成员保持一致，不可随意调整。如果批准通知中“项目评审意见及修改意见表”中“对研究方案的修改意见”栏目有调整项目组成员相关要求的，待项目开始执行后，按照项目成员变更程序另行办理。
 - （四）资金预算表：按批准资助的直接费用填报资金预算表和预算说明书，其中的劳务费、专家咨询费金额不应高于申请书中相应金额。国家重大科研仪器研制项目、重大项目还应按照预算评审后批复的直接费用各科目金额填报资金预算表、预算说明书及相应的预算明细表。
 - （五）正文：
 1. 面上项目、青年科学基金项目、地区科学基金项目：如果《批准通知》中没有修改要求的，只需选择“研究内容和研究目标按照申请书执行”即可；如果《批准通知》中“项目评审意见及修改意见表”中“对研究方案的修改意见”栏目明确要求调整研究期限和研究内容等的，须选择“根据研究方案修改意见更改”并填报相关修改内容。
 2. 重点项目、重点国际（地区）合作研究项目、重大项目、国家重大科研仪器研制项目：须选择“根据研究方案修改意见更改”，根据《批准通知》的要求填写研究（研制）内容，不得自行降低、更改研究目标（或仪器研制的技术性能与主要技术指标以及验收技术指标）或缩减研究（研制）内容。此外，还要突出以下几点：
 - （1）研究的难点和在实施过程中可能遇到的问题（或仪器研制风险），拟采用的研究（研制）方案和技术路线；
 - （2）项目主要参与者分工，合作研究单位之间的关系与分工，重大项目还需说明课题之间的关联；
 - （3）详细的年度研究（研制）计划。



3. 国家杰出青年科学基金、优秀青年科学基金和海外及港澳学者合作研究基金项目：须选择“根据研究方案修改意见更改”，按下列提纲撰写：
 - (1) 研究方向；
 - (2) 结合国内外研究现状，说明研究工作的学术思想和科学意义（限两个页面）；
 - (3) 研究内容、研究方案及预期目标（限两个页面）；
 - (4) 年度研究计划；
 - (5) 研究队伍的组成情况。
4. 对于其他类型项目，参照面上项目的方式进行选择和填写。



简表

申请者信息	姓 名	刘林川	性 别	男	出生年月	1983年01月	民 族	汉族
	学 位	博士			职称	副研究员		
	电 话	021-57078263		电子邮件	liulinchuan@163.com			
	传 真			个人网页				
	工 作 单 位	中国科学院上海生命科学研究院						
	所 在 院 系 所	上海植物逆境生物研究中心						
依托单位信息	名 称	中国科学院上海生命科学研究院					代码	20003108B1308
	联 系 人	王江		电子邮件	jiangwang@sibs.ac.cn			
	电 话	021-54920062		网站地址	http://www.sibs.ac.cn			
合作单位信息	单 位 名 称							代 码
项目基本信息	项 目 名 称	核苷酸单糖转运蛋白ROCK1/EBS8在拟南芥内质网蛋白质质量控制中的作用机制研究						
	资 助 类 别	青年科学基金项目				亚 类 说 明		
	附 注 说 明							
	申 请 代 码	C060102:植物分子遗传				C020101:植物形态结构与功能		
	基 地 类 别							
	执 行 年 限	2017.01-2019.12						
	直 接 费 用	21万元						



项目摘要

中文摘要(500字以内):

蛋白质正常功能的行使依赖于形成正确的天然构象,内质网是分泌蛋白和膜蛋白折叠修饰的场所。植物在长期进化过程中形成了保守的内质网蛋白质质量控制机制,对错误折叠蛋白进行识别修复,只有正确折叠的蛋白质才被转运至其它细胞器发挥作用。近年来的研究表明许多定位在内质网膜上的核苷酸单糖转运蛋白参与了拟南芥内质网蛋白质质量控制过程。尽管这些蛋白质的基本生物学功能已被阐述,但它们在该过程中的具体作用方式和作用机制还不是很清楚。本研究利用我们实验室建立的遗传筛选与鉴定体系,结合生物化学方法重点研究核苷酸单糖转运蛋白ROCK1/EBS8在拟南芥内质网蛋白质质量控制中的分子机制,同时研究它与另外两个内质网定位的核苷酸单糖转运蛋白AtUtr1和AtUtr3之间的关系。该项研究有助于我们更好的认识植物内质网蛋白质质量控制系统,同时可以为酵母和动物中该领域的研究提供参考。

关键词: 模式植物; 表型变异; 基因的遗传互作; 蛋白质质量控制; 核苷酸单糖转运蛋白

Abstract(limited to 4000 words):

It is well known that the proper function of a protein depends on its correct native conformation. The endoplasmic reticulum (ER) is the folding compartment for secretory and membrane proteins. Plants have evolved a conserved ER-mediated protein quality control (ERQC) mechanism to recognize and repair incorreced folded protein, only corrected folded proteins can be exported to their physiological destinations. Recent studies revealed that several ER-localized nucleotide sugar transporters (NSTs) were involved in ER protein quality control in Arabidopsis. Despite the physiological functions of these proteins have been presented, their molecular mechanisms in ERQC remains undefined. Here, we attempt to investigate the mechanisms of ROCK1/EBS8, a NST protein, in ERQC by using our developed screening system and examined the role of two other ER-localized NSTs proteins, AtUtr1 and AtUtr3. Elaborating the mechanism of Arabidopsis ROCK1/EBS8 and other NSTs proteins can help us to better understand ERQC in plant and throw light on the ERQC research in yeast and mammalian.

Keywords: Model Plant; Phenotypic Variation; Genetic Interaction; Protein Quality Control; Nucleotide Sugar Transporter



项目组主要成员

编号	姓名	出生年月	性别	职称	学位	单位名称	电话	证件号码	项目分工	每年工作时间（月）				
1	刘林川	1983.01	男	副研究员	博士	中国科学院上海生命科学研究	021-57078263	21100219830126013X	项目负责人	10				
2	王牧阳	1980.10	女	高级工程师	博士	中国科学院上海生命科学研究	021-57078263	320522198010040740	蛋白质相互作用分析	10				
3	张聪聪	1989.10	男	博士生	学士	中国科学院上海生命科学研究	021-57078263	370126198910090439	突变体的筛选与鉴定	8				
4	陈永武	1989.03	男	博士生	学士	中国科学院上海生命科学研究	021-57078263	350825198903135414	蛋白表达与纯化	8				
5	刘晓玲	1990.02	女	博士生	学士	中国科学院上海生命科学研究	021-57078263	370783199002106006	糖链结构鉴定与分析	8				
总人数			高级		中级		初级		博士后		博士生		硕士生	
5			2								3			



国家自然科学基金项目直接费用预算表（定额补助）

项目批准号：31600996

项目负责人：刘林川

金额单位：万元

序号	科目名称	金额
1	一、项目直接费用	21.0000
2	1、设备费	1.0000
3	(1)设备购置费	1.0000
4	(2)设备试制费	0.0000
5	(3)设备改造与租赁费	0.0000
6	2、材料费	8.4800
7	3、测试化验加工费	3.5000
8	4、燃料动力费	0.0000
9	5、差旅/会议/国际合作与交流费	2.70
10	6、出版/文献/信息传播/知识产权事务费	1.0000
11	7、劳务费	4.3200
12	8、专家咨询费	0.00
13	9、其他支出	0.00
14	二、自筹资金	0.00



预算说明书（定额补助）

（请按《国家自然科学基金项目资金预算表编制说明》中的要求，对各项支出的主要用途和测算理由及合作研究外拨资金、单价 ≥ 10 万元的设备费等内容进行详细说明，可根据需要另加附页。）

一、项目直接费用

1. 设备费

预算经费：1.00 万元

用于购置本项目所需要的小型仪器设备。

2. 材料费

预算经费：8.48 万元

用于购置本项目所需要常用化学试剂、酶、抗体和同位素等。

预算依据如下：

PCR 反应用试剂，用于基因克隆及转基因植株的检测，包括普通 Taq 酶、高保真 KOD 酶和 dNTP 等，预算经费 0.48 万元。

DNA 内切酶（包括稀有内切酶）、外切酶、连接酶、反转录酶、糖苷酶等酶类，用于基因克隆、载体构建和糖化学研究等，预算经费 1.40 万元。

DNA、RNA 提取、纯化用试剂盒及高纯度大量质粒提取试剂盒，预算经费 0.50 万元。

蛋白纯化及相互作用检测用试剂，主要包括蛋白纯化所用的填料、标签抗体、用于免疫共沉淀的抗体偶联磁珠、western blot 所需要的常用耗材等。预算经费 3.00 万元。

本项目中用于转运活性测定所需的同位素标记底物，预算经费 1.20 万元。

用于购买质谱实验所需的胰蛋白酶，糖链标准品蛋白和样品浓缩试剂盒等，预算经费 1.50 万元。

植物组织培养试剂，用于转基因的遗传筛选和种植，预计经费 0.40 万元。

3. 测试化验加工费

预算经费：3.50 万元

主要用于各类引物合成、基因测序分析、抗体制备、蛋白质质谱鉴定、高效液相色谱分析等。预算依据如下：

用于载体构建、遗传鉴定的引物合成和测序，预计经费 0.80 万元。制备多克隆抗体 2 个，预计经费 1.00 万元。蛋白质质谱鉴定糖蛋白糖链结构，预计经费 1.20 万元。高效液相色谱分析糖蛋白糖链结构，预计经费 0.5 万元。

4. 燃料动力费

无

5. 差旅/会议/国际合作与交流费

预算经费：2.7 万元



本申请项目中酵母NSTs转运活性分析需要开展国内合作。中科院遗传发育所周奕华实验室在酵母微粒体、脂质体分离、同位素标记检测等方面有很好的基础。合作研究预计出差2次，每次1个星期，交通费、住宿费每次0.30万元，合计预算经费0.60万元。

参加国内学术会议交流2次，植物分子遗传学和细胞生物学领域各一次，每次2-3天。会议注册费、交通费、住宿费每次0.30万元，合计预算经费0.60万元。

由于本项目中糖链结构鉴定需要不同糖链类型的标准品蛋白作为参考，目前国际上只有日本少数公司和实验室具有合成该标准品的能力。因此，本申请项目中糖化学实验需要开展国际合作。我们与日本大阪大学Fujiyama实验室有着很好的合作关系，该实验室在植物糖蛋白和糖化学研究领域有着丰富的经验。因此需要赴日本与该实验室合作完成这部分工作。交通费、住宿费预算合计1.00万元。

参加植物膜生物学和生物化学国际会议，了解植物科学的最新研究进展和动态，并与国外同行交流我们的科研成果。交通费、住宿费预算合计0.50万元。

6. 出版/文献/信息传播/知识产权事务费

预算经费：1.00万元

预计发表SCI论文2篇，平均每篇版面费用0.50万元，合计预算经费1.00万元。

7. 劳务费

预算经费：4.32万元

参加课题研究工作的博士研究生3人，主要参与项目中遗传材料的构建和蛋白质相互作用分析。按照中国科学院上海生命科学研究院的博士研究生待遇标准每人每月补助600元，3名博士研究生共计72人月，合计预算经费4.32万元。

8. 专家咨询费

无

9. 其他支出

无

二. 自筹资金

无

项目负责人签字：

科研部门公章：

财务部门公章：



报告正文

研究内容和研究目标按照申请书执行。



国家自然科学基金资助项目签批审核表

<p>我接受国家自然科学基金的资助，将按照申请书、项目批准意见和计划书负责实施本项目（批准号：31600996），严格遵守国家自然科学基金委员会关于资助项目管理、财务等各项规定，切实保证研究工作时间，认真开展研究工作，按时报送有关材料，及时报告重大情况变动，对资助项目发表的论著和取得的研究成果按规定进行标注。</p> <p>项目负责人（签章）： 年 月 日</p>	<p>我单位同意承担上述国家自然科学基金项目，将保证项目负责人及其研究队伍的稳定和研究项目实施所需的条件，严格遵守国家自然科学基金委员会有关资助项目管理、财务等各项规定，并督促实施。</p> <p>依托单位（公章） 年 月 日</p>														
本栏目由基金委填写	<p>科学处审查意见：</p> <p>建议年度拨款计划（本栏目为自动生成，单位：万元）：</p> <table border="1" data-bbox="201 947 1045 1072"><thead><tr><th>年度</th><th>总额</th><th>第一年</th><th>第二年</th><th>第三年</th><th>第四年</th><th>第五年</th></tr></thead><tbody><tr><td>金额</td><td></td><td></td><td></td><td></td><td></td><td></td></tr></tbody></table> <p>负责人（签章）： 年 月 日</p>	年度	总额	第一年	第二年	第三年	第四年	第五年	金额						
	年度	总额	第一年	第二年	第三年	第四年	第五年								
	金额														
<p>科学部审查意见：</p> <p>负责人（签章）： 年 月 日</p>															
本栏目主要用于重大项目等	<p>相关局室审核意见：</p> <p>负责人（签章）： 年 月 日</p>														
	<p>委领导审批意见：</p> <p>委领导（签章）： 年 月 日</p>														

国家自然科学基金资助项目批准通知

刘林川 先生/女士：

根据《国家自然科学基金条例》和专家评审意见，国家自然科学基金委员会（以下简称自然科学基金委）决定批准资助您的申请项目。项目批准号：31970187，项目名称：植物ABCB1的质量控制及其协同油菜素内酯信号和生长素运输的分子机制，直接费用：58.00万元，项目起止年月：2020年01月至2023年12月，有关项目的评审意见及修改意见附后。

请尽早登录科学基金网络信息系统（<https://isisn.nsfc.gov.cn>），获取《国家自然科学基金资助项目计划书》（以下简称计划书）并按要求填写。对于有修改意见的项目，请按修改意见及时调整计划书相关内容；如对修改意见有异议，须在电子版计划书报送截止日期前向相关科学处提出。

电子版计划书通过科学基金网络信息系统（<https://isisn.nsfc.gov.cn>）上传，依托单位审核后提交至自然科学基金委进行审核。审核未通过者，返回修改后再行提交；审核通过者，打印纸质版计划书（一式两份，双面打印），依托单位审核并加盖单位公章后报送至自然科学基金委项目材料接收工作组。电子版和纸质版计划书内容应当保证一致。向自然科学基金委提交和报送计划书截止时间节点如下：

- 1、提交电子版计划书截止时间为**2019年9月11日16点**（视为计划书正式提交时间）；
- 2、提交电子修改版计划书截止时间为**2019年9月18日16点**；
- 3、报送纸质版计划书截止时间为**2019年9月26日16点**。

请按照以上规定及时提交电子版计划书，并报送纸质版计划书，未说明理由且逾期不报计划书者，视为自动放弃接受资助。

附件：项目评审意见及修改意见表

国家自然科学基金委员会
2019年8月16日

附件：项目评审意见及修改意见表

项目批准号	31970187	项目负责人	刘林川	申请代码1	C020101
项目名称	植物ABCB1的质量控制及其协同油菜素内酯信号和生长素运输的分子机制				
资助类别	面上项目		亚类说明		
附注说明					
依托单位	华南农业大学				
直接费用	58.00 万元		起止年月	2020年01月 至 2023年12月	
<p>通讯评审意见：</p> <p><1>具体评价意见：</p> <p>一、请针对创新点详细评述申请项目的创新性、科学价值以及对相关领域的潜在影响。</p> <p>本项申请拟以拟南芥为材料，采用遗传学、生物化学、分子生物学和细胞生物学等研究手段，研究植物ABCB1在内质网中的质量控制和降解机制，同时，探讨其在油菜素内酯信号和生长素运输中的协同作用。</p> <p>该项研究目标明确，技术路线可行，具有很好的研究基础。</p> <p>二、请结合申请项目的研究方案与申请人的研究基础评述项目的可行性。</p> <p>申请书中正在承担的科研项目中，在研青年科学基金项目起始日期“2007.01-2009.12”应该是错误了。</p> <p>三、其他建议</p> <p><2>具体评价意见：</p> <p>一、请针对创新点详细评述申请项目的创新性、科学价值以及对相关领域的潜在影响。</p> <p>真核细胞内质网中的蛋白质质量控制以及错误折叠蛋白的降解机制是细胞完成生命活动的重要保证，相关的机制研究是包括植物在内的真核生物科学研究领域内的重点和热点。在植物科学研究领域，生长素和BR是非常重要的内源激素，相互作用调控植物生长发育的众多过程。该项目提出对生长素转运蛋白ABCB1在内质网中的质量控制机制进行研究，并探索其如何协同BR信号与生长素的运输，有很好的创新性和科研价值，具有重要的科学理论意义。</p> <p>二、请结合申请项目的研究方案与申请人的研究基础评述项目的可行性。</p> <p>申请人在相关领域有较强的背景，而且已开展了前期研究工作取得了一定的成果，为该项目的进一步研究奠定了良好的基础，所提的方案切实可行，所依托的单位能提供良好的条件。</p> <p>三、其他建议</p> <p><3>具体评价意见：</p> <p>一、请针对创新点详细评述申请项目的创新性、科学价值以及对相关领域的潜在影响。</p> <p>该研究拟对ABC转运蛋白ABCB1在内质网中受到的质量控制作用开展系统的研究，通过多学科的手段揭示TWD1对ABCB1在内质网中的质量控制机制，并探究ABCB1在油菜素内酯信号和生长素运输中的作用。研究具有一定的创新性。</p> <p>二、请结合申请项目的研究方案与申请人的研究基础评述项目的可行性。</p> <p>申请人拟应用遗传学、生物化学、蛋白质组学等多种手段，研究ABCB1在内质网的滞留和降解在蛋白质量控制中的作用、及其对油菜素内酯信号和生长素运输的影响，解析ABCB1的功能，揭示内质网中的蛋白质量控制机制。研究内容翔实，研究方案较为合理，技术路线可行，前期工作基础扎实。</p> <p>三、其他建议</p>					

修改意见：

生命科学部

2019年8月16日



项目批准号	31970187
申请代码	C020101
归口管理部门	
依托单位代码	51064208A0499-0932



3 1970187 1003 819

国家自然科学基金委员会 资助项目计划书

资助类别：面上项目

亚类说明：

附注说明：

项目名称：植物ABCB1的质量控制及其协同油菜素内酯信号和生长素运输的分子机制

直接费用：58万元 执行年限：2020.01-2023.12

负责人：刘林川

通讯地址：广东省广州市天河区五山路483号华南农业大学林学与风景园林学院617房间

邮政编码：201602 电 话：020-85280256

电子邮件：liulinchuan@163.com

依托单位：华南农业大学

联系人：倪慧群 电 话：020-85280070

填表日期：2019年08月23日

国家自然科学基金委员会制

Version: 1.003.819



国家自然科学基金委员会资助项目计划书填报说明

- 一、项目负责人收到《关于国家自然科学基金资助项目批准及有关事项的通知》（以下简称《批准通知》）后，请认真阅读本填报说明，参照国家自然科学基金相关项目管理办法及《国家自然科学基金资助项目资金管理办法》（请查阅国家自然科学基金委员会官方网站首页“政策法规”栏目），按《批准通知》的要求认真填写和提交《国家自然科学基金委员会资助项目计划书》（以下简称《计划书》）。
- 二、填写《计划书》时要求科学严谨、实事求是、表述清晰、准确。《计划书》经国家自然科学基金委员会相关项目管理部门审核批准后，将作为项目研究计划执行和检查、验收的依据。
- 三、《计划书》各部分填写要求如下：
 - （一）简表：由系统自动生成。
 - （二）摘要及关键词：各类获资助项目都必须填写中、英文摘要及关键词。
 - （三）项目组主要成员：计划书中列出姓名的项目组主要成员由系统自动生成，与申请书原成员保持一致，不可随意调整。如果批准通知中“项目评审意见及修改意见表”中“对研究方案的修改意见”栏目有调整项目组成员相关要求的，待项目开始执行后，按照项目成员变更程序另行办理。
 - （四）资金预算表：根据批准资助的直接费用，按照《国家自然科学基金项目预算表编制说明》填报资金预算表和预算说明书。国家重大科研仪器研制项目、重大项目还应按照预算评审后批复的直接费用各科目金额填报资金预算表、预算说明书及相应的预算明细表。
 - （五）正文：
 1. 面上项目、青年科学基金项目、地区科学基金项目：如果《批准通知》中没有修改要求的，只需选择“研究内容和研究目标按照申请书执行”即可；如果《批准通知》中“项目评审意见及修改意见表”中“对研究方案的修改意见”栏目明确要求调整研究期限和研究内容等的，须选择“根据研究方案修改意见更改”并填报相关修改内容。
 2. 重点项目、重点国际（地区）合作研究项目、重大项目、国家重大科研仪器研制项目：须选择“根据研究方案修改意见更改”，根据《批准通知》的要求填写研究（研制）内容，不得自行降低、更改研究目标（或仪器研制的技术性能与主要技术指标以及验收技术指标）或缩减研究（研制）内容。此外，还要突出以下几点：
 - （1）研究的难点和在实施过程中可能遇到的问题（或仪器研制风险），拟采用的研究（研制）方案和技术路线；
 - （2）项目主要参与者分工，合作研究单位之间的关系与分工，重大项目还需说明课题之间的关联；
 - （3）详细的年度研究（研制）计划。



3. 国家杰出青年科学基金、优秀青年科学基金和海外及港澳学者合作研究基金项目：须选择“根据研究方案修改意见更改”，按下列提纲撰写：
 - (1) 研究方向；
 - (2) 结合国内外研究现状，说明研究工作的学术思想和科学意义（限两个页面）；
 - (3) 研究内容、研究方案及预期目标（限两个页面）；
 - (4) 年度研究计划；
 - (5) 研究队伍的组成情况。
4. 国家自然科学基金基础科学中心项目：须选择“根据研究方案修改意见更改”，应当根据评审委员会和现场考察专家组的意见和建议，进一步完善并细化研究计划，作为评估和验收的依据。按下列提纲撰写：
 - (1) 五年拟开展的研究工作（包括主要研究方向、关键科学问题与研究内容）；
 - (2) 研究方案（包括骨干成员之间的分工及合作方式、学科交叉融合研究计划等）；
 - (3) 年度研究计划；
 - (4) 五年预期目标和可能取得的重大突破等；
 - (5) 研究队伍的组成情况。
5. 对于其他类型项目，参照面上项目的方式进行选择和填写。



简表

申请者信息	姓 名	刘林川	性 别	男	出生年月	1983年01月	民 族	汉族
	学 位	博士			职称	教授		
	是否在站博士后	否			电子邮件	liulinchuan@163.com		
	电 话	020-85280256			个人网页			
	工 作 单 位	华南农业大学						
	所 在 院 系 所	林学与风景园林学院						
依托单位信息	名 称	华南农业大学					代码	51064208A0499
	联 系 人	倪慧群			电子邮件	kyc.jhk@scau.edu.cn		
	电 话	020-85280070			网站地址	http://kjc.scau.edu.cn/		
合作单位信息	单 位 名 称							
项目基本信息	项 目 名 称	植物ABCB1的质量控制及其协同油菜素内酯信号和生长素运输的分子机制						
	资 助 类 别	面上项目				亚 类 说 明		
	附 注 说 明							
	申 请 代 码	C020101:植物结构与功能				C020407:植物激素与生长调节物质		
	基 地 类 别							
	执 行 年 限	2020.01-2023.12						
	直 接 费 用	58万元						



项目摘要

中文摘要:

植物ABC转运蛋白利用ATP水解提供能量将底物进行逆浓度梯度转运,在植物的生长和发育过程中起着非常重要的作用。生长素在特定的细胞合成后需要转运至不同的组织来行使生理功能,ABCB1作为一种重要的ABC转运蛋白在细胞膜上参与了对生长素的转运。然而,我们发现ABCB1在拟南芥twd1-6突变体背景下被滞留在内质网中并且被快速降解,特别是twd1-6和ABCB1蛋白能够共同定位于内质网。尽管我们目前对动物、酵母和植物细胞中糖蛋白在内质网中的质量控制和降解机制有了一定的了解,但是对转运蛋白的内质网滞留和降解途径认识还十分有限。在本项目申请中,我们以遗传学为基础,结合生物化学和细胞生物学研究手段,研究ABCB1在内质网中的质量控制机制。同时,我们还探索植物生长过程中ABCB1是如何来协同油菜素内酯信号和生长素的运输。

Abstract:

ABC transporters are essential for plant growth and development, which can transport complex organic materials against concentration gradients energized by ATP. Auxin are synthesized in specialized cells and are transported to target tissues. ABCB1, an ABC transporter, has been shown to be involved in auxin transport in plasma membrane. However, we found a single missense Arabidopsis twd1(twisted dwarf1) mutant, twd1-6, in which ABCB1 was retained in the ER and rapidly degraded. Especially, twd1-6 is co-localized with ABCB1 in the ER. Despite primary understanding of ERQC/ERAD of glycosylated proteins has been ascertained through investigating yeast, mammalian and plant cells, the functional studies of the ERQC/ERAD processes on membrane transporter proteins remained rather limited. In this study, we will focus on the folding, maturation, and degradation of ABCB1 to screen and identify the components involved in these processes by using genetics methods combined with biochemical and cell biology approaches. In addition, we are going to explore the critical roles of ABCB1 in the interactions between BR signaling and auxin transport during plant growth.

关键词(用分号分开): 运输途径; 蛋白质分选; 蛋白质降解; 油菜素内酯信号; 生长素运输

Keywords(用分号分开): transport pathway; protein sorting; protein degradation; BR signaling; auxin transport



项目组主要成员

编号	姓名	出生年月	性别	职称	学位	单位名称	电话	证件号码	项目分工	每年工 作时间 (月)
1	刘林川	1983.01	男	教授	博士	华南农业大学	020-85280256	21100219830126013X	项目负责人	10
2	李青粉	1987.02	女	工程师	博士	华南农业大学	18998825286	410901198702052023	遗传材料构建与分析	10
3	胡莉	1994.05	女	博士生	硕士	华南农业大学	18320726497	430621199405101041	蛋白质磷酸化修饰分析	10
4	韦健烺	1993.09	男	博士生	硕士	华南农业大学	13570444591	440681199309212639	细胞生物学分析	10
5	段志豪	1996.03	男	硕士生	学士	华南农业大学	18825195959	361127199603044213	蛋白质相互作用分析	10
6	周淑瑶	1997.02	女	硕士生	学士	华南农业大学	13422003209	440681199702234746	细胞生物学分析	10
7	伍慧祥	1997.12	男	硕士生	学士	华南农业大学	13632190418	360782199712094419	蛋白质相互作用分析	10
总人数		高级		中级		初级		博士后	博士生	硕士生
7		1		1		0		0	2	3



国家自然科学基金项目直接费用预算表（定额补助）

项目批准号：31970187

项目负责人：刘林川

金额单位：万元

序号	科目名称	金额
1	项目直接费用合计	58.0000
2	1、设备费	0.0000
3	(1)设备购置费	0.0000
4	(2)设备试制费	0.0000
5	(3)设备升级改造与租赁费	0.0000
6	2、材料费	22.0000
7	3、测试化验加工费	11.0000
8	4、燃料动力费	0.0000
9	5、差旅/会议/国际合作与交流费	5.8000
10	6、出版/文献/信息传播/知识产权事务费	3.2000
11	7、劳务费	16.0000
12	8、专家咨询费	0.0000
13	9、其他支出	0.0000



预算说明书（定额补助）

（请按照《国家自然科学基金项目预算表编制说明》等的有关要求，对各项支出的主要用途和测算理由，以及合作研究外拨资金、单价 ≥ 10 万元的设备费等内容进行必要说明。）

1.设备费

无

目前，本团队和所在科研平台已具备开展本项目所需的实验条件，如各种仪器设备等，因此本项目无仪器设备购置的预算。

2.材料费

预算经费：22.00 万元

(1) 基因克隆和载体构建，预算经费 8.60 万元。

Taq 酶（1000U/支，Takara），每支 200 元，购置 50 支，合计 1.00 万元；
高保真 Taq 酶（1000U，Vazyme），每支 800 元，购置 20 支，合计 1.60 万元；
购买电泳普通琼脂糖每瓶 300 元，购置 50 瓶，合计 1.50 万元；
DNA 内切酶、连接酶、反转录酶和重组酶等酶类，合计 2.50 万元；
植物 DNA 提取试剂盒、RNA 提取试剂盒、琼脂糖凝胶 DNA 回收试剂盒等，合计 2.00 万元。

(2) 基因表达分析，预算经费 1.12 万元。

定量 PCR 试剂盒（Bio-Rad，100 次，iScript cDNA Synthesis Kit），每个 1600 元，购置 7 盒，合计 1.12 万元；

(3) 蛋白表达纯化及功能检测，预算经费 6.20 万元。

原核表达蛋白 His 标签、GST 标签、MBP 标签纯化用介质，合计 0.90 万元；
BCA 蛋白质定量试剂盒，合计 0.30 万元；
蛋白浓缩用超滤管，每个 50 元，购置 100 个，合计 0.50 万元；
购买标签抗体、磁珠，用于免疫共沉淀和蛋白质相互作用检测，合计 4.50 万元。

(4) 植物组织培养试剂，预算经费 2.70 万元。

植物组培用琼脂粉、培养基、糖类等培养基，合计 1.20 万元。
转基因筛选用抗生素，潮霉素、头孢霉素、利福平、卡那霉素等，合计 1.50 万元；

(5) 常用低值易耗品，预算经费 3.38 万元。

一次性培养皿，每箱 160 元，购置 30 箱，合计 0.48 万元；
一次性移液吸头和离心管，合计 2.00 万元；
一次性 96 孔 PCR 板（Axygen），每包 30 元，购置 200 包，合计 0.60 万元；
一次性乳胶手套、口罩等，合计 0.30 万元；

3.测试化验加工费

预算经费：11.00 万元

(1) 引物合成，用于基因的图位克隆，基因表达的鉴定，载体构建等实验，合计 1.80 万元；

(2) DNA 测序，用于基因克隆、载体构建，定点突变的鉴定等，合计 1.50 万；

(3) 蛋白质质谱分析，用于蛋白质定性和定量分析，磷酸化位点分析等，合计 2.50 万元。

(4) 抗体制备，用于蛋白质稳定性检测和其它生化实验。每个 8000 元，制备 4 个，



合计 3.20 万元；
进行转录组测序分析，每个样本 2000 元，预计 10 个样本，合计 2.00 万元。

4.燃料动力费
无

5.差旅/会议/国际合作与交流费

预算经费：5.80 万元

用于参加国内、国际学术会议注册费用和住宿、交通费用。

课题人员参加国内学术会议交流 6 人次，会议注册费、交通费、住宿费合计 3.00 万元。参加国际学术会议 2 人次，会议注册费、交通费、住宿费合计 2.80 万元。

6.出版/文献/信息传播/知识产权事务费

预算经费：3.20 万元

项目研究期间发表高水平 SCI 国际论文 2 篇，论文版面费以每篇 1.50 万元计；资料查阅、文献检索费等 0.20 万元；合计 3.20 万元。

7.劳务费

预算经费：16.00 万元

参加课题研究工作的博士研究生 2 人，按照华南农业大学的博士研究生待遇标准课题组每人每月平均补助 800 元，2 名博士研究生共计 80 人月，合计 6.40 万元；

参加课题研究工作的硕士研究生 3 人，按照华南农业大学硕士研究生待遇标准每人每月平均补助 800 元，3 名硕士研究生共计 120 人月，合计 9.60 万元。

8.专家咨询费

无

9.其他支出

无

项目负责人签字：

科研部门公章：

财务部门公章：



报告正文

研究内容和研究目标按照申请书执行。



国家自然科学基金资助项目签批审核表

<p>我接受国家自然科学基金的资助，将按照申请书、项目批准意见和计划书负责实施本项目（批准号：31970187），严格遵守国家自然科学基金委员会关于资助项目管理、财务等各项规定，切实保证研究工作时间，认真开展研究工作，按时报送有关材料，及时报告重大情况变动，对资助项目发表的论著和取得的研究成果按规定进行标注。</p> <p>项目负责人（签章）： 年 月 日</p>		<p>我单位同意承担上述国家自然科学基金项目，将保证项目负责人及其研究队伍的稳定和研究项目实施所需的条件，严格遵守国家自然科学基金委员会有关资助项目管理、财务等各项规定，并督促实施。</p> <p>依托单位（公章） 年 月 日</p>						
本栏目由基金委填写	<p>科学处审查意见：</p>							
	<p>建议年度拨款计划（本栏目为自动生成，单位：万元）：</p>							
	年度	总额	第一年	第二年	第三年	第四年	第五年	
	金额							
本栏目主要用于重大项目等	<p>科学部审查意见：</p> <p>负责人（签章）： 年 月 日</p>							
	<p>相关局室审核意见：</p> <p>负责人（签章）： 年 月 日</p>							
		<p>委领导审批意见：</p> <p>委领导（签章）： 年 月 日</p>						

国家自然科学基金资助项目批准通知

（预算制项目）

刘林川 先生/女士：

根据《国家自然科学基金条例》、相关项目管理办法规定和专家评审意见，国家自然科学基金委员会（以下简称自然科学基金委）决定资助您申请的项目。项目批准号：32370269，项目名称：植物DOA10介导的内质网蛋白质数量调控机制研究，直接费用：50.00万元，项目起止年月：2024年01月至2027年12月，有关项目的评审意见及修改意见附后。

请您尽快登录科学基金网络信息系统（<https://grants.nsfc.gov.cn>），**认真阅读《国家自然科学基金资助项目计划书填报说明》并按要求填写《国家自然科学基金资助项目计划书》（以下简称计划书）**。对于有修改意见的项目，请您按修改意见及时调整计划书相关内容；如您对修改意见有异议，须在电子版计划书报送截止日期前向相关科学处提出。

请您将电子版计划书通过科学基金网络信息系统（<https://grants.nsfc.gov.cn>）提交，由依托单位审核后提交至自然科学基金委。自然科学基金委审核未通过者，将退回的电子版计划书修改后再行提交；审核通过者，打印纸质版计划书（一式两份，双面打印）并在项目负责人承诺栏签字，由依托单位科研、财务管理等部门审核、签章并在承诺栏加盖依托单位公章，且将申请书纸质签字盖章页订在其中一份计划书之后，一并报送至自然科学基金委项目材料接收工作组。纸质版计划书应当保证与审核通过的电子版计划书内容一致。**自然科学基金委将对申请书纸质签字盖章页进行审核，对存在问题的，允许依托单位进行一次修改或补齐。**

向自然科学基金委提交电子版计划书、报送纸质版计划书并补交申请书纸质签字盖章页截止时间节点如下：

1. **2023年9月7日16点**：提交电子版计划书的截止时间；
2. **2023年9月14日16点**：提交修改后电子版计划书的截止时间；
3. **2023年9月21日**：报送纸质版计划书（一式两份，其中一份包含申请书纸质签字盖章页）的截止时间。
4. **2023年10月7日**：报送修改后的申请书纸质签字盖章页的截止时间。

请按照以上规定及时提交电子版计划书，并报送纸质版计划书和申请书纸质签字盖章页，逾期不报计划书或申请书纸质签字盖章页且未说明理由的，视为自动放弃接受资助；未按要求修改或逾期提交申请书纸质签字盖章页者，将视情况给予暂缓拨付经费等处理。

附件：项目评审意见及修改意见表

国家自然科学基金委员会
2023年8月24日

附件：项目评审意见及修改意见表

项目批准号	32370269	项目负责人	刘林川	申请代码1	C0204
项目名称	植物DOA10介导的内质网蛋白质数量调控机制研究				
资助类别	面上项目		亚类说明		
附注说明					
依托单位	华南农业大学				
直接费用	50.00 万元		起止年月	2024年01月 至 2027年12月	

通讯评审意见：

<1>具体评价意见：

一、该申请项目的研究思想或方案是否具有新颖性和独特性？请详细阐述判断理由。

该项目主要研究内质网相关蛋白降解系统（ERAD）调控植物生长发育和逆境响应的相关机理。为了充分理解ERAD的降解机制，那么就需要了解哪些蛋白是受ERAD降解的。申请人利用定量蛋白质组学和泛素化组学筛选受E3泛素连接酶DOA10介导ERAD途径降解的天然底物蛋白。发现DOA10可能与三萜类物质合成相关蛋白SQE1和SQE3互作。项目将以此互作重点解析ERAD介导天然蛋白降解的机制。项目具有一定的原创性，特别是ERAD介导的蛋白质降解具有相对重要的意义。

二、请评述申请项目所关注问题的科学价值以及对相关前沿领域的潜在贡献。

ERAD最初被认为负责降解错误折叠的蛋白质，但是后来发现ERAD也降解天然底物蛋白，但是有关方面的研究还不够深入。因此申请人重点解析ERAD的天然底物蛋白，发现SQE1和SQE3可能为ERAD的潜在底物，可能影响三萜类化合物合成。本研究将进一步丰富ERAD介导天然蛋白降解的理论知识。

三、请评述申请人的研究基础与研究方案的可行性。

申请人具有较好的研究基础，在高水平期刊上发表一定数量的论文，具有蛋白泛素化、蛋白质组学相关知识背景。

此外，建议申请人对figure legends详细描述。

四、其他建议

<2>具体评价意见：

一、该申请项目的研究思想或方案是否具有新颖性和独特性？请详细阐述判断理由。

内质网只蛋白折叠和分泌及组装的重要细胞器，在植物生长和应激响应中起着重要调控作用。该项目拟利用定量蛋白质组学和泛素化组学角度挖掘分析受内质网调控的天然底物分子，该研究对于拓展植物内质网蛋白的认识及为植物次生代谢产物合成和物质转运的调控提供新的策略。

二、请评述申请项目所关注问题的科学价值以及对相关前沿领域的潜在贡献。

该项目提出的关键科学问题有点大和泛，难以通过一个国家基金去完成，建议聚焦于某个确实参与了内质网底物蛋白合成的基因，研究其分子机制和生物学功能。

三、请评述申请人的研究基础与研究方案的可行性。

该项目申报人及其课题组在内质网蛋白研究方面具有一定的研究基础，但是该项目拟解决的科学问题太大，且归纳总结的该项目的特色与创新之处没有厘清，研究目标不够明确。

四、其他建议

<3>具体评价意见：

一、该申请项目的研究思想或方案是否具有新颖性和独特性？请详细阐述判断理由。

该申请项目聚焦植物蛋白降解系统，采用定量蛋白组学的方法筛选和挖掘受DOA10介导的ERAD

途径降解的天然底物，研究思想独特，具有一定创新性。申请人通过新的手段和方法寻找受ERAD调控的植物天然底物分子，有望丰富植物中内质网蛋白质数量调控网络。

二、请评述申请项目所关注问题的科学价值以及对相关前沿领域的潜在贡献。

三、请评述申请人的研究基础与研究方案的可行性。

蛋白质在细胞中的降解机制和降解途径是生物学的研究热点之一，该项目围绕此核心问题，研究方案设计合理，可行性强。该项目前期研究基础扎实，研究目标明确，团队具备完成该项目的条件，且申请人前期发表过高水平科研论文。综上所述，该项目有望达到预期成果。

四、其他建议

修改意见：

生命科学部

2023年8月24日



项目批准号	32370269
申请代码	C0204
归口管理部门	
依托单位代码	51064208A0499-0932



323702691003728

国家自然科学基金 资助项目计划书 (预算制项目)

资助类别：面上项目

亚类说明：

附注说明：

项目名称：植物DOA10介导的内质网蛋白质数量调控机制研究

直接费用：50万元 执行年限：2024.01-2027.12

负责人：刘林川

通讯地址：广东省广州市天河区五山路483号华南农业大学科技楼1002房间

邮政编码：510642 电话：020-85280256

电子邮件：liulinchuan@163.com

依托单位：华南农业大学

联系人：唐家林 电话：020-85280070

填表日期：2023年08月30日

国家自然科学基金委员会制

Version: 1.003.728



国家自然科学基金资助项目计划书填报说明 （预算制项目）

- 一、项目负责人收到《国家自然科学基金资助项目批准通知》（以下简称《批准通知》）后，请认真阅读本填报说明，参照国家自然科学基金相关项目管理办​​法和新修订的《国家自然科学基金资助项目资金管理办法》（以下简称《资金管理办法》，请查阅国家自然科学基金委员会官方网站首页“政策法规”栏目），按《批准通知》的要求认真填写和提交《国家自然科学基金资助项目计划书》（以下简称《计划书》）。
- 二、填写《计划书》时要科学严谨、实事求是、表述清晰、准确。《计划书》经国家自然科学基金委员会相关项目管理部门审核批准后，将作为项目研究计划执行、检查和验收的依据。
- 三、《计划书》各部分填写要求如下：
 - （一）简表：由系统自动生成。
 - （二）摘要及关键词：各类获资助项目都应当填写中、英文摘要及关键词。
 - （三）项目组主要成员：计划书中列出姓名的项目组主要成员由系统自动生成，与申请书原成员保持一致，不可随意调整。如果《批准通知》所附“项目评审意见及修改意见表”中“修改意见”栏目有调整项目组成员相关要求的，待项目开始执行后，按照项目成员变更程序另行办理。
 - （四）资金预算表：根据批准的项目资助额度，按规定调整项目预算，并按照《国家自然科学基金项目计划书预算表编制说明》填报资金预算表和预算说明书。
 - （五）正文：
 1. 面上项目、地区科学基金项目：如果《批准通知》所附“项目评审意见及修改意见表”中“修改意见”栏目没有修改要求的，只需选择“研究内容和研究目标按照申请书执行”即可；如果《批准通知》中上述栏目明确要求调整研究期限或研究内容等的，须选择“根据研究方案修改意见更改”并填报相关修改内容。
 2. 重点项目、重点国际（地区）合作研究项目、重大项目、国家重大科研仪器研制项目、原创探索计划项目：须选择“根据研究方案修改意见更改”，根据《批准通知》的要求填写研究（研制）内容，不得自行降低、更改研究目标（或仪器研制的技术性能与主要技术指标、验收技术指标等）或缩减研究（研制）内容。此外，还要突出以下几点：
 - （1）研究的难点和在实施过程中可能遇到的问题（或仪器研制风险），拟采用的研究（研制）方案和技术路线；
 - （2）项目主要参与者分工，合作研究单位（如有）之间的关系与分工，重大项目还需说明课题之间的关联；
 - （3）详细的年度研究（研制）计划。
 3. 创新研究群体项目：须选择“根据研究方案修改意见更改”，按下列提纲撰写：
 - （1）研究方向；



- (2) 结合国内外研究现状，说明研究工作的学术思想和科学意义（限两个页面）；
 - (3) 研究内容、研究方案及预期目标（限两个页面）；
 - (4) 年度研究计划；
 - (5) 研究队伍的组成情况。
4. 基础科学中心项目：须选择“根据研究方案修改意见更改”，根据《批准通知》的要求和现场考察专家组的意见和建议，进一步完善并细化研究计划，按下列提纲撰写：
 - (1) 五年拟开展的研究工作（包括主要研究方向、关键科学问题与研究内容）；
 - (2) 研究方案（包括骨干成员之间的分工及合作方式、学科交叉融合研究计划等）；
 - (3) 年度研究计划；
 - (4) 五年预期目标和可能取得的重大突破等；
 - (5) 研究队伍的组成情况。
5. 对于其他类型项目，参照面上项目的方式进行选择和填写。



简表

项目负责人信息	姓 名	刘林川	性 别	男	出生年月	1983年01月	民 族	汉族
	学 位	博士			职称	教授		
	是否在站博士后	否			电子邮件	liulinchuan@163.com		
	电 话	020-85280256			个人网页			
	工 作 单 位	华南农业大学						
	所 在 院 系 所	林学与风景园林学院						
依托单位信息	名 称	华南农业大学					代码	51064208A0499
	联 系 人	唐家林			电子邮件	kyc.jhk@scau.edu.cn		
	电 话	020-85280070			网站地址	http://kjc.scau.edu.cn/		
合作单位信息	单 位 名 称							
项目基本信息	项 目 名 称	植物D0A10介导的内质网蛋白质数量调控机制研究						
	资 助 类 别	面上项目				亚 类 说 明		
	附 注 说 明							
	申 请 代 码	C0204:水分和营养物质的运输与代谢				C0708:细胞代谢、应激及稳态调控		
	基 地 类 别	亚热带农业生物资源保护与利用国家重点实验室						
	执 行 年 限	2024.01-2027.12						
	直 接 费 用	50万元						



项目摘要

中文摘要:

内质网是膜蛋白和分泌蛋白折叠和组装的场所，真核生物在长期进化中形成了保守的内质网相关蛋白质降解系统(ERAD)，能够对内质网中的错误折叠蛋白进行降解。近年来，一些证据表明细胞内的一些正常状态的蛋白也可以通过ERAD途径降解，为细胞提供了一种能够在数量上快速调节内质网驻留蛋白和分泌蛋白水平的调控方式。植物内质网是三萜类化合物合成的主要场所，也是植物质膜蛋白进入分泌途径的起点。在本研究中，我们将利用定量蛋白质组学的方法筛选和挖掘拟南芥中受DOA10介导ERAD途径降解的天然底物分子，并通过遗传学和生物化学手段对目前已发现的参与三萜类物质合成的角鲨烯环氧酶家族蛋白成员和部分质膜转运蛋白进行鉴定和功能研究，探索他们在细胞中的调控机制。该研究为深入理解植物细胞中代谢途径的适应性与蛋白质的内稳态调节提供理论依据和参考。

Abstract:

The endoplasmic reticulum (ER) is an essential organelle involved in the folding and assembly of membrane and secretory proteins, and eukaryotes have evolved a conserved endoplasmic reticulum-associated protein degradation (ERAD) system for eliminating misfolded proteins in the ER. Recent studies have demonstrated an increasing number of native enzymes and transporters that are also targeted for ERAD, which provides a way to rapidly and quantitatively downregulate the levels of proteins that mature or reside in the ER. The plant ER is the main site for the synthesis of triterpenoids and the entry for secretory of plant plasma membrane proteins. In the present study, quantitative proteomics will be performed to seek native substrates that can be degraded by DOA10 ERAD system. Importantly, we will explore the regulatory mechanisms of squalene epoxidase (SQE) family proteins and some transporter proteins degraded in the ER by genetic and biochemical approaches. This study can provide a framework to understand metabolic adaptation and protein homeostasis in plant cells.

关键词(用分号分开): 拟南芥; 内质网; 泛素化; 蛋白质降解; 内稳态

Keywords(用分号分开): Arabidopsis; ER; Ubiquitination; Protein degradation; Homeostasis



项目组主要成员

编号	姓名	出生年月	性别	职称	学位	单位名称	电话	证件号码	项目分工	每年工作时间（月）
1	刘林川	1983.01	男	教授	博士	华南农业大学	020-85280256	21100219830126013X	项目负责人	10
2	毛娟	1984.09	女	副研究员	博士	华南农业大学	020-85280256	21052219840918322X	生化与蛋白质组分析	10
总人数		高级		中级		初级		博士后	博士生	硕士生
7		2		0		0		0	2	3



国家自然科学基金预算制项目预算表

项目批准号：32370269

项目负责人：刘林川

金额单位：万元

序号	科目名称	金额
1	一、基金资助项目直接费用合计	50.0000
2	1、设备费	0.0000
3	其中：设备购置费	0.0000
4	2、业务费	37.5000
5	3、劳务费	12.5000
6	二、其他来源资金	0.0000
7	三、合计	50.0000

注：请按照项目研究实际需要合理填写各科目预算金额。



预算说明书

（请按照《国家自然科学基金项目申请书预算表编制说明》等的有关要求，按照政策相符性、目标相关性和经济合理性原则，实事求是编制项目预算。填报时，直接费用应按设备费、业务费、劳务费三个类别填报，每个类别结合科研任务按支出用途进行说明。对单价 ≥ 50 万元的设备详细说明，对单价 < 50 万元的设备费用分类说明，**对合作研究单位资质及资金外拨情况、自筹资金进行必要说明。**）

一.设备费 0.00万元

无仪器设备购置的预算。

二.业务费 37.50万元

1. 材料费：预算 18.00 万元。

- (1)基因克隆和遗传分析，预算经费 5.90 万元；
- (2)基因表达分析，预算经费 1.60 万元；
- (3)蛋白表达纯化及功能检测，预算经费 5.40 万元；
- (4)植物组织培养试剂，预算经费 1.70 万元；
- (5)常用低值易耗品，预算经费 3.40 万元；

2. 测试化验加工费：预算 12.00 万元。

- (1)引物合成，预算经费 1.20 万元；
- (2) DNA 测序，预算经费 1.50 万元；
- (3)蛋白质质谱鉴定和分析，预算经费 4.50 万元；
- (4)抗体制备，预算经费 2.80 万元；
- (5)转录组测序，预算经费 2.00 万元；

3. 差旅/会议/国际合作与交流费：预算 4.00 万元。

- (1)参加国内学术会议 5 人次，预算经费 1.50 万元；
- (2)参加国际学术会议 2 人次，预算经费 2.50 万元；

4. 出版/文献/信息传播/知识产权事务费：预算 3.50 万元。

三.劳务费 12.50万元

支付参加本课题的 5 名研究生助学金，预算 12.50 万元。



报告正文

研究内容和研究目标按照申请书执行。



国家自然科学基金项目负责人、依托单位承诺书

国家自然科学基金项目负责人承诺书

本人郑重承诺：我接受国家自然科学基金的资助，严格遵守中共中央办公厅、国务院办公厅《关于进一步加强科研诚信建设的若干意见》《关于进一步弘扬科学家精神加强作风和学风建设的意见》《关于加强科技伦理治理的意见》等规定，及国家自然科学基金委员会关于资助项目管理、项目资金管理等各项规章，在《计划书》填写及项目执行过程中：

（一）按照《批准通知》《国家自然科学基金资助项目计划书填报说明》的要求填写《计划书》，未自行降低、更改目标任务或约定要求，或缩减研究（研制）内容；

（二）树立“红线”意识，严格履行科研合同义务，按照《计划书》负责实施本项目（批准号：32370269），切实保证研究工作时间，按时报送有关材料，及时报告重大情况变动，不违规将科研任务转包、分包他人，不以项目实施周期外或不相关成果充抵交差；

（三）遵守科研诚信、科技伦理规范和学术道德，认真开展研究工作，对资助项目发表的论著和取得的科研成果按规定进行标注，不在非本项目资助的成果或其他无关成果上标注本项目批准号，反对无实质学术贡献者“挂名”，不在成果署名、知识产权归属等方面侵占他人合法权益，并如实报告本人及项目组成员发生的违背科研诚信要求的任何行为；

（四）尊重科研规律，弘扬科学家精神，严谨求实，追求卓越，反对浮夸浮躁、投机取巧，不人为夸大学术或技术价值，不传播未经科学验证的现象和观点；

（五）将项目资金全部用于与本项目研究工作相关的支出，并结合科研活动需要，科学合理安排项目资金支出进度；

（六）做好项目组成员的教育和管理，确保遵守以上相关要求。

如违背上述承诺，本人愿接受国家自然科学基金委员会和相关部门做出的各项处理决定。

项目负责人（签字）：

年 月 日

依托单位科研管理部门：

负责人（签章）：

年 月 日

依托单位财务管理部门：

负责人（签章）：

年 月 日

国家自然科学基金项目依托单位承诺书

我单位同意承担上述国家自然科学基金项目，将保证项目负责人及其研究队伍的稳定和研究项目实施所需的条件，严格遵守国家自然科学基金委员会有关资助项目管理、项目资金管理、科研诚信管理和科技伦理管理等各项规定，并督促实施。

依托单位（公章）

年 月 日

受理编号: c22140500002556

项目编号: 2022A1515010803

文件编号: 粤基金字(2022)3号

广东省基础与应用基础研究基金项目 任务书

项目名称: 油菜素甾醇信号途径调控黄梁木生长发育的分子机制

项目类别: 广东省自然科学基金-面上项目

项目起止时间: 2022-01-01 至 2024-12-31

管理单位(甲方): 广东省基础与应用基础研究基金委员会

依托单位(乙方): 华南农业大学

通讯地址: 广东省广州市天河区五山路483号

邮政编码: 510642

单位电话: 020-85283435

项目负责人: 刘林川

联系电话: 13301685636



(广东科技微信公众号)



(查看任务书信息)



(受理纸质材料二维码)

广东省基础与应用基础研究
基金委员会
二〇二〇年制

填写说明

一、项目任务书内容原则上要求与申报书相关内容保持一致，不得无故修改。

二、项目承担单位通过广东省科技业务管理阳光政务平台下载项目任务书，按要求完成签名盖章后提交至省科技厅受理窗口。

三、签名盖章说明。请分别在单位工作分工及经费分配情况页、人员信息页、签约各方页等地方按要求签字或盖章，签章不合规或错漏将不予受理。其中，人员信息页要求所有参与人员本人亲笔签名，代签或印章无效，漏签将不予受理。

四、本任务书自签字并加盖公章之日起生效，各方均应负本任务书的法律责任，不应受机构、人事变动影响。

2022A1515010803

一、主要研究内容和要达到的目标

本项目主要研究内容和要达到的目标包括以下两个部分：一是建立并优化黄梁木遗传转化及再生体系，获得黄梁木转基因植株。建立发根农杆菌介导的黄梁木遗传转化及再生体系，克服传统组培过程周期长，抗生素筛选压力选择困难，转化效率低等问题，以实现快速鉴定；同时优化根癌农杆菌介导的黄梁木子叶节遗传转化体系，提高黄梁木遗传转化效率。通过转基因体系的建立，可缩短林木育种周期、加快新品种培育，为林木功能基因研究提供技术保障。为实现林木基因挖掘与功能验证提供科学便捷、稳定高效的遗传研究手段。二是揭示植物激素油菜素甾醇调控黄梁木木质部生长发育的分子机制。目前有许多证据表明BR的合成和信号传导可以调控植物木质部的形成与分化，但在木本植物中，其具体的分子机制还不明确，特别是该性状与木材的形成息息相关，具有重要的研究意义。分别对黄梁木BR信号途径中最为关键的两个蛋白激酶基因NcBRI1和NcBIN2进行克隆和功能鉴定，结合遗传学和转录组测序等手段，研究BR信号在黄梁木中生理生化功能，帮助我们更好地理解BR在木本植物中的调控作用。

二、项目预期获得的研究成果及形式

论文及专著情况	国家统计源刊物以上刊物 发表论文（篇）		2		科技报告（篇）		1	
	其中被SCI/EI/ISTP收录 论文数（篇）		2		培养人才（人）		3	
	专著（册）		0		引进人才（人）		0	
专利情况(项)	发明专利		实用新型专利		外观设计专利		国外专利	
	申请	授权	申请	授权	申请	授权	申请	授权
	0	0	0	0	0	0	0	0

三、项目进度和阶段目标

(一) 项目起止时间： 2022-01-01 至 2024-12-31		
(二) 项目实施进度及阶段主要目标：		
开始日期	结束日期	主要工作内容
2022-01-01	2022-12-31	(1). 利用拟南芥遗传突变体验证NcBRI1和NcBIN2 (NcBIN2-1, NcBIN2-2)的功能; (2). 构建适用于黄梁木毛状根遗传转化和快速鉴定的载体; (3). 构建目的基因与WUS和DRN共表达载体, 优化黄梁木转基因体系。
2023-01-01	2023-12-31	(1). 对拟南芥转基因植株进行生理生化分析, 包括细胞、组织结构和信号响应; (2). 对黄梁木转基因毛状根(过量表达和基因编辑)和转基因植株进行表型观察和组织结构分析; (3). 对转基因黄梁木进行转录组测序分析, 获得可能受BR信号调控的参与黄梁木维管组织发育和木质部形成的下游调控基因。
2024-01-01	2024-12-31	(1). 对受BR调控的相关基因进行验证; (2). 总结BR信号调控黄梁木木质部生长发育的分子机制; (3). 论文的撰写和发表。

四、项目总经费及省基金委经费预算

1. 省基金委经费下达总额：（大写）壹拾万圆整；（小写）10万元；					
2. 省基金委经费年度下达计划：					
年度	2022 年	年	年	年	年
经费(万元)	10.00				
3. 总经费及省基金委经费开支预算计划：					
经费筹集情况：					(单位：万元)
省基金委经费	自筹资金				合计
	自有资金	贷款	地方政府投入	其它	
10.00	0.00	0.00	0.00	0.00	10.00
政府部门、境外资金及其他资金投入情况说明：	无				
与本项目相关的其他经费来源			(单位：万元)		
其他计划资助经费：			0.00		
单位配套经费：			0.00		
其他经费资助：			0.00		
其他经费来源合计：					

五、人员信息

项目负责人								
姓名	证件号码	年龄	性别	职称	学历	在项目中承担的任务	所在单位	签名
刘林川	21100219830126013X	39	男	教授	博士研究生	项目负责人	华南农业大学	刘林川

项目组主要成员								
姓名	证件号码	年龄	性别	职称	学历	在项目中承担的任务	所在单位	签名
陈凯	430421199811230219	24	男	未取得	本科	载体构建与表型分析	华南农业大学	陈凯
刘文杰	41282819931029573X	29	男	未取得	本科	黄梁木转基因体系建立与优化	华南农业大学	刘文杰
段志豪	361127199603044213	26	男	未取得	本科	细胞与生化实验	华南农业大学	段志豪

六、工作分工及经费分配

承担/参与单位名称 (盖章)	工作分工	总经费分摊 (万元)	省基金委经费分配 (万元)
华南农业大学	本项目由依托单位独立完成。	10.00	10.00
	合计	10.00	10.00

七、任务书条款

第一条 甲方与乙方根据《中华人民共和国民法典》及国家有关法规和规定，按照《广东省科学技术厅关于广东省基础与应用基础研究基金（省自然科学基金、联合基金等）项目管理的实施细则（试行）》《广东省省级科技计划项目验收结题工作规程（试行）》等规定，为顺利完成（2022）年油菜素甾醇信号途径调控黄梁木生长发育的分子机制专项项目（文件编号：粤基金字（2022）3号）经协商一致，特订立本任务书，作为甲乙双方在项目实施管理过程中共同遵守的依据。

第二条 甲方的权利义务：

1. 按任务书规定进行经费核拨的有关工作协调。
2. 根据甲方需要，在不影响乙方工作的前提下，定期或不定期对乙方项目的实施情况和经费使用情况进行检查或抽查。
3. 根据《广东省科研诚信管理办法(试行)》等规定对乙方进行科技计划信用管理。

第三条 乙方的权利义务：

1. 确保落实自筹经费及有关保障条件。
2. 按任务书规定，对甲方核拨的经费实行专款专用，单独列账，并随时配合甲方进行监督检查。
3. 经费使用按照广东省级财政科研项目经费使用等有关规定进行管理。
4. 项目依托单位应制定经费使用“负面清单+包干制”内部管理制度并报甲方备案。
5. 使用财政资金采购设备、原材料等，按照《广东省实施〈中华人民共和国招标投标法〉办法》有关规定，符合招标条件的须进行招标。
6. 项目任务书任务完成后，或任务书规定的任务、指标及经费投入等提前完成的，乙方可提出验收结题申请，并按甲方要求做好项目验收结题工作。
7. 若项目发生需要终止结题的情况，乙方须提出终止结题申请，并按甲方要求做好项目终止结题工作。
8. 在每年规定时间内向甲方如实提交上年度工作情况报告，报告内容包含上年度项目进展情况、经费决算和取得的成果等。
9. 按照国家和省有关规定，提交科技报告及其他材料。
10. 利用甲方的经费获得的研究成果，项目负责人和参与者应当注明获得“广东省基础与应用基础研究基金（英文：Guangdong Basic and Applied Basic Research Foundation）（项目编号）”资助或作有关说明。
11. 乙方要恪守科学道德准则，遵守科研活动规范，践行科研诚信要求，不得抄袭、剽窃他人科研成果或者伪造、篡改研究数据、研究结论；不得购买、代写、代投论文，虚构同行评议专家及评议意见；不得违反论文署名规范，擅自标注或虚假标注获得科技计划（专项、基金等）等资助；不得弄虚作假，骗取科技计划（专项、基金等）项目、科研经费以及奖励、荣誉等；不得有其他违背科研诚信要求的行为。
12. 确保本项目开展的研究工作符合我国科技伦理管理相关规定。

第四条 在履行本任务书的过程中，如出现广东省相关政策法规重大改变等不可抗力情况，甲方有权对所核拨经费的数量和时间进行相应调整。

第五条 在履行本任务书的过程中，当事人一方发现可能导致项目整体或部分失败的情形时，应及时通知另一方，并采取适当措施减少损失，没有及时通知并采取适当措施，致使损失扩大的，应当就扩大的损失承担责任。

第六条 本项目技术成果的归属、转让和实施技术成果所产生的经济利益的分享，除双方另有约定外，按国家和广东省有关法规执行。

第七条 根据项目具体情况，经双方另行协商订立的附加条款，作为本任务书正式内容的一部分，与本任务书具有同等效力。

第八条 本任务书一式三份，各份具有同等效力。甲、乙方及项目负责人各执一份，三方签字、盖章后即生效，有效期至项目结题后一年内。各方均应负任务书的法律责任，不应受机构、人事变动的影响。

第九条 乙方必须接受甲方聘请的本项目任务书监理单位的监督和管理。监理单位按照甲方赋予的权利对本项目任务书的履行进行审核、进度调查，对项目任务书变更、经费使用情况进行监督管理及组织项目验收。

说明：1. 本任务书中，凡是当事人约定无需填写的内容，应在空白处划（/）。

2. 委托代理人签订本任务书的，应出具合法、有效的委托书。

八、本任务书签约各方

管理单位（甲方）：

广东省基础与应用基础研究基金委员会（盖章）

法定代表人（或法人代理）：

曾路

（签章）

2022 年 04 月 21 日

依托单位（乙方）：华南农业大学

（盖章）

法定代表人（或法人代理）：

刘雅红

（签章）

联系人（项目主管）姓名：

倪慧群

（签章）

Email: kjcgxk@scau.edu.cn

电话：020-85283435 / 15920301530

开户单位名称：华南农业大学

开户银行名称：广东广州工行五山支行

开户银行帐号：3602002609000310520

2022年04月28日

年 月 日

联系人（项目负责人）姓名：刘林川

（签名）

Email: liulinchuan@163.com

电话：13301685636

2022 年 4 月 26 日



科研动态

我的办公

我的项目

我的经费

我的成果

我的学术交流

我的考核

我的主页

常用下载

项目立项

项目申报 (1)

所有项目

总数:4项 (表中经费单位: 万元)

导出

打印

职称评定

主持的项目

参与的项目

博硕导评定

主持的项目

参与的项目

项目性质

纵向(8项)

项目分类

国家自然科学基金项目(4项)

广东省林业科技创新专项资金

项目(1项)

广州市科技计划项目(1项)

教育厅其它项目(1项)

面上项目(1项)

参与形式

主持(4项)

参与(4项)

☐ 全选

序号 项目名称

评审等级 项目来源

合同经费/
实到经费

立项时间

开始时间

结题时间

负责人

本人排名

课题组
总人数

是否结题

☐

1

植物内质网介导的蛋白质
降解机制研究

T1

国家自然科学基金基
金委员会

278.0

2017-08-15

2018-01-01

2022-12-31

李建明

2

3

是

☐

2

与麻楝蛀斑螟啃食密切相
关的红椿单萜类物质合成
关键酶基因的功能研究

C

广东省教育厅

15.0

2019-11-30

2020-01-01

2021-12-31

李培

2

8

是

☐

3

黄梁木优良种源/家系功能
性定向培育及产业化开发
利用(2019)

B

广东省林业局

50.0

2019-01-01

2019-01-01

2021-01-31

彭昌操

4

5

否

☐

4

黄梁木速生等关键机理研
究

A

广州市科技局

200.0

2019-04-01

2019-04-01

2022-03-31

吴蔼民

10

20

否



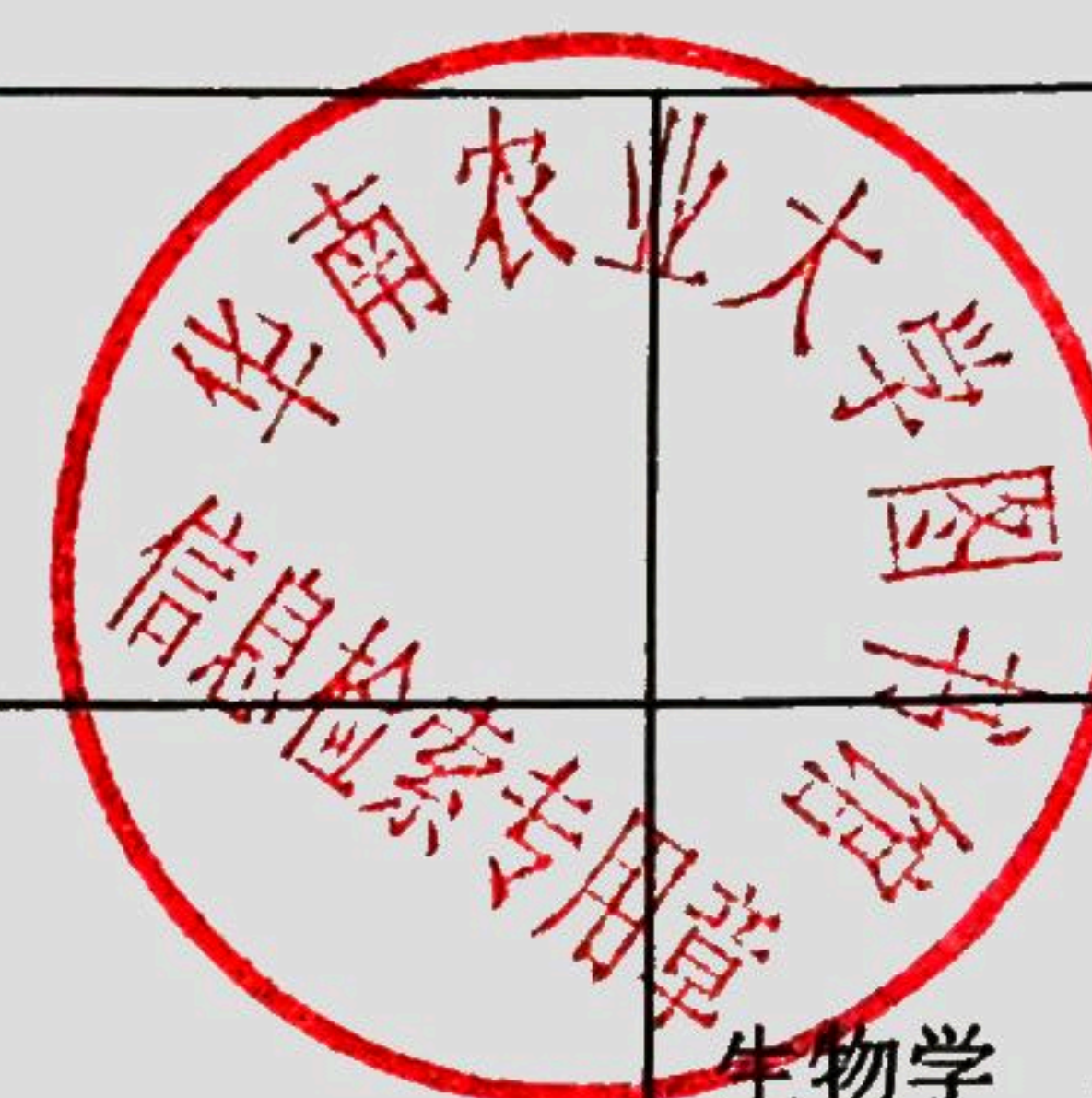
检索证明

根据委托人提供的论文材料，委托人华南农业大学林学与风景园林学院 刘林川 8 篇论文收录情况如下表。

序号	论文名称	发表刊物及发表的年月卷期/页码等	作者排名	论文等级	作者文中单位	收录情况	影响因子	中科院大分类分区
1	A Temperature-Sensitive Misfolded bril-301 Receptor Requires Its Kinase Activity to Promote Growth	PLANT PHYSIOLOGY 出版年：2018 出版日期：DEC 卷期：178 4 页码：1704- 1719 文献类型：Article	通讯作者	A 类	华南农业大学	SCI	IF2-year=6.305 IF5-year=7.024 (2018)	生物 2 区 Top 期刊：是 (2018)
2	PAWH1 and PAWH2 are plant-specific components of an Arabidopsis endoplasmic reticulum-associated degradation complex	NATURE COMMUNICATIONS 出版年：2019 出版日期：AUG 2 卷期：10 页码：- 文献号：3492 文献类型：Article	共同通讯 作者	T2 类	华南农业大学	SCI	IF2-year=12.121 IF5-year=13.611 (2019)	综合性期刊 1 区 Top 期刊：是 (2019)
3	Communications Between the Endoplasmic Reticulum and Other Organelles During Abiotic Stress Response in Plants	FRONTIERS IN PLANT SCIENCE 出版年：2019 出版日期：JUN 12 卷期：10 页码：- 文献号：749	第一作者	A 类	华南农业大学	SCI	IF2-year=4.402 IF5-year=5.207 (2019)	生物学 2 区 Top 期刊：否 (2019)



		文献类型: Review						
4	A Predominant Role of AtEDEMI in Catalyzing a Rate-Limiting Demannosylation Step of an Arabidopsis Endoplasmic Reticulum-Associated Degradation Process	FRONTIERS IN PLANT SCIENCE 出版年: 2022 出版日期: JUL 7 卷期: 13 页码: - 文献号: 952246 文献类型: Article	共同通讯作者	A类	华南农业大学	SCI	IF2-year=5.6 IF5-year=6.8 (2022)	生物学 2区 Top 期刊: 是 (2022)
5	Mechanisms of Endoplasmic Reticulum Protein Homeostasis in Plants	INTERNATIONAL JOURNAL OF MOLECULAR SCIENCES 出版年: 2023 出版日期: DEC 卷期: 24 24 页码: - 文献号: 17599 文献类型: Review	共同通讯作者(倒数第一)	A类	华南农业大学	SCI	IF2-year=4.9 IF5-year=5.6 (2023)	生物学 2区 Top 期刊: 否 (2023)
6	Post-translational Regulation of BRI1-EMS Suppressor 1 and Brassinazole-Resistant 1	PLANT AND CELL PHYSIOLOGY 出版年: 2024 出版日期: JUL 10 卷期: 65 10 页码: 1544-1551 文献类型: Article	共同通讯作者	A类	华南农业大学	SCI	IF2-year=4.0 IF5-year=4.7 (2024)	生物学 2区 Top 期刊: 否 (2025)



7	Interaction of the Transcription Factors BES1/BZR1 in Plant Growth and Stress Response	INTERNATIONAL JOURNAL OF MOLECULAR SCIENCES 出版年: 2024 出版日期: JUL 卷期: 25 13 页码: - 文献号: 6836 文献类型: Review	共同通讯作者	B类	华南农业大学	SCI	IF2-year=4.9 IF5-year=5.7 (2024)	生物学 3区 Top 期刊: 否 (2025)
8	植物激素转运研究进展	植物生理学报 出版年: 2022 卷期: 页码: - 文献号: 文献类型:	通讯作者	C类	华南农业大学	北大核心	无	无

说明: 论文等级和中科院大类分区按《华南农业大学学术论文评价方案(试行)》划分。

报告免责声明: 如未盖章, 报告无效



检索证明

根据委托人提供的论文材料，委托人华南农业大学林学与风景园林学院 刘林川 2 篇论文收录情况如下表。

序号	论文名称	发表刊物及发表的年月卷期/页码等	作者排名	论文等级	作者文中单位	收录情况	影响因子	中科院大类分区
1	NcBRI1 positively regulate vascular development and promote biomass production in Neolamarckia cadamba	PLANT SCIENCE 出版年：2025 出版日期：MAR 卷期：352 页码：- 文献号：112352 文献类型：Article	通讯作者	A 类	华南农业大学	SCI	IF2-year=4.1 IF5-year=5.1 (2024)	生物学 2 区 Top 期刊：否 (2025)
2	利用拟南芥生长素转运突变体开展细胞生物学教学探索与实践	生物学杂志 出版年：2024 卷期： 页码：- 文献号： 文献类型：	第一作者	C 类	华南农业大学	北大核心, CNKI	无	无

说明：论文等级和中科院大类分区按《华南农业大学学术论文评价方案（试行）》划分。

报告免责声明:如未盖章,报告无效



2025-07-14

Plant Physiology

December 2008 • Volume 138 • Number 12 • www.plantphysiology.org

第 87 页

On the Cover: Scanning Electron Micrograph of the tip of a young maize tassel, showing several axillary meristems developing from an apical inflorescence meristem. Liu et al. show that the transcriptional corepressor REL2 is involved in the initiation and maintenance of these meristems. Image credit: Andrea Gallavotti.

Note: The article affiliated with this image will be appearing in the January 2019 issue of Plant Physiology, Volume 179 Issue 1.

ON THE INSIDE

Peter V. Minorsky 1426

NEWS AND VIEWS

Discovery of Mitochondrial Endonucleases. Masanori Izumi 1428

Alternative Splice Variant Sheds Light on Temperature Acclimation in Algae. Nathaniel Butler 1430

Spot the Difference: Distinct Cargo-Specific Functionality of Two Closely Related SNAREs. Magdalena M. Julkowska 1432

Highlighting the Fast Signals that Establish Remote Metabolite Profiles. Amna Mhamdi and Scott Hayes 1434

BREAKTHROUGH TECHNOLOGIES

^[OPEN]MAPINS, a Highly Efficient Detection Method That Identifies Insertional Mutations and Complex DNA Rearrangements. Huawen Lin, Paul F. Cliften, and Susan K. Dutcher

A fast and efficient whole-genome sequencing method identifies insertional mutations and reveals complex DNA rearrangements accompanied insertional mutagenesis in *Chlamydomonas reinhardtii*. 1436

Micro Imaging Displays the Sucrose Landscape within and along Its Allocation Pathways. André Guendel, Hardy Rolletschek, Steffen Wagner, Aleksandra Muszynska, and Ljudmilla Borisjuk

A procedure for the quantitative mapping of sucrose in plant tissue with spatial resolution sufficient to measure sucrose in individual phloem bundles and across transport boundaries. 1448

RESEARCH REPORTS

^[OPEN]Local and Systemic Metabolic Responses during Light-Induced Rapid Systemic Signaling. Feroza K. Choudhury, Amith R. Devireddy, Rajeev K. Azad, Vladimir Shulaev, and Ron Mittler

Rapid systemic signaling is accompanied by coordinated metabolic changes in local, transport, and systemic tissues. 1461

^[OPEN]NRT1.1-Related NH_4^+ Toxicity Is Associated with a Disturbed Balance between NH_4^+ Uptake and Assimilation. Shaofen Jian, Qiong Liao, Haixing Song, Qiang Liu, Joe Eugene Lepo, Chunyun Guan, Jianhua Zhang, Abdelbagi M. Ismail, and Zhenhua Zhang

Nitrate transporter NRT1.1 enhances NH_4^+ accumulation, disturbs NH_4^+ metabolism, and aggravates NH_4^+ toxicity in *Arabidopsis* grown in a high concentration of NH_4^+ as the sole N source. 1473

RESEARCH ARTICLES

BIOCHEMISTRY AND METABOLISM

A Musashi Splice Variant and Its Interaction Partners Influence Temperature Acclimation in *Chlamydomonas*. Wenshuang Li, David Carrasco Flores, Juliane Füssel, Jan Euteneuer, Hannes Dathe, Yong Zou, Wolfram Weisheit, Volker Wagner, Jan Petersen, and Maria Mittag

Three RNA metabolism proteins are part of an interaction network that integrates temperature information and confers acclimation to changes in ambient temperature in the green alga Chlamydomonas.

1489

[OPEN] Identification of Genes Encoding Enzymes Catalyzing the Early Steps of Carrot Polyacetylene Biosynthesis. Lucas Busta, Won Cheol Yim, Evan William LaBrant, Peng Wang, Lindsey Grimes, Kiah Malyszka, John C. Cushman, Patricia Santos, Dylan K. Kosma, and Edgar B. Cahoon

Members of a large family of fatty acid desaturase enzymes in carrot control the production of dehydrocrepenynic acid, an intermediate in the falcarin-type polyacetylene biosynthesis pathway.

1507

[OPEN] The Spermine Synthase OsSPMS1 Regulates Seed Germination, Grain Size, and Yield. Yajun Tao, Jun Wang, Jun Miao, Jie Chen, Shujun Wu, Jinyan Zhu, Dongping Zhang, Houwen Gu, Huan Cui, Shuangyue Shi, Mingyue Xu, Youli Yao, Zhiyun Gong, Zefeng Yang, Minghong Gu, Yong Zhou, and Guohua Liang

OsSPMS1, a spermine synthase that participates in polyamine and ethylene homeostasis, plays an important role in seed germination, plant architecture, and yield in rice.

1522

CELL BIOLOGY

The Mitochondrial Endonuclease M20 Participates in the Down-Regulation of Mitochondrial DNA in Pollen Cells. Fei Ma, Hui Qi, Yu-Fei Hu, Qian-Ru Jiang, Li-Guang Zhang, Peng Xue, Fu-Quan Yang, Rui Wang, Yan Ju, Hidenobu Uchida, Quan Zhang, and Sodmergen

The mitochondrial endonuclease M20 is an H-N-H/N nuclease that degrades linear and circular DNA and participates in mitochondrial DNA regulation during pollen development.

1537

CLASP Facilitates Transitions between Cortical Microtubule Array Patterns. David Thoms, Laura Vineyard, Andrew Elliott, and Sidney L. Shaw

The microtubule associated protein, CLASP, impacts polymer dynamics leading to a slowdown in microtubule array pattern transitions without altering the ability to form specific array patterns.

1551

ECOPHYSIOLOGY AND SUSTAINABILITY

ARSENATE INDUCED CHLOROSIS 1/ TRANSLOCON AT THE OUTER ENVELOPE MEMBRANE OF CHLOROPLASTS 132 Protects Chloroplasts from Arsenic Toxicity. Peitong Wang, Xi Chen, Xuan Xu, Chenni Lu, Wei Zhang, and Fang-Jie Zhao

The translocon at the outer envelope membrane of chloroplast Toc132 plays an important role in alleviating arsenic toxicity in chloroplasts.

1568

[OPEN] The Causes of Leaf Hydraulic Vulnerability and Its Influence on Gas Exchange in *Arabidopsis thaliana*. Christine Scoffoni, Caetano Albuquerque, Hervé Cochard, Thomas N. Buckley, Leila R. Fletcher, Marissa A. Caringella, Megan Bartlett, Craig R. Brodersen, Steven Jansen, Andrew J. McElrone, and Lauren Sack

Declines in leaf outside-xylem hydraulic conductance prior to turgor loss point contribute strongly to stomatal closure, and improve performance, survival and efficient water use during drought.

1584

Diurnal Variation in Nonstructural Carbohydrate Storage in Trees: Remobilization and Vertical Mixing.
Aude Tixier, Jessica Orozco, Adele Amico Roxas, J. Mason Earles, and Maciej A. Zwieniecki

NSC storage is highly dynamic at the diurnal timescale, exhibiting vertical mixing and a potential role for the xylem as a secondary pathway for sugar redistribution.

1602

GENES, DEVELOPMENT AND EVOLUTION

[OPEN]RNA Polymerase II Read-Through Promotes Expression of Neighboring Genes in SAL1-PAP-XRN Retrograde Signaling. Peter A. Crisp, Aaron B. Smith, Diep R. Ganguly, Kevin D. Murray, Steven R. Eichten, Anthony A. Millar, and Barry J. Pogson

Consequences of transcription out of bounds: a retrograde signal can trigger RNA Polymerase II read-through, upregulating the expression of downstream genes.

1614

[OPEN]Enhancer-Promoter Interaction of SELF PRUNING 5G Shapes Photoperiod Adaptation. Shuaibin Zhang, Zhicheng Jiao, Lei Liu, Ketao Wang, Deyi Zhong, Shengben Li, Tingting Zhao, Xiangyang Xu, and Xia Cui

Loss of an enhancer element in the 3' untranslated region of SP5G conferred day-length insensitivity to domesticated tomato cultivars and helped the species spread worldwide.

1631

[OPEN]Efficient Replication of the Plastid Genome Requires an Organellar Thymidine Kinase. Monique Le Ret, Susan Belcher, Stéphanie Graindorge, Clémentine Wallet, Sandrine Koechler, Mathieu Erhardt, Rosalind Williams-Carrier, Alice Barkan, and José M. Gualberto

Depletion of organellar thymidine kinase affects plastid genome replication and repair, leading to the accumulation of truncated genomes and the apparent mobilization of new replication origins.

1643

MEMBRANES, TRANSPORT AND BIOENERGETICS

K⁺ Efflux Antiporters 4, 5, and 6 Mediate pH and K⁺ Homeostasis in Endomembrane Compartments. Xiaojie Zhu, Ting Pan, Xiao Zhang, Ligang Fan, Francisco J. Quintero, Hong Zhao, Xiaomeng Su, Xiaojiao Li, Irene Villalta, Imelda Mendoza, Jinbo Shen, Liwen Jiang, Jose M. Pardo, and Quan-Sheng Qiu

Arabidopsis thaliana KEA4, KEA5, and KEA6 are endosomal K⁺ transporters that function in maintaining pH and ion homeostasis in the endomembrane network.

1657

[OPEN]SNAREs SYP121 and SYP122 Mediate the Secretion of Distinct Cargo Subsets. Sakham Waghmare, Edita Lileikyte, Rucha Karnik, Jennifer K. Goodman, Michael R. Blatt, and Alexandra M.E. Jones

Two closely related SNAREs mediate secretion of specific cargo proteins in Arabidopsis thaliana.

1679

[OPEN]Going with the Flow: Multiscale Insights into the Composite Nature of Water Transport in Roots. Valentin Couvreur, Marc Faget, Guillaume Lobet, Mathieu Javaux, François Chaumont, and Xavier Draye

A bio-physical model of the "root hydraulic anatomy" allows testing hypotheses related to radial water transport down to the cell level and proves complementary to current experimental approaches.

1689

SIGNALING AND RESPONSE

[OPEN]A Temperature-Sensitive Misfolded bri1-301 Receptor Requires Its Kinase Activity to Promote Growth. Xiaowei Zhang, Linyao Zhou, Yukuo Qin, Yongwu Chen, Xiaolei Liu, Muyang Wang, Juan Mao, Jianjun Zhang, Zuhua He, Linchuan Liu, and Jianming Li

bri1-301 is a temperature-sensitive misfolded brassinosteroid receptor that requires kinase activity to promote growth and is rapidly degraded in the endoplasmic reticulum and on the cell surface.

1704

Continued from preceding page

[OPEN] Network Analysis Reveals a Role for Salicylic Acid Pathway Components in Shade Avoidance.

Kazunari Nozue, Upendra Kumar Devisetty, Saradadevi Lekkala, Patricia Mueller-Moulé, Aurélie Bak,
Clare L. Casteel, and Julin N. Maloof

Shade avoidance involves complex regulation of multiple hormone network modules, and salicylic acid pathway genes are required for petiole shade avoidance.

1720

[OPEN] Articles can be viewed without a subscription.

A Temperature-Sensitive Misfolded *bri1-301* Receptor Requires Its Kinase Activity to Promote Growth^{1[OPEN]}

Xiawei Zhang,^{a,b,c} Linyao Zhou,^{a,c} Yukuo Qin,^{a,c} Yongwu Chen,^{a,c} Xiaolei Liu,^a Muyang Wang,^b Juan Mao,^{d,e} Jianjun Zhang,^{d,e} Zuhua He,^b Linchuan Liu,^{d,e,2,3} and Jianming Li^{a,d,e,f,2}

^aShanghai Center for Plant Stress Biology, Chinese Academy of Sciences, Shanghai 201602, China

^bShanghai Institute of Plant Physiology and Ecology, Chinese Academy of Sciences, Shanghai 200032, China

^cUniversity of Chinese Academy of Sciences, Beijing 100004, China

^dGuangdong Key Laboratory for Innovative Development and Utilization of Forest Plant Germplasm, College of Forestry and Landscape Architecture, South China Agricultural University, Guangzhou 510642, China

^eState Key Laboratory for Conservation and Utilization of Subtropical Agro-Bioresources, South China Agriculture University, Guangzhou 510642, China

^fDepartment of Molecular, Cellular, and Developmental Biology, University of Michigan, Ann Arbor, Michigan 48109-1048

ORCID IDs: 0000-0002-0340-6351 (X.Z.); 0000-0003-2656-5731 (Y.Q.); 0000-0003-0524-9895 (J.M.); 0000-0003-3798-4114 (J.Z.); 0000-0002-6098-7893 (Z.H.); 0000-0002-8669-7202 (L.L.); 0000-0003-3231-0778 (J.L.)

BRASSINOSTEROID-INSENSITIVE1 (BRI1) is a leucine-rich-repeat receptor-like kinase that functions as the cell surface receptor for brassinosteroids (BRs). Previous studies showed that BRI1 requires its kinase activity to transduce the extracellular BR signal into the nucleus. Among the many reported mutant *bri1* alleles, *bri1-301* is unique, as its glycine-989-to-isoleucine mutation completely inhibits its kinase activity in vitro but only gives rise to a weak dwarf phenotype compared with strong or null *bri1* alleles, raising the question of whether kinase activity is essential for the biological function of BRI1. Here, we show that the *Arabidopsis* (*Arabidopsis thaliana*) *bri1-301* mutant receptor exhibits weak BR-triggered phosphorylation in vivo and absolutely requires its kinase activity for the limited growth that occurs in the *bri1-301* mutant. We also show that *bri1-301* is a temperature-sensitive misfolded protein that is rapidly degraded in the endoplasmic reticulum and at the plasma membrane by yet unknown mechanisms. A temperature increase from 22°C to 29°C reduced the protein stability and biochemical activity of *bri1-301*, likely due to temperature-enhanced protein misfolding. The *bri1-301* protein could be used as a model to study the degradation machinery for misfolded membrane proteins with cytosolic structural lesions and the plasma membrane-associated protein quality-control mechanism.

Brassinosteroids (BRs) are important plant growth hormones that regulate a wide range of plant developmental and physiological processes, such as pollen development, seed germination, vascular differentiation, hypocotyl/petiole elongation, senescence, stomata development, and flowering time (Clouse, 2011).

¹This work was partially supported by a grant from the Chinese Academy of Sciences (2012CSP004 to J.L.), grants from the Natural Science Foundation of China (NSFC31600996 to L.L. and NSFC31730019 to J.L.), and the Shanghai Center for Plant Stress Biology.

²Senior author.

³ Author for contact: lcliu@scau.edu.cn.

The author responsible for distribution of materials integral to the findings presented in this article in accordance with the policy described in the Instructions for Authors (www.plantphysiology.org) is: Jianming Li (lian@umich.edu).

J.L. conceived the research plans; J.L. and L.L. supervised the project, suggested experiments, and wrote the article with support from J.M., J.Z., and Z.H.; Y.Q. initiated the project and X.Z. performed most of the experiments, analyzed data, and prepared figures with assistance from L.Z., Y.C., X.L., and M.W.

[OPEN] Articles can be viewed without a subscription.

www.plantphysiol.org/cgi/doi/10.1104/pp.18.00452

Genetic, biochemical, and structural biology studies have shown that these plant steroids are perceived at the cell surface by BRASSINOSTEROID-INSENSITIVE1 (BRI1), a leucine-rich-repeat receptor-like kinase (LRR-RLK; Li and Chory, 1997; He et al., 2000; Wang et al., 2001; Kinoshita et al., 2005; Hothorn et al., 2011; She et al., 2011). Upon BR binding, BRI1 heterodimerizes with and transphosphorylates BRI1-ASSOCIATED RECEPTOR KINASE (BAK1), a similar but smaller LRR-RLK (Li et al., 2002; Nam and Li, 2002), to initiate a protein phosphorylation-mediated signaling cascade, which controls the activities of several key transcription factors regulating the expression of thousands of BR-responsive genes important for plant growth (for review, see Belkhadir and Jaillais, 2015). Loss-of-function mutations in BR-biosynthesis enzymes or BRI1 result in characteristic BR-deficient/insensitive phenotypes that include short hypocotyls in the dark, dwarf stature in the light, altered vascular development, prolonged vegetative phase, and reduced male fertility (Clouse, 1996; Li et al., 1996; Szekeres et al., 1996; Li and Chory, 1997).

BRI1 is the only BR signaling component identified by loss-of-function mutations in multiple forward

genetic screens (Clouse, 1996; Li and Chory, 1997; Noguchi et al., 1999), and over 30 mutant *bri1* alleles have been reported so far (Friedrichsen et al., 2000; Wang et al., 2001, 2005; Xu et al., 2008; Kang et al., 2010; Shang et al., 2011; She et al., 2011; Santiago et al., 2013; Bojar et al., 2014; Sun et al., 2017), most of which carry missense mutations in the BR-binding extracellular domain and the cytoplasmic kinase domain and exhibit dwarf phenotypes of varying strength (Table 1). Previous biochemical and structural studies have demonstrated or suggested that some *bri1* mutations affect BRI1 binding with its ligand or its coreceptor BAK1 (He et al., 2000; Wang et al., 2001; Santiago et al., 2013; Bojar et al., 2014), some prevent BRI1 intracellular trafficking (Jin et al., 2007; Hong et al., 2008), while others inhibit BRI1's kinase activity (Friedrichsen et al., 2000; Wang et al., 2005; Kang et al., 2010; Sun et al., 2017). Among these characterized *bri1* alleles, *bri1-301* is very interesting, as this mutant was generated by ethylmethanesulfonate mutagenesis, which often causes G-to-A and C-to-T transitions (Greene et al., 2003), but carries a GG-AT two-nucleotide change in the *BRI1* gene, resulting in the Gly-989-Ile (G989I) missense mutation in the kinase domain (Xu et al., 2008). Morphologically, it is one of the weakest known *bri1* mutants reported so far. However, two previous studies show that *bri1-301* has an inactive kinase when assayed by in vitro phosphorylation or in yeast cells that coexpressed the full-length proteins of BRI1/*bri1-301* and the wild-type BAK1 (Xu et al., 2008; Kang et al., 2010). It is interesting that a recently reported *bri1* allele, known as *bri1-702*, carrying a mutation of Pro-1050-Ser, exhibited significantly reduced but detectable in vitro autophosphorylation activity but caused a growth phenotype stronger than *bri1-301* (Sun et al., 2017). That study also included a transgenic experiment showing that the GFP-tagged BAK1 was constitutively phosphorylated in *bri1-301* but not in a T-DNA insertional null *bri1* mutant background (Sun et al., 2017), suggesting that *bri1-301* might be an active kinase in Arabidopsis (*Arabidopsis thaliana*). Because the detected BAK1 phosphorylation might not be catalyzed by *bri1-301* but a yet unknown *bri1-301*-dependent mechanism, it remains to be determined if *bri1-301* requires its kinase activity for the observed weak growth phenotype. It is also worth mentioning that another recently reported mutant BR receptor, *bri1-707* (with the same Gly-989 residue mutated to Glu), exhibits slightly reduced in vitro autophosphorylation activity but does not cause any detectable growth alteration (Sun et al., 2017).

Because *bri1-301* is widely used in many studies investigating BR signaling and its cross talk with many other plant signaling processes (Li and Nam, 2002; Nam and Li, 2002; Kim et al., 2007; Wang et al., 2009, 2016; Kang et al., 2010; Schwessinger et al., 2011; Albrecht et al., 2012; Shi et al., 2015; Unterholzner et al., 2015; Ha et al., 2016; Hao et al., 2016), we decided to investigate the mechanism of the *bri1-301* mutation. During our study, we also discovered that *bri1-301* exhibited a severe growth defect when grown in a 29°C

growth chamber. Our biochemical and genetic experiments revealed that *bri1-301* is a temperature-sensitive misfolded BR receptor that is unstable in the endoplasmic reticulum (ER) and at the plasma membrane (PM) and requires its kinase activity for the observed weak growth phenotype. Our study suggests that *bri1-301* may serve as a model protein to study the PM-associated quality-control mechanism in Arabidopsis.

RESULTS

The Weak Growth Phenotype of *bri1-301* Is Caused by the *bri1-301* Mutation

Because no severe dwarf phenotype segregated out in our previous genetic studies with the *bri1-301* mutant (Li and Nam, 2002; Nam and Li, 2002; Wang et al., 2009; Kang et al., 2010), we initially hypothesized that the weak growth phenotype of the *bri1-301* mutant might be caused by a linked unknown mutation that suppresses the dwarf phenotype of the "kinase-dead" BR receptor. To test this hypothesis, we crossed *bri1-301* with the heterozygous T-DNA insertional mutant *bri1-701/+* and discovered that the *bri1-301/bri1-701* heterozygous mutants were smaller than *bri1-301* (Fig. 1A), suggesting that the enhanced dwarfism could be caused by eliminating a recessive suppressor mutation or by reducing *bri1-301* abundance. Genome sequencing of the *bri1-301* mutant revealed three nucleotide changes in the bottom 3,100-kb region of chromosome 4 (15,522,789–18,660,050; Fig. 1B), including the two-nucleotide change (GG-AT at positions of 18,327,790–18,327,791) in the *BRI1* gene (*At4g39400*; Xu et al., 2008) and a single-nucleotide change (G-T at position 18,334,855) in the immediate downstream gene (*At4g39410*) of *BRI1*. Because the third nucleotide change occurs in the annotated promoter region of *At4g39410* that encodes an Arabidopsis WRKY transcription factor, AtWRKY13, and thus might affect *At4g39410* transcript abundance, we performed reverse transcription quantitative PCR (RT-qPCR) and found that the G-T nucleotide change had little effect on *At4g39410* transcript abundance (Fig. 1C), suggesting that the weak growth phenotype of *bri1-301* is unlikely to be caused by the G-T mutation but rather is the result of the two-nucleotide change in the *BRI1* gene.

Further support for our conclusion came from our transgenic experiment. We generated a *pBRI1::bri1-301* construct (driven by the *BRI1* promoter), transformed it into heterozygous *bri1-701* plants, and analyzed the phenotypes of the resulting transgenic lines that were homozygous for the *bri1-701* mutation. As shown in Figure 1D, the *pBRI1::bri1-301* construct complemented the null *bri1-701* mutation, and the growth phenotypes observed with the *pBRI1::bri1-301 bri1-701* transgenic lines matched well with *bri1-301* protein abundance, with the wild type-like lines accumulating higher

Table 1. Summary of previously reported *bri1* alleles
Ecotypes are as follows: Col-0, Columbia-0; Ws-2, Wassilewskija-2.

<i>bri1</i> Allele	Mutation Site	Dwarfism	Ecotype	Biochemical Effect	Reference
<i>bri1-1</i>	G2725A	Strong	Col-0	A909T, extremely weak in vivo BL-stimulated BAK1 phosphorylation	Clouse et al. (1996); Wang et al. (2008)
<i>bri1-2 (cbb2)</i>	Unknown	Strong	C24	Unknown	Kauschmann et al. (1996)
<i>bri1-3</i>	4-bp deletion at 2,745	Strong	Ws-2	Premature termination	Noguchi et al. (1999)
<i>bri1-4</i>	10-bp deletion at 459	Strong	Ws-2	Premature termination	Noguchi et al. (1999)
<i>bri1-5</i>	G206A	Weak	Ws-2	C69Y, ER retention	Noguchi et al. (1999)
<i>bri1-5R1</i>	G260A	Weak	<i>bri1-5</i> Ws-2	Partially suppresses the <i>bri1-5</i> mutation	Belkhadir et al. (2010)
<i>bri1-6/bri1-119</i>	G1931A	Weak	Enkheim-2	G644D, unknown	Noguchi et al. (1999); Friedrichsen et al. (2000)
<i>bri1-7</i>	G1838A	Weak	Ws-2	G613S, unknown	Noguchi et al. (1999)
<i>bri1-8/bri1-108-102</i>	G2948A	Intermediate	Ws-2/Col-0	R983N, no detectable in vitro kinase activity	Noguchi et al. (1999)
<i>bri1-9</i>	C1985T	Weak	Ws-2/Col-0	S662F, ER retention	Noguchi et al. (1999); Jin et al. (2007)
<i>bri1-101</i>	G3232A	Strong	Col-0	E1078K, extremely weak in vitro kinase activity	Li and Chory (1997); Friedrichsen et al. (2000)
<i>bri1-102</i>	C2249T	Strong	Col-0	T750I	Friedrichsen et al. (2000)
<i>bri1-103/104</i>	G3091A	Strong	Col-0	A1031T	Li and Chory (1997); Friedrichsen et al. (2000)
<i>bri1-105-107</i>	C3175T	Strong	Col-0	Q1059Stop	Li and Chory (1997); Friedrichsen et al. (2000)
<i>bri1-113</i>	G1832A	Strong	Col-0	G611E	Li and Chory (1997)
<i>bri1-114/116</i>	C1747T	Strong	Col-0	Q583Stop	Friedrichsen et al. (2000)
<i>bri1-115</i>	G3143A	Strong	Col-0	G1048D	Li and Chory (1997)
<i>bri1-117/118</i>	G3415A	Strong	Col-0	D1139N	Friedrichsen et al. (2000)
<i>bri1-120</i>	T1196C	Weak	Landsberg erecta	S399F in the 13th LRR	Shang et al. (2011)
<i>bri1-201</i>	G1831A	Strong	Ws-2	G611R	Domagalska et al. (2007)
<i>bri1-202</i>	C2854T	Strong	Ws-2	R952W	Domagalska et al. (2007)
<i>bri1-301</i>	GG2965/6AT	Very weak	Col-0	No detectable kinase activity in vitro or in yeast cells	Xu et al. (2008); Kang et al. (2010); this study
<i>bri1-401</i>	G2714A/G3582A	Strong	Ws	G895R/G1194E	Tanaka et al. (2005)
<i>bri1-701</i>	T-DNA insertion at 1,245	Strong	Col-0	Knockout of BRI1	Gou et al. (2012)
<i>bri1-702</i>	C3148T	Weak	Col-0	P1050S, reduced in vitro kinase activity	Sun et al. (2017)
<i>bri1-703</i>	G3166A	Strong	Col-0	E1056K, no detectable in vitro kinase activity	Sun et al. (2017)
<i>bri1-704</i>	G3079A	Strong	Col-0	D1027N, no detectable in vitro kinase activity	Sun et al. (2017)
<i>bri1-705</i>	C2156T	Subtle	Col-0	P719L, likely affects the interaction of BL, BRI1, and BAK1	Sun et al. (2017)
<i>bri1-706</i>	C758T	Subtle	Col-0	S253F	Sun et al. (2017)
<i>bri1-708</i>	C2947G	Strong	Col-0	R983G, no detectable in vitro kinase activity	Sun et al. (2017)
<i>bri1-709</i>	G2543A	Strong	Col-0	W848Stop, premature termination	Sun et al. (2017)
<i>bri1-710</i>	G1858A	Subtle	Col-0	G620R	Sun et al. (2017)
<i>bri1-711</i>	G2236A	Subtle	Col-0	G746S	Sun et al. (2017)

amounts of *bri1-301* (Fig. 1E). It is important to note that a line exhibiting *bri1-301*-like morphology contained a similar amount of *bri1-301* protein as the *bri1-301* mutant (Fig. 1, D and E). Importantly, this line also exhibited similar BR sensitivity to the *bri1-301* mutant revealed by the BR-induced BRI1-EMS-SUPPRESSOR1 (BES1) dephosphorylation assay (Mora-García et al., 2004) and by RT-qPCR analysis of three BR-responsive genes, *CONSTITUTIVE PHOTOMORPHOGENESIS AND DWARFISM* (CPD; Mathur et al., 1998), *DWARF4* (DWF4;

Bancoş et al., 2002), and *SMALL-AUXIN-UP-RNA-ARABIDOPSIS COLUMBIA1* (*SAUR-AC1*; Nakamura et al., 2003; Fig. 1, F–H; Supplemental Fig. S1A). Consistent with their growth morphology, the two wild-type-like *pBRI1::bri1-301 bri1-701* transgenic lines displayed wild-type-like BR sensitivity, as shown in Figure 1, F to H, and Supplemental Figure S1A. Taken together, these results showed that the weak growth phenotype of *bri1-301* is due to the G989I substitution in BRI1 rather by the G-T mutation in the *At4g39410* promoter.

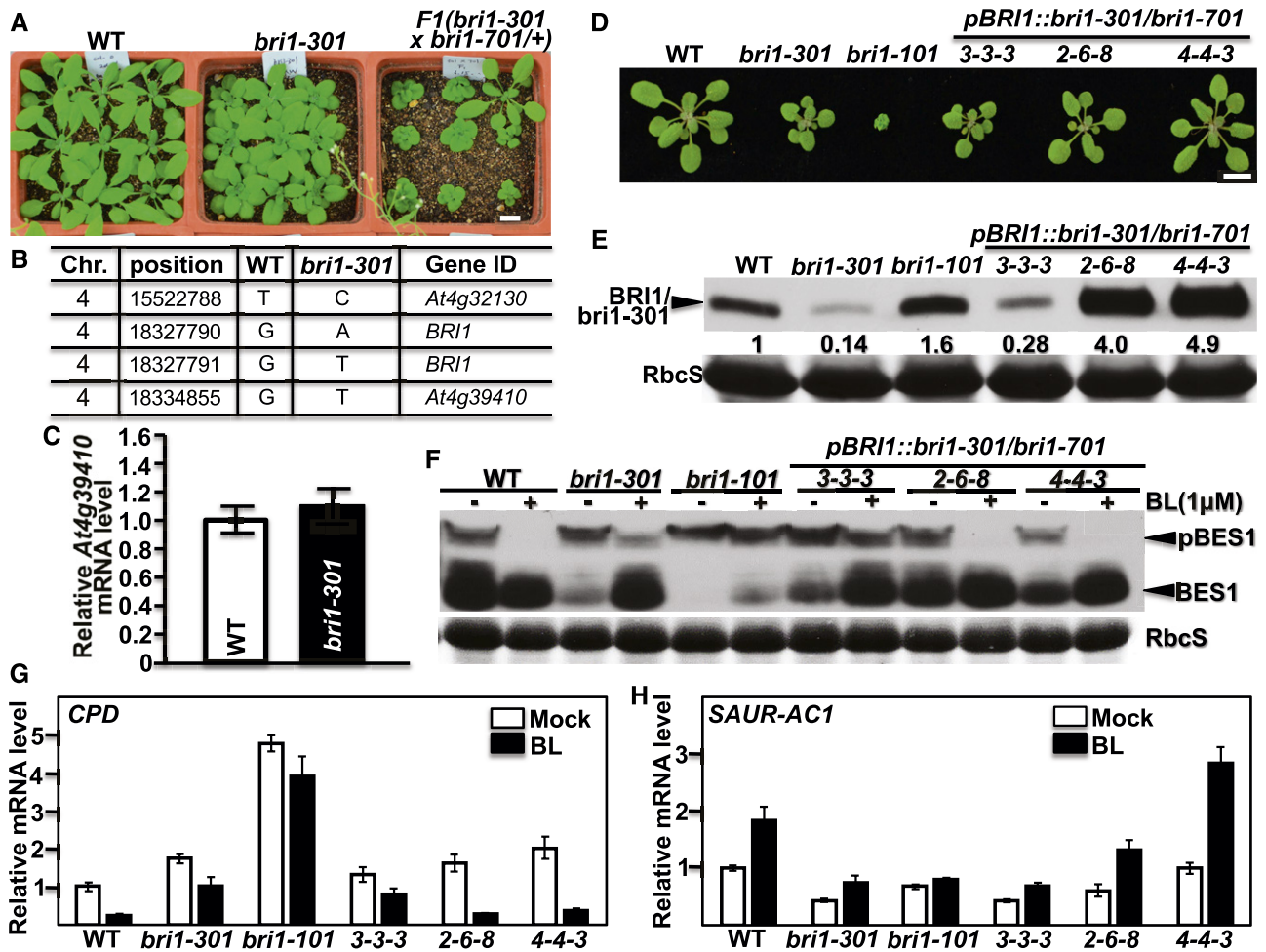


Figure 1. The G989I mutation of *BRI1* is responsible for the weak growth phenotype of *bri1-301*. **A**, Photographs of 26-d-old soil-grown plants in a 22°C growth chamber. **B**, Nucleotide changes between *bri1-301* and its wild-type control (WT) within the bottom 3,000-kb region of chromosome 4. **C**, RT-qPCR analysis of the relative transcript abundance of *At4g39410* between 10-d-old seedlings of the wild type and *bri1-301* grown in a 22°C growth room. **D**, Photographs of 18-d-old soil-grown seedlings in a 22°C growth room. **E**, Immunoblot analysis of *BRI1/bri1-301* abundance of the Arabidopsis seedlings shown in **D**. The numbers shown below the anti-*BRI1* strip are the relative values of anti-*BRI1* signals after normalization with the signal intensity of the corresponding Coomassie Blue-stained *RbcS* bands. The signal intensity of each band was quantified by ImageJ. **F**, Immunoblot analysis of *BES1* phosphorylation status. Eight-day-old seedlings grown on one-half-strength Murashige and Skoog (1/2 MS) medium were carefully transferred into liquid 1/2 MS medium supplemented with or without 1 μM brassinolide (BL) and incubated for 2 h. Their total protein extracts were separated by 10% SDS-PAGE and analyzed by Coomassie Blue staining or immunoblotting with an anti-*BES1* antibody. **G** and **H**, RT-qPCR analyses of the relative transcript abundance of *CPD* (**G**) and *SAUR-AC1* (**H**) using total RNAs extracted from 8-d-old seedlings treated with or without 1 μM BL for 2 h. The transcript abundance of *CPD* or *SAUR-AC1* in nontreated wild-type seedlings was set as 1. In **C**, **G**, and **H**, for each sample, the RT-qPCR assays were repeated four times, and the error bars denote ±SD. Bars in **A** and **D** = 1 cm.

The *bri1-301* Protein Requires Its Kinase Activity for Its Weak Growth Phenotype

Our second hypothesis to explain the discrepancy between the nondetectable kinase activity of *bri1-301* in vitro or in yeast cells and its weak growth phenotype is that *bri1-301* is a rather active kinase in vivo. To test this hypothesis, we performed two different experiments capable of detecting in vivo phosphorylated proteins. First, we performed Phos-tag immunoblotting with total proteins extracted from seedlings

of the wild type, *bri1-301*, and *bri1-101* treated with or without 1 μM BL (the most active member of the BR family). Due to the presence of Phos-tag, a selective phosphate-binding tag molecule, in the SDS-polyacrylamide gel, phosphorylated proteins move slower than their corresponding nonphosphorylated forms (Kinoshita et al., 2009). As shown in Figure 2A, a 4-h treatment with 1 μM BL caused the appearance of highly abundant slower-moving *BRI1* bands in the wild-type sample, while the same treatment resulted

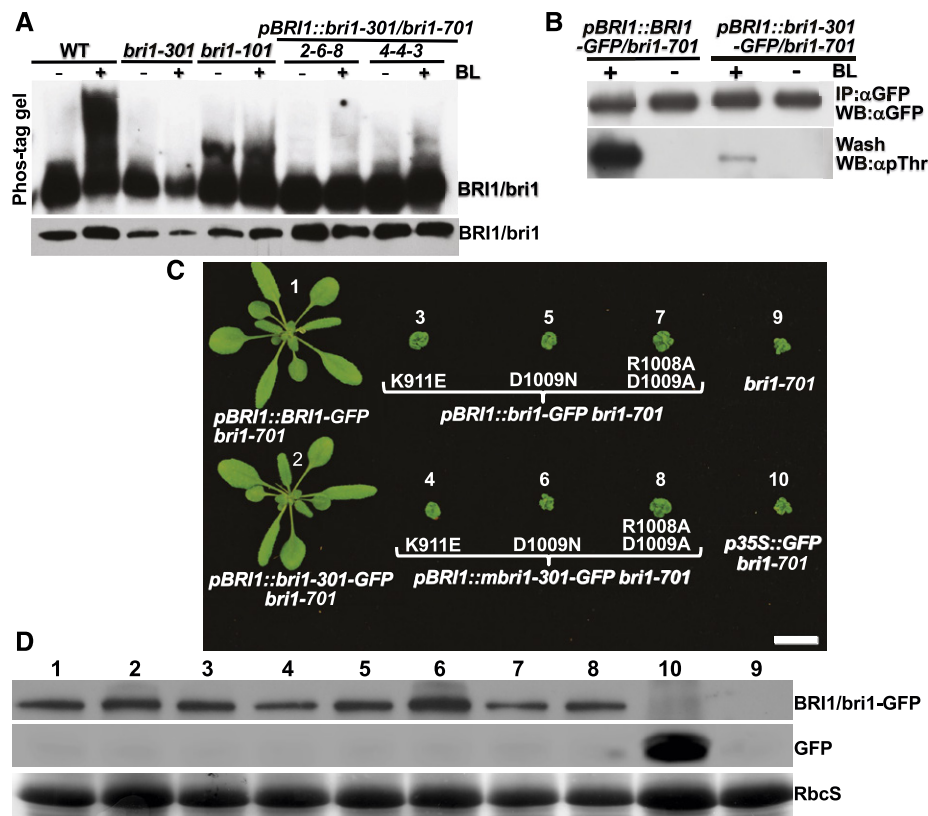


Figure 2. *bri1-301* is weakly phosphorylated in vivo and requires its kinase activity for the weak growth phenotype. A, Phos-tag assay of BL-triggered BRI1/bri1 phosphorylation (top strip; for details, see “Materials and Methods”) and immunoblot analysis of BRI1/bri1-301 abundance (bottom strip). WT, Wild type. B, Immunoblot analysis of BL-induced BRI1/bri1-301 phosphorylation by an anti-pThr antibody with 18-d-old seedlings treated with or without 1 μ M BL. IP, immunoprecipitation; WB, western blot. C, Photographs of 26-d-old soil-grown seedlings of transgenic *bri1-701* lines. Bar = 1 cm. D, Immunoblot analysis of the transgenically expressed BRI1/bri1-301-GFP fusion proteins in the lines shown in C. The numbers shown above the blots correspond to the numbered lines shown in C. The bottom strip shows the Coomassie Blue-stained RbcS bands for the loading control.

in no detectable slower-moving bands in the *bri1-301* sample. To address the concern that our failure to detect slower-moving *bri1-301* bands could be due simply to the lower abundance of total *bri1-301* proteins (Fig. 2A), we included two wild-type-looking *pBRI1::bri1-301 bri1-701* transgenic lines with similar or higher *bri1-301* abundance than the wild-type BRI1 abundance (Fig. 2, A and B). As shown in Figure 2A, the 4-h BL treatment did show slower-moving *bri1-301* bands in the two transgenic lines; however, the abundance of these slower-moving bands was much lower than that of the corresponding wild-type BRI1 bands, suggesting that *bri1-301* exhibits a very low level of BR-induced phosphorylation. This conclusion was further supported by our second immunoblot experiment with a *pBRI1::BRI1-GFP bri1-701* transgenic line and a wild-type-like *pBRI1::bri1-301-GFP bri1-701* transgenic line (Fig. 2B) using an anti-pThr antibody capable of detecting phosphorylated Thr residues in BRI1 and its coreceptor BAK1 (Wang et al., 2005).

The detected *bri1-301* phosphorylation could be caused by its autophosphorylation activity or trans-

phosphorylation by a BRI1-associated kinase, such as BAK1 that functions as a BRI1 coreceptor (Li et al., 2002; Nam and Li, 2002). To directly test if *bri1-301* requires its kinase activity for the observed weak growth phenotype, we mutated three residues in the kinase domain of BRI1 known to be essential for its kinase activity: Lys-911 mutated to Glu (K911E), which is known to form the salt bridge with Glu-927 essential to maintain an active conformation of BRI1 (Bojar et al., 2014); Arg-1008 mutated to Asn (R1008N) or Ala (R1008A); and Asp-1009 mutated to Ala (D1009A) in combination with the R1008A mutation of the catalytic His-Arg-Asp loop motif, known to be highly conserved throughout the protein kinase family (Hanks et al., 1988). We individually transformed the mutated *pBRI1::BRI1-GFP* or *pBRI1::bri1-301-GFP* transgene into the heterozygous *bri1-701* plants and screened T1 plants homozygous for the *bri1-701* mutation. We discovered that every homozygous *bri1-701* transgenic plant was morphologically identical to the parental *bri1-701* mutant (Fig. 2C), indicating that the kinase activity is absolutely required for the weak growth phenotype of the mutant *bri1-301* receptor.

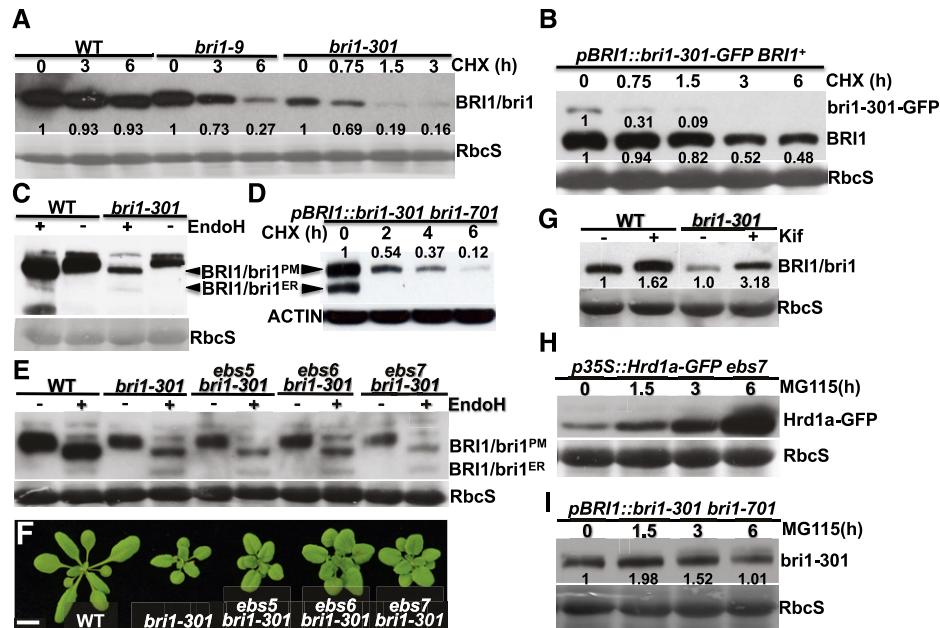


Figure 3. *bri1-301* is an unstable protein that is degraded in the ER and at the PM. A, Immunoblot analysis of BRI1/bri1 stability after treatment with CHX. B, Immunoblot analysis of the protein stability of the endogenous BRI1 and the transgenically expressed *bri1-301*-GFP fusion proteins. C and D, Endo-H analysis of BRI1/bri1-301 and transgenically expressed *bri1-301* in the *bri1-701* background. E, Immunoblot analysis of BRI1/bri1-301 abundance with total proteins treated with or without Endo-H. F, Photographs of 18-d-old soil-grown plants in a 22°C growth room. Bar = 1 cm. G, Immunoblot analysis of the impact of Kif treatment on BRI1/bri1-301 abundance. H and I, Immunoblot analysis of the effect of MG115 on the stability of Hrd1a-GFP (H; used as a positive control) and *bri1-301* (I). In A to C, E, and G to I, Coomassie Blue staining of duplicate gels was used as the loading control, while in D, immunoblotting of a duplicate blot with anti-ACTIN antibody served as the loading control. In A, B, D, and G to I, the numbers on the gel images or in the space between gel images are relative values of the anti-BRI1 signals (against the nontreated sample of the same genotype) after normalization with the signal intensity of the corresponding RbcS or ACTIN band. ImageJ was used to quantify the signal intensity of each band. WT, wild type.

bri1-301 Is an Unstable Protein in the ER and on the PM

During our experiment assaying the BR-induced BRI1/*bri1-301* phosphorylation, we discovered that the protein abundance of *bri1-301* was much lower than that of wild-type BRI1 (Figs. 1E and 2A), suggesting that *bri1-301* is an unstable protein. To determine if the low *bri1-301* abundance is caused by increased degradation or decreased biosynthesis of *bri1-301*, we performed a cycloheximide (CHX)-chasing experiment by treating Arabidopsis seedlings of *bri1-9*, *bri1-301*, and their wild-type control with CHX, a widely used protein biosynthesis inhibitor. As shown in Figure 3A, while the wild-type BRI1 protein was rather stable, *bri1-301* was rapidly degraded in the treated *bri1-301* seedlings. Interestingly, it seemed that *bri1-301* disappeared more rapidly than the ER-retained *bri1-9*, which is degraded by an endoplasmic reticulum-associated degradation (ERAD) mechanism (Hong et al., 2009). A similar study was performed with a transgenic line that expresses a GFP-tagged *bri1-301* (driven by the *BRI1* promoter) in a wild-type background. As shown in Figure 3B, the GFP-tagged *bri1-301* degraded much more rapidly than the endogenous wild-type BRI1. Taken together, our experiments demonstrated that *bri1-301* is rapidly degraded in Arabidopsis plants.

Our earlier endoglycosidase H (Endo-H) assay revealed that *bri1-301* is not retained in the ER but is localized mainly on the PM (Hong et al., 2008), as Endo-H is an endoglycosidase capable of cleaving high-mannose (Man)-type Asn-linked glycans (N-glycans) of ER-retained glycoproteins but not the Golgi-processed complex-type N-glycans (Robbins et al., 1984). However, Figure 3C shows a low but detectable level of the Endo-H-sensitive form of *bri1-301* on the immunoblot, suggesting that the G989I mutation leads to the presence of a very small pool of *bri1-301* proteins in the ER. Consistently, a similar Endo-H assay of *bri1-301* from a wild-type-looking *pBRI1::bri1-301 bri1-701* line revealed the presence of a high level of an ER-retained form of *bri1-301*, which was degraded much faster than the PM-localized *bri1-301* proteins (Fig. 3D). We hypothesized that *bri1-301* is a misfolded protein with a cytosolic structural lesion that is not efficiently retained in the ER. In addition, its ER-retained form is rapidly degraded and remains unstable even when it reaches the PM.

To investigate if the low abundance of the ER-retained *bri1-301* pool is due to rapid degradation by the ERAD pathway known for degrading *bri1-5* and *bri1-9*, two ER-retained mutant BR receptors (Jin et al.,

2007; Hong et al., 2008), we crossed *bri1-301* with three previously reported Arabidopsis ERAD mutants: *EMS-mutagenized bri1 suppressor5* (*ebs5*), *ebs6*, and *ebs7* (Su et al., 2011, 2012; Liu et al., 2015). EBS5, an ER transmembrane protein, works together with the ER luminal lectin EBS6, which binds to α 1,2-Man-trimmed N-glycans to recruit a terminally misfolded glycoprotein to the ER membrane-anchored ubiquitin ligase HMG-CoA-reductase degradation protein1 (Hrd1), while EBS7 regulates the protein stability of Hrd1 (Liu and Li, 2014; Liu et al., 2015). As shown in Figure 3, E and F, none of the three ERAD mutations was able to suppress the *bri1-301* growth phenotype and to stabilize the ER-retained form of *bri1-301*, indicating that degradation of the ER-retained *bri1-301* does not involve the ERAD machinery that degrades *bri1-5* and *bri1-9*. Surprisingly, treatment of the *bri1-301* mutant with kifunensine (Kif), a widely used inhibitor of α 1,2-mannosidases and ERAD of glycoproteins (Elbein et al., 1990), increased the protein abundance of *bri1-301*, suggesting the involvement of N-glycosylation in *bri1-301* degradation (Fig. 3G). Because Kif inhibits not only the ER-mediated α 1,2-Man trimming of terminally misfolded glycoproteins but also the Golgi-mediated α 1,2-Man trimming of correctly folded glycoproteins that are destined to the PM or other cellular organelles, it is possible that Kif treatment might affect the activity of yet unknown glycoproteins to degrade *bri1-301*. It is worth noting that treatment with MG115, which could block the degradation of the Arabidopsis ER-localized E3 ligase Hrd1a that becomes unstable in an *ebs7* mutant background (Liu et al., 2015; Fig. 3H), showed very limited impact on *bri1-301* abundance (Fig. 3I), suggesting that the cytosolic proteasome might not make a major contribution to degrading the ER-retained or PM-localized *bri1-301*.

The *bri1-301* Mutant Is Highly Sensitive to Higher Temperatures

During our study, we noticed that *bri1-301* grown in a 22°C growth chamber was a weak dwarf but became an extreme dwarf when grown in a 29°C growth chamber (Fig. 4A), suggesting that *bri1-301* is a temperature-sensitive mutant. Indeed, when grown in a 25°C growth chamber, the rosette size of *bri1-301* was between that of the 22°C-grown and 29°C-grown *bri1-301* mutants (Fig. 4B). We also tested the temperature sensitivity of other *bri1* mutants. As shown in Figure 4C, while the temperature increase of 22°C to 29°C stimulated the growth of the wild type and weak *bri1* mutants such as *bri1-5*, *bri1-702*, and *bri1-707*, which was likely mediated by high-temperature-induced auxin biosynthesis (Gray et al., 1998; Koini et al., 2009), it had little impact on stronger *bri1* mutants, including *bri1-9*, *bri1-101*, *bri1-701*, *bri1-703*, *bri1-704*, and *bri1-708*. It is interesting that the temperature-triggered severe dwarfism was not observed in the dark (Fig. 4D). A quantitative assay, which measures the sensitivity of dark-grown seedlings to a BR biosynthesis inhibitor,

brassinazole (BRZ; Asami et al., 2000; Nagata et al., 2000), showed that the temperature shift had little effect on the BRZ sensitivity of the weak receptor mutant, although the 22°C to 29°C temperature shift did enhance the BRZ resistance of the dark-grown wild-type seedlings (Fig. 4E).

The Thermosensitivity of *bri1-301* Is Caused by the G989I Mutation of *BR11*

There are two possible explanations for the observed 29°C-triggered growth inhibition of *bri1-301*. It might be due to an unknown mutation that confers warm temperature-induced growth inhibition to *bri1-301*, or it may be caused by a warm temperature-triggered reduction in the activity and/or protein abundance of *bri1-301*. To investigate the first possibility, we crossed *bri1-301* with the wild type and *bri1-701*, analyzed their F2 offspring (more than 3,000 F2 individual seedlings for each cross), and discovered a close linkage of the thermosensitive phenotype with the *BR11* locus. As mentioned before, there are only three detected nucleotide changes in the bottom 3,100-kb region of chromosome 4: two in the *BR11* gene and one in the promoter region of *At4g39410* located immediately downstream of the *BR11* locus (Fig. 1B). Therefore, we performed RT-qPCR analysis of the *At4g39410* gene with the 22°C- and 29°C-grown *bri1-301* mutants but detected no obvious difference in its transcript abundance between temperatures (Fig. 5A), suggesting that the temperature-triggered severe dwarfism of *bri1-301* is likely due to the G989I mutation of *bri1-301* but not the nucleotide change in the *At4g39410* promoter. Further support came from our analysis of the growth phenotypes of the above-mentioned *pBR11::bri1-301 bri1-701* transgenic lines grown in the 29°C growth chamber. As shown in Figure 5B, the *bri1-301*-like *pBR11::bri1-301 bri1-701* line (3-3-3), which contains a similar amount of *bri1-301* to the *bri1-301* single mutant (Fig. 5C), was an extreme dwarf resembling the 29°C-grown *bri1-301* (Fig. 5B). Interestingly, the two other *pBR11::bri1-301 bri1-701* transgenic lines (2-6-8 and 4-4-3), which accumulated higher levels of *bri1-301* mRNA and *bri1-301* protein than the wild type (Fig. 5C; Supplemental Fig. S2), were larger than the 22°C-grown *bri1-301* mutant and morphologically similar to the 22°C-grown wild-type plants (Fig. 5B). Consistent with the morphological phenotypes, the BR-induced BES1 dephosphorylation assay and RT-qPCR experiments of three BR-responsive genes showed that the 29°C-grown wild-type-looking *pBR11::bri1-301 bri1-701* lines still responded to BL, whereas the 29°C-grown seedlings of *bri1-301* and the *bri1-301*-like *pBR11::bri1-301 bri1-701* line became insensitive to the exogenously applied BL (Fig. 5, D–F; Supplemental Fig. S1B). Together, these results demonstrated that the 29°C-triggered growth inhibition is caused by the *bri1-301* mutation itself. In addition, our experiments revealed that *bri1-301* remains active in promoting plant growth even at 29°C, when its protein abundance is high enough to compensate

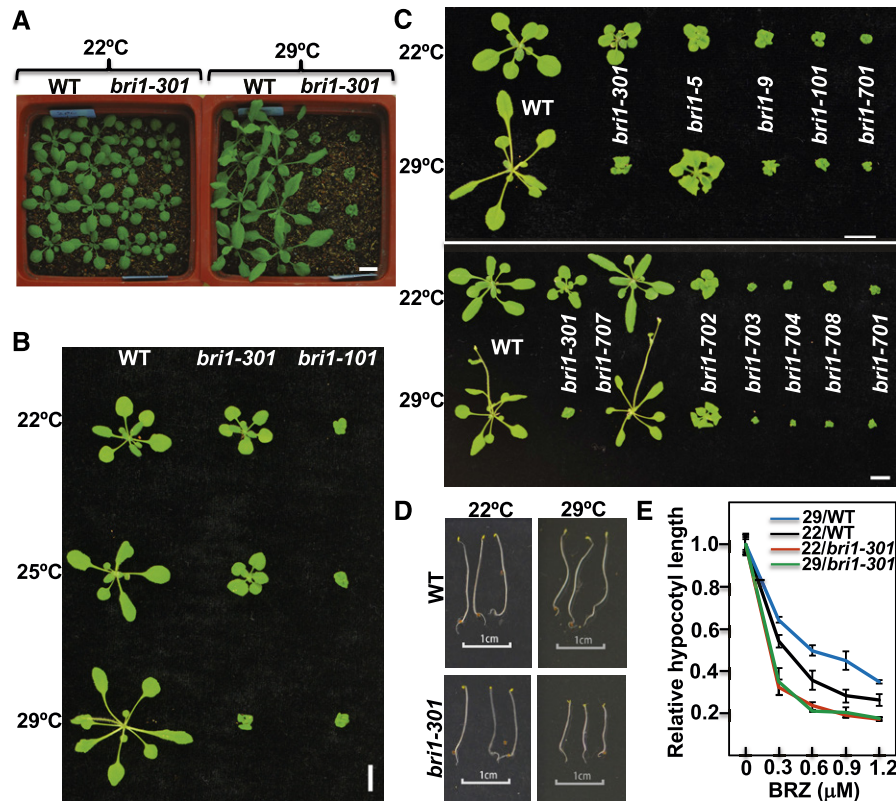


Figure 4. *bri1-301* is a thermosensitive dwarf mutant. A, Photographs of 26-d-old soil-grown plants in a 22°C growth chamber (left pot) and in a 29°C growth chamber (right pot). B, Photographs of 20-d-old soil-grown plants at three different temperatures. C, Photographs of 18-d-old (top) and 23-d-old (bottom) soil-grown wild-type (WT) and various *bri1* mutant plants in 22°C and 29°C growth chambers. D, Photographs of 5-d-old 22°C- and 29°C-grown etiolated seedlings. E, Quantitative analysis of seedling sensitivity to BRZ. Five-day-old dark-grown seedlings were carefully removed from petri dishes and photographed, and their hypocotyl lengths were measured by ImageJ. The data points are relative hypocotyl lengths of seedlings grown on BRZ-containing medium in comparison with seedlings grown on normal 1/2 MS medium at 22°C or 29°C. For each data point, the average length was obtained through three replicates of 20 seedlings each. The error bars indicate \pm SD. Bars in A to D = 1 cm.

for its reduced activity at a higher growth temperature (Fig. 5, B and C).

The Warmer Temperature-Enhanced Protein Misfolding Is Likely Responsible for the Severe Dwarfism of 29°C-Grown *bri1-301*

Given the fact that the 29°C-induced severe dwarf phenotype of *bri1-301* could be suppressed by increased production of the mutant BR receptor (Fig. 5, B and C), we suspected that the warm temperature-triggered dwarfism enhancement might be caused by a reduction in the activity and/or abundance of *bri1-301*. We first compared the protein abundance of the mutant BR receptor between 22°C- and 29°C-grown *bri1-301* seedlings. As shown in Figure 6A, the temperature increase of 22°C to 29°C had a marginal impact on the protein level of the wild-type BRI1 but caused an ~4-fold reduction in *bri1-301* abundance. A subsequent CHX-chasing experiment showed that *bri1-301* was degraded slightly faster in the 29°C-grown *bri1-301*

seedlings than in the 22°C-grown seedlings (Fig. 6B). Additional support for the suspected causal relationship between reduced *bri1-301* abundance and severe dwarfism came from our immunoblot experiment with 22°C-grown seedlings of *bri1-301*, a *pBRI1::bri1-301 bri1-701* transgenic line, the F1 offspring of the *bri1-301* \times *bri1-701* cross, and their wild-type control plus our analysis of BRI1/*bri1-301* abundance of wild-type and *bri1-301* seedlings grown at 18°C, 22°C, 25°C, and 29°C. Figure 6C reveals an association between BRI1 abundance and the severity of dwarfism among 22°C-grown seedlings of various genotypes, while Figure 6, D and E, show that *bri1-301* abundance decreased with the increased severity of dwarfism when the growth temperature increased.

Based on our findings of the temperature-dependent reduction in the protein abundance of *bri1-301* and its increased degradation rate at 29°C, we hypothesized that *bri1-301* is a temperature-sensitive misfolded BR receptor that becomes even more misfolded at higher temperatures. If so, we would expect that more *bri1-301*

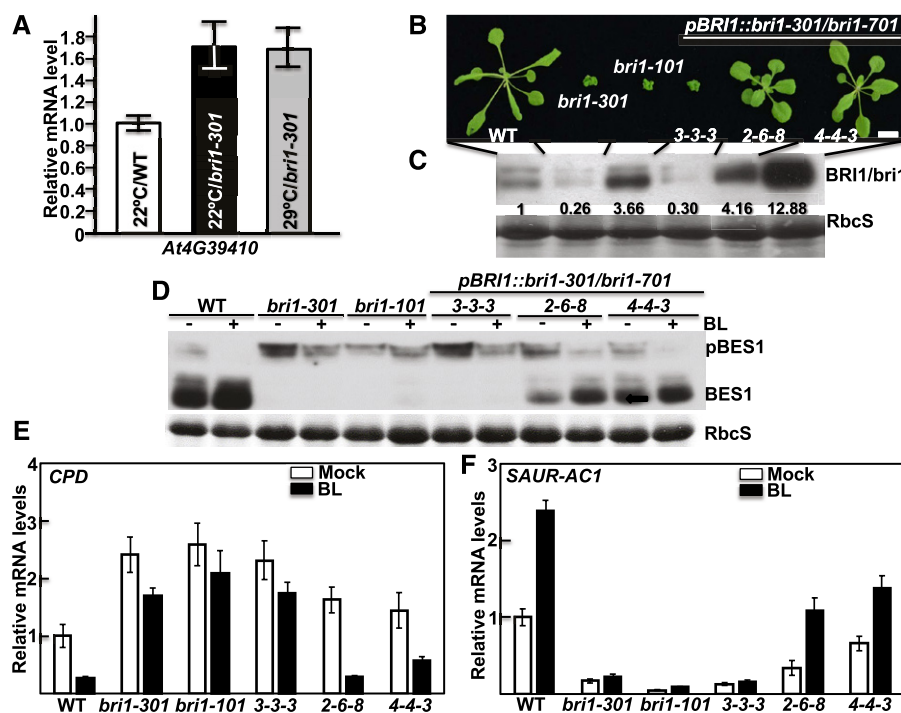


Figure 5. The G989I mutation is responsible for warm temperature-triggered severe dwarfism. A, RT-qPCR analysis of *At4g39410* transcript abundance. B, Photographs of 20-d-old soil-grown plants in a 29°C growth chamber. Bar = 1 cm. C, Immunoblot analysis of BRI1/*bri1-301* protein abundance in the plants shown in B. The numbers shown on the anti-BRI1 strip are the values of anti-BRI1 signal intensity relative to the wild-type (WT) BRI1 after normalization with the signal intensity of the corresponding Coomassie Blue-stained RbcS bands. The signal intensity of each band was quantified by ImageJ. D, Immunoblot analysis of BL-triggered changes in BES1 phosphorylation status. E and F, RT-qPCR analysis of the relative transcript abundance of *CPD* and *SAUR-AC1* in 29°C-grown seedlings treated with or without 1 μ M BL for 2 h. In A, E, and F, the error bars represent \pm SD, and each bar is the average of four replicate RT-qPCR results.

proteins would be retained in the ER. To test this hypothesis, we performed an Endo-H experiment, which indeed showed an increased ratio of ER-retained *bri1-301* (Endo-H-sensitive form) to the PM-localized *bri1-301* (Endo-H-resistant form) despite a remarkable reduction in the total amount of *bri1-301* by the temperature increase (Fig. 6F). Similar to what was observed in 22°C-grown seedlings, degradation of the ER-retained *bri1-301* in 29°C-grown seedlings did not involve EBS5, EBS6, or EBS7 (Fig. 6G). Consistently, the morphology of 29°C-grown *ews5 bri1-301*, *ews6 bri1-301*, or *ews7 bri1-301* was indistinguishable from that of the 29°C-grown *bri1-301* single mutant (Fig. 6G). Additional support for a more misfolded state of *bri1-301* in 29°C-grown *bri1-301* mutants came from a trypsin sensitivity assay, which is widely used to assess if a protein is misfolded compared with its correctly folded conformer (<https://bio-protocol.org/e1953>). As shown in Figure 6H, the *bri1-301* protein extracted from the 29°C-grown seedlings was more sensitive to the trypsin digestion than that extracted from the 22°C-grown seedlings. Together, these results strongly suggested that *bri1-301* becomes more misfolded at 29°C, leading to its increased ER retention and further reduced protein stability on the PM.

The temperature-enhanced misfolding and increased degradation of *bri1-301* suggested that the activity of the mutant receptor also could be reduced by higher growth temperatures. Consistent with this assessment, morphological and immunoblot analyses of additional 29°C-grown *pBRI1::bri1-301 bri1-701* transgenic lines, which were generated by an independent transformation experiment (Fig. 7A), showed that two transgenic lines (#1 and #2, with ~4- and 11-fold higher *bri1-301* abundance than that of the 29°C-grown *bri1-301* mutant, respectively) were still severe dwarfs (Fig. 7, B and C). If the temperature increase had only affected *bri1-301* stability, a 29°C-grown *pBRI1::bri1-301 bri1-701* transgenic line accumulating greater than 4 times more *bri1-301* than the 29°C-grown *bri1-301* would be morphologically similar to the 22°C-grown *bri1-301*, as the *bri1-301* abundance of 22°C-grown *bri1-301* was ~4-fold higher than that of the 29°C-grown *bri1-301* (Fig. 6A). Further support for a temperature-triggered reduction of *bri1-301* activity came from a Phos-tag experiment that measured the BR-induced BRI1/*bri1-301* phosphorylation level in 29°C-grown seedlings. As shown in Figure 7D, despite the similar abundance of transgenically expressed *bri1-301* in the *bri1-701* mutant background to that of wild-type BRI1 in the

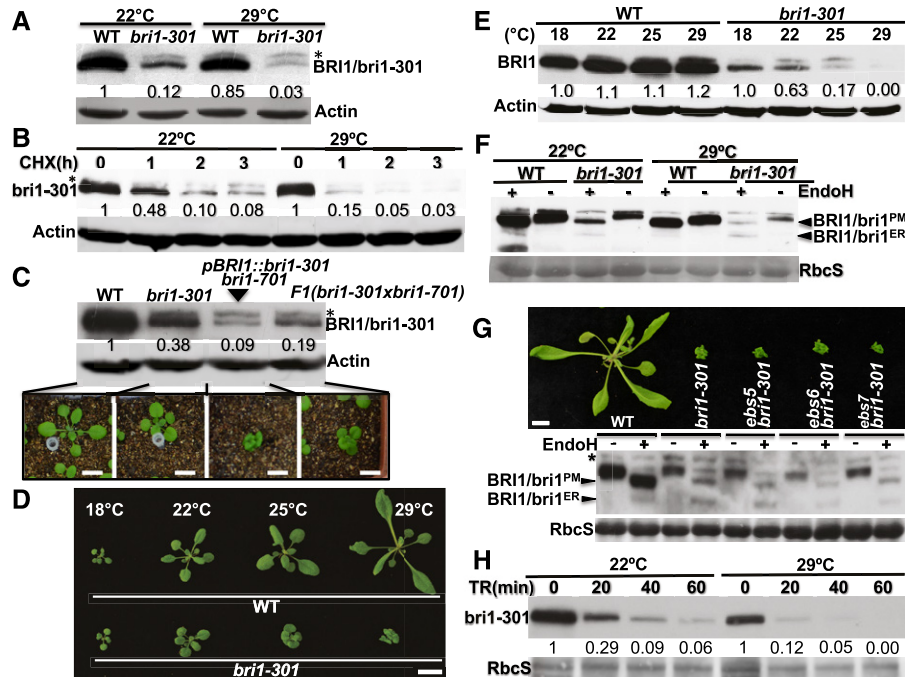


Figure 6. The 22°C to 29°C temperature increase reduces *bri1-301* stability. A, Immunoblot analysis of BRI1/*bri1-301* protein abundance. B, Immunoblot analysis of *bri1-301* protein stability after the CHX treatment. C, Immunoblot analysis of BRI1/*bri1-301* protein abundance in 18-d-old soil-grown seedlings (shown below the gel strips) of the wild type (WT), *bri1-301*, a *pBRI1::bri1-301 bri1-701* line, and an F1 plant of the *bri1-301* × *bri1-701* cross. D, Photographs of 18-d-old seedlings grown at different temperatures. E, Immunoblot analysis of BRI1/*bri1-301* protein abundance in the seedlings shown in D. F, Endo-H analysis of BRI1/*bri1-301* proteins with total proteins extracted from wild-type and *bri1-301* seedlings grown in 22°C and 29°C growth chambers. G, Photographs (top) and immunoblot analysis (bottom) of 20-d-old seedlings grown in soil at 29°C. H, Immunoblot analysis of trypsin sensitivity of the *bri1-301* protein from the 22°C- and 29°C-grown *bri1-301* mutant. TR, trypsin. In A to C, E, and H, the numbers shown in the space between two gel strips are BRI1/*bri1* abundance (relative to that of the wild-type BRI1 in lane 1 in A and C, to that of nontreated samples in B and H, or to that of 18°C-grown seedlings of the same genotype in E) after normalization with the signals of corresponding ACTIN (A–C and E) or RbcS (H) bands. Bars in C, D, and G = 1 cm.

wild-type control, the BL treatment resulted in no detectable BR-triggered *bri1-301* phosphorylation in the two *pBRI1::bri1-301 bri1-701* transgenic lines. This is quite different from what was observed with the same two transgenic lines grown in a 22°C growth chamber (Fig. 2A). Together, these two experiments strongly suggested that the temperature-enhanced *bri1-301* misfolding not only increases the degradation rate of the mutant BR receptor but also reduces its biochemical activity.

DISCUSSION

The Mutant *bri1-301* Receptor Requires Its Kinase Activity to Promote Plant Growth

Among various reported alleles of the Arabidopsis BR receptor, *bri1-301* is very interesting because it lacks a detectable auto/transphosphorylation activity in vitro or in yeast cells but only causes a weak growth

phenotype (Xu et al., 2008; Kang et al., 2010; Sun et al., 2017), which led us to question whether the kinase activity is required for BRI1's physiological activity. In this study, we eliminated the possibility of a linked suppressor mutation being responsible for the apparent inconsistency between an inactive kinase and the weak growth phenotype and demonstrated by a transgenic approach that the weak growth phenotype of *bri1-301* is caused by the G989I mutation in the BRI1 protein. Our analysis of in vivo *bri1-301* phosphorylation with an anti-pThr antibody and Phos-tag gel electrophoresis revealed that *bri1-301* was very weakly phosphorylated in response to BR treatment, which is quite different from what was reported recently for the strong BR-independent BAK1 phosphorylation in the *bri1-301* mutant background (Sun et al., 2017). Although we could not tell if the detected *bri1-301* phosphorylation was caused by autophosphorylation of *bri1-301* or transphosphorylation by a BAK1 or other yet unknown BRI1-interacting kinases, our transgenic experiments using several kinase-dead mutant *pBRI1::bri1-301* constructs that were transformed into

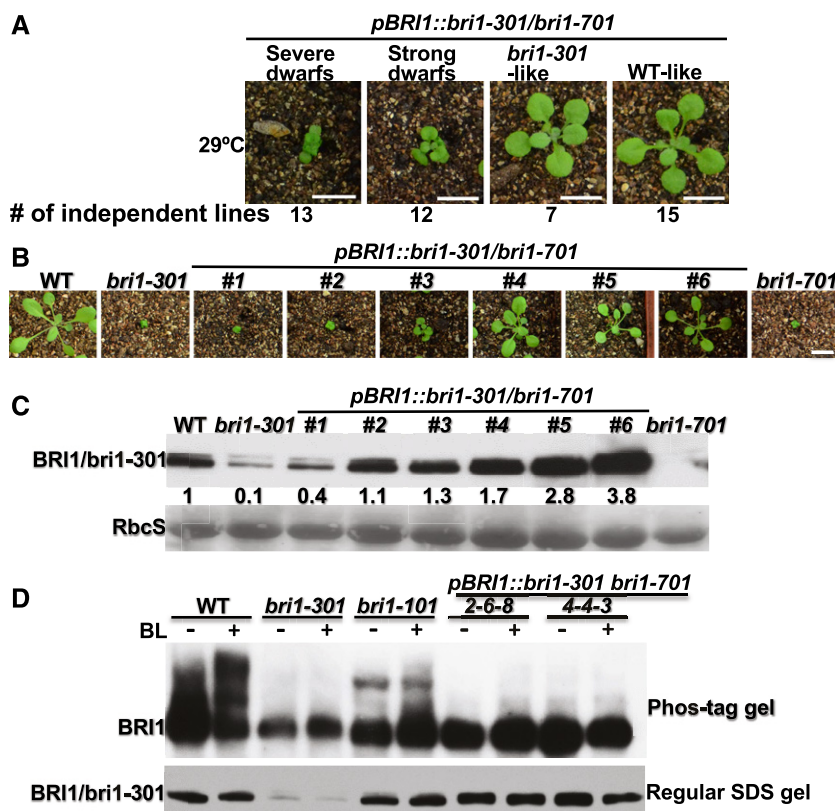


Figure 7. The 22°C to 29°C temperature increase also inhibits *bri1-301* activity. **A**, Phenotypic grouping of transgenic *pBRI1::bri1-301 bri1-701* lines grown in a 29°C growth chamber. The numbers indicate the numbers of transgenic lines (out of the same transformation experiment) exhibiting similar growth morphology to the plant shown above. **B**, Photographs of 18-d-old soil-grown plants in the 29°C growth chamber. **C**, Immunoblot analysis of BRI1/*bri1-301* protein abundance of the plants shown in **B**. The numbers shown between the two gel strips are the relative signal intensity of the *bri1-301* bands after normalization with the signals of the corresponding Coomassie Blue-stained RbcS bands. The signal intensity of each band was measured by ImageJ. **D**, Immunoblot analysis of BRI1/*bri1-301* phosphorylation status in 29°C-grown plants of the two characterized wild-type-like *pBRI1::bri1-301 bri1-701* lines shown in Figure 1D. The top strip is the anti-BRI1 immunoblot from a Phos-tag gel, while the bottom strip is the anti-BRI1 immunoblot from a regular SDS-PAGE of the same set of protein samples. WT, wild type.

the null *bri1-701* mutant clearly demonstrated that *bri1-301* absolutely requires its kinase activity for the weak growth phenotype, as all of the transgenic lines expressing these mutant *pBRI1::bri1-301* transgenes were morphologically indistinguishable from *bri1-701* (Fig. 2C).

The G989I Mutation Might Cause a Structural Defect of the BRI1 Kinase Domain That Is Partially Stabilized by Chaperones/Cochaperones in Planta

The Gly-989 residue mutated in *bri1-301* is located in the conserved kinase subdomain VIa (Li and Chory, 1997). While this residue is not conserved among the plant LRR-RLKs, it is absolutely conserved between BRI1 and its plant homologs (Sun et al., 2017). Analysis of the BRI1 kinase's crystal structure revealed that this residue is solvent exposed in the middle of the α E helix and is tightly packed against Asn-938 and Ala-1023 residues (Bojar et al., 2014; Fig. 8). Asn-938

occupies a strategic position in the α C- β 4 loop that facilitates the interaction of Leu-942 of the β 4 strand with Ile-931 of the α C helix. Ala-1023 is the first residue of the β 8 strand that flanks the highly conserved Asp-Phe-Gly motif of the activation loop, with the Asp-1027 residue interacting with the ATP-bound Mg^{2+} ion and Phe-1028 making hydrophobic interactions with Ile-931 of the α C helix and His-1007 of the His-Arg-Asp motif of the catalytic loop (Fig. 8). Leu-942, Ile-931, Phe-1028, and His-1007 form the so-called regulatory spine (R-spine) that is a hallmark of activated protein kinases (Taylor and Kornev, 2011). We suspected that the substitution of a small Gly-989 residue by a large hydrophobic Ile residue might affect the spatial positioning of the R-spine residues, thus preventing the assembly of the R-spine and greatly inhibiting BRI1's kinase activity. It is interesting that the same Gly-989 residue is changed to Glu in a newly discovered *bri1* allele, *bri1-707*, that has no observable growth phenotype (Sun et al., 2017).

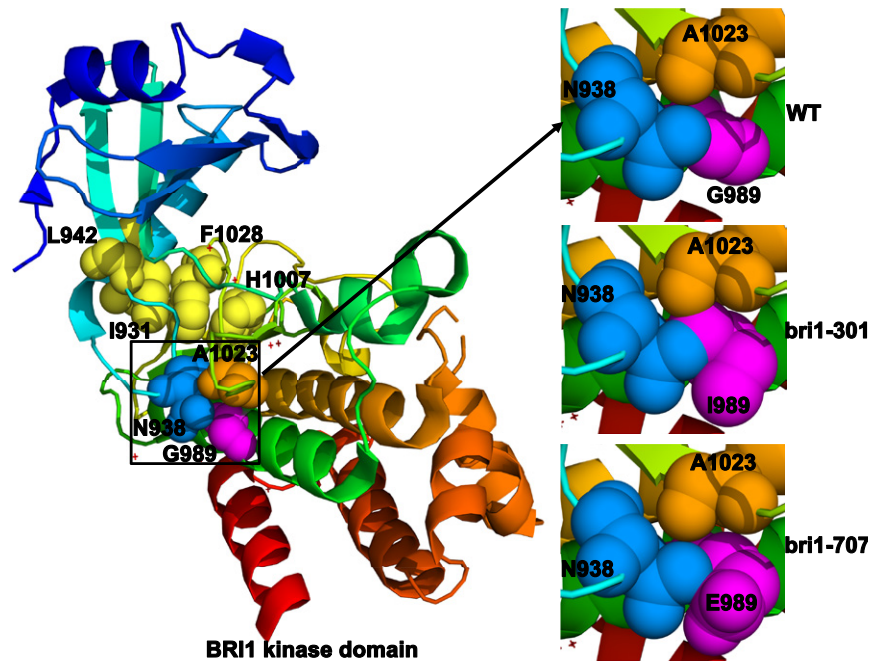


Figure 8. The G989I mutation likely causes a structural change in the BRI1 kinase domain. Shown on the left is the colored ribbon model of the crystal structure of the BRI1 kinase domain (Protein Data Bank no. 5LPY). The four hydrophobic amino acids that make up the conserved regulatory spine are shown with yellow spheres, Gly-989 is shown with purple spheres, Asn-938 is represented by pale blue spheres, and Ala-1023 is indicated by orange spheres. The relative positioning of the three tightly packed residues in wild-type BRI1 (WT), *bri1-301*, and *bri1-707* is shown on the right. The mutagenesis of Gly-989 to Ile-989 (in *bri1-301*) or Glu-989 (in *bri1-707*) was performed with PyMol (<http://www.pymol.org>).

Structural analysis by PyMol (<http://www.pymol.org>) revealed that the G989E substitution only slightly affects its packing with Asn-938 but not with Ala-1023 (Fig. 8), explaining its slightly reduced *in vitro* kinase activity and its slight impact on plant growth (Sun et al., 2017). This revelation is consistent with the recent finding that Gly-989 is often replaced by Glu and Asp in other Arabidopsis LRR-RLKs (Sun et al., 2017). It is quite possible that certain chaperones and/or cochaperones, such as HEAT SHOCK PROTEIN70 (HSP70)/90s, could buffer the structural defect of *bri1-301*, similar to what was demonstrated previously for the Arabidopsis HSP90s (Queitsch et al., 2002; Sangster et al., 2008). Consistent with our hypothesis, a loss-of-function mutation in Arabidopsis TWISTED DWARF1, a 42-kD FK506-binding protein (FKBP42) known to interact with HSP90 (Kamphausen et al., 2002), was shown recently to exhibit a strong synergistic interaction with *bri1-301* (Zhao et al., 2016). These chaperones and cochaperones might work together to allow the mutant *bri1-301* protein to exhibit a low kinase activity in planta, which is necessary and sufficient to confer the weak growth phenotype. Previous mathematical modeling coupled with a root growth stimulation assay suggested that the receptor activity of *bri1-301* is only ~1% to 3% that of the wild-type BRI1 (van Esse et al., 2012). It remains to be

tested if a 97% to 99% reduction in the BRI1 protein abundance could recapitulate the *bri1-301* phenotype.

The Rapid Degradation of the ER-Retained Form of *bri1-301* Is Not Mediated by the ERAD Machinery That Degrades *bri1-5and bri1-9*

In this study, we discovered the presence of a small pool of the ER-retained form of *bri1-301* at 22°C (Fig. 3, C and D), which was greatly increased when the mutant was grown at 29°C (Fig. 6F). A CHX-chasing experiment with a *bri1-301*-overexpressing *bri1-701* (*pBRI1::bri1-301 bri1-701*) transgenic line indicated that the ER-retained form of *bri1-301* is degraded very rapidly (Fig. 3D). These results suggested that Arabidopsis contains an inefficient quality-control system that recognizes and retains a transmembrane protein carrying a cytosolic structural defect yet houses a very efficient degradation system to remove such an ERAD-C client (an ERAD client carrying a structural defect in its cytosolic domain). Consistent with what has been learned in yeast cells (Carvalho et al., 2006), the degradation of such an ERAD-C substrate does not involve components of the highly conserved ERAD machinery that degrades ERAD-L and ERAD-M substrates carrying structural abnormalities in their luminal domain and transmembrane segment, respectively. Loss-of-function mutations of EBS5, EBS6, and EBS7 did not

suppress the *bri1-301* dwarfism or increase the accumulation of the ER-retained form of *bri1-301* at 22°C or 29°C (Figs. 3, E and F, and 6G). In yeast and mammalian cells, the removal of ERAD-C clients involves a different ERAD system that builds around a different ER membrane-anchored E3 ligase known as Degradation of alpha factor2-10 (Doa10; yeast) or Membrane associated RING-CH-type finger6 (MARCH6; mammalian cells; Hassink et al., 2005; Carvalho et al., 2006). Interestingly, the Arabidopsis genome encodes two homologs of the Doa10/MARCH6 protein, including SUPPRESSOR OF DRY2 DEFECTS1 (SUD1; also known as ECERIFERUM9) that was shown recently to be involved in cuticular wax biosynthesis (Lü et al., 2012; Doblas et al., 2013; Zhao et al., 2014). Further investigation is needed to fully understand the Arabidopsis quality-control mechanism that recognizes and degrades an ERAD-C substrate. A simple genetic cross with the T-DNA insertional mutants of SUD1 and its homolog will reveal if rapid removal of the ER-retained *bri1-301* proteins involves SUD1 and/or its close homolog, while proteomic studies of a transgenically expressed *bri1-301*-GFP fusion protein could identify proteins involved in recognizing and retaining *bri1-301* in the ER.

***bri1-301* Could Be a Model Protein to Study the PM-Associated Protein Quality-Control Mechanism in a Plant Model Organism**

Likely due to the presence of an inefficient ER recognition and retention system for an ERAD-C client, a large amount of *bri1-301* proteins successfully reach the PM. However, the G989I mutation that makes the ER-retained *bri1-301* protein extremely unstable also leads to accelerated degradation of the PM-localized *bri1-301* (Fig. 3D), suggesting the existence of a PM-associated quality-control (PMQC) system that detects the structural lesion of *bri1-301* and targets the mutant BR receptor for degradation. The PMQC system is an integral part of the cellular proteostasis network that constantly monitors the folding status of all cellular proteins and removes their incorrectly folded and structurally damaged conformers at all subcellular locations (Babst, 2014). Recent studies in yeast and mammalian cells have revealed at least two PMQC mechanisms for removing the structurally unstable proteins from the cell surface via ubiquitination, endocytosis, and lysosomal degradation (Okuyoneda et al., 2011; Apaja and Lukacs, 2014). These studies have implicated two E3 ubiquitin ligases in ubiquitinating the structurally defective PM proteins, including the mammalian Carboxy terminus of Hsc70-interacting protein (CHIP), a U-box domain-containing E3 ligase (Edkins, 2015), and the yeast HECT-type E3 ligase Reverses Spt-phenotype5 (Zhao et al., 2013). The Arabidopsis genome encodes a potential CHIP homolog known as AtCHIP1, which was implicated in stress tolerance, plant immunity, and chloroplast function (Yan et al., 2003; Luo et al., 2006; Shen et al., 2007a, 2007b; Wei et al., 2015;

Copeland et al., 2016), and at least seven HECT-type E3 ligases (Downes et al., 2003; Marín, 2013). Compared with what has been learned about the PMQC system in yeast and mammalian cells, almost nothing is known about a similar system in plants. Despite its faster degradation rate than the wild-type BRI1, *bri1-301* might share the same degradation pathway with wild-type BRI1, which was suggested recently to involve K63-linked polyubiquitination, endocytosis, and vacuolar degradation for its removal from the PM in a ligand-independent manner (Martins et al., 2015). The *bri1-301* mutant could be used as a convenient system for genetic dissection of a plant PMQC mechanism.

MATERIALS AND METHODS

Plant Materials and Growth Conditions

Arabidopsis (*Arabidopsis thaliana*) ecotypes Columbia-0 and Wassilewskija-2 were used as the wild-type controls for genetic, transgenic, and phenotypic analyses. The Arabidopsis mutants that were used in this study were all described previously, including *bri1-5* (Noguchi et al., 1999), *bri1-9* (Jin et al., 2007), *bri1-101* (Li and Chory, 1997), *bri1-301* (Xu et al., 2008), *bri1-701* (Gou et al., 2012), *bri1-702*, *bri1-703*, *bri1-704*, *bri1-707*, and *bri1-708* (Sun et al., 2017), *ehs5* (Su et al., 2011), *ehs6* (Su et al., 2012), and *ehs7* (Liu et al., 2015). Seed sterilization and seedling growth were performed following previously described protocols (Li et al., 2001).

Generation of Plasmid Constructs and Transgenic Plants

The *pBRI1::BRI1-GFP* construct was described previously (Friedrichsen et al., 2000) and was used to generate the *pBRI1::BRI1* plasmid by deleting the GFP-coding sequence using the ClonExpress II One Step cloning kit (Vazyme) and the *BRI1::BRI1* primer set (Supplemental Table S1). Both plasmids were used as templates to generate *pBRI1::bri1-301-GFP*, *pBRI1::bri1-301*, and other mutant constructs via a PCR-driven overlapping extension mutagenesis approach (Heckman and Pease, 2007) with mutagenesis primers and flanking primers listed in Supplemental Table S1. These newly created plasmids were fully sequenced to ensure no PCR-introduced error and used subsequently to transform the null *bri1-701* mutant and its wild-type control via the *Agrobacterium tumefaciens*-mediated floral dip method (Clough and Bent, 1998). Every analyzed transgenic plant was genotypically verified by PCR, and the expression of *bri1-301/BRI1* or their GFP fusions was analyzed by immunoblotting.

RNA Analysis

Total RNAs were isolated from 8-d-old Arabidopsis seedlings grown on 1/2 MS medium with the RNeasy plant mini kit (Qiagen) and were subsequently converted into first-strand cDNAs using the iScript gDNA Clear cDNA Synthesis Kit (Bio-Rad) according to the manufacturer's recommended protocols. To analyze the transcript abundance of the genes of interest, 0.5 µL of the first-strand cDNA templates was used for RT-qPCR amplification on a Bio-Rad CFX96 Touch system with the primer sets shown in Supplemental Table S1 and iTaq Universal SYBR Green Supermix (Bio-Rad). The *ACTIN* transcript was amplified using the *ACTIN* primer set (Supplemental Table S1) for an internal reference. For each transcript, the RT-qPCR assay was repeated four times.

Protein Analysis

Total proteins were extracted from whole seedlings grown on 1/2 MS agar medium or rosette leaves of soil-grown plants. Briefly, 30 mg of plant tissue for each sample was quickly frozen in liquid nitrogen, cryogenically ground into fine powder with steel beads in a mixer mill (MM400; Retsch), and dissolved in 150 µL of 2× SDS loading buffer (100 mM Tris-HCl, pH 6.8, 20%

[v/v] glycerol, 4% [w/v] SDS, 0.02% [w/v] Bromophenol Blue, and 100 mM DTT). The mixed crude extracts were heated at 95°C for 10 min and centrifuged immediately at 10,000g for 10 min. The cleared supernatants were used immediately for gel electrophoresis or treated with or without 1,000 units of Endo-Hf in 1× G5 buffer (New England Biolabs) for 1 h at 37°C. The treated or nontreated total proteins were separated by SDS-PAGE, transferred onto a polyvinylidene difluoride membrane (Bio-Rad), and analyzed by Coomassie Blue staining (for loading controls) or immunoblotting with antibodies generated against BRI1 (Mora-García et al., 2004), GFP (632381; Clontech), BES1 (Mora-García et al., 2004), or ACTIN (CW0264; Beijing CWBio). The quantification of relative BRI1/*brl1* abundance was performed using ImageJ (<https://imagej.nih.gov/ij/>) with scanned images of Coomassie Blue-stained gels or immunoblots after normalizing anti-BRI1 signals with the signal intensity of the corresponding RbcS or anti-ACTIN bands.

To perform coimmunoprecipitation experiments, seedlings were collected, immediately ground into fine powder in liquid nitrogen, and extracted with the immunoprecipitation buffer (2–3 mL g⁻¹ plant tissue; 50 mM Tris-HCl, pH 7.5, 50 mM NaCl, 0.2% [v/v] Triton X-100, 1 mM phenylmethylsulfonyl fluoride [Sigma-Aldrich], 1× cOmplete protease inhibitor cocktail [Roche], and 1× phosphatase inhibitor cocktail [BioTool Chemicals] that was added only for the immunoprecipitation experiments to detect protein phosphorylation). The dissolved crude extracts were centrifuged twice at 20,000g for 15 min each at 4°C. The resulting supernatants were collected and incubated with prewashed anti-GFP monoclonal antibody-agarose beads (D153-8; MBL) at 4°C for 4 h. The agarose beads were subsequently washed four times with the immunoprecipitation buffer and four additional times with the washing buffer (the immunoprecipitation buffer excluding Triton X-100). The proteins remaining on the beads were removed with 2× SDS loading buffer and 5 min of boiling at 95°C. After 10 min of centrifugation, the supernatants were subject to SDS-PAGE and analyzed by Coomassie Blue staining or immunoblotting with appropriate antibodies.

To analyze the phosphorylation status of BRI1 and *brl1*-301, total protein extracts were loaded onto Zn²⁺-Phos-tag SDS-PAGE gels containing 50 μM Phos-tag Acrylamide (Wako Laboratory Chemicals). The detailed procedure was performed according to a manufacturer's recommended protocol (http://www.wako-chem.co.jp/english/labchem/product/life/Phos-tag/pdf/AAL107_v12.pdf).

Treatment with Chemicals

To analyze BRZ sensitivity, sterilized Arabidopsis seeds were planted directly on 1/2 MS agar medium containing varying concentrations of BRZ (TCI Chemicals). After 2 h of light exposure, the petri dishes were wrapped with light-proof aluminum foil and kept in total darkness for 5 d in a 22°C or 29°C growth chamber for seed germination and seedling growth. Seedlings were removed carefully from the petri dishes, photographed immediately, and their hypocotyl lengths were quantified by ImageJ (<https://imagej.nih.gov/ij/>). To investigate the effect of BL on the BES1 phosphorylation status and transcript abundance of selected BR-responsive genes, 8-d-old light-grown seedlings were removed carefully from petri dishes, immediately transferred into liquid 1/2 MS medium supplemented with or without 1 μM BL (Wako Chemicals), incubated for 2 h, and subsequently harvested and placed in liquid nitrogen for the extraction of total proteins and RNAs or storage in a -80°C freezer. To analyze the protein stability of BRI1 and its mutant variants, 2-week-old seedlings grown on 1/2 MS agar medium were transferred carefully into liquid 1/2 MS medium supplemented with or without 180 μM CHX (Sigma-Aldrich), 50 μM Kif (Toronto Research Chemicals), or 80 μM MG115 (Sigma-Aldrich), incubated for different times, and subsequently collected into liquid nitrogen for total protein extraction.

Endo-H and Trypsin Sensitivity Assays

The Endo-H assay was performed according to a previously described procedure (Hong et al., 2008). To carry out the trypsin sensitivity assay, 10-d-old seedlings grown on 1/2 MS agar medium were collected, immediately ground into a fine powder in liquid nitrogen, dissolved in 100 μL of phosphate-buffered saline solution (137 mM NaCl, 2.7 mM KCl, 10 mM Na₂HPO₄, and 1.8 mM KH₂PO₄, pH 7.4) containing 0.4% (v/v) Triton X-100, and centrifuged at 10,000g for 5 min at 4°C to remove cellular debris and insoluble materials. The resulting supernatant was mixed with trypsin (Sigma-Aldrich) at 5 μg mL⁻¹ and incubated on ice. Aliquots of 30 μL of the reaction mixtures were removed at different time points, immediately mixed with 20 μL of 2× SDS

loading buffer for denaturing by 15 min of boiling, and subsequently frozen in liquid nitrogen. The frozen samples were reheated, separated by SDS-PAGE, and subsequently analyzed by immunoblotting.

Accession Numbers

Sequence data from this article can be found in the GenBank/EMBL data libraries under the following accession numbers: *BRI1*, AAC49810.1; *CPD*, NM120651; *DWF4*, AF044216; *SAUR-AC1*, S70188.1; and *WRKY13*, NM120101.

Supplemental Data

The following supplemental materials are available.

Supplemental Figure S1. RT-qPCR analysis of *DWF4* transcript abundance.

Supplemental Figure S2. RT-qPCR analysis of *BRI1/brl1*-301 transcript abundance.

Supplemental Table S1. Oligonucleotides used in this study.

ACKNOWLEDGMENTS

We thank Dr. Yanhai Yin for supplying the anti-BES1 antibody and Dr. Jia Li for seeds of Arabidopsis *brl1*-701-704, *brl1*-707, and *brl1*-708 mutants and for discussing his similar study with us. We also thank additional members of the Li laboratory for stimulating discussion throughout this study.

Received April 13, 2018; accepted October 9, 2018; published October 17, 2018.

LITERATURE CITED

- Albrecht C, Boutrot F, Segonzac C, Schwessinger B, Gimenez-Ibanez S, Chinchilla D, Rathjen JP, de Vries SC, Zipfel C (2012) Brassinosteroids inhibit pathogen-associated molecular pattern-triggered immune signaling independent of the receptor kinase BAK1. *Proc Natl Acad Sci USA* **109**: 303–308
- Apaja PM, Lukacs GL (2014) Protein homeostasis at the plasma membrane. *Physiology (Bethesda)* **29**: 265–277
- Asami T, Min YK, Nagata N, Yamagishi K, Takatsuto S, Fujioka S, Murofushi N, Yamaguchi I, Yoshida S (2000) Characterization of brassinazole, a triazole-type brassinosteroid biosynthesis inhibitor. *Plant Physiol* **123**: 93–100
- Babst M (2014) Quality control at the plasma membrane: One mechanism does not fit all. *J Cell Biol* **205**: 11–20
- Bancoş S, Nomura T, Sato T, Molnár G, Bishop GJ, Koncz C, Yokota T, Nagy E, Szekeres M (2002) Regulation of transcript levels of the Arabidopsis cytochrome P450 genes involved in brassinosteroid biosynthesis. *Plant Physiol* **130**: 504–513
- Belkhadir Y, Jaillais Y (2015) The molecular circuitry of brassinosteroid signaling. *New Phytol* **206**: 522–540
- Belkhadir Y, Durbak A, Wierzbza M, Schmitz RJ, Aguirre A, Michel R, Rowe S, Fujioka S, Tax FE (2010) Intragenic suppression of a trafficking-defective brassinosteroid receptor mutant in Arabidopsis. *Genetics* **185**: 1283–1296
- Bojar D, Martinez J, Santiago J, Rybin V, Bayliss R, Hothorn M (2014) Crystal structures of the phosphorylated BRI1 kinase domain and implications for brassinosteroid signal initiation. *Plant J* **78**: 31–43
- Carvalho P, Goder V, Rapoport TA (2006) Distinct ubiquitin-ligase complexes define convergent pathways for the degradation of ER proteins. *Cell* **126**: 361–373
- Clough SJ, Bent AF (1998) Floral dip: A simplified method for Agrobacterium-mediated transformation of Arabidopsis thaliana. *Plant J* **16**: 735–743
- Clouse SD (1996) Molecular genetic studies confirm the role of brassinosteroids in plant growth and development. *Plant J* **10**: 1–8
- Clouse SD (2011) Brassinosteroids. *The Arabidopsis Book* **9**: e0151
- Clouse SD, Langford M, McMorris TC (1996) A brassinosteroid-insensitive mutant in Arabidopsis thaliana exhibits multiple defects in growth and development. *Plant Physiol* **111**: 671–678
- Copeland C, Ao K, Huang Y, Tong M, Li X (2016) The evolutionarily conserved E3 ubiquitin ligase AtCHIP contributes to plant immunity. *Front Plant Sci* **7**: 309

- Doblas VG, Amorim-Silva V, Posé D, Rosado A, Esteban A, Arró M, Azevedo H, Bombarely A, Borsani O, Valpuesta V, (2013) The SUD1 gene encodes a putative E3 ubiquitin ligase and is a positive regulator of 3-hydroxy-3-methylglutaryl coenzyme A reductase activity in Arabidopsis. *Plant Cell* 25: 728–743
- Domagalska MA, Schomburg FM, Amasino RM, Vierstra RD, Nagy F, Davis SJ (2007) Attenuation of brassinosteroid signaling enhances FLC expression and delays flowering. *Development* 134: 2841–2850
- Downes BP, Stupar RM, Gingerich DJ, Vierstra RD (2003) The HECT ubiquitin-protein ligase (UPL) family in Arabidopsis: UPL3 has a specific role in trichome development. *Plant J* 35: 729–742
- Edkins AL (2015) CHIP: A co-chaperone for degradation by the proteasome. *Subcell Biochem* 78: 219–242
- Elbein AD, Tropea JE, Mitchell M, Kaushal GP (1990) Kifunensine, a potent inhibitor of the glycoprotein processing mannosidase I. *J Biol Chem* 265: 15599–15605
- Friedrichsen DM, Joazeiro CA, Li J, Hunter T, Chory J (2000) Brassinosteroid-insensitive-1 is a ubiquitously expressed leucine-rich repeat receptor serine/threonine kinase. *Plant Physiol* 123: 1247–1256
- Gou X, Yin H, He K, Du J, Yi J, Xu S, Lin H, Clouse SD, Li J (2012) Genetic evidence for an indispensable role of somatic embryogenesis receptor kinases in brassinosteroid signaling. *PLoS Genet* 8: e1002452
- Gray WM, Ostin A, Sandberg G, Romano CP, Estelle M (1998) High temperature promotes auxin-mediated hypocotyl elongation in Arabidopsis. *Proc Natl Acad Sci USA* 95: 7197–7202
- Greene EA, Codomo CA, Taylor NE, Henikoff JG, Till BJ, Reynolds SH, Enns LC, Burtner C, Johnson JE, Odden AR, (2003) Spectrum of chemically induced mutations from a large-scale reverse-genetic screen in Arabidopsis. *Genetics* 164: 731–740
- Ha Y, Shang Y, Nam KH (2016) Brassinosteroids modulate ABA-induced stomatal closure in Arabidopsis. *J Exp Bot* 67: 6297–6308
- Hanks SK, Quinn AM, Hunter T (1988) The protein kinase family: Conserved features and deduced phylogeny of the catalytic domains. *Science* 241: 42–52
- Hao Y, Wang H, Qiao S, Leng L, Wang X (2016) Histone deacetylase HDA6 enhances brassinosteroid signaling by inhibiting the BIN2 kinase. *Proc Natl Acad Sci USA* 113: 10418–10423
- Hassink G, Kikkert M, van Voorden S, Lee SJ, Spaapen R, van Laar T, Coleman CS, Bartee E, Früh K, Chau V, (2005) TEB4 is a C4HC3 RING finger-containing ubiquitin ligase of the endoplasmic reticulum. *Biochem J* 388: 647–655
- He Z, Wang ZY, Li J, Zhu Q, Lamb C, Ronald P, Chory J (2000) Perception of brassinosteroids by the extracellular domain of the receptor kinase BRI1. *Science* 288: 2360–2363
- Heckman KL, Pease LR (2007) Gene splicing and mutagenesis by PCR-driven overlap extension. *Nat Protoc* 2: 924–932
- Hong Z, Jin H, Tzfira T, Li J (2008) Multiple mechanism-mediated retention of a defective brassinosteroid receptor in the endoplasmic reticulum of Arabidopsis. *Plant Cell* 20: 3418–3429
- Hong Z, Jin H, Fitchette AC, Xia Y, Monk AM, Faye L, Li J (2009) Mutations of an α 1,6 mannosyltransferase inhibit endoplasmic reticulum-associated degradation of defective brassinosteroid receptors in Arabidopsis. *Plant Cell* 21: 3792–3802
- Hothorn M, Belkhadir Y, Dreux M, Dabi T, Noel JP, Wilson IA, Chory J (2011) Structural basis of steroid hormone perception by the receptor kinase BRI1. *Nature* 474: 467–471
- Jin H, Yan Z, Nam KH, Li J (2007) Allele-specific suppression of a defective brassinosteroid receptor reveals a physiological role of UGGT in ER quality control. *Mol Cell* 26: 821–830
- Kamphausen T, Fanghänel J, Neumann D, Schulz B, Rahfeld JU (2002) Characterization of Arabidopsis thaliana AtFKBP42 that is membrane-bound and interacts with Hsp90. *Plant J* 32: 263–276
- Kang B, Wang H, Nam KH, Li J, Li J (2010) Activation-tagged suppressors of a weak brassinosteroid receptor mutant. *Mol Plant* 3: 260–268
- Kauschmann A, Jessop A, Koncz C, Szekeres M, Willmitzer L, Altmann T (1996) Genetic evidence for an essential role of brassinosteroids in plant development. *Plant J* 9: 701–713
- Kim TW, Lee SM, Joo SH, Yun HS, Lee Y, Kaufman PB, Kirakosyan A, Kim SH, Nam KH, Lee JS, (2007) Elongation and gravitropic responses of Arabidopsis roots are regulated by brassinolide and IAA. *Plant Cell Environ* 30: 679–689
- Kinoshita E, Kinoshita-Kikuta E, Koike T (2009) Separation and detection of large phosphoproteins using Phos-tag SDS-PAGE. *Nat Protoc* 4: 1513–1521
- Kinoshita T, Caño-Delgado A, Seto H, Hiranuma S, Fujioka S, Yoshida S, Chory J (2005) Binding of brassinosteroids to the extracellular domain of plant receptor kinase BRI1. *Nature* 433: 167–171
- Koini MA, Alvey L, Allen T, Tilley CA, Harberd NP, Whitelam GC, Franklin KA (2009) High temperature-mediated adaptations in plant architecture require the bHLH transcription factor PIF4. *Curr Biol* 19: 408–413
- Li J, Chory J (1997) A putative leucine-rich repeat receptor kinase involved in brassinosteroid signal transduction. *Cell* 90: 929–938
- Li J, Nam KH (2002) Regulation of brassinosteroid signaling by a GSK3/SHAGGY-like kinase. *Science* 295: 1299–1301
- Li J, Nagpal P, Vitart V, McMorris TC, Chory J (1996) A role for brassinosteroids in light-dependent development of Arabidopsis. *Science* 272: 398–401
- Li J, Nam KH, Vafeados D, Chory J (2001) BIN2, a new brassinosteroid-insensitive locus in Arabidopsis. *Plant Physiol* 127: 14–22
- Li J, Wen J, Lease KA, Doke JT, Tax FE, Walker JC (2002) BAK1, an Arabidopsis LRR receptor-like protein kinase, interacts with BRI1 and modulates brassinosteroid signaling. *Cell* 110: 213–222
- Liu Y, Li J (2014) Endoplasmic reticulum-mediated protein quality control in Arabidopsis. *Front Plant Sci* 5: 162
- Liu Y, Zhang C, Wang D, Su W, Liu L, Wang M, Li J (2015) EBS7 is a plant-specific component of a highly conserved endoplasmic reticulum-associated degradation system in Arabidopsis. *Proc Natl Acad Sci USA* 112: 12205–12210
- Lü S, Zhao H, Des Marais DL, Parsons EP, Wen X, Xu X, Bangarusamy DK, Wang G, Rowland O, Juenger T, (2012) Arabidopsis ECERIFERUM9 involvement in cuticle formation and maintenance of plant water status. *Plant Physiol* 159: 930–944
- Luo J, Shen G, Yan J, He C, Zhang H (2006) AtCHIP functions as an E3 ubiquitin ligase of protein phosphatase 2A subunits and alters plant response to abscisic acid treatment. *Plant J* 46: 649–657
- Marín I (2013) Evolution of plant HECT ubiquitin ligases. *PLoS ONE* 8: e68536
- Martins S, Dohmann EM, Cayrel A, Johnson A, Fischer W, Pojer F, Satiat-Jeunemaitre B, Jaillais Y, Chory J, Geldner N, (2015) Internalization and vacuolar targeting of the brassinosteroid hormone receptor BRI1 are regulated by ubiquitination. *Nat Commun* 6: 6151
- Mathur J, Molnár G, Fujioka S, Takatsuto S, Sakurai A, Yokota T, Adam G, Voigt B, Nagy F, Maas C, (1998) Transcription of the Arabidopsis CPD gene, encoding a steroidogenic cytochrome P450, is negatively controlled by brassinosteroids. *Plant J* 14: 593–602
- Mora-García S, Vert G, Yin Y, Caño-Delgado A, Cheong H, Chory J (2004) Nuclear protein phosphatases with Kelch-repeat domains modulate the response to brassinosteroids in Arabidopsis. *Genes Dev* 18: 448–460
- Nagata N, Min YK, Nakano T, Asami T, Yoshida S (2000) Treatment of dark-grown Arabidopsis thaliana with a brassinosteroid-biosynthesis inhibitor, brassinazole, induces some characteristics of light-grown plants. *Planta* 211: 781–790
- Nakamura A, Shimada Y, Goda H, Fujiwara MT, Asami T, Yoshida S (2003) AXR1 is involved in BR-mediated elongation and SAUR-AC1 gene expression in Arabidopsis. *FEBS Lett* 553: 28–32
- Nam KH, Li J (2002) BRI1/BAK1, a receptor kinase pair mediating brassinosteroid signaling. *Cell* 110: 203–212
- Noguchi T, Fujioka S, Choe S, Takatsuto S, Yoshida S, Yuan H, Feldmann KA, Tax FE (1999) Brassinosteroid-insensitive dwarf mutants of Arabidopsis accumulate brassinosteroids. *Plant Physiol* 121: 743–752
- Okiyonedo T, Apaja PM, Lukacs GL (2011) Protein quality control at the plasma membrane. *Curr Opin Cell Biol* 23: 483–491
- Queitsch C, Sangster TA, Lindquist S (2002) Hsp90 as a capacitor of phenotypic variation. *Nature* 417: 618–624
- Robbins PW, Trimble RB, Wirth DF, Hering C, Maley F, Maley GF, Das R, Gibson BW, Royal N, Biemann K (1984) Primary structure of the Streptomyces enzyme endo-beta-N-acetylglucosaminidase H. *J Biol Chem* 259: 7577–7583
- Sangster TA, Salathia N, Lee HN, Watanabe E, Schellenberg K, Morneau K, Wang H, Undurraga S, Queitsch C, Lindquist S (2008) HSP90-buffered genetic variation is common in Arabidopsis thaliana. *Proc Natl Acad Sci USA* 105: 2969–2974
- Santiago J, Henzler C, Hothorn M (2013) Molecular mechanism for plant steroid receptor activation by somatic embryogenesis co-receptor kinases. *Science* 341: 889–892
- Schwessinger B, Roux M, Kadota Y, Ntoukakis V, Sklenar J, Jones A, Zipfel C (2011) Phosphorylation-dependent differential regulation of plant growth,






- cell death, and innate immunity by the regulatory receptor-like kinase BAK1. *PLoS Genet* 7: e1002046
- Shang Y, Lee MM, Li J, Nam KH (2011) Characterization of cp3 reveals a new *bri1* allele, *bri1-120*, and the importance of the LRR domain of BRI1 mediating BR signaling. *BMC Plant Biol* 11: 8
- She J, Han Z, Kim TW, Wang J, Cheng W, Chang J, Shi S, Wang J, Yang M, Wang ZY, (2011) Structural insight into brassinosteroid perception by BRI1. *Nature* 474: 472–476
- Shen G, Adam Z, Zhang H (2007a) The E3 ligase AtCHIP ubiquitylates FtsH1, a component of the chloroplast FtsH protease, and affects protein degradation in chloroplasts. *Plant J* 52: 309–321
- Shen G, Yan J, Pasapula V, Luo J, He C, Clarke AK, Zhang H (2007b) The chloroplast protease subunit ClpP4 is a substrate of the E3 ligase AtCHIP and plays an important role in chloroplast function. *Plant J* 49: 228–237
- Shi C, Qi C, Ren H, Huang A, Hei S, She X (2015) Ethylene mediates brassinosteroid-induced stomatal closure via *Ga* protein-activated hydrogen peroxide and nitric oxide production in Arabidopsis. *Plant J* 82: 280–301
- Su W, Liu Y, Xia Y, Hong Z, Li J (2011) Conserved endoplasmic reticulum-associated degradation system to eliminate mutated receptor-like kinases in Arabidopsis. *Proc Natl Acad Sci USA* 108: 870–875
- Su W, Liu Y, Xia Y, Hong Z, Li J (2012) The Arabidopsis homolog of the mammalian OS-9 protein plays a key role in the endoplasmic reticulum-associated degradation of misfolded receptor-like kinases. *Mol Plant* 5: 929–940
- Sun C, Yan K, Han JT, Tao L, Lv MH, Shi T, He YX, Wierzbza M, Tax FE, Li J (2017) Scanning for new BRI1 mutations via TILLING analysis. *Plant Physiol* 174: 1881–1896
- Szekeres M, Németh K, Koncz-Kálmán Z, Mathur J, Kauschmann A, Altmann T, Rédei GP, Nagy F, Schell J, Koncz C (1996) Brassinosteroids rescue the deficiency of CYP90, a cytochrome P450, controlling cell elongation and de-etiolation in Arabidopsis. *Cell* 85: 171–182
- Tanaka K, Asami T, Yoshida S, Nakamura Y, Matsuo T, Okamoto S (2005) Brassinosteroid homeostasis in Arabidopsis is ensured by feedback expressions of multiple genes involved in its metabolism. *Plant Physiol* 138: 1117–1125
- Taylor SS, Kornev AP (2011) Protein kinases: Evolution of dynamic regulatory proteins. *Trends Biochem Sci* 36: 65–77
- Unterholzner SJ, Rozhon W, Papacek M, Ciomas J, Lange T, Kugler KG, Mayer KF, Sieberer T, Poppenberger B (2015) Brassinosteroids are master regulators of gibberellin biosynthesis in Arabidopsis. *Plant Cell* 27: 2261–2272
- van Esse GW, van Mourik S, Stigter H, ten Hove CA, Molenaar J, de Vries SC (2012) A mathematical model for BRASSINOSTEROID INSENSITIVE1-mediated signaling in root growth and hypocotyl elongation. *Plant Physiol* 160: 523–532
- Wang H, Zhu Y, Fujioka S, Asami T, Li J, Li J (2009) Regulation of Arabidopsis brassinosteroid signaling by atypical basic helix-loop-helix proteins. *Plant Cell* 21: 3781–3791
- Wang R, Liu M, Yuan M, Osés-Prieto JA, Cai X, Sun Y, Burlingame AL, Wang ZY, Tang W (2016) The brassinosteroid-activated BRI1 receptor kinase is switched off by dephosphorylation mediated by cytoplasm-localized PP2A B' subunits. *Mol Plant* 9: 148–157
- Wang X, Goshe MB, Soderblom EJ, Phinney BS, Kuchar JA, Li J, Asami T, Yoshida S, Huber SC, Clouse SD (2005) Identification and functional analysis of in vivo phosphorylation sites of the Arabidopsis BRASSINOSTEROID-INSENSITIVE1 receptor kinase. *Plant Cell* 17: 1685–1703
- Wang X, Kota U, He K, Blackburn K, Li J, Goshe MB, Huber SC, Clouse SD (2008) Sequential transphosphorylation of the BRI1/BAK1 receptor kinase complex impacts early events in brassinosteroid signaling. *Dev Cell* 15: 220–235
- Wang ZY, Seto H, Fujioka S, Yoshida S, Chory J (2001) BRI1 is a critical component of a plasma-membrane receptor for plant steroids. *Nature* 410: 380–383
- Wei J, Qiu X, Chen L, Hu W, Hu R, Chen J, Sun L, Li L, Zhang H, Lv Z, (2015) The E3 ligase AtCHIP positively regulates Clp proteolytic subunit homeostasis. *J Exp Bot* 66: 5809–5820
- Xu W, Huang J, Li B, Li J, Wang Y (2008) Is kinase activity essential for biological functions of BRI1? *Cell Res* 18: 472–478
- Yan J, Wang J, Li Q, Hwang JR, Patterson C, Zhang H (2003) AtCHIP, a U-box-containing E3 ubiquitin ligase, plays a critical role in temperature stress tolerance in Arabidopsis. *Plant Physiol* 132: 861–869
- Zhao B, Lv M, Feng Z, Campbell T, Liscum E, Li J (2016) TWISTED DWARF 1 associates with BRASSINOSTEROID-INSENSITIVE 1 to regulate early events of the brassinosteroid signaling pathway. *Mol Plant* 9: 582–592
- Zhao H, Zhang H, Cui P, Ding F, Wang G, Li R, Jenks MA, Lü S, Xiong L (2014) The putative E3 ubiquitin ligase ECERIFERUM9 regulates abscisic acid biosynthesis and response during seed germination and postgermination growth in Arabidopsis. *Plant Physiol* 165: 1255–1268
- Zhao Y, Macgurn JA, Liu M, Emr S (2013) The ART-Rsp5 ubiquitin ligase network comprises a plasma membrane quality control system that protects yeast cells from proteotoxic stress. *eLife* 2: e00459

ARTICLE

<https://doi.org/10.1038/s41467-019-11480-7>

OPEN

PAWH1 and PAWH2 are plant-specific components of an Arabidopsis endoplasmic reticulum-associated degradation complex

Liangguang Lin ^{1,2,7}, Congcong Zhang^{1,2,7}, Yongwu Chen^{1,2}, Yi Wang^{1,2}, Dinghe Wang^{1,3}, Xiaolei Liu¹, Muyang Wang ³, Juan Mao ^{4,5}, Jianjun Zhang ^{4,5}, Weiman Xing¹, Linchuan Liu^{4,5} & Jianming Li ^{4,5,6}

Endoplasmic reticulum-associated degradation (ERAD) is a unique mechanism to degrade misfolded proteins via complexes containing several highly-conserved ER-anchored ubiquitin ligases such as HMG-CoA reductase degradation1 (Hrd1). Arabidopsis has a similar Hrd1-containing ERAD machinery; however, our knowledge of this complex is limited. Here we report two closely-related Arabidopsis proteins, Protein Associated With Hrd1-1 (PAWH1) and PAWH2, which share a conserved domain with yeast Altered Inheritance of Mitochondria24. PAWH1 and PAWH2 localize to the ER membrane and associate with Hrd1 via EMS-mutagenized Bri1 Suppressor7 (EBS7), a plant-specific component of the Hrd1 complex. Simultaneously elimination of two PAWHs constitutively activates the unfolded protein response and compromises stress tolerance. Importantly, the *pawh1 pawh2* double mutation reduces the protein abundance of EBS7 and Hrd1 and inhibits degradation of several ERAD substrates. Our study not only discovers additional plant-specific components of the Arabidopsis Hrd1 complex but also reveals a distinct mechanism for regulating the Hrd1 stability.

¹Shanghai Center for Plant Stress Biology, Chinese Academy of Sciences, 201602 Shanghai, China. ²University of Chinese Academy of Sciences, 100004 Beijing, China. ³Shanghai Institute of Plant Physiology and Ecology, The Center of Excellence for Molecular Plant Sciences, Chinese Academy of Sciences, 300 Fenglin Road, 200032 Shanghai, China. ⁴Guangdong Key Laboratory for Innovative Development and Utilization of Forest Plant Germplasm, College of Forestry and Landscape Architecture, South China Agricultural University, 510642 Guangzhou, China. ⁵State Key Laboratory for Conservation and Utilization of Subtropical Agro-Bioresources, South China Agricultural University, 510642 Guangzhou, China. ⁶Department of Molecular, Cellular, and Developmental Biology, University of Michigan, Ann Arbor, MI 48109-1048, USA. ⁷These authors contributed equally: Liangguang Lin, Congcong Zhang. Correspondence and requests for materials should be addressed to L.L. (email: lliu@scau.edu.cn) or to J.L. (email: jian@umich.edu)

Endoplasmic reticulum-associated degradation (ERAD) is an integral part of the ER-mediated protein quality control system, which constantly monitors the folding status of secretory and membrane proteins, repairs misfolding proteins, and degrades irreparable terminally misfolded proteins¹. ERAD is a highly conserved degradation mechanism that involves substrate recognition, ubiquitination at the cytosolic surface of the ER membrane, retrotranslocation through ER membrane-embedded retrotranslocons, and eventual degradation by cytosolic proteasome². The ERAD machinery builds around several ER membrane-anchored ubiquitin (E3) ligases that recognize different types of ERAD clients carrying structural defects in their luminal domains, transmembrane domains, or cytosolic domains (known as ERAD-L, ERAD-M, and ERAD-C substrates, respectively)³. One of the well-studied ERAD system is a multiprotein complex centered around an ER membrane-anchored ubiquitin E3 ligase known as HMG-CoA reductase degradation1 (Hrd1) in yeast⁴ [HRD1 and glycoprotein 78 (gp78) in mammals^{5,6}]. The Hrd1 complex is known to degrade ERAD-L and ERAD-M substrates and contains several other highly conserved membrane and luminal proteins³. They include Hrd3⁷ [Sel1L (Suppressor of lin-12-like) in mammals⁸], Yos9 (Yeast OS-9 homolog)^{9,10} [OS-9 (Osteosarcoma amplified 9), and XTP3-B (XTP3-transactivated protein B) in mammals^{11,12}], Usa1¹³ [U1 SNP1-associated protein 1; HERP for Homocysteine-induced ER Protein in mammals¹⁴], Der1 (Degradation in the endoplasmic reticulum1)¹⁵ [DERLIN1-3 (Der-like domain-containing 1-3) in mammals¹⁶]. The Hrd1 complex also includes one or more ubiquitin-conjugating enzyme (E2), such as the ER membrane-anchored UBC6 (Ubiquitin-Conjugating 6) [Ube2j2 (Ubiquitin-conjugating enzyme E2 j2) in mammals¹⁷] and a cytosolic E2 UBC7 (Ube2g2 in mammals¹⁸) with its ER membrane-anchored recruiter Cue1 (Coupling of Ubiquitin conjugation to ER degradation that has no mammalian homolog)¹⁹. Biochemical and genetic studies in yeast and mammalian cells have shown that terminally misfolded glycoproteins with a unique asparagine-linked glycan (N-glycan) structure carrying an exposed α 1,6-mannose residue are recruited to Hrd1 through a bipartite recruitment mechanism that uses Yos9/OS-9 to bind the α 1,6-mannose-exposed N-glycans and Hrd3/Sel1L to bind exposed hydrophobic amino acid patches of misfolded glycoproteins²⁰. A recruited ERAD client is subsequently ubiquitinated and retrotranslocated, which is likely mediated by Hrd1 in yeast²¹, into the cytosol where the ubiquitinated ERAD substrate is degraded by the 26S proteasome. In both yeast and mammalian cells, deleting Hrd3/Sel1L significantly reduces the stability of Hrd1/HRD1^{7,22,23}. Interestingly, while the Δ hrd3-induced autodegradation requires Usa1 in yeast cells²⁴, the loss-of-Sel1L-caused HRD1 instability does not involve HERP in mammalian cells^{23,25}.

Recent studies have revealed that Arabidopsis has a similar Hrd1-mediated ERAD machinery²⁶. This system is known to degrade two ER-retained mutant forms of the brassinosteroid (BR) receptor BRASSINOSTEROID-INSENSITIVE 1 (BRI1), bri1-5 and bri1-9^{27,28}, a misfolded conform of an Arabidopsis immunity receptor EF-Tu Receptor (EFR) produced in an Arabidopsis mutant defective in an ER-luminal protein folding sensor^{29,30}, several engineered ERAD substrates^{31–34}, and an ERAD component³⁵. These studies not only identified conserved ERAD components in Arabidopsis, such as Hrd1a and Hrd1b^{35,36}, EBS5 (EMS-mutagenized bri1 suppressor 5; also known as HRD3A)^{34,36}, EBS6 (also known as AtOS9)^{37,38}, and UBC32 (Ubiquitin Conjugase 32)³³, which are homologs of the yeast Hrd1, Hrd3, Yos9, and Ubc7, respectively, but also discovered a plant-specific component known as EBS7 that regulates the protein stability of Hrd1a³⁹. Analysis of the Arabidopsis genome fails to discover Arabidopsis homologs of Cue1 and Usa1

but identified three Arabidopsis homologs of Der1 [(Der1, Der2.1, and Der2.2)⁴⁰]. Compared to what has learnt from the yeast and mammalian systems, our knowledge of the plant Hrd1 ERAD complex remains limited²⁶. For example, little is known about the composition and organization of the Arabidopsis Hrd1 complex, and it remains to be determined if the Arabidopsis Hrd1 ERAD complex contains a Der1/Derlin homolog. We also know little about how the protein stability and biochemical activity of Hrd1 are regulated in plants and whether or not the Arabidopsis Hrd1 is also involved in retrotranslocating its ERAD clients. In order to expand our understanding of the plant ERAD mechanism, we took a proteomic approach with independently generated transgenic lines expressing epitope-tagged Hrd1a/EBS7 to identify proteins that interact with both EBS7 and Hrd1a. Our subsequent biochemical and genetic studies demonstrated that two paralogous Arabidopsis proteins, named hereinafter as PAWH1 and 2 for Protein Associated With Hrd1, are crucial core components of the Arabidopsis Hrd1-containing ERAD machinery and are required to maintain the protein stability of both EBS7 and Hrd1a.

Results

Identification of PAWH1 and PAWH2 via a proteomic approach. To identify additional components of the Arabidopsis Hrd1-complex, we employed a proteomic approach of immunoprecipitation coupled with mass spectrometry. We generated several transgenic lines expressing a fusion protein of green fluorescent protein (GFP) with the Arabidopsis Hrd1a (Hrd1a-GFP)³⁶, one of the two Arabidopsis Hrd1 homologs, or MYC/HA-tagged EBS7, a newly identified plant-specific component of the Arabidopsis ERAD machinery crucial for maintaining the Hrd1a stability³⁹. Our previous studies have shown that simultaneous elimination of the two Arabidopsis Hrd1 homologs, Hrd1a and Hrd1b, or loss-of-function mutations in EBS7, inhibit ERAD of bri1-5 and bri1-9, two ER-retained mutant variant of the BR receptor BRI1 carrying a Cys⁶⁹-Tyr mutation and a Ser⁶⁶²-Phe mutation in its extracellular domain, respectively^{28,41}. Consequently, a small percentage of ER-accumulated bri1-5 and bri1-9 proteins leak out of the ER, likely due to saturation of their retention mechanisms, to reach the PM where the two mutant receptors bind extracellular BRs to promote plant growth, resulting in phenotypic suppression of the corresponding bri1-5 and bri1-9 dwarf mutants^{36,39}. The three transgenes were able to rescue the corresponding hrd1a hrd1b bri1-9 and ebs7-3 bri1-5 mutants (Supplementary Fig. 1), respectively, indicating that all three tagged proteins are physiologically functional. We used one representative transgenic line for each transgene to extract total proteins or microsomal proteins and subsequently performed immunoprecipitation (IP) experiments with antibody-conjugated beads. The resulting immunoprecipitates were analyzed by liquid chromatography coupled with tandem mass spectrometry (LC-MS/MS) to identify proteins that were coimmunoprecipitated with the GFP-fused Hrd1a or MYC/HA-tagged EBS7. We also included the non-transgenic wild-type plant as our negative control to eliminate proteins that bound non-specifically to antibody-conjugated beads. Comparison of the five sets of coimmunoprecipitated proteins identified nine common proteins (Fig. 1a, b), including Hrd1a, EBS7, and a previously demonstrated component of the Arabidopsis ERAD machinery, EBS5³⁶ (also known as HRD3A³⁴ or SEL1L³⁸ that is the Arabidopsis homolog of the yeast Hrd3 and mammalian Sel1L). It is interesting to note that the three IP experiments with total proteins also identified Hrd1b and EBS6 (the Arabidopsis homolog of Yos9/OS-9^{37,38}; Supplementary Fig. 2), suggesting the presence of multimeric Hrd1 in the Arabidopsis Hrd1 complex. The

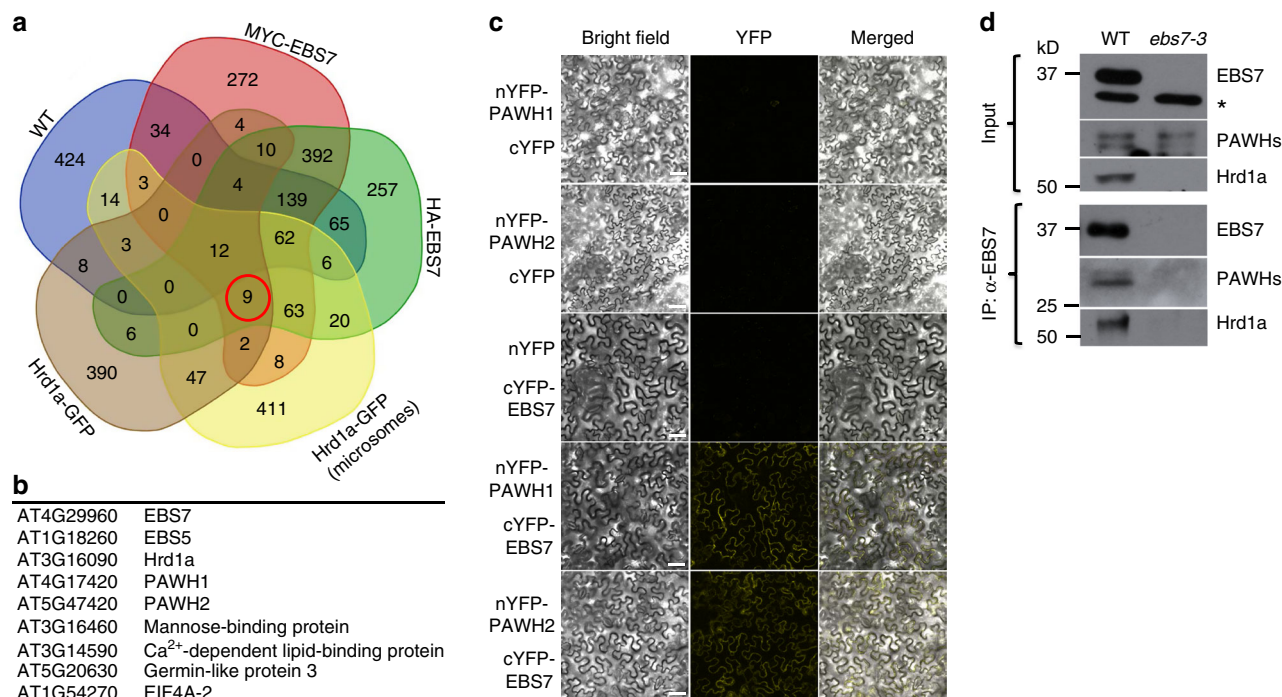


Fig. 1 Discovery and verification of the two EBS7/Hrd1a-interacting PAWHs. **a** A Venn diagram of the immunoprecipitated proteins from total/microsomal proteins of the wild-type control or transgenic mutants expressing Hrd1a-GFP or MYC/HA-tagged EBS7. **b** The list of the nine proteins that were identified in all four IP-MS experiments. **c** The BiFC analysis of the PAWH1/2-EBS7 interaction in tobacco leaf epidermal cells. Bar = 50 μm. **d** CoIP of EBS7 with PAWH1/2 and Hrd1a in Arabidopsis plants. The total proteins (Input) and anti-EBS7 immunoprecipitates (IP:α-EBS7) were separated by SDS-PAGE and analyzed by immunoblotting with antibodies to EBS7, PAWH, and Hrd1a. The star indicates a non-specific cross-reactive band used to control equal amounts of proteins used for the coIP assays. The positions of molecular mass standards are indicated on the left. The raw data of the IP-MS experiments can be accessed at <https://www.ebi.ac.uk/pride/archive> with the dataset identifier PXD013400, and other source data are provided as a Source Data file

identification of known ERAD components as the abundant interacting proteins of both Hrd1a and EBS7 indicated success of our proteomic approach, whereas the failure to detect Hrd1b and EBS6 in the anti-GFP immunoprecipitates of the microsomal preparation was likely caused by low recovery of the immunoprecipitated proteins, evidenced by lower coverage of Hrd1a and EBS5 compared to a similar coimmunoprecipitation (coIP) experiment using the total proteins (Supplementary Fig. 2). Our analysis also identified two highly homologous proteins, At4g17420 (285 amino acids) and At5g47420 (282 amino acids) that were previously annotated as tryptophan RNA-binding attenuator protein-like proteins (TRAPs) and were renamed hereinafter as Protein Associated With Hrd1-1 (PAWH1) and PAWH2, respectively (Fig. 1b and Supplementary Fig. 2). A simple BLAST search revealed that PAWH1 and PAWH2 are highly conserved in the plant kingdom and contain AIM24 domain (Supplementary Fig. 3), which is originally discovered in the yeast mitochondria AIM24 (Altered Inheritance of Mitochondria protein 24) recently implicated in stabilizing the mitochondria contact site complex and the respiratory chain supercomplexes⁴². The four other proteins recovered in all 4 IP-MS experiments include a jacalin-related lectin (At3g16460), a calcium-dependent lipid-binding protein (At3g14590), a germin-like protein (At5g20630), and one of the three Arabidopsis translational initiation factor EIF4As (At1g54270). Further studies are needed to determine whether they are bona fide components of the Arabidopsis Hrd1 complex.

Analysis of PAWH interactions with EBS7 and Hrd1a. To test if PAWHs directly interact with Hrd1a and EBS7, we performed three experiments. The first one was a simple yeast two-hybrid

assay with the predicted AIM24 domain-containing N-terminal 260 amino acids (AAs) of PAWH1 (PAWH1-N260) or 257 AAs of PAWH2 (PAWH2-N257) and the N-terminal soluble domain of EBS7 containing its N-terminal 142 AAs (EBS7-N142) or the cytoplasmic RING finger domain of Hrd1a (Hrd1a-CD). These assays showed that while PAWH1-N260 (also PAWH2-N257) interacted well with the EBS7-N142 fragment, it failed to interact with Hrd1a-CD that was previously shown to interact with the EBS7-N142 fragment³⁹ (Supplementary Figs. 4 and 5a). The second experiment was a transient bimolecular fluorescence complementation assay (better known as BiFC⁴³) in tobacco leaf epidermal cells using the full-length PAWH1 and PAWH2 fused at their N-termini with the N-terminal half of the yellow fluorescent protein (nYFP-PAWH1 and nYFP-PAWH2) and the full-length EBS7 fused at its N-terminus with the C-terminal half of YFP (cYFP-EBS7) or the full-length Hrd1a fused with cYFP at its C-terminus (Hrd1a-cYFP). While yellow fluorescent signals were detected in tobacco leaf cells coexpressing nYFP-PAWH1 or nYFP-PAWH2 with cYFP-EBS7 (Fig. 1c), no fluorescent signal was detected in tobacco leaf cells coexpressing nYFP-PAWH1 or nYFP-PAWH2 with Hrd1a-cYFP (Supplementary Fig. 5b). In addition, we performed a coIP experiment with total proteins from the wild-type Arabidopsis seedlings using anti-EBS7 antibody³⁹, a custom-made anti-Hrd1a antibody (Supplementary Fig. 6), and a custom-made anti-PAWH antibody that could identify both PAWH1 and PAWH2 proteins (see Supplementary Fig. 11d). As shown in Fig. 1d, the anti-EBS7 antibody not only immunoprecipitated the endogenous EBS7 protein but also brought down Hrd1a and the two PAWH proteins. By contrast, neither Hrd1a nor PAWHs were detected in a similar coIP assay with the total proteins extracted from the null *esb7-3* mutant³⁹ (Fig. 1d). These results suggested that PAWH1/2 could directly

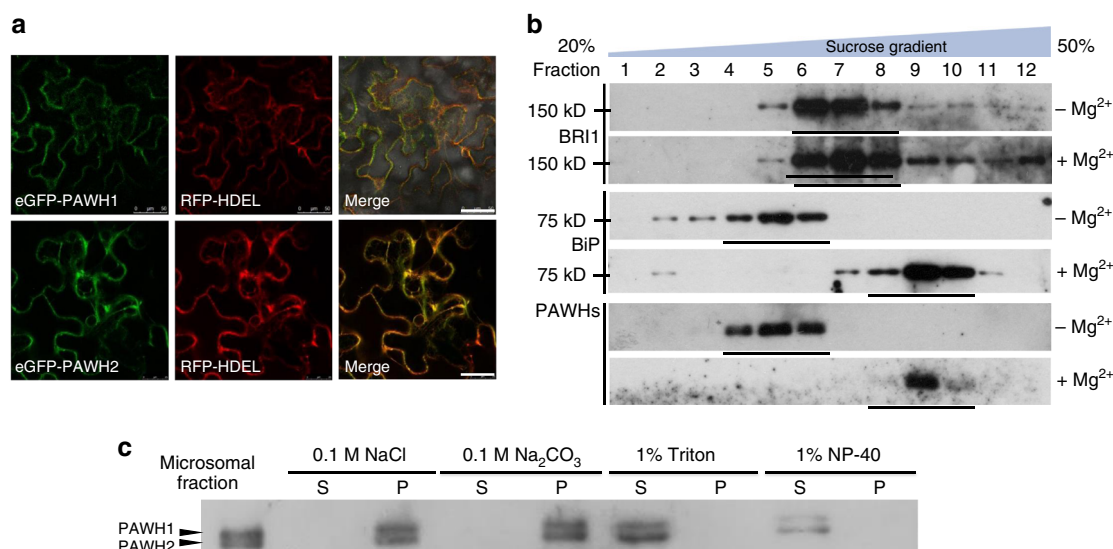


Fig. 2 PAWHs are ER membrane-anchored proteins. **a** The confocal microscopic images of tobacco leaf epidermal cells that transiently express GFP-PAWH1/2 (left), the ER-localized RFP-HDEL (middle), and merged images of green and red fluorescent signals (right). Bar = 50 μ m. **b** Sucrose gradient ultracentrifugation of PAWH1/2 proteins/protein complexes. Protein samples from collected gradient fractions of a linear (20–50%) sucrose gradient in the presence (+) or absence (–) of Mg^{2+} were separated by SDS-PAGE and analyzed by immunoblotting with antibodies to BRI1, BiPs, and PAWH. The positions of molecular mass standards are shown on the left. **c** Solubilization of PAWHs by various solvents/detergents. The microsomal preparations of 10-day-old Arabidopsis seedlings were treated with 0.1 M NaCl, 0.1 M Na_2CO_3 , 1% (v/v) Triton X-100, or 1% (v/v) Nonidet P-40 for 4 h and centrifuged at 100,000 \times g for 60 min to generate both supernatant (S) and pellet (P) fractions, which were subsequently separated by SDS-PAGE and analyzed by immunoblotting with anti-PAWH antibody. Source data are provided as a Source Data file

bind EBS7 but not Hrd1a and that the coIP-detected Hrd1a-PAWH1/2 association is likely mediated by EBS7 known to interact directly with Hrd1a³⁹.

PAWHs are ER membrane proteins and induced by ER stress.

Both *PAWH* genes are widely expressed in various tissues/organs throughout the Arabidopsis development with *PAWH1* exhibiting high expression at later stages of seed development and reaching its highest expression level in dry seed (Supplementary Fig. 7). The two *PAWH* genes were previously shown to coexpress with genes known/predicted to be involved in protein folding and/or protein quality control (Supplementary Fig. 8)⁴⁴. Many *PAWH*-coexpressed genes were known to be induced by ER stress⁴⁵. To test if *PAWH* transcripts and PAWH proteins are also induced by ER stress, we treated the wild-type seedlings with or without tunicamycin (TM), a widely used ER stress inducer that inhibits the first biosynthetic step of the N-glycan precursor, and used the treated seedlings to examine the abundance of *PAWH* transcripts and PAWH proteins by RT-PCR and immunoblotting, respectively. We found that the TM treatment increased the mRNA levels of both *PAWH* genes and elevated the protein abundance of both PAWHs (Supplementary Fig. 9).

Both PAWHs lack the N-terminal signal peptide or the C-terminal ER retrieval motifs but were predicted to contain a potential transmembrane (TM) segment near their C-termini (Supplementary Fig. 10). To directly determine their subcellular localization, we generated GFP-fusion transgenes for the two *PAWH* genes and transiently expressed them in tobacco leaf epidermal cells. Confocal microscopy analysis of agro-infiltrated tobacco leaves revealed that the green fluorescent signals of the GFP-PAWH1/2 fusion proteins overlapped with the fluorescent signals of the red fluorescent protein (RFP) tagged at its C-terminus with the HDEL (histidine-aspartate-glutamate-leucine) ER retrieval motif (Fig. 2a), a widely used ER-localized marker, strongly suggesting that PAWH1/2 are localized to the ER. A further confirmation was provided by sucrose density-gradient

centrifugation with Arabidopsis microsomal proteins in the presence or absence of Mg^{2+} . Because Mg^{2+} is required for polyribosome binding to the ER and that the density of the ribosome-bound ER membrane is higher than that of the ribosome-free ER or other microsomal membranes, an ER-localized protein should undergo a diagnostic Mg^{2+} -dependent shift from lower density to higher density on a sucrose gradient⁴⁶. Figure 2b shows that PAWHs exhibited a similar Mg^{2+} -dependent density shift as BiPs (binding immunoglobulin proteins, ER-localized Heat Shock Protein 70), but differs from BRI1 known to be localized to the PM⁴⁷. Consistent with the predicted C-terminal TM segments (Supplementary Fig. 10), immunoblot analysis of PAWHs in soluble and insoluble fractions of resuspended Arabidopsis microsomal pellets in 0.1 M NaCl, 0.1 M Na_2CO_3 , 1% (v/v) Triton X-100, or 1% (v/v) Nonidet P-40 solution showed that only the two nonionic detergents could release the two PAWHs from microsomes, suggesting that both PAWHs are likely anchored to the ER membrane (Fig. 2c).

Mutating both PAWHs stabilizes several ERAD substrates.

To investigate if the two PAWHs are involved in an Arabidopsis ERAD process, we obtained T-DNA insertion mutants for the two *PAWH* genes from the Arabidopsis Biological Resource Center (<http://abrc.osu.edu/>)⁴⁸ (Supplementary Fig. 11a, b). RT-PCR analysis indicated that the two mutants failed to produce the full-length transcript of the corresponding *PAWH* gene while immunoblot analysis failed to detect one of the two crossing-reacting bands of the wild-type plant (Supplementary Fig. 11c, d), indicating that the two T-DNA insertion mutants are null mutants. We crossed each mutant into *bri1-9* and found that the resulting *pawh1 bri1-9* and *pawh2 bri1-9* mutants were morphologically indistinguishable from *bri1-9* (Fig. 3a–c). A further cross between the two double mutants generated a *pawh1 pawh2 bri1-9* triple mutant that was morphologically similar to the wild-type (Fig. 3a–c), indicating that simultaneous elimination of PAWH1 and PAWH2 suppressed the *bri1-9* dwarf phenotype.

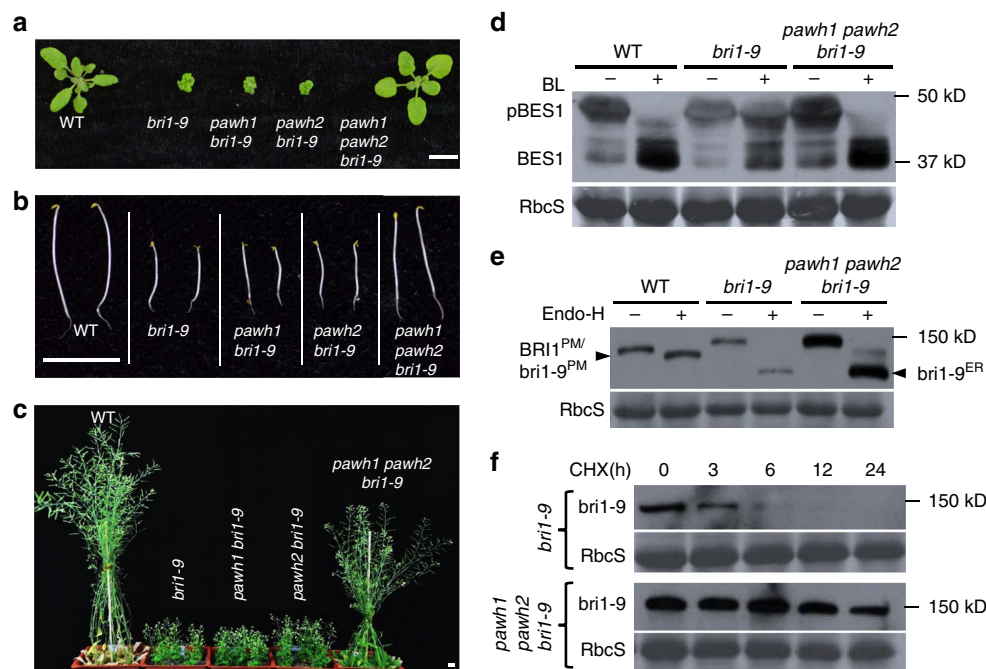


Fig. 3 Mutating two PAWHs suppresses the *bri1-9* phenotype and inhibits *bri1-9* degradation. **a–c** Photographs of 3-week-old light-grown seedlings (**a**), 7-day-old dark-grown seedlings (**b**), and 2-month-old mature soil-grown plants (**c**). Scale bar = 1 cm. **d–f** Immunoblot analysis of BR-triggered BES1 dephosphorylation (**d**), the Endo H sensitivity of BRI1/*bri1-9* (**e**), and the protein stability of *bri1-9* (**f**). Total proteins were extracted from 10-day-old Arabidopsis seedlings treated with (+) or without (–) 1 μ M brassinolide (BL, the most active member of the BR family) for 1 h (**d**) or 180 μ M CHX (**f**) for indicated durations. Proteins extracted from non-treated seedlings were treated with (+) or without (–) Endo H (**e**). These protein samples were separated by SDS-PAGE and analyzed by immunoblotting with antibodies to BES1 (**d**) or BRI1 (**e**, **f**). The lower strips in **d–f** showing the Ponceau Red-stained small subunit of the ribulose-1,5-bisphosphate carboxylase/oxygenase (RbcS), were used as loading controls. The positions of the molecular mass standards are shown on the right. In **e** BRI1^{PM}/*bri1-9*^{PM} and *bri1-9*^{ER} denote BRI1/*bri1-9* proteins localized on the PM and in the ER, respectively. Source data are provided as a Source Data file

Consistent with the phenotypic suppression, the *pawh1 pawh2* double mutation partially restored the BR sensitivity to the *bri1-9* mutant revealed by the BR-triggered root growth inhibition assay⁴⁹ (Supplementary Fig. 12) and the BR-induced BES1 dephosphorylation assay⁵⁰ (Fig. 3d). Importantly, immunoblot analysis showed that the *pawh1 pawh2* double mutation greatly increased the *bri1-9* abundance, which was much higher than the abundance of the wild-type BRI1 that undergoes a phosphorylation-dependent endocytosis and ubiquitin-mediated degradation⁵¹. We also treated total proteins with endoglycosidase H (Endo H) that cleaves high mannose-type N-glycans of ER-localized/retained glycoproteins but does not cut Golgi-processed N-glycans of glycoproteins. We found that the *pawh1 pawh2* mutation increased abundance of the Endo H-resistant form of *bri1-9* (Fig. 3e), suggesting increased presence of *bri1-9* on the PM to promote growth. Indeed, our transgenic experiment showed that overexpression of EBS2 known to retain *bri1-9* in the ER⁵², significantly decreased the amount of the Endo H-resistant form of *bri1-9* and nullified the suppressive effect of the *pawh1 pawh2* double mutation on the *bri1-9* dwarfism while having a little effect on the total amount of *bri1-9* proteins (Supplementary Fig. 13). To determine the biochemical basis of increased *bri1-9* abundance in the *pawh1 pawh2 bri1-9* mutant, we performed a cycloheximide (CHX)-chasing experiment and found that increased *bri1-9* abundance is caused by decreased protein degradation rather by increased protein biosynthesis (Fig. 3f). A subsequent rescue experiment showed that the effect on growth and biochemical phenotypes were indeed caused by the double *pawh1 pawh2* mutation (Supplementary Fig. 14). Taken together, these experiments demonstrated that PAWH1 and PAWH2 are

crucial components of the Arabidopsis ERAD machinery that degrades the ER-retained mutant *bri1-9* receptor.

A similar set of experiments revealed that simultaneous elimination of the two PAWHs by the T-DNA insertional mutations or by CRISPR/Cas9-mediated genome editing inhibited the degradation of *bri1-5* and suppressed the dwarf phenotype of the corresponding *bri1-5* mutant (Supplementary Figs. 15 and 16). We also tested if the *pawh1 pawh2* double mutation could inhibit degradation of other misfolded Arabidopsis proteins. Previous studies showed that the Arabidopsis EF-Tu receptor (EFR), a cell surface-localized receptor that detects and binds a small peptide derived from the highly conserved translation factor EF-TU (elongation factor thermo unstable) of pathogenic bacteria⁵³, becomes misfolded and degraded in an Arabidopsis mutant defective in an ER-luminal protein homologous to the mammalian UDP-glucose:glycoprotein glucosyltransferase^{29,30} (also known as EBS1⁴¹). We crossed the *pawh1 pawh2* mutation into an *ebc1* mutant and analyzed the EFR abundance in *ebc1*, *pawh1 pawh2*, *ebc1 pawh1 pawh2*, and their wild-type control. Consistent with the previous findings^{29,30}, EFR was non-detectable in *ebc1* but its level was greatly increased in the *ebc1 pawh1 pawh2* triple mutant (Supplementary Fig. 17), demonstrating that the two PAWHs are also involved in degrading a misfolded EFR. We thus concluded that PAWH1 and PAWH2 are likely general components of the Arabidopsis Hrd1-containing ERAD complex.

The loss of PAWHs activates UPR and reduces stress tolerance. Previous studies have shown that loss-of-function ERAD

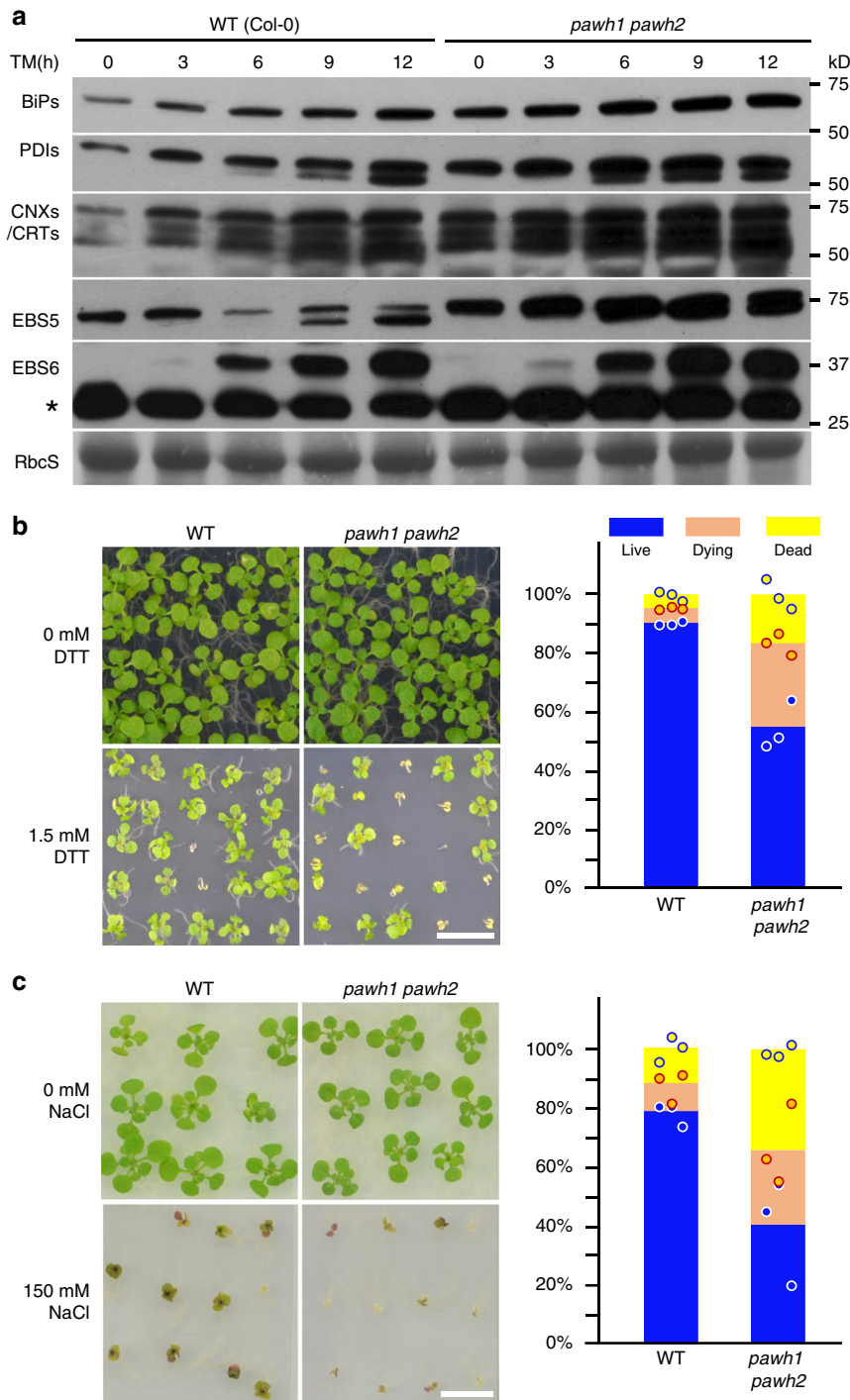


Fig. 4 The *pawh1 pawh2* mutation activates UPR and reduces stress tolerance. **a** Immunoblot analysis of various ER-localized proteins in seedlings treated with TM for different durations. The faster moving bands detected by anti-PDI and anti-EBS5 antibody are non-glycosylated forms of PDIs and EBS5, respectively. The star indicates a non-specific band. The lower strip is the Ponceau Red-stained RbcS bands used as the loading control. **b, c** The left are photographs of 15-day-old Arabidopsis seedlings grown on ½ MS medium supplemented with or without 1.5 mM DTT (**b**) or 150 mM NaCl (**c**), while the right are the bar graphs showing the percentage of three kinds of seedlings: blue (alive), brown (dying), and yellow (dead). Scale bar = 1 cm. The stress sensitivity experiments were repeated three times with ~100 seedlings/each for the DTT assay and ~50 seedlings/each for the NaCl experiment with individual data points shown as open circles distributed above or below the average values of the three repeats. Source data are provided as a Source Data file

mutations often result in constitutive activation of the Arabidopsis unfolded protein response (UPR) pathway^{36–39}, a highly conserved ER stress response pathway that upregulates production of ER chaperones and ERAD components to maintain proteostasis^{54,55}. To examine if the *pawh1 pawh2* mutation also

activates UPR, we performed an immunoblot analysis with total proteins of the wild-type and *pawh1 pawh2* mutant treated with or without TM for variable durations. Figure 4a shows that the protein abundance of BiPs, protein disulfide isomerases (PDIs), calreticulins/calnexins (CRT/CNXs), EBS5, and EBS6 was higher

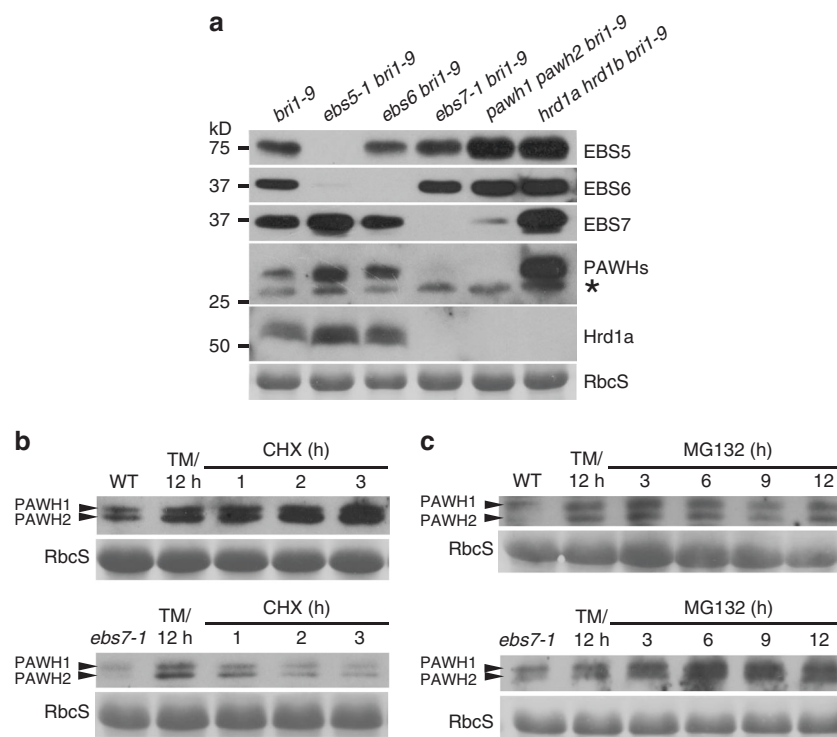


Fig. 5 Impact of ERAD mutations on the stability of EBS7, PAWHs, and Hrd1a. **a** Immunoblot analysis of the protein abundance of EBS5, EBS6, EBS7, PAWH1/2, and Hrd1a in 4-week-old seedlings of various ERAD mutants. Asterisk indicates a non-specific band. **b, c** Immunoblot analysis of the protein abundance of PAWHs. Total proteins extracted from 10-day-old seedlings treated with 5 μ g/mL TM for 12 h followed by treatment with 180 μ M CHX (**b**) or 80 μ M MG132 (**c**) for different durations were separated by SDS-PAGE and analyzed by immunoblotting with anti-PAWH antibody. In **a–c**, the RbcS-labeled strips show the Ponceau Red-stained RbcS band and were used as the loading controls for the experiments. Source data are provided as a Source data file

in *pawh1 pawh2* seedlings treated with or without TM than the corresponding wild-type seedlings, indicating that the *pawh1 pawh2* mutation constitutively activates the UPR pathway. The detected enhancement of UPR prompted us to test if the *pawh1 pawh2* double mutation affects the plant stress tolerance, which is known to involve the UPR pathway⁵⁵. We germinated seeds and grew seedlings on $\frac{1}{2}$ MS medium containing 1.5 mM dithiothreitol (DTT, a widely used ER stress-inducer that interferes with oxidative protein folding) and 150 mM NaCl known to cause salt stress in Arabidopsis. As shown in Fig. 4b, c, the percentages of dying and dead seedlings on DTT/NaCl-containing medium were markedly higher for the *pawh1 pawh2* mutant than the wild-type control, indicating that the *pawh1 pawh2* double mutation compromises the plant stress tolerance.

Both PAWH1 and PAWH2 are unstable in the *ebs7-1* mutant.

Given the facts that EBS7 interacts with both Hrd1a and PAWHs and that *ebs7* mutations greatly destabilize Hrd1a³⁹, we were interested in examining the impact of the *ebs7-1* mutation on the PAWH1/2 abundance as well as the impact of the *pawh1 pawh2* mutation on the protein stability of both EBS7 and Hrd1a. We also included three other ERAD mutants, *ebs5 bri1-9*, *ebs6 bri1-9*, and *hrd1a hrd1b bri1-9* in our experiment. Consistent with our earlier finding³⁹, the missense *ebs7-1* mutation (Ala¹³¹-Thr) caused disappearance of not only the mutated *ebs7-1* protein but also Hrd1a (Fig. 5a). Interestingly, *ebs7-1* also markedly reduced the protein abundance of the two PAWHs (Fig. 5a). By contrast, the *ebs6* mutation seemed to have a marginal effect on the abundance of EBS7, PAWHs, or Hrd1a, whereas the *ebs5* mutation increased the protein levels of EBS7 and PAWHs (Fig. 5a), which could be caused by non-significant and significant impact

of the *ebs6* and *ebs5* mutations, respectively, on the transcript abundance of EBS7 and PAWHs (Supplementary Fig. 18). To determine if the *ebs7-1*-caused reduction of PAWH abundance is attributed to increased protein degradation, we first treated seedlings of wild-type and *ebs7-1* with TM for 12 h to increase the PAWH1/2 abundance, subsequently treated these seedlings with CHX or MG132 (a widely used proteasome inhibitor) for different durations, and analyzed the PAWH abundance by immunoblotting. Figure 5b shows that while the CHX treatment had little impact on the PAWH1/2 abundance in wild-type seedlings, the same treatment led to a rapid decrease in the PAWH1/2 abundance in *ebs7-1* seedlings. Consistently, a 12-h-treatment of MG132 caused little change or slightly reduction in the PAWH abundance in wild-type seedlings, whereas the same MG132 treatment actually increased the PAWH1/PAWH2 protein levels in the *ebs7-1* mutant (Fig. 5c). Together, these experiments indicated that *ebs7-1* destabilizes the two PAWH proteins that are likely degraded via a proteasome-mediated process.

The *pawh1 pawh2* mutation destabilizes EBS7 and Hrd1a. Our immunoblot assays of various ERAD mutants also revealed that the *pawh1 pawh2* double mutation greatly reduced the protein abundance of both EBS7 and Hrd1a (Fig. 5a), while our quantitative real-time RT-PCR (qPCR) analyses showed that the *pawh1 pawh2* double mutation slightly elevated the levels of the EBS7 mRNA but had a marginal impact on the *Hrd1a* transcript abundance (Supplementary Fig. 18). To determine if the observed reduction in EBS7 and Hrd1a protein abundance is due to increased protein degradation or decreased protein synthesis, we used the same TM-CHX/MG132 protocol described above to

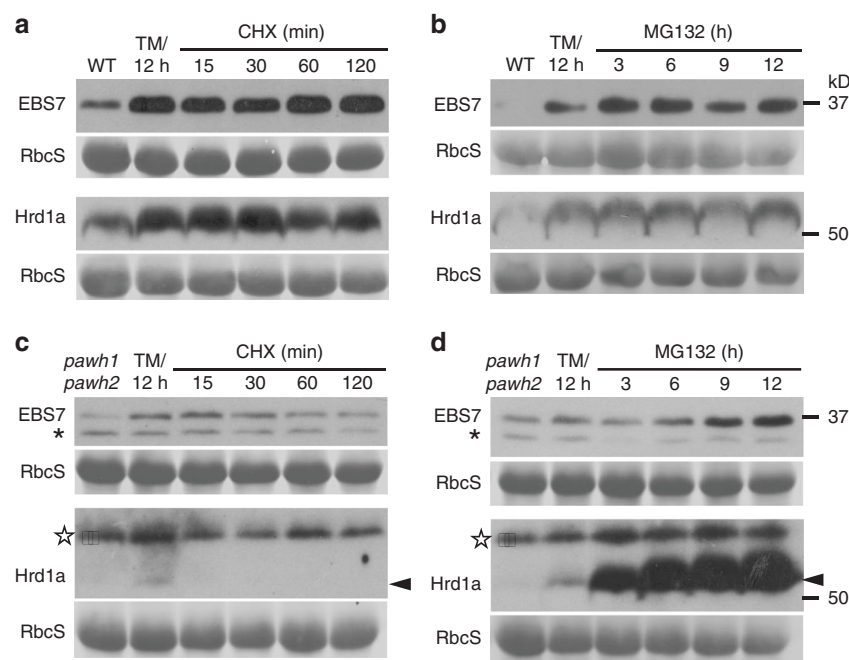


Fig. 6 The *pawh1 pawh2* double mutation reduces the stability of EBS7 and Hrd1a. **a–d** Immunoblot analysis of EBS7 and Hrd1a in the wild-type (**a, b**) and *pawh1 pawh2* double mutant (**c, d**). Total proteins were extracted from 10-day-old seedlings that were initially treated with 5 μ g/mL TM for 12 h and subsequently treated with 180 μ M CHX (**a, c**) or 80 μ M MG132 (**b, d**) for different durations, separated by SDS-PAGE, and analyzed by immunoblotting using anti-EBS7 and anti-Hrd1a antibodies. In each immunoblotting experiment, the RbcS-labeled strip was used as a loading control. Asterisks and stars denote cross-reacting bands to anti-EBS7 and anti-Hrd1a antibodies, respectively, while arrows indicate the Hrd1a band. Source data are provided as a Source Data file

treat seedlings of the wild-type and the *pawh1 pawh2* double mutant and analyzed the protein abundance of EBS7 and Hrd1a by immunoblotting. As shown in Fig. 6a, b, neither CHX or MG132 treatment had an observable effect on the protein abundance of EBS7 or Hrd1a in the wild-type seedlings. However, the CHX treatment caused a gradual reduction of EBS7 but very rapid disappearance of the TM-induced Hrd1a (Fig. 6c), whereas the MG132 treatment gradually stabilized EBS7 and caused rapid and significant stabilization of the ER-anchored E3 ligase (Fig. 6d). We concluded that the *pawh1 pawh2* double mutation destabilizes both EBS7 and Hrd1a that are likely degraded via a proteasome-mediated mechanism.

Because PAWHs fail to interact directly with Hrd1a (Supplementary Fig. 5) and the *pawh1 pawh2* mutation greatly reduces the protein abundance of EBS7 (Fig. 5a), which is known to be important to maintain the Hrd1a stability³⁹, we wondered whether the impact of the *pawh1 pawh2* mutation on Hrd1a stability is a secondary effect caused by reduced EBS7 abundance. We therefore overexpressed EBS7 using the strong *p35S* promoter to drive the expression of HA-tagged EBS7 in the *pawh1 pawh2 bri1-9* triple mutant. This experiment revealed that while the *p35S::HA-EBS7* transgene did lead to increased EBS7 protein abundance in the triple mutant, it failed to stabilize Hrd1a or decrease the *bri1-9* abundance (Supplementary Fig. 19), suggesting that PAWHs exert their direct impact on the ER-anchored E3 ligase via a yet unknown mechanism.

Our immunoblot analysis also revealed that the *hrd1a hrd1b* double mutation did not reduce but increased the abundance of EBS5, EBS6, EBS7, and the two PAWH proteins (Fig. 5a). Because our qPCR experiments showed that the *hrd1a hrd1b* double mutation significantly increased the transcript levels of both PAWH genes but had a marginal impact on the EBS7 transcript abundance (Supplementary Fig. 18), we suspected that Hrd1a and/or Hrd1b might be the E3 ligase that ubiquitinates EBS7 in

the *pawh1 pawh2* mutant to promote EBS7 degradation. Consistent with this hypothesis, overexpression of a GFP-tagged Hrd1a driven by the strong *p35S* promoter not only reduced the *bri1-9* abundance and complemented the phenotypes of the *hrd1a hrd1b bri1-9* triple mutant, but also greatly lowered the protein levels of *bri1-9*, EBS7, and the two PAWHs (Supplementary Fig. 20). Because both EBS7 and PAWHs remained stable in the *hrd1a hrd1b* mutant background, we also used total proteins of the *hrd1a hrd1b bri1-9* mutant to analyze the EBS7-PAWHs interaction and discovered that the *hrd1a hrd1b* mutation had no detectable impact on the EBS7-PAWHs interaction (Supplementary Fig. 21).

Discussion

In this study, we used a proteomic approach to identify two redundant proteins, PAWH1 and PAWH2, which were coimmunoprecipitated with GFP-tagged AtHrd1a and MYC/HA-tagged EBS7 expressed in their corresponding loss-of-function Arabidopsis mutants. Previous transcriptome analyses indicated that both PAWH genes were co-expressed with genes known or predicted to encode ER chaperone, folding catalysts, and ERAD components, while our current study confirmed that both PAWH1 and PAWH2 proteins were induced by chemically triggered ER stress. Despite the lack of an N-terminal signal peptide and known ER retention/retrieval sequence motifs, both PAWHs were found to be localized at the ER membrane, likely through its predicted C-terminal transmembrane segment, as evidenced by confocal microscopy, sucrose-gradient ultracentrifugation, and solubilization of microsomal proteins with different solvents and detergents.

In addition, our yeast two-hybrid assay, transient BiFC assay in tobacco leaves, and coIP experiments using transgenic Arabidopsis plants showed that PAWHs interact directly with EBS7 but

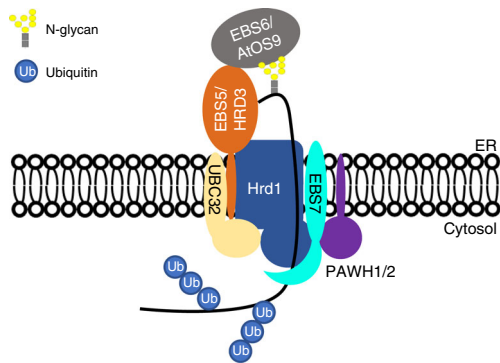


Fig. 7 A model of the Arabidopsis Hrd1 complex. An ERAD-L substrate is recognized and recruited by both EBS6/AtOS9 and EBS5/HRD3 to the ER membrane-anchored Hrd1 that works with the E2 UBC32 to ubiquitinate the ERAD client. EBS7 and PAWH1/2 interact with Hrd1 to regulate the stability and activity of the E3 ligase

associate with Hrd1a indirectly, most likely mediated by the previously demonstrated EBS7-Hrd1a interaction³⁹. Furthermore, we showed that the *pawh1 pawh2* double mutation constitutively activated the UPR pathway and greatly compromised plant tolerance against salt stress and DTT-triggered ER stress, similar to what were previously reported for Arabidopsis ERAD mutants^{36–39}. More importantly, we have shown that the *pawh1 pawh2* mutation blocked degradation of two ER-retained mutant BR receptors, bri1-5 and bri1-9, allowing them to accumulate and consequently leak out of the ER to reach the PM where the two mutant BR receptors could respond to BRs to stimulate plant growth. Our study also showed that the *pawh1 pawh2* mutation also inhibited degradation of misfolded EFR in the *els1* mutant background, strongly suggesting that the two redundant PAWH proteins are likely general components of the Arabidopsis Hrd1-containing ERAD complex that degrades many misfolded proteins. Thus, our study, coupled with previously reported results, revealed that such an Arabidopsis ERAD complex consists of not only evolutionarily conserved components, including EBS5/HRD3A^{34,36}, EBS6/AtOS9^{37,38}, Hrd1a/1b³⁶, and their associated E2 conjugase UBC32³³, but also plant-specific components, such as EBS7³⁹ and PAWH1/PAWH2 (Fig. 7).

Our results have shown that the plant-specific components, EBS7 and PAWHs, are important to maintain the protein stability of Hrd1a. In the absence of the two homologous PAWH proteins, the stability of EBS7 and Hrd1 was significantly reduced. Our previous study demonstrated that *els7* mutations significantly reduce the Hrd1 stability³⁹, raising a question if reduction of Hrd1 stability by the *pawh1 pawh2* mutation is an indirect consequence of reduced abundance of EBS7 that directly binds PAWHs. However, our transgenic experiment showed that increased production of EBS7 driven by the *p35S* promoter failed to increase Hrd1a abundance, suggesting a direct role of PAWHs in maintaining the Hrd1a stability. This finding and our earlier results of the EBS7-AtHrd1a interaction demonstrated that EBS7 and PAWHs work together to regulate the stability of the ER membrane-anchored Hrd1a.

Studies in yeast and mammalian cells showed that Hrd3/Sel1L is essential to maintain the stability of Hrd1 and that mutations in Hrd3 in yeast or Sel1L in mammalian cells resulted in a significant reduction in the stability of the yeast or mammalian Hrd1 E3 ligase^{7,22,23}. However, mutations of EBS5, the Arabidopsis homolog of Hrd3/Sel1L³⁶, had no detectable impact on the Hrd1a stability. Our results thus revealed a novel mechanism that regulates the protein stability/activity of a plant ERAD E3 ligase, which is quite diverged from a conserved regulatory mechanism

that controls the stability of yeast and mammalian Hrd1s. In yeast, the *hrd3Δ*-triggered Hrd1 loss is caused by autodegradation facilitated by the Hrd1's own catalytic RING domain²⁴. It remains to be tested whether or not the disappearance of Hrd1a in *els7* or *pawh1 pawh2* mutant is caused by self-destruction of Hrd1a or by other ER-anchored E3 ligases such as SUPPRESSOR OF DRY2 DEFECTS1⁵⁶, an Arabidopsis homolog of the yeast Degradation of alpha factor2-10 (Doa10) that is known to be involved in degrading misfolded transmembrane proteins carrying a cytosolic structural defect³ or one of the three Arabidopsis RING finger proteins with membrane anchor (RMA1-3)⁵⁷.

While loss-of-function mutations in EBS7 and PAWHs destabilize PAWHs/Hrd1a and EBS7/Hrd1a, respectively, the *hrd1a hrd1b* double mutation does not reduce but increases the protein abundance of both EBS7 and PAWHs. We hypothesize that this is caused by increased transcription and reduced protein degradation. The *hrd1a hrd1b* double mutation may cause accumulation of misfolded proteins in the ER and consequently activates the UPR pathway, which increases production of many chaperones, folding enzymes, and components of the ERAD machinery such as EBS7 and PAWHs. Moreover, the two functionally redundant Hrd1 homologs likely trans-ubiquitinate EBS7 to regulate its protein abundance via the so-called ER-tuning mechanism^{35,58} to tightly and rapidly regulate the ERAD capacity to adapt to fluctuations in the amount of misfolded proteins accumulated in the ER, thus maintaining the ER proteostasis essential for cell survival. A further investigation is needed to fully understand the role of Hrd1 in such an ER-tuning regulatory mechanism.

Although our study demonstrated an essential role of PAWHs in maintaining the stability of Hrd1a, it remains unknown how the two PAWHs execute this function. Both PAWH1 and PAWH2 carry a highly conserved domain that was first discovered in the yeast AIM24 protein, a mitochondria protein tightly associated with the inner membrane and required for the ultrastructure, composition, and function of mitochondria^{42,59}. It was previously thought that AIM24 is a fungal invention⁶⁰, but the 32nd release of the Pfam database of protein families in Sept. 2018 (<https://pfam.xfam.org>) revealed a total of 5937 AIM24 domain-containing proteins from 3272 species in all three domains of life, with >93% of them containing only the AIM24 domain (Supplementary Fig. 22). Despite wide occurrence of the AIM24 domain-containing proteins (a total of 4535 sequences) in bacteria, nothing is known about physiological function of any of these bacterial proteins. Interestingly, crystal structures of at least two bacterial AIM24 domain-containing proteins were solved: an unknown protein of 248 AAs (PA3696) from *Pseudomonas aeruginosa* strain PA01 (PDB: 1YOX), and a hypothetical protein of 243 AAs (SpyM3_0169) from *Streptococcus pyogenes* (PDB: 1PG6). Structural modeling at SWISS-MODEL server (<https://swissmodel.expasy.org>) using the structures of these two bacterial proteins as templates suggested that PAWH1/2 likely adopt a similar monomeric structure consisting of three structural repeats of beta-sandwich (Supplementary Fig. 23a, b), each having two beta-sheets of 3/4 anti-parallel beta-strands. It is worth mentioning that each structure unit resembles the crystal structure of the bacterial tryptophan RNA-binding attenuation protein (PDB: 1WAP)⁶¹, explaining the original names of the two PAWHs as tryptophan RNA-binding attenuator-like proteins. Our structural modeling also suggested that PAWHs could form a homotrimeric subcomplex with a flat surface on the bottom (Supplementary Fig. 23c–f). It is important to note that the predicted C-terminal transmembrane α -helix is not included in the models and that the C-terminal α -helices shown in the two models correspond to the peptide fragment of 239–250 of PAWH1 (236–247 in PAWH2), which is unlikely a transmembrane domain due to its short length.

Such a modeled PAWH structure suggests that PAWHs likely rely on their flat ring-surface to interact with other proteins and use the protruding α -helices (corresponding to the consensus C-terminal transmembrane α -helical domain, see Supplementary Fig. 10) to attach the trimeric PAWH complex into the ER membrane. Further studies are needed to determine if the predicted C-terminal transmembrane domain is needed for the biological function of PAWHs, and more importantly, to identify additional PAWH-interacting proteins and/or crucial amino acid residues of PAWH1/2, which could help to understand the biochemical mechanism(s) by which PAWHs regulate the protein stability and catalytic activity of the plant Hrd1.

Methods

Plant materials and growth conditions. Most of the Arabidopsis wild-type, mutants, and transgenic lines are in the Columbia (Col-0) ecotype except for mutants and transgenic lines that carry the *bri1-5* mutation, which are in the Wassilewskija-2 (Ws-2) ecotype. The Arabidopsis mutants used in this study include *bri1-5*⁶², *bri1-941*, *ebf1*⁴¹, *ebf3*³⁶, *ebf6*³⁷, *ebf7-1*³³⁹, and *hrd1a hrd1b*³⁶. The T-DNA insertional mutants CS335767 (*pawh1*) and SALK_111654 (*pawh2*) were obtained from Arabidopsis Biological Resource Center (ABRC) at Ohio State University^{48,63}. The *pawh1-c* and *pawh2-c* mutants were created by CRISPR/Cas9-mediated genome editing in the *bri1-5* mutant background (see below for the experimental details). Seed were surface sterilized using the ethanol-washing protocol⁶⁴ and seedling were grown at 22 °C in growth chamber or growth room under long-day (16 h-light/8 h-dark) photoperiodic condition.

Chemical treatment of Arabidopsis seedlings. To study the stress tolerance, seeds were germinated, and young seedlings were grown on ½ Murashige and Skoog (MS, Sigma) medium supplemented with or without 1.5 mM DTT (Roche) or 150 mM NaCl for 15 days and the numbers of seedlings that were green (alive), yellowish (dying), or dead were counted and recorded. To analyze UPR activation, 10-day-old Arabidopsis seedlings were carefully transferred into liquid ½ MS medium supplemented with 5 µg/mL TM (BioMol) and were incubated for 0, 3, 6, 9, or 12 hours before samples were harvested into liquid nitrogen. To analyze the BR sensitivity, seeds were germinated, and seedlings were grown on ½ MS medium containing varying concentration of brassinolide (BL, Wako Chemical) for 7 days under a long-day (16-h-light/8-h-dark) photoperiodic growth condition. The seedlings were photographed, and their root length were measured digitally by ImageJ (<https://imagej.nih.gov/ij/>). Source data of the measurement are provided as a Source Data file. To study the BR-induced BES1 dephosphorylation, 10-day-old Arabidopsis seedlings were carefully transferred into liquid ½ MS medium supplemented with or without 1 µM BL, incubated for 2 hours, and subsequently harvested into liquid nitrogen. To study protein degradation, 10-day-old Arabidopsis seedlings were carefully transferred into liquid ½ MS medium containing 180 µM CHX (Sigma), incubated for varying durations, and harvested into liquid nitrogen for protein extraction. To study the impact of *ebf3* and *pawh1 pawh2* mutations on protein stability, 10-day-old Arabidopsis seedlings were pretreated with 5 µg/mL TM in liquid ½ MS medium for 12 hours before being treated with 180 µM CHX or 80 µM MG132 (Sigma).

Generation of transgene constructs and transgenic plants. A ~4.1-kb genomic fragment for each PAWH gene was amplified from genomic DNAs of the wild-type Arabidopsis Col-0 seedlings using the *gPAWH1* and *gPAWH2* primer sets (see Supplementary Table 1) and cloned into *pCambia1300* (<https://cambia.org/welcome-to-cambialabs/>) to generate *pCambia1300-gPAWH1* and *pCambia1300-gPAWH2* transgenes. The *p35S::Hrd1a-GFP* transgene was created by cloning a 1,479-bp *Hrd1a* cDNA fragment amplified from the 1st strand cDNAs converted from total RNAs of the wild-type Arabidopsis seedlings using the *Hrd1a-GFP* primer set (Supplementary Table 1) into the *pCambia1300-p35S::C-GFP* vector. To create *p35S::HA-EBS7* or *p35S::MYC-EBS7* transgene, an 876-bp *EBS7* cDNA fragment was amplified from the same Arabidopsis 1st cDNA preparation using the *HA-EBS7* and *MYC-EBS7* primer set (Supplementary Table 1) and cloned into the *pCambia1300-p35S::N-HA* or *pCambia1300-p35S::N-MYC* vector, respectively. To generate the *pEFR::EFR-FLAG* transgene, a 5.2-kb *EFR* genomic fragment (*gEFR* without its 3'-UTR sequence) was PCR amplified from the genomic DNAs of the wild-type Arabidopsis seedlings using the *gEFR-FLAG* primer set (Supplementary Table 1) and cloned into the *pCambia1300-C-FLAG* vector. The *gEBS2* construct is a genomic transgene for *EBS2*⁵². All created transgenes were fully sequenced to ensure no PCR-introduced sequence error, and were individually transformed into the *Agrobacterium tumefaciens* strain GV3101 by electroporation and the resulting *Agrobacterium* strains were subsequently used to transform Arabidopsis plants using the floral-dipping method⁶⁵.

CRISPR/Cas9-mediated genome editing to create *pawh* mutants. The CRISPR/Cas9 vectors used to create *pawh1/2-c* mutation were provided by Dr. Jian-Kang

Zhu⁶⁶. The target sites for introducing mutations into *PAWH1* and *PAWH2* genes were selected using the web program CRISPR-PLANT (<http://crispr.hzau.edu.cn/cgi-bin/CRISPR/CRISPR>), and the oligonucleotides for generating guide RNAs are listed in Supplementary Table 1. The CRISPR/Cas9 constructs were introduced into the *Agrobacterium* strain GV3101 by electroporation, which were subsequently used to transform *bri1-5* mutant by the floral-dipping method⁶⁵. T0 seeds were harvested, sterilized, and subsequently screened on ½ MS medium for T1 lines that carried the CRISPR/Cas9 constructs, which were subsequently screened for intended mutations of *PAWH1/PAWH2* genes and verified in T2 and T3 generations. The verified *pawh1-c bri1-5* and *pawh2 bri1-5* mutants were crossed to get the *pawh1-c pawh2-c bri1-5* triple mutant.

Expression of fusion proteins and generation of antibodies. The 1st cDNA preparation derived from total RNAs of wild-type Arabidopsis seedlings and the *antigen-PAWH1* primer sets (Supplementary Table 1) were used to amplify a 480-bp *PAWH1* cDNA fragment corresponding to its N-terminal 160 AAs. The amplified fragment was cloned into *pGEX-4T-3* (GE Healthcare) and *pMALc-H*⁶⁷ vectors, which were subsequently transformed into BL21-competent cells. The same cDNA preparation was also used to amplify a *Hrd1a* cDNA fragment encoding the N-terminal fragment of 73 AAs using the *antigen-Hrd1a* primer sets (Supplementary Table 1), and two copies of the amplified *Hrd1a* cDNA were cloned into the *pGEX-4T-3* and *pMALc-H* vectors. The induction of GST and MBP fusion proteins and their subsequent purification using Glutathione Sepharose™ 4 Fast Flow beads (GE Healthcare) and Amylose Resin beads (New England Biolabs), respectively, were carried out following the manufacturers' recommended protocols. The purified MBP-PAWH1 and GST-Hrd1a fusion proteins were used to make custom antibody by Abmart (<http://www.ab-mart.com.cn>) while the purified GST-PAWH1 and MBP-Hrd1a fusion proteins were used to affinity-purify anti-PAWH and anti-Hrd1a antibodies from Abmart-generated anti-PAWH and anti-Hrd1a antisera, respectively, using an online protocol with nitrocellulose membrane (<http://post.queensu.ca/~chinsang/lab-protocols/antibody-purification.html>). The specificity of the purified anti-PAWH and anti-Hrd1a antibodies was analyzed by immunoblotting with total proteins extracted from 2-week-old seedlings of wild-type Arabidopsis plant and relevant mutants. Source data are provided as a Source Data file.

Yeast two-hybrid assay. The Clontech's yeast two-hybrid system was used to examine the interactions of PAWHs, EBS7, and Hrd1a in yeast cells (AH109). The 1st cDNA preparation described above was used to amplify cDNA fragments of the N-terminal 260 amino acids of PAWH1 (PAWH1-N260) or the N-terminal 257 amino acids of PAWH2 (PAWH2-N257) with the *Y2H-PAWH1/2* primer sets (Supplementary Table 1). The PCR-amplified *PAWH1/2* cDNA fragments were subsequently cloned into the vectors, *pGADT7* (for expressing a fusion protein of the GAL4 activation domain with a target protein) and *pGBKT7* (for producing a fusion protein of the GAL4 DNA-binding domain with a protein of interest). The *pGADT7* and *pGBKT7* constructs of EBS7-N142 and the catalytic domain of Hrd1a (Hrd1a-CD containing amino acids of 247–492) were described previously³⁹. Yeast cells containing different combinations of *pGADT7* and *pGBKT7* plasmids were selected by growth on synthetic media lacking leucine and tryptophan. Several independent colonies were picked, resuspended in the liquid yeast growth medium, subsequently spotted via serial dilutions onto solid synthetic medium lacking leucine, tryptophan, and histidine for visual observation of their growth.

RNA isolation and analysis. Ten-day-old Arabidopsis seedlings grown on ½ MS medium supplemented with or without certain chemicals were harvested and ground in liquid nitrogen into a fine powder and their total RNAs were extracted using the RNeasy Plant Mini Kit (QIAGEN). One microgram of the purified total RNAs were treated with RNase-free DNase I (TIANGEN) and subsequently reverse transcribed into 1st strand cDNAs by the iScript™ cDNA synthesis Kit (Bio-Rad). The resulting cDNAs were used for classical PCR or quantitative real-time PCR (qPCR) analysis with gene-specific oligonucleotides listed in Supplementary Table 1. The qPCR assays were performed on the CFX96 Real-Time System (Bio-Rad) with SYBR® GREEN PCR Master Mix (Bio-Rad) following the manufacturer's instruction. Three biological replicates each with three technical repeats were conducted for each target mRNA and each sample. The *ACTIN8* cDNA was used as an internal control. The classical RT-PCR assays were carried out on a C1000 Touch™ Thermal Cycler (Bio-Rad) with 2xHiEff™ PCR Master Mix (Yeasten). The PCR amplified cDNA fragments were separated by agarose gel electrophoresis and visualized by Gel Doc™ XR+ Molecular Imager (Bio-Rad) with Image Lab™ software. The β -Tubulin was used as an internal reference. Source data are provided as a Source Data file.

Protein extraction and analyses. To isolate microsomal proteins, 1 g of 10-day-old Arabidopsis seedlings was harvested directly into liquid N₂ and immediately ground in liquid nitrogen into fine powder, dissolved in a homogenization buffer [50 mM Tris-HCl (pH 8.2), 20% (v/v) glycerol, 1 mM phenylmethylsulphonyl fluoride (PMSF, Sigma), 2 mM ethylenediaminetetraacetic acid (EDTA), 1 mM DTT, 2 protease inhibitor Cocktail Tablets (Roche) per 100 mL solution], and centrifuged for 10 min at 8000 × g at 4 °C. The supernatant (total proteins) was

centrifuged further at $100,000 \times g$ at 4°C for 60 min to collect the microsomal pellet. The resulting pellet was dissolved in the homogenization buffer as the microsomal fraction. Both the total proteins and microsomal fraction were used to immunoprecipitate the GFP-tagged Hrd1a and MYC/HA-tagged EBS7 using anti-GFP mAb-agarose (D153-8, MBL) and anti-MYC/anti-HA-agarose affinity gels (Sigma) for mass spectrometric analysis of Hrd1/EBS7-associated proteins. The microsomal fraction of the wild-type seedlings was subsequently treated with solutions of 0.1 M NaCl, 0.1 M Na_2CO_3 , 1% (v/v) Triton X-100 (Sigma) or 1% (v/v) Nonidet P-40 (Roche) at 4°C for 4 h. After treatment, the four fractions were centrifuged at $100,000 \times g$ at 4°C for 60 min to collect the supernatants (soluble fraction) and the pellets, which were mixed with 2x SDS buffer, boiled for 10 min, separated by 12% SDS/PAGE, and analyzed by immunoblotting.

We used 10-day-old seedlings to perform the coIP assays³⁹. In brief, 10-day-old Arabidopsis seedlings were harvested, ground into fine powder in liquid N_2 . Total proteins were extracted in the extraction buffer [50 mM Tris-HCl (pH 8.0), 150 mM NaCl, 5 mM EDTA, 0.1% (v/v) Triton X-100, 0.2% (v/v) Nonidet P-40 (Roche), 2 tablets of the protease inhibitor cocktail (Roche) per 100 mL] and the extracts were centrifuge at $14,000 \times g$ for 15 min at 4°C . The resulting supernatants were incubated with anti-EBS7 antibody³⁹ followed by protein-A/G-agarose beads (Abmart) at 4°C for 8 h. The immunoprecipitates were washed five times with the extraction buffer, resuspended in 2X SDS sample buffer, boiled at 95°C for 10 min, and separated by SDS/PAGE. For other immunoblot assays, 10-day-old Arabidopsis seedlings treated with or without a chemical of interest were harvested into liquid N_2 and stored in -80°C freezer for later analysis or immediately ground into fine powder in liquid N_2 . The broken plant tissues were dissolved in 2x SDS sample buffer, boiled at 95°C for 10 min, and centrifuged for 10 min at the top speed in an Eppendorf 5424 centrifuge. The resulting supernatants were immediately used for immunoblotting analysis or incubated with or without 1000 U Endo-Hf in 1x G5 buffer (New England Biolabs) at 37°C for 1.5 h. The treated/non-treated total proteins were separated by 7, 10, or 12% SDS-PAGE. For all the immunoblotting performed throughout this study, after transfer from SDS-PAGE gels to PVDF membranes (Bio-Rad), proteins were analyzed by immunoblot with antibodies against BESI⁵⁰, BRI1⁵⁰, BiP (at-95, Santa Cruz Biotechnology), maize-CRT⁶⁸, PDI (Rose Biotechnology Inc), EBS5³⁶, EBS6³⁷, EBS7³⁹, PAWHs (this study), Hrd1a (this study), GFP [living color® A.v.monoclonal antibody (JL-8), 632381, Takara], or HA (H9658, Sigma). The signals on those immunoblots were detected with horseradish peroxidase-conjugated secondary antibodies, ECL Select™ Western Blotting Detection Reagent (GE Healthcare), and Medical X-ray Processor (Kodak). The resulting signals on X-ray films were scanned and digitalized. Source data are provided as a Source Data file.

Sucrose density-gradient centrifugation. Sixteen grams of 10-day-old Arabidopsis seedlings were ground in liquid N_2 into a fine powder and immediately extracted by the homogenization buffer (see above) at 4°C . The protein extracts were first filtered through Miracloth (CalBiochem) to remove insoluble plant debris and subsequently centrifuged at $5000 \times g$ for 5 min at 4°C to remove cellular debris and organelles. The supernatant was centrifuged at $100,000 \times g$ for 45 min to pellet the microsomes, which was resuspended in 1 mL resuspension buffer [25 mM Tris-HCl (pH 7.5), 10% (w/v) sucrose, 1 mM PMSF, 2 mM EDTA, 1 mM DTT, 2 protease inhibitor Cocktail Tablets (Roche) per 100 mL]. The microsome resuspension was loaded onto the top of a 11-mL 20–50% (w/w) sucrose gradient in 10 mM Tris-HCl (pH 7.5), 2 mM EDTA, 1 mM DTT, 0.1 mM PMSF, and centrifuged at $100,000 \times g$ for 16 h. After centrifugation, 1 mL fractions (12 fractions) were hand collected, and 50 μL protein sample for each fraction was mixed with 2x SDS buffer, boiled for 10 min, separated by 10 and 12% SDS/PAGE, and analyzed by immunoblotting. For the Mg^{2+} -plus experiments, 5 mM MgCl_2 was added to the buffers of homogenization, resuspension, and ultracentrifugation. Source data are provided as a Source Data file.

Confocal analysis of PAWH1/2 fusion proteins. To generate *p35S::GFP-PAWH1* and *p35S::GFP-PAWH2* transgenes for visualization of PAWH1/2 subcellular localization patterns, an 858-bp PAWH1 cDNA fragment and an 849-bp PAWH2 cDNA fragment were amplified from the 1st cDNA preparation of the wild-type Arabidopsis seedlings using the GFP-PAWH1 and GFP-PAWH2 primer sets (Supplementary Table 1) and subsequently cloned into the *pCambia1300-p35S::N-GFP* vector. The plasmid *p35S::RFP-HDEL* was the same as used in the EBS7 study³⁹. To analyze the protein interaction using the bimolecular fluorescence complementation (BiFC) assay, an 858-bp PAWH1 cDNA or an 849-bp PAWH2 cDNA fragment amplified from the 1st strand cDNAs of wild-type Arabidopsis seedlings using the *NER-PAWH1* or *NER-PAWH2* primer set (see Supplementary Table 1) was cloned into the *pVYNER* vector⁶⁹. The same 1st cDNA preparation was also used to amplify the full-length (876-bp) EBS7 cDNA using the *CER-EBS7* primer set and the full-length (1479 bp) *Hrd1a* cDNA using the *CER-Hrd1a* primer set (Supplementary Table 1), which were subsequently cloned into the *pVYCER* and *pVYCE* vectors⁶⁹. These plasmids and the corresponding empty vectors, after verifying no PCR-introduced error, were individually transformed into the *Agrobacterium tumefaciens* strain GV3101. The *p35S::RFP-HDEL*-carrying GV3101 cells were mixed with the *p35S::GFP-PAWH1* or *p35S::GFP-PAWH2*-transformed GV3101 strain and co-transformed into leaves of 3-week-old tobacco (*Nicotiana benthamiana*) plants by the agro-infiltration

method⁷⁰. Similarly, a mixture of two *Agrobacterium* strains, one carrying a *pVYNER* plasmid and the other containing a *pVYCER* or *pVYCE* plasmid, was used to infiltrate young leaves of 3-week-old tobacco. Two days after infiltration, the transformed tobacco leaves were examined by confocal microscopy on a Leica SP8 (with LAS AF software, Leica Microsystems) for the subcellular localization patterns of GFP-tagged PAWH1/2 and the ER-localized RFP-HDEL or the reconstituted YFP signal. GFP, YFP, and RFP were excited by using 488-, 514-, and 542-nm laser light, respectively.

Liquid chromatography-tandem mass spectrometry. Immunoprecipitated proteins were eluted from antibody-conjugated beads with 0.2 M Glycine (pH 2.5), dried, and solubilized in 8 M urea containing 50 mM iodoacetamide. The alkylated proteins were digested by sequencing-grade trypsin (Promega) in 25 mM NH_4HCO_3 at an enzyme:substrate ratio of 1:100 (w/w) in a 37°C shaking incubator for 18 h. The tryptic peptides were collected after centrifugation at $13,523 \times g$ and freeze-dried with a refrigerated CentriVap concentrator (Labconco). Protein samples were reconstituted in 0.1% formic acid (FA) and analyzed by online nanoAcquity ultraperformance LC (Waters) coupled with an Orbitrap Fusion Tribrid mass spectrometer (Thermo Fisher Scientific). Nanospray was controlled by a PicoView Nanospray Source (PV550; New Objective) at a spray voltage of 1.9 kV. The peptides were trapped by a 2G-V/MT Trap symmetry C18 column (5 μm particles, 180 μm inner diameter \times 20 mm length) at a flow rate of 3 $\mu\text{L min}^{-1}$ for 3 min, and separated on a BEH130 C18 analytical column (1.7 μm particles, 100 μm inner diameter \times 250 mm length) at a flow rate of 250 nL min^{-1} . Peptides were eluted using mobile phases consisting of solvent A (0.1% FA in water) and solvent B (0.1% FA in acetonitrile) through a linear gradient, and then 85% of solvent B at a duration of 90 min. Data-dependent MS/MS acquisition was performed following a full MS survey scan by Orbitrap at a resolution of 70,000 over the m/z range of 350–1800, and MS/MS measurements of the top 20 most intense precursor ions. The MS raw data from the LC-MS/MS analyses were separately converted to mascot generic format (MGF) files using the Proteome Discoverer 1.4 software (Thermo Fisher Scientific) and then searched against in-house databases using Mascot Daemon 2.4 (MatrixSciences). The search parameter for tryptic digestion was restricted to a maximum of two missed cleavages of proteins. Cysteine carbamidomethylation was designated as a fixed modification. Mass tolerances were set up to 20 ppm for the Orbitrap-MS ions, and 0.2 or 1 Da for ion-trap MS/MS fragment ions.

Reporting summary. Further information on research design is available in the Nature Research Reporting Summary linked to this article.

Data availability

The mass spectrometry proteomic data have been deposited to the ProteomeXchange Consortium via the PRIDE partner repository (<https://www.ebi.ac.uk/pride/archive/>) with the dataset identifier PXD013400. The source data underlying Figs. 1d, 2b, c, 3d–f, 4a, 5a–c, and 6a–d and Supplementary Figs. 6, 9b, c, 11b–d, 12, 13b, 14b, c, e, f, 15d–f, 16d, 17–19, 20b, and 21 are provided by a Source Data file. The source data for generating Supplementary Figs. 7 and 8 were obtained from http://bar.utoronto.ca/cfp_arabidopsis (using At4g17420 and At5g47420 as queries) and atted.jp (using At5g47420 as query), respectively. All other data are available from the corresponding authors upon a reasonable request.

Received: 25 December 2018 Accepted: 16 July 2019

Published online: 02 August 2019

References

- Christianson, J. C. & Ye, Y. Cleaning up in the endoplasmic reticulum: ubiquitin in charge. *Nat. Struct. Mol. Biol.* **21**, 325–335 (2014).
- Vembar, S. S. & Brodsky, J. L. One step at a time: endoplasmic reticulum-associated degradation. *Nat. Rev. Mol. Cell Biol.* **9**, 944–957 (2008).
- Carvalho, P., Goder, V. & Rapoport, T. A. Distinct ubiquitin-ligase complexes define convergent pathways for the degradation of ER proteins. *Cell* **126**, 361–373 (2006).
- Bordallo, J., Plempner, R. K., Finger, A. & Wolf, D. H. Der3p/Hrd1p is required for endoplasmic reticulum-associated degradation of misfolded luminal and integral membrane proteins. *Mol. Biol. Cell* **9**, 209–222 (1998).
- Kikkert, M. et al. Human HRD1 is an E3 ubiquitin ligase involved in degradation of proteins from the endoplasmic reticulum. *J. Biol. Chem.* **279**, 3525–3534 (2004).
- Fang, S. et al. The tumor autocrine motility factor receptor, gp78, is a ubiquitin protein ligase implicated in degradation from the endoplasmic reticulum. *Proc. Natl Acad. Sci. USA* **98**, 14422–14427 (2001).
- Gardner, R. G. et al. Endoplasmic reticulum degradation requires lumen to cytosol signaling. Transmembrane control of Hrd1p by Hrd3p. *J. Cell Biol.* **151**, 69–82 (2000).

8. Mueller, B., Lilley, B. N. & Ploegh, H. L. SEL1L, the homologue of yeast Hrd3p, is involved in protein dislocation from the mammalian ER. *J. Cell Biol.* **175**, 261–270 (2006).
9. Kim, W., Spear, E. D. & Ng, D. T. Yos9p detects and targets misfolded glycoproteins for ER-associated degradation. *Mol. Cell* **19**, 753–764 (2005).
10. Szathmary, R., Biemann, R., Nita-Lazar, M., Burda, P. & Jakob, C. A. Yos9 protein is essential for degradation of misfolded glycoproteins and may function as lectin in ERAD. *Mol. Cell* **19**, 765–775 (2005).
11. Hosokawa, N., Kamiya, Y., Kamiya, D., Kato, K. & Nagata, K. Human OS-9, a lectin required for glycoprotein endoplasmic reticulum-associated degradation, recognizes mannose-trimmed N-glycans. *J. Biol. Chem.* **284**, 17061–17068 (2009).
12. Hosokawa, N. et al. Human XTP3-B forms an endoplasmic reticulum quality control scaffold with the HRD1-SEL1L ubiquitin ligase complex and BiP. *J. Biol. Chem.* **283**, 20914–20924 (2008).
13. Awasthi, S., Palmer, R., Castro, M., Mobarak, C. D. & Ruby, S. W. New roles for the Snp1 and Exo84 proteins in yeast pre-mRNA splicing. *J. Biol. Chem.* **276**, 31004–31005 (2001).
14. Schulze, A. et al. The ubiquitin-domain protein HERP forms a complex with components of the endoplasmic reticulum associated degradation pathway. *J. Mol. Biol.* **354**, 1021–1027 (2005).
15. Gauss, R., Sommer, T. & Jarosch, E. The Hrd1p ligase complex forms a linchpin between ER-lumenal substrate selection and Cdc48p recruitment. *EMBO J.* **25**, 1827–1835 (2006).
16. Wang, X., Ye, Y., Lencer, W. & Hansen, T. H. The viral E3 ubiquitin ligase mK3 uses the Derlin/p97 endoplasmic reticulum-associated degradation pathway to mediate down-regulation of major histocompatibility complex class I proteins. *J. Biol. Chem.* **281**, 8636–8644 (2006).
17. Lenk, U. et al. A role for mammalian Ubc6 homologues in ER-associated protein degradation. *J. Cell Sci.* **115**, 3007–3014 (2002).
18. Webster, J. M., Tiwari, S., Weissman, A. M. & Wojcikiewicz, R. J. Inositol 1,4,5-trisphosphate receptor ubiquitination is mediated by mammalian Ubc7, a component of the endoplasmic reticulum-associated degradation pathway, and is inhibited by chelation of intracellular Zn²⁺. *J. Biol. Chem.* **278**, 38238–38246 (2003).
19. Biederer, T., Volkwein, C. & Sommer, T. Role of Cue1p in ubiquitination and degradation at the ER. *Surf. Sci.* **278**, 1806–1809 (1997).
20. Ruggiano, A., Foresti, O. & Carvalho, P. Quality control: ER-associated degradation: protein quality control and beyond. *J. Cell. Biol.* **204**, 869–879 (2014).
21. Baldrige, R. D. & Rapoport, T. A. Autoubiquitination of the Hrd1 ligase triggers protein retrotranslocation in ERAD. *Cell* **166**, 394–407 (2016).
22. Iida, Y. et al. SEL1L protein critically determines the stability of the HRD1-SEL1L endoplasmic reticulum-associated degradation (ERAD) complex to optimize the degradation kinetics of ERAD substrates. *J. Biol. Chem.* **286**, 16929–16939 (2011).
23. Sun, S. et al. Sel1L is indispensable for mammalian endoplasmic reticulum-associated degradation, endoplasmic reticulum homeostasis, and survival. *Proc. Natl Acad. Sci. USA* **111**, E582–E591 (2014).
24. Carroll, S. M. & Hampton, R. Y. Usa1p is required for optimal function and regulation of the Hrd1p endoplasmic reticulum-associated degradation ubiquitin ligase. *J. Biol. Chem.* **285**, 5146–51456 (2010).
25. Huang, C. H., Chu, Y. R., Ye, Y. & Chen, X. Role of HERP and a HERP-related protein in HRD1-dependent protein degradation at the endoplasmic reticulum. *J. Biol. Chem.* **289**, 4444–4454 (2014).
26. Strasser, R. Protein quality control in the endoplasmic reticulum of plants. *Annu. Rev. Plant Biol.* **69**, 147–172 (2018).
27. Hong, Z. et al. Evolutionarily conserved glycan signal to degrade aberrant brassinosteroid receptors in Arabidopsis. *Proc. Natl Acad. Sci. USA* **109**, 11437–11442 (2012).
28. Hong, Z. et al. Mutations of an alpha1,6 mannosyltransferase inhibit endoplasmic reticulum-associated degradation of defective brassinosteroid receptors in Arabidopsis. *Plant Cell* **21**, 3792–3802 (2009).
29. Li, J. et al. Specific ER quality control components required for biogenesis of the plant innate immune receptor EFR. *Proc. Natl Acad. Sci. USA* **106**, 15973–15978 (2009).
30. Saijo, Y. et al. Receptor quality control in the endoplasmic reticulum for plant innate immunity. *EMBO J.* **28**, 3439–3449 (2009).
31. Huttner, S. et al. A context-independent N-glycan signal targets the misfolded extracellular domain of Arabidopsis STRUBBELIG to endoplasmic-reticulum-associated degradation. *Biochem. J.* **464**, 401–411 (2014).
32. Shin, Y. J., Vavra, U., Veit, C. & Strasser, R. The glycan-dependent ERAD machinery degrades topologically diverse misfolded proteins. *Plant J.* **94**, 246–259 (2018).
33. Cui, F. et al. Arabidopsis ubiquitin conjugase UBC32 is an ERAD component that functions in brassinosteroid-mediated salt stress tolerance. *Plant Cell* **24**, 233–244 (2012).
34. Liu, L. et al. The endoplasmic reticulum-associated degradation is necessary for plant salt tolerance. *Cell Res.* **21**, 957–969 (2011).
35. Chen, Q. et al. HRD1-mediated ERAD tuning of ER-bound E2 is conserved between plants and mammals. *Nat. Plants* **2**, 16094 (2016).
36. Su, W., Liu, Y., Xia, Y., Hong, Z. & Li, J. Conserved endoplasmic reticulum-associated degradation system to eliminate mutated receptor-like kinases in Arabidopsis. *Proc. Natl Acad. Sci. USA* **108**, 870–875 (2011).
37. Su, W., Liu, Y., Xia, Y., Hong, Z. & Li, J. The Arabidopsis homolog of the mammalian OS-9 protein plays a key role in the endoplasmic reticulum-associated degradation of misfolded receptor-like kinases. *Mol. Plant* **5**, 929–940 (2012).
38. Huttner, S., Veit, C., Schoberer, J., Grass, J. & Strasser, R. Unraveling the function of Arabidopsis thaliana OS9 in the endoplasmic reticulum-associated degradation of glycoproteins. *Plant Mol. Biol.* **79**, 21–33 (2012).
39. Liu, Y. et al. EBS7 is a plant-specific component of a highly conserved endoplasmic reticulum-associated degradation system in Arabidopsis. *Proc. Natl Acad. Sci. USA* **112**, 12205–12210 (2015).
40. Liu, Y. & Li, J. Endoplasmic reticulum-mediated protein quality control in Arabidopsis. *Front. Plant Sci.* **5**, 162 (2014).
41. Jin, H., Yan, Z., Nam, K. H. & Li, J. Allele-specific suppression of a defective brassinosteroid receptor reveals a physiological role of UGGT in ER quality control. *Mol. Cell* **26**, 821–830 (2007).
42. Harner, M. E. et al. Aim24 and MICOS modulate respiratory function, tafazzin-related cardiolipin modification and mitochondrial architecture. *eLife* **3**, e01684 (2014).
43. Hu, C. D. & Kerppola, T. K. Simultaneous visualization of multiple protein interactions in living cells using multicolor fluorescence complementation analysis. *Nat. Biotechnol.* **21**, 539–545 (2003).
44. Aoki, Y., Okamura, Y., Tadaka, S., Kinoshita, K. & Obayashi, T. ATTED-II in 2016: a plant coexpression database towards lineage-specific coexpression. *Plant Cell Physiol.* **57**, e5 (2016).
45. Martinez, I. M. & Chrispeels, M. J. Genomic analysis of the unfolded protein response in Arabidopsis shows its connection to important cellular processes. *Plant Cell* **15**, 561–576 (2003).
46. Lord, J. M., Kagawa, T., Moore, T. S. & Beevers, H. Endoplasmic reticulum as the site of lecithin formation in castor bean endosperm. *J. Cell Biol.* **57**, 659–667 (1973).
47. Friedrichsen, D. M., Joazeiro, C. A., Li, J., Hunter, T. & Chory, J. Brassinosteroid-insensitive-1 is a ubiquitously expressed leucine-rich repeat receptor serine/threonine kinase. *Plant Physiol.* **123**, 1247–1256 (2000).
48. Alonso, J. M. et al. Genome-wide insertional mutagenesis of Arabidopsis thaliana. *Science* **301**, 653–657 (2003).
49. Clouse, S. D., Langford, M. & McMorris, T. C. A brassinosteroid-insensitive mutant in Arabidopsis thaliana exhibits multiple defects in growth and development. *Plant Physiol.* **111**, 671–678 (1996).
50. Mora-Garcia, S. et al. Nuclear protein phosphatases with Kelch-repeat domains modulate the response to brassinosteroids in Arabidopsis. *Genes Dev.* **18**, 448–460 (2004).
51. Zhou, J. et al. Regulation of Arabidopsis brassinosteroid receptor BRI1 endocytosis and degradation by plant U-box PUB12/PUB13-mediated ubiquitination. *Proc. Natl Acad. Sci. USA* **115**, E1906–E1915 (2018).
52. Jin, H., Hong, Z., Su, W. & Li, J. A plant-specific calreticulin is a key retention factor for a defective brassinosteroid receptor in the endoplasmic reticulum. *Proc. Natl Acad. Sci. USA* **106**, 13612–13617 (2009).
53. Zipfel, C. et al. Perception of the bacterial PAMP EF-Tu by the receptor EFR restricts Agrobacterium-mediated transformation. *Cell* **125**, 749–760 (2006).
54. Walter, P. & Ron, D. The unfolded protein response: from stress pathway to homeostatic regulation. *Science* **334**, 1081–1086 (2011).
55. Howell, S. H. Endoplasmic reticulum stress responses in plants. *Annu. Rev. Plant Biol.* **64**, 477–499 (2013).
56. Doblas, V. G. et al. The SUD1 gene encodes a putative E3 ubiquitin ligase and is a positive regulator of 3-hydroxy-3-methylglutaryl coenzyme A reductase activity in Arabidopsis. *Plant Cell* **25**, 728–743 (2013).
57. Son, O., Cho, S. K., Kim, E. Y. & Kim, W. T. Characterization of three Arabidopsis homologs of human RING membrane anchor E3 ubiquitin ligase. *Plant Cell Rep.* **28**, 561–569 (2009).
58. Bernasconi, R. et al. Role of the SEL1L:LC3-I complex as an ERAD tuning receptor in the mammalian ER. *Mol. Cell* **46**, 809–819 (2012).
59. Deckers, M. et al. Aim24 stabilizes respiratory chain supercomplexes and is required for efficient respiration. *FEBS Lett.* **588**, 2985–2992 (2014).
60. Munoz-Gomez, S. A., Slamovits, C. H., Dacks, J. B. & Wideman, J. G. The evolution of MICOS: ancestral and derived functions and interactions. *Commun. Integr. Biol.* **8**, e1094593 (2015).
61. Antton, A. A. et al. The structure of trp RNA-binding attenuation protein. *Nature* **374**, 693–700 (1995).
62. Noguchi, T. et al. Brassinosteroid-insensitive dwarf mutants of Arabidopsis accumulate brassinosteroids. *Plant Physiol.* **121**, 743–752 (1999).

63. Rosso, M. G. et al. An *Arabidopsis thaliana* T-DNA mutagenized population (GABI-Kat) for flanking sequence tag-based reverse genetics. *Plant Mol. Biol.* **53**, 247–259 (2003).
64. Li, J., Nam, K. H., Vafeados, D. & Chory, J. BIN2, a new brassinosteroid-insensitive locus in *Arabidopsis*. *Plant Physiol.* **127**, 14–22 (2001).
65. Clough, S. J. & Bent, A. F. Floral dip: a simplified method for *Agrobacterium*-mediated transformation of *Arabidopsis thaliana*. *Plant J.* **16**, 735–743 (1998).
66. Feng, Z. et al. Efficient genome editing in plants using a CRISPR/Cas system. *Cell Res.* **23**, 1229–1232 (2013).
67. Pryor, K. D. & Leiting, B. High-level expression of soluble protein in *Escherichia coli* using a His6-tag and maltose-binding-protein double-affinity fusion system. *Protein Expr. Purif.* **10**, 309–319 (1997).
68. Baluska, F., Samaj, J., Napier, R. & Volkmann, D. Maize calreticulin localizes preferentially to plasmodesmata in root apex. *Plant J.* **19**, 481–488 (1999).
69. Waadt, R. et al. Multicolor bimolecular fluorescence complementation reveals simultaneous formation of alternative CBL/CIPK complexes in planta. *Plant J.* **56**, 505–516 (2008).
70. Voinnet, O., Rivas, S., Mestre, P. & Baulcombe, D. An enhanced transient expression system in plants based on suppression of gene silencing by the p19 protein of tomato bushy stunt virus. *Plant J.* **33**, 949–956 (2003).

Acknowledgements

We are grateful to the Core Facilities at Shanghai Center for Plant Stress biology for their excellent technical supports, the Arabidopsis Biological Resource Center at Ohio State University for providing seeds of the T-DNA insertional *pawh1* and *pawh2* mutants, Dr. Frans Tax for *bri1-5* seeds, Dr. Yanhai Yin for anti-BES1 antibody, and Dr. Jian-Kang Zhu for the CRISPR/Cas9 vectors. We thank other members of the J.L. laboratory for stimulating discussions. This work was partially supported by grants from National Natural Science Foundation of China (NSFC31730019 to J.L. and NSFC31600996 to L.Liu.), a grant from the Chinese Academy of Sciences (2012CSP004 to J.L.), and research funds from Shanghai Center for Plant Stress Biology and South China Agricultural University.

Author contributions

J.L. conceived the research plans, J.L., L.Liu., and W.X. supervised the project, suggested experiments, analyzed results, and wrote the manuscript with support from J.M. and J.Z.;

C.Z. initiated the project and carried out the immunoprecipitation-mass spectrometry experiments, L.Lin. performed a majority of the experiments, analyzed data, and prepared figures with technical assistance from Y.C., Y.W., D.W., X.L., and M.W.

Additional information

Supplementary Information accompanies this paper at <https://doi.org/10.1038/s41467-019-11480-7>.

Competing interests: The authors declare no competing interests.

Reprints and permission information is available online at <http://npg.nature.com/reprintsandpermissions/>

Peer review information: *Nature Communications* thanks Alessandro Vitale and other anonymous reviewer(s) for their contribution to the peer review of this work. Peer reviewer reports are available.

Publisher's note: Springer Nature remains neutral with regard to jurisdictional claims in published maps and institutional affiliations.



Open Access This article is licensed under a Creative Commons Attribution 4.0 International License, which permits use, sharing, adaptation, distribution and reproduction in any medium or format, as long as you give appropriate credit to the original author(s) and the source, provide a link to the Creative Commons license, and indicate if changes were made. The images or other third party material in this article are included in the article's Creative Commons license, unless indicated otherwise in a credit line to the material. If material is not included in the article's Creative Commons license and your intended use is not permitted by statutory regulation or exceeds the permitted use, you will need to obtain permission directly from the copyright holder. To view a copy of this license, visit <http://creativecommons.org/licenses/by/4.0/>.

© The Author(s) 2019

UNDERSTANDING THE MOLECULAR MECHANISMS OF PLANT RESPONSES TO ABIOTIC STRESS

EDITED BY: Sang Yeol Lee, Dae-Jin Yun, Jose M. Pardo, Motoaki Seki,
Yan Guo and Abel Rosado
PUBLISHED IN: *Frontiers in Plant Science*





frontiers

Frontiers eBook Copyright Statement

The copyright in the text of individual articles in this eBook is the property of their respective authors or their respective institutions or funders. The copyright in graphics and images within each article may be subject to copyright of other parties. In both cases this is subject to a license granted to Frontiers.

The compilation of articles constituting this eBook is the property of Frontiers.

Each article within this eBook, and the eBook itself, are published under the most recent version of the Creative Commons CC-BY licence.

The version current at the date of publication of this eBook is CC-BY 4.0. If the CC-BY licence is updated, the licence granted by Frontiers is automatically updated to the new version.

When exercising any right under the CC-BY licence, Frontiers must be attributed as the original publisher of the article or eBook, as applicable.

Authors have the responsibility of ensuring that any graphics or other materials which are the property of others may be included in the CC-BY licence, but this should be checked before relying on the CC-BY licence to reproduce those materials. Any copyright notices relating to those materials must be complied with.

Copyright and source acknowledgement notices may not be removed and must be displayed in any copy, derivative work or partial copy which includes the elements in question.

All copyright, and all rights therein, are protected by national and international copyright laws. The above represents a summary only. For further information please read Frontiers' Conditions for Website Use and Copyright Statement, and the applicable CC-BY licence.

ISSN 1664-8714

ISBN 978-2-88963-491-0

DOI 10.3389/978-2-88963-491-0

About Frontiers

Frontiers is more than just an open-access publisher of scholarly articles: it is a pioneering approach to the world of academia, radically improving the way scholarly research is managed. The grand vision of Frontiers is a world where all people have an equal opportunity to seek, share and generate knowledge. Frontiers provides immediate and permanent online open access to all its publications, but this alone is not enough to realize our grand goals.

Frontiers Journal Series

The Frontiers Journal Series is a multi-tier and interdisciplinary set of open-access, online journals, promising a paradigm shift from the current review, selection and dissemination processes in academic publishing. All Frontiers journals are driven by researchers for researchers; therefore, they constitute a service to the scholarly community. At the same time, the Frontiers Journal Series operates on a revolutionary invention, the tiered publishing system, initially addressing specific communities of scholars, and gradually climbing up to broader public understanding, thus serving the interests of the lay society, too.

Dedication to Quality

Each Frontiers article is a landmark of the highest quality, thanks to genuinely collaborative interactions between authors and review editors, who include some of the world's best academicians. Research must be certified by peers before entering a stream of knowledge that may eventually reach the public - and shape society; therefore, Frontiers only applies the most rigorous and unbiased reviews.

Frontiers revolutionizes research publishing by freely delivering the most outstanding research, evaluated with no bias from both the academic and social point of view. By applying the most advanced information technologies, Frontiers is catapulting scholarly publishing into a new generation.

What are Frontiers Research Topics?

Frontiers Research Topics are very popular trademarks of the Frontiers Journals Series: they are collections of at least ten articles, all centered on a particular subject. With their unique mix of varied contributions from Original Research to Review Articles, Frontiers Research Topics unify the most influential researchers, the latest key findings and historical advances in a hot research area! Find out more on how to host your own Frontiers Research Topic or contribute to one as an author by contacting the Frontiers Editorial Office: researchtopics@frontiersin.org

Table of Contents

- 06** *Pectin Methylesterases: Cell Wall Remodeling Proteins Are Required for Plant Response to Heat Stress*
Hui-Chen Wu, Victor P. Bulgakov and Tsung-Luo Jinn
- 27** *Overexpression of the Wheat (Triticum aestivum L.) TaPEPKR2 Gene Enhances Heat and Dehydration Tolerance in Both Wheat and Arabidopsis*
Xinshan Zang, Xiaoli Geng, Kexiang He, Fei Wang, Xuejun Tian, Mingming Xin, Yingyin Yao, Zhaorong Hu, Zhongfu Ni, Qixin Sun and Huiru Peng
- 35** *OsDIRP1, a Putative RING E3 Ligase, Plays an Opposite Role in Drought and Cold Stress Responses as a Negative and Positive Factor, Respectively, in Rice (Oryza sativa L.)*
Li Hua Cui, Hye Jo Min, Mi Young Byun, Hyeong Geun Oh and Woo Taek Kim
- 49** *The Rice SPOTTED LEAF4 (SPL4) Encodes a Plant Spastin That Inhibits ROS Accumulation in Leaf Development and Functions in Leaf Senescence*
Giha Song, Choon-Tak Kwon, Suk-Hwan Kim, Yejin Shim, Chaemyeong Lim, Hee-Jong Koh, Gynheung An, Kiyoon Kang and Nam-Chon Paek
- 63** *Emerging Roles of LSM Complexes in Posttranscriptional Regulation of Plant Response to Abiotic Stress*
Rafael Catalá, Cristian Carrasco-López, Carlos Perea-Resa, Tamara Hernández-Verdeja and Julio Salinas
- 77** *Modulation of Ethylene and Ascorbic Acid on Reactive Oxygen Species Scavenging in Plant Salt Response*
Juan Wang and Rongfeng Huang
- 83** *Salinity and ABA Seed Responses in Pepper: Expression and Interaction of ABA Core Signaling Components*
Alessandra Ruggiero, Simone Landi, Paola Punzo, Marco Possenti, Michael J. Van Oosten, Antonello Costa, Giorgio Morelli, Albino Maggio, Stefania Grillo and Giorgia Batelli
- 97** *Regulation of K⁺ Nutrition in Plants*
Paula Ragel, Natalia Raddatz, Eduardo O. Leidi, Francisco J. Quintero and José M. Pardo
- 118** *Submergence and Waterlogging Stress in Plants: A Review Highlighting Research Opportunities and Understudied Aspects*
Takeshi Fukao, Blanca Estela Barrera-Figueroa, Piyada Juntawong and Julián Mario Peña-Castro
- 142** *Chloroplast Redox Regulatory Mechanisms in Plant Adaptation to Light and Darkness*
Francisco Javier Cejudo, Valle Ojeda, Víctor Delgado-Requerey, Maricruz González and Juan Manuel Pérez-Ruiz
- 153** *Endoplasmic Reticulum Plays a Critical Role in Integrating Signals Generated by Both Biotic and Abiotic Stress in Plants*
Chang-Jin Park and Jeong Mee Park

- 161 ***Early Brassica Crops Responses to Salinity Stress: A Comparative Analysis Between Chinese Cabbage, White Cabbage, and Kale***
Iva Pavlović, Selma Mlinarić, Danuše Tarkowská, Jana Oklestkova, Ondřej Novák, Hrvoje Lepeduš, Valerija Vujčić Bok, Sandra Radić Brkanac, Miroslav Strnad and Branka Salopek-Sondi
- 177 ***Epitranscriptomic RNA Methylation in Plant Development and Abiotic Stress Responses***
Jianzhong Hu, Stefano Manduzio and Hunseung Kang
- 188 ***Acetic Acid Treatment Enhances Drought Avoidance in Cassava (Manihot esculenta Crantz)***
Yoshinori Utsumi, Chikako Utsumi, Maho Tanaka, Chien Van Ha, Satoshi Takahashi, Akihiro Matsui, Tomoko M. Matsunaga, Sachihito Matsunaga, Yuri Kanno, Mitsunori Seo, Yoshie Okamoto, Erika Moriya and Motoaki Seki
- 200 ***A Wall-Associated Kinase Gene CaWAKL20 From Pepper Negatively Modulates Plant Thermotolerance by Reducing the Expression of ABA-Responsive Genes***
Hu Wang, Huanhuan Niu, Minmin Liang, Yufei Zhai, Wei Huang, Qin Ding, Yu Du and Minghui Lu
- 213 ***The 26S Proteasome is Required for the Maintenance of Root Apical Meristem by Modulating Auxin and Cytokinin Responses Under High-Boron Stress***
Takuya Sakamoto, Naoyuki Sotta, Takamasa Suzuki, Toru Fujiwara and Sachihito Matsunaga
- 226 ***Genome-Wide Characterization and Expression Analysis of Soybean TGA Transcription Factors Identified a Novel TGA Gene Involved in Drought and Salt Tolerance***
Bo Li, Ying Liu, Xi-Yan Cui, Jin-Dong Fu, Yong-Bin Zhou, Wei-Jun Zheng, Jin-Hao Lan, Long-Guo Jin, Ming Chen, You-Zhi Ma, Zhao-Shi Xu and Dong-Hong Min
- 246 ***Luciferase-Based Screen for Post-translational Control Factors in the Regulation of the Pseudo-Response Regulator PRR7***
Yeon Jeong Kim and David E. Somers
- 259 ***Corrigendum: Luciferase-Based Screen for Post-Translational Control Factors in the Regulation of the Pseudo-Response Regulator PRR7***
Yeon Jeong Kim and David E. Somers
- 260 ***The Physiological Functions of Universal Stress Proteins and Their Molecular Mechanism to Protect Plants From Environmental Stresses***
Yong Hun Chi, Sung Sun Koo, Hun Taek Oh, Eun Seon Lee, Joung Hun Park, Kieu Anh Thi Phan, Seong Dong Wi, Su Bin Bae, Seol Ki Paeng, Ho Byoung Chae, Chang Ho Kang, Min Gab Kim, Woe-Yeon Kim, Dae-Jin Yun and Sang Yeol Lee
- 273 ***Communications Between the Endoplasmic Reticulum and Other Organelles During Abiotic Stress Response in Plants***
Linchuan Liu and Jianming Li
- 287 ***ABA Alleviates Uptake and Accumulation of Zinc in Grapevine (Vitis vinifera L.) by Inducing Expression of ZIP and Detoxification-Related Genes***
Changzheng Song, Yifan Yan, Abel Rosado, Zhenwen Zhang and Simone Diego Castellarin

- 299** *OoNAC72, a NAC-Type Oxytropis ochrocephala Transcription Factor, Conferring Enhanced Drought and Salt Stress Tolerance in Arabidopsis*
Huirui Guan, Xin Liu, Fei Niu, Qianqian Zhao, Na Fan, Duo Cao, Dian Meng, Wei He, Bin Guo, Yahui Wei and Yanping Fu
- 313** *The Roles of GmERF135 in Improving Salt Tolerance and Decreasing ABA Sensitivity in Soybean*
Meng-Jie Zhao, Li-Juan Yin, Jian Ma, Jia-Cheng Zheng, Yan-Xia Wang, Jin-Hao Lan, Jin-Dong Fu, Ming Chen, Zhao-Shi Xu and You-Zhi Ma
- 324** *Transcriptome Analysis of the Hierarchical Response of Histone Deacetylase Proteins That Respond in an Antagonistic Manner to Salinity Stress*
Minoru Ueda, Akihiro Matsui, Shunsuke Watanabe, Makoto Kobayashi, Kazuki Saito, Maho Tanaka, Junko Ishida, Miyako Kusano, Mitsunori Seo and Motoaki Seki



Communications Between the Endoplasmic Reticulum and Other Organelles During Abiotic Stress Response in Plants

Linchuan Liu^{1,2} and Jianming Li^{1,2,3*}

¹State Key Laboratory for Conservation and Utilization of Subtropical Agro-Bioresources, South China Agricultural University, Guangzhou, China, ²Guangdong Key Laboratory for Innovative Development and Utilization of Forest Plant Germplasm, College of Forestry and Landscape Architecture, South China Agricultural University, Guangzhou, China, ³Department of Molecular, Cellular, and Developmental Biology, University of Michigan, Ann Arbor, MI, United States

OPEN ACCESS

Edited by:

Abel Rosado,
University of British Columbia, Canada

Reviewed by:

Giovanni Stefano,
Michigan State University,
United States
Yohann Boutté,
UMR5200 Laboratoire de biogenèse
membranaire (LBM), France

*Correspondence:

Jianming Li
jmlumaa@scau.edu.cn;
jian@umich.edu

Specialty section:

This article was submitted to
Plant Abiotic Stress,
a section of the journal
Frontiers in Plant Science

Received: 24 December 2018

Accepted: 21 May 2019

Published: 12 June 2019

Citation:

Liu L and Li J (2019)
Communications Between the
Endoplasmic Reticulum and Other
Organelles During Abiotic Stress
Response in Plants.
Front. Plant Sci. 10:749.
doi: 10.3389/fpls.2019.00749

To adapt to constantly changing environmental conditions, plants have evolved sophisticated tolerance mechanisms to integrate various stress signals and to coordinate plant growth and development. It is well known that inter-organellar communications play important roles in maintaining cellular homeostasis in response to environmental stresses. The endoplasmic reticulum (ER), extending throughout the cytoplasm of eukaryotic cells, is a central organelle involved in lipid metabolism, Ca^{2+} homeostasis, and synthesis and folding of secretory and transmembrane proteins crucial to perceive and transduce environmental signals. The ER communicates with the nucleus via the highly conserved unfolded protein response pathway to mitigate ER stress. Importantly, recent studies have revealed that the dynamic ER network physically interacts with other intracellular organelles and endomembrane compartments, such as the Golgi complex, mitochondria, chloroplast, peroxisome, vacuole, and the plasma membrane, through multiple membrane contact sites between closely apposed organelles. In this review, we will discuss the signaling and metabolite exchanges between the ER and other organelles during abiotic stress responses in plants as well as the ER-organelle membrane contact sites and their associated tethering complexes.

Keywords: membrane contact sites, endoplasmic reticulum, unfolded protein response, lipid exchange and transport, calcium homeostasis, reactive oxygen species

INTRODUCTION

Plants growing under natural habitats have to deal with various environmental stresses during their growth and development. Abiotic stresses such as extreme cold and hot temperatures, drought, salinity, and nutrient deficiency can greatly affect plant growth and crop productivity. Plants have evolved various sophisticated strategies to respond to different environmental stimuli at different levels from alternations in gene expression to changes in morphology (Nakashima et al., 2009; Su et al., 2013). The sensing and transduction of the environmental signals in stressed plants were intensively studied in the past several decades, revealing potential strategies to improve plant stress tolerance and agricultural productivity. It is generally believed that

plant cells sense external environmental stimuli by various sensors, which are localized on the plasma membrane (PM), in the cytosol, or inside organelles. These environmental sensors activate intracellular signaling cascades that involve Ca^{2+} , lipids, reactive oxygen species (ROS), and phytohormones (Osakabe et al., 2013; Zhu, 2016), ultimately inducing changes in gene expression, protein production, and metabolic pathways to enhance plant stress tolerance. Therefore, coordinated signaling between various intracellular compartments with distinct biochemical processes plays an important role in maintaining cellular homeostasis for the plant stress tolerance.

The endoplasmic reticulum (ER) is a central network of interconnected tubules and flattened cisternae that extend throughout the entire cytoplasm of the eukaryotic cells (Figure 1). The ER network occupies a large volume of the cytoplasm, with its membrane accounting for ~50% of total cellular membranes, and functions in protein processing and folding, lipid biosynthesis, and Ca^{2+} storage (Stefano and Brandizzi, 2018). In eukaryote cells, about one-third of newly synthesized proteins enter the ER where they are glycosylated, folded, and/or assembled into protein complexes. The ER houses several stringent quality control mechanisms that export only correctly folded and properly assembled proteins to continue their secretory journeys (Hetz et al., 2015). However, protein folding in the ER is an error-prone process that could easily be disturbed by various abiotic and biotic stresses, leading to accumulation of mis/unfolded

proteins in the ER and causing ER stress (Angelos et al., 2017). Currently, the unfolded protein response (UPR) is widely considered as a significant intracellular signaling pathway that links the ER proteostasis with gene regulation in the nucleus to alleviate the ER stress. Given its characteristic dynamic architecture and its essential roles in producing proteins and lipids for other organelles and maintaining Ca^{2+} homeostasis, the ER makes numerous physical contacts with other organelles and endomembrane compartments (Figure 1; Stefano and Brandizzi, 2018; Wu et al., 2018). Recent studies have identified many so-called ER-membrane contact sites (MCSs) that facilitate exchanges of important metabolites and signaling molecules between the ER and various organelles (Prinz, 2014; Wang and Dehesh, 2018; Wu et al., 2018). In this review, we will discuss recent results on the inter-organellar communications between the ER and other organelles during plant abiotic stress responses as well as the ER-organelle physical contacts and their associated tethering complexes.

THE ENDOPLASMIC RETICULUM-NUCLEUS INTERACTION VIA UNFOLDED PROTEIN RESPONSE

In addition to the physical ER-nuclear envelop connection (Figure 1), the ER-nucleus interaction is mediated by a highly conserved signaling mechanism known as UPR, which is activated by accumulation of misfolded proteins in the ER. Because protein folding is an error-prone process that can easily be disturbed by various environmental stresses, UPR is closely connected to the plant stress tolerance (Liu and Howell, 2016). In plants, the UPR pathway is principally mediated by two major branches that are conserved in mammalian cells (Howell, 2013). One arm is mediated by two homologous ER membrane-anchored bZIP-family transcription factors, bZIP17 and bZIP28 that are activated by regulated intradomain proteolysis (Liu et al., 2007a). bZIP17 was originally identified as a transcription factor activated by salt stress (Liu et al., 2007b), while bZIP28 was discovered to be activated by heat stress (Gao et al., 2008). Both bZIP17 and bZIP28 are type II transmembrane proteins with a single transmembrane domain (TMD) and a DNA-binding/transcriptional activation bZIP domain facing the cytosol, and a C-terminal domain inside the ER lumen (Sun et al., 2013). In response to ER stress, bZIP17 and bZIP28 dissociate from the major ER luminal chaperone, binding immunoglobulin proteins (BiPs), and traffic from the ER to the Golgi where the two bZIP proteins are proteolytically processed by the Golgi-resident site-1 and site-2 proteases (S1P and S2P), thus releasing their N-terminal cytosolic domains that move into the nucleus (Andersson et al., 2007; Liu et al., 2007b; Gao et al., 2008; Srivastava et al., 2012; Iwata et al., 2017). The nuclear-localized bZIP17/28 proteins bind to their target promoters to increase expression of genes encoding ER chaperones, folding catalysts, and components of the ER-associated degradation (ERAD) machinery, which work together to restore the ER homeostasis (Liu and Howell, 2010). Interestingly, high light intensity increases ER stress sensitivity of plants *via* a competitive inhibitory interaction of bZIP28 with LONG HYPOCOTYL5 (HY5), a bZIP protein that positively regulates

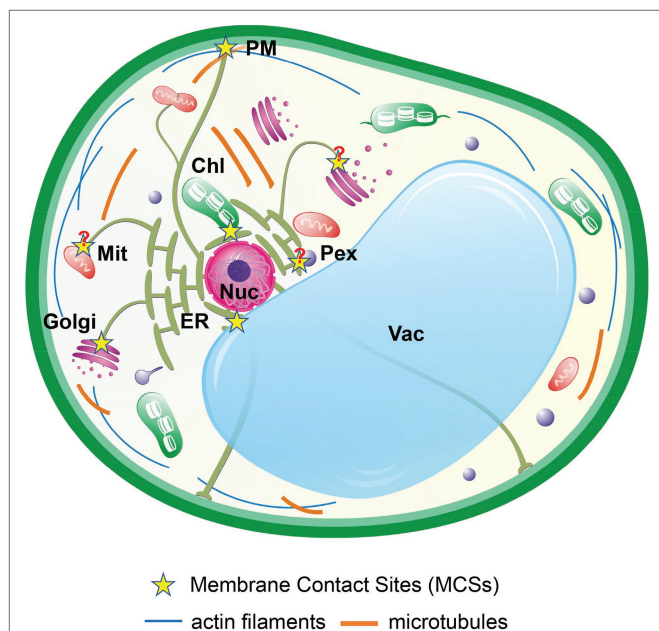


FIGURE 1 | Interactions of the ER network with other organelles in plant cells. The dynamic ER network physically interacts with other subcellular compartments, such as the Golgi (*cis*- and *trans*-), mitochondria (Mit), chloroplasts (Chl), peroxisomes (PEX), vacuole (Vac), nucleus (Nuc), and the plasma membrane (PM) through MCSs. The pointed extensions of a peroxisome and a chloroplast represent peroxule and stromules, respectively. Question marks indicate MCSs that have not yet characterized. MCS-enriched proteins are directly involved in physical tethering; mediate organelle biogenesis; and regulate exchanges of lipids, Ca^{2+} , ROS, and other important metabolites and signaling molecules.

light signaling but suppresses the UPR pathway (Nawkar et al., 2017). The other arm of the plant UPR pathway involves the unconventional splicing of the mRNA of another bZIP transcription factor, bZIP60, which is catalyzed by the ER membrane-anchored inositol-requiring enzyme 1 (IRE1) (Deng et al., 2011; Nagashima et al., 2011). IRE1 is the most conserved ER stress sensor among yeast, plants, and animals and is a dual-functional protein with both protein serine/threonine kinase and endoribonuclease (RNase) activities. *Arabidopsis* has two IRE1 homologs, IRE1a and IRE1b (Koizumi et al., 2001). Under the ER stress, IRE1a and IRE1b can form homodimers or heterodimers to trigger their RNase activities, which splice the *bZIP60* mRNA (Howell, 2013). The frame-shift splicing of the *bZIP60* mRNA causes production of the active form of bZIP60 (bZIP60s, s for spliced) that lacks a transmembrane domain and can thus move into the nucleus to bind promoters of its target genes (Deng et al., 2011; Nagashima et al., 2011; Iwata and Koizumi, 2012). In addition to its *bZIP60* mRNA splicing role, the *Arabidopsis* IRE1s also participate in selective degradation of certain mRNAs of secretory pathway proteins and inhibitory proteins of the ER stress-induced autophagy, a process known as regulated IRE1-dependent decay of mRNAs (RIDD) (Mishiba et al., 2013; Bao et al., 2018). In plants, the ER stress responses are closely related to abiotic stress tolerance. *Arabidopsis* mutants defective in bZIP17, bZIP28, and/or bZIP60 show increased sensitivity to various environmental stresses whereas overexpression of the active forms of the three bZIP proteins enhances the plant stress tolerance (Fujita et al., 2007; Liu et al., 2007b; Kataoka et al., 2017; Ruberti et al., 2018). A recent study also implicated bZIP17 and a component of the *Arabidopsis* ERAD machinery in salt acclimation memory that enables plants to tolerate severe salt stress (Tian et al., 2018).

THE ENDOPLASMIC RETICULUM-GOLGI RELATIONSHIP

The ER and the Golgi apparatus are the first two membrane compartments in the protein secretory pathway. Unlike the mammalian cells in which the ER and the Golgi apparatus are separated by the ER-Golgi intermediate compartment (ERGIC, also known as the vesicular-tubular cluster or VTC), the ER and the Golgi complex are often physically attached in plant cells at ER exit sites (ERES) (Figure 1; Sparkes et al., 2009), although recent studies suggested the presence of an ERGIC-like compartment termed as GECCO for Golgi entry core compartment in plant cells (Ito et al., 2012, 2018). The ER-Golgi interaction involves the coat protein complex II (COPII)-mediated cargo export from the ER and the COPI-mediated retrieval of ER-resident proteins from the Golgi. Due to the existence of high stringent quality control mechanisms, only the correctly folded and properly assembled proteins can be exported from the ER into the Golgi, whereas those incompletely-/misfolded and improperly assembled proteins are retained in the ER for chaperone-assisted refolding or removal by ERAD that involves cytosolic proteasomes (Brandizzi and Barlowe, 2013; Liu and Li, 2014). In the Golgi complex that includes the *trans*-Golgi network (TGN), the ER-derived protein cargos undergo N-glycan maturation and are sorted

by vesicle-dependent/independent trafficking pathways to specific destinations to carry out their cellular functions. Live cell imaging revealed that the plant Golgi apparatus is a highly dynamic organelle with dispersed stacks of cisternae that are often physically attached to the ER tubules (Figure 1; Sparkes et al., 2009). Additionally, the shape and architecture of the Golgi complex are flexible enough to adapt to the functional status of different plant cells (Dupree and Sherrier, 1998). These functional and physical connections between the ER and the Golgi complex not only ensure normal cellular activities but are also essential for the survival of plant cells during stress conditions.

Recent studies have shown that several *Arabidopsis* mutants deficient in the ER-Golgi/Golgi-ER vesicle trafficking exhibit the ER stress and are hypersensitive to abscisic acid (ABA) and salt stress (Zhao et al., 2013, 2018; Pastor-Cantizano et al., 2018), suggesting that the bidirectional vesicle transport between the ER and Golgi is crucial for maintaining cellular homeostasis and adaptation to environment stresses. In addition to vesicular trafficking, accumulating evidence indicates the existence of non-vesicular transport connecting the ER and Golgi. Three-dimensional electron microscopy and Forster resonance energy transfer-based fluorescence lifetime imaging microscopy revealed the physical contacts between the ER subdomains and *trans*-Golgi/TGN in mammalian cells (Ladinsky et al., 1999; Venditti et al., 2019b). No ER-*trans*-Golgi/TGN (referred hereinafter as ER-TG) contact has been observed so far in plant cells, but laser trap was used to reveal the ER-*cis*-Golgi interaction in plant cells, which occurs at ERES where the mobile Golgi stacks are associated with COPII components (Figure 1; Dasilva et al., 2004; Hawes et al., 2008; Sparkes et al., 2009). AtCASP, a homolog of a yeast/mammalian transmembrane Golgi protein known as CCAAT-displacement protein alternatively spliced product (CASP) was recently identified as a component of a novel tethering complex that connects ERES with the *cis*-Golgi to form the so-called “mobile secretory unit” (Osterrieder et al., 2017). The *cis*-Golgi-localized AtCASP could interact with ERES-enriched proteins to mediate the ER-*cis*-Golgi tethering that likely increases the efficiency of COPII vesicle-mediated cargo transport *via* the so-called “hug-and-kiss” mechanism (Kurokawa et al., 2014). Identification of potential AtCASP-binding proteins that are enriched at ERES could discover additional components of the ER-*cis*-Golgi tethering complex that might help to resolve the controversy on the mechanism of the ER-Golgi transport (Robinson et al., 2015) and explain the “sticky” nature of the plant *cis*-Golgi cisterna (Sparkes et al., 2009).

Mammalian cells lack the ER-*cis*-Golgi physical contact but contain multiple ER-TG contact sites that are implicated in the non-vesicle-mediated lipid exchange (Figure 1; Mesmin et al., 2019; Venditti et al., 2019b). Several lipid transfer proteins (LTPs) localized at the ER-TG interface were identified, such as CERT (ceramide-transfer protein), FAPP2 (four-phosphate adaptor protein 2), and OSBP (oxysterol-binding protein), which mediate the vesicle-independent ER-TG transport of ceramide, glucosylceramide, and cholesterol (coupled with counter-transport of phosphatidylinositol-4-phosphate), respectively (Mesmin et al.,

2019; Venditti et al., 2019a). All three LTPs share similar protein domains important for the ER-TG bridging, including a TGN-binding N-terminal pleckstrin homology (PH) domain, a central FFAT (diphenylalanine in an acidic tract) motif exhibiting specific binding to the ER-localized vesicle-associated membrane protein-associated proteins (VAPs), and the C-terminal oxysteroid-binding domain. Almost nothing is known about the ER-TG contact in plant cells, but the *Arabidopsis* genome encodes multiple homologs of CERT/FAPP2/OSBP (Umate, 2011) that lack the FFAT motif and a total of 12 VAP homologs known as plant VAP homologs (PVAs) (Sutter et al., 2006). One of the *Arabidopsis* OSBP-related proteins (ORPs), ORP3a, is localized to the ER *via* its interaction with an ER-localized PVA, PVA12 through a WFDE (tryptophan-phenylalanine-aspartate-glutamate) motif located on the surface of ORP3a (Saravanan et al., 2009). It remains to be investigated whether or not plant cells have the ER-TG physical contacts, and if so, whether some of the *Arabidopsis* homologs of CERT/FAPP2/OSBP interact with ER-localized PVAs to mediate the ER-TG tethering and the ER-TG lipid/sterol exchanges.

THE ENDOPLASMIC RETICULUM-MITOCHONDRIA CONNECTION

Mitochondrion is an intracellular double-membrane organelle found in all eukaryotic cells. It not only provides cellular energy and metabolic intermediates but also participates in many other cellular processes, such as ROS signaling, Ca^{2+} buffering, cell differentiation, and apoptosis (Labbé et al., 2014). Under changing environmental conditions, plants have to adjust their metabolism to balance their energy production and consumption through mitochondria. Recently, a growing body of evidence suggests that mitochondria and the ER cooperate in several biosynthetic pathways and exchange signaling molecules during stress conditions (Mueller and Reski, 2015; Wang and Dehesh, 2018). It is well known that environmental stresses, such as heat, drought, salinity, and high light intensity, increase production and accumulation of ROS in mitochondria, which not only serves an important intracellular signal (at low concentrations) to regulate various cellular pathways but also causes oxidative damage (at high concentrations) to the cellular components (Suzuki et al., 2012; Das and Roychoudhury, 2014). ROS can also be generated in the ER lumen, which has a higher redox potential (~100 mV) than that of other cellular compartments (Birk et al., 2013). The oxidative protein folding process in the ER is mediated by protein disulfide isomerases (PDIs) and a flavin adenine dinucleotide-binding protein, ER oxidoreductase 1 (Ero1), which produces H_2O_2 as a result of electron flow from target proteins *via* the PDI-Ero1 couple to O_2 (Tü and Weissman, 2002; Santos et al., 2009; Higa and Chevet, 2012). Due to the H_2O_2 permeability of the ER membrane (Ramming et al., 2014), the ER-induced oxidative stress can influence the production of mitochondrial ROS likely mediated by the ER-mitochondria physical contacts (Bhandary et al., 2012; Murphy, 2013; Zeeshan et al., 2016). On the other hand,

the mitochondrial ROS can induce expression of the ER UPR target genes (Ozgur et al., 2015).

The ER-mitochondria contact is also essential to build the membrane system of mitochondria that import most lipids from other organelles (Li-Beisson et al., 2017). The ER-mitochondria tethering allows lipid exchanges between two apposed membranes and/or permits access of the membrane-localized enzymes to lipid substrates on the tethered membrane (Michaud et al., 2017). In yeast, the ER-mitochondria encounter structure (ERMES) is the most well-defined ER-mitochondria tethering complex that facilitates the ER-mitochondria phospholipid exchanges (Figure 1; Michel and Kornmann, 2012; Lang et al., 2015). The yeast ER-mitochondria tethering also involves another complex known as the ER membrane complex (EMC)-translocase of outer membrane 5 kDa subunit (TOM5) complex (Lahiri et al., 2014). In mammalian cells, the ER-mitochondria interface, known as mitochondria-associated ER membrane (MAM), has more complicated protein complexes involved in physical tethering, Ca^{2+} regulation, lipid exchanges, mitochondrial fission, autophagy, and apoptosis (Lee and Min, 2018). In plants, despite visual evidence for the ER-mitochondria physical interaction that likely plays a role in mitochondrial fission and the ER-mitochondria coordinated biosynthesis and exchanges of phospholipids (Figure 1; Mueller and Reski, 2015; Michaud et al., 2017), no homologs of the yeast ERMES were found in plants that also lack homologs of a majority of known mammalian MAM proteins (Duncan et al., 2013; Michaud et al., 2017). The *Arabidopsis* genome does encode homologs of three of the six components (EMC1, 2, 3, 5, 6, and TOM5) of the EMC-TOM5 complex (Michaud et al., 2016) and homologs of mitofusin1 (MFN1), a mitochondrial fusion GTPase that interacts with its ER-localized homolog MFN2 to mediate the ER-mitochondria tethering (Detmer and Chan, 2007; de Brito and Scorrano, 2008). However, the two *Arabidopsis* MFN1/2 homologs, DRP3A/3B and FZL, are not involved in mitochondrial fusion (Arimura, 2018), and there is no report on the involvement of the three homologs of the yeast EMC-TOM5 complex in the ER-mitochondria tethering in plant cells. A recent study identified a *Physcomitrella patens* protein, MELL1 (mitochondria-ER-localized LEA-related LysM domain protein 1) that regulates the numbers of the ER-mitochondria contact sites and could thus be a component of the plant ER-mitochondria tethering complex (Mueller and Reski, 2015). It will be interesting to determine whether MELL1 is conserved in higher plants and if so, whether the MELL1 homologs are a component of the yet to be identified ERMES/MAM in higher plants and required for the phospholipid biosynthesis/exchange of the ER and mitochondria. The lipid exchanges between the ER and mitochondria also involve lipid trafficking between the inner membrane (IM) and outer membrane (OM) of the mitochondria. A recent study implicated a mitochondrial transmembrane lipoprotein (MTL) complex containing the TOM complex and IM-localized AtMIC60, an *Arabidopsis* homolog of the yeast MIC60 that is a component of the well-studied mitochondria contact site and cristae organizing system (MICOS) (Pfanner et al., 2014), in the IM-OM lipid trafficking (Michaud et al., 2016). It is thus possible that the TOM complex, through its interaction with IM-localized AtMIC60 capable of extracting

membrane lipid and the ER-localized homologs of the yeast EMC-TOM5 complex, functions as a crucial component of a plant ER-mitochondria tethering complex to mediate lipid exchanges or coordinate lipid biosynthesis.

The ER-mitochondria physical contact is also essential for the Ca^{2+} cross talk between the two organelles, which is often influenced by ROS. In plants, a variety of environmental stimuli trigger Ca^{2+} transients, such as the influx of Ca^{2+} into the mitochondrial matrix, to regulate gene expression and metabolism (Carraretto et al., 2016). However, the ER is generally considered the main intracellular Ca^{2+} store. The Ca^{2+} channels located at the ER-mitochondria contact sites, such as the mitochondrial outer membrane-localized VDAC (voltage-dependent anion-selective channel) and the ER membrane-anchored inositol triphosphate-dependent calcium channel IP_3R , are believed to mediate the transport of Ca^{2+} between the ER and mitochondria in response to ER stress in mammalian cells (Lee and Min, 2018). The mammalian ER-localized Ca^{2+} -release channel ryanodine receptor is activated by Ero1 -generated H_2O_2 (Anelli et al., 2012). It remains to be determined if the ER ROS also regulates the ER Ca^{2+} release in plant cells that lack the homologs of the mammalian ER Ca^{2+} efflux channels IP_3R and ryanodine receptor (Stael et al., 2012).

Two recent studies revealed another interesting mechanism by which the ER interacts with the mitochondria in plant cells. The mitochondrial retrograde regulation (MRR), which transmits the stress-induced mitochondrial signal into the nucleus to increase production of certain mitochondrial proteins for sustaining or restoring the mitochondrial functions during stressful conditions (Dojcinovic et al., 2005), was shown to involve two ER-anchored NAC transcription factors, ANAC013 and ANAC017 (De Clercq et al., 2013; Ng et al., 2013). ANAC013 knockdown lines and an ANAC017 knockout mutant were hypersensitive to stress than their wild-type controls. It was hypothesized that the mitochondrial stress somehow activates yet unknown proteases that proteolytically activate the two ER-anchored ANAC proteins that can subsequently translocate into the nucleus (Wang et al., 2018c). It will be interesting to test if the proteolytic activation of the two NAC-type transcription factors occurs at ERMES/MAM in plant cells. Proteomic experiments with stressed *Arabidopsis* plants expressing non-cleavable variants of ANAC013/017 might lead to identification of potential components of the *Arabidopsis* ERMES/MAM. It is also interesting to note that the two ANACs were recently implicated in coordinating mitochondrial and chloroplast functions *via* their physical interactions with a nuclear protein Radical-induced Cell Death1 (RCD1) that was known to be regulated by ROS (Shapiguzov et al., 2019).

THE ENDOPLASMIC RETICULUM-PLASMA MEMBRANE CONTACT

The plasma membrane (PM), a lipid bilayer embedded with proteins, is an essential cellular component for the plant stress tolerance. It not only serves as a physical barrier to shield

cellular contents from the extracellular environment and controls the flux of solutes and macromolecules but also contains a wide range of sensors and receptors that perceive and transmit all kinds of environmental signals. As discussed above, the ER not only produces, folds, and assembles the PM-localized channels/transporters and receptors/sensors but also delivers lipids to the PM and other intracellular compartments *via* vesicle-dependent and/or independent mechanisms.

The ER-PM contact sites (EPCSs) are evolutionarily conserved microdomains that are important for the ER-PM communications, such as lipid homeostasis, and Ca^{2+} influx (Figure 1; Saheki and De Camilli, 2017). The composition of EPCSs and their molecular functions have been well established in the yeast and mammalian cells in the last decade (Stefan, 2018). The yeast EPCSs consists of six proteins: three tricalbins, Increased sodium tolerance protein 2 (Ist2), and the ER-resident protein Scs2/22 (Suppressor of choline sensitivity 2/22) (Manford et al., 2012). The mammalian EPCSs contains three tricalbin homologs known as E-Syts for extended synaptotagmin (Giordano et al., 2013) and two Scs2/22 homologs, VAP-A and VAP-B, but lacks an Ist2 homolog (Selitrennik and Lev, 2016). In plants, the EPCS complex is the best known protein tether of the plant ER MCSs and consists of VAP27, VAP-Related Suppressor of TMM (VST), an actin-binding protein NETWORKED 3C (NET3C), actin filaments, and microtubule networks (Figure 1; Wang et al., 2014, 2016, 2017, 2018a; Ho et al., 2016). In particular, a phospholipid-binding protein Synaptotagmin1 (SYT1), which is the plant homolog of tricalbin/E-Syts, was found in the plant EPCS complex (Perez-Sancho et al., 2015) and subsequently used as a marker for the plant EPCS for microscopic studies (McFarlane et al., 2017; Lee et al., 2019). SYT1 has been previously described as an essential component for maintaining the PM integrity, especially under conditions of high risks of membrane disruption such as osmotic shock, freezing, and salt stresses (Schapire et al., 2008). Other studies have shown that SYT1 is required for tethering the ER to the PM and plays an essential role in regulating the ER remodeling and the stability of EPCSs (Siao et al., 2016). A recent study revealed that the ER-anchored SYT1 directly binds the PM-localized phosphatidylinositol 4,5-bisphosphate [PI (4,5)P₂] to establish EPCSs (Lee et al., 2019), thus revealing a physiological function of the stressed-induced PM accumulation PI(4,5)P₂ (Heilmann, 2008). It is likely that the protein-lipid tether could be disrupted or strengthened by additional SYT1/PI(4,5)P₂-binding proteins.

EPCSs are now widely accepted as important sites for the non-vesicular lipid transport, which appears to be the major transport route of certain lipid species (Lev, 2012). Plants exposed to abiotic stresses have to adapt their membrane lipid composition and fluidity to changing environmental conditions by adjusting the relative amounts of various lipids, such as phospholipids and galactolipids (Hou et al., 2016). It is well known that lipids synthesized in the ER need to be delivered to other membranes for assembly of biological membranes or for lipid-mediated signaling cascades. It is proposed that the lipid transfer proteins (LTPs) are localized at the EPCSs and function as dynamic tethers between the two membranes with their lipid transfer module regulating lipid exchange (Dickson et al., 2016; Quon et al., 2018). Mammalian VAPs are known

to interact with proteins involved in lipid transfer (Gatta et al., 2015) while SYT1 contains a synaptotagmin-like mitochondria-lipid-binding protein (SMP) domain that is implicated in lipid transfer in mammals (Schauder et al., 2014). It is likely that the plant EPCSs are also involved in the ER-PM lipid transfer and thus play important role in plant stress tolerance by modulating the composition and fluidity of the PM. The EPCS is also important for the intracellular Ca^{2+} homeostasis in mammalian cells. The ER-PM contacts are critically implicated in generating the cytosolic Ca^{2+} signals, which is likely mediated by Ca^{2+} release from the ER in response to the PM-perceived environmental stimuli, and in replenishing the depleted ER Ca^{2+} store (Chung et al., 2017). Given the importance of Ca^{2+} signaling in plant stress response (Ranty et al., 2016), it would be interesting to investigate the role of EPCSs in regulating the stress-triggered intracellular Ca^{2+} dynamics in plants.

In addition to the EPCS-mediated exchange of lipids and Ca^{2+} , there are other mechanisms that connect the ER physiology to the PM function in plant stress response. A recent study implicated a PM-localized NAC transcription factor, ANAC062, in the ER-nucleus-mediated UPR pathway (Yang et al., 2014). It is quite possible that the ER stress could increase the EPCS formation, altering the local membrane lipid composition to enhance the proteolytic processing of the PM-anchored ANAC062 (Seo et al., 2010). The cleaved ANAC062 can then move into the nucleus to regulate UPR-related genes, thus helping to mitigate the ER stress. Other studies found that the increased cytosolic Ca^{2+} caused by the stress-triggered Ca^{2+} release from the ER could activate the PM-localized NADPH oxidase, which was known to be induced by UPR and is required to survive ER stress (Ozgur et al., 2015, 2018; Angelos and Brandizzi, 2018). It is quite tempting to speculate that the Ca^{2+} -mediated activation of the PM-localized NADPH oxidase might require EPCSs. It is important to note that the plant NADPH oxidase is the most well-studied ROS enzymatic system and plays a key role in ROS signaling involved in plant growth, stress tolerance, and plant immunity (Marino et al., 2012).

One unique type of the plant ER-PM contact occurs at plasmodesmata (PD), which consist of the cylindrically apposed PM and the tightly compressed ER (desmotubule) with unique lipid/protein compositions (Grison et al., 2015; Leijon et al., 2018). The PD-PM and the desmotubule are connected by spoke-like elements (Ding et al., 1992; Nicolas et al., 2017) whose molecular identities remain to be defined, but recent studies suggested the PD association of AtSYT1 (Levy et al., 2015) and VAP27 (Wang et al., 2016). The space between the PD-PM and the desmotubule constitutes the actual channel (the cytoplasmic sleeve) that transports a wide range of molecular cargos across cell walls of neighboring cells (Tilsner et al., 2016). Given the key role of PD in generating cytosolic and membrane continuity that are essential for growth and development, stress tolerance, and plant defense, the permeability of PD (also known as size exclusion limit), governed by the size of the cytoplasmic sleeve and distribution of spokes that creates nanochannels, is constantly regulated by various of developmental and environmental signals (Sun et al., 2019). Although PD exhibits the essential features of MCS (Scorrano et al., 2019), it remains to be investigated if

the ER-PM contacts in PD play any role in inter-organelle exchanges of lipids, Ca^{2+} , and/or other signaling molecules.

THE ENDOPLASMIC RETICULUM-CHLOROPLAST JUNCTION

Chloroplasts conduct photosynthesis and produce energy for plant growth, development, and defense. In addition, chloroplasts are essential for synthesizing certain amino acids, lipids, and fatty acids. Like mitochondrion, chloroplast is also a semiautonomous organelle with its own genome and a majority of chloroplast proteins are encoded by the nuclear genome and imported from the cytosol. Accordingly, the plant cells execute anterograde and retrograde communications between the chloroplast and the nucleus to respond to changing environment (Watson et al., 2018). Under stress conditions, ROS such as singlet oxygen and superoxide were generated from electron transport chain in the chloroplasts, which cause oxidative damage to the photosynthetic organelle. Consequently, the chloroplasts use ROS and several metabolites, such as 3'-phosphoadenosine 5'-phosphate (PAP) (Chan et al., 2016) and methylerythritol cyclodiphosphate (MEcPP) (Xiao et al., 2012), to relay the stress signal into the nucleus to reprogram gene expression for damage mitigation and stress acclimation (Woodson and Chory, 2012). The chloroplast-nucleus signaling might also involve chloroplast-nucleus contact sites consisting of stromules, the stroma-filled tubular protrusions from the chloroplast outer membrane (Figure 1; Kohler and Hanson, 2000; Hanson and Hines, 2018), which facilitate translocations of chloroplast-sequestered transcription factors into the nucleus in response to various stresses (Caplan et al., 2008; Sun et al., 2011; Foyer et al., 2014). Stromules were also known to be associated with the ER, Golgi apparatus, PM, mitochondria, and peroxisomes (Kwok and Hanson, 2004; Schattat et al., 2011; Hanson and Hines, 2018); however, the physiological significance of these associations remains to be investigated in the coming years.

The ER and chloroplasts are the two major sites of lipid biosynthesis (van Meer et al., 2008; Hurlock et al., 2014) and the ER-chloroplast interaction is essential for lipid homeostasis in plant cells under normal growth condition and in response to various environmental stresses (Negi et al., 2018; Lavell and Benning, 2019). The ER-chloroplast-mediated lipid biosynthesis involving *de novo* synthesis of fatty acids (FAs) in chloroplasts, the chloroplast-ER transport of FAs, the ER-catalyzed assembly and modification of glycerolipids that move back to chloroplasts for producing galactolipids (Benning and Ohta, 2005), the major chloroplast lipids (Dormann and Benning, 2002). Studies in recent years strongly suggest that the chloroplast-ER physical contact sites, better known as plastid-associated membranes [PLAMs, (Andersson et al., 2007)], are directly involved in the lipid exchange (Tan et al., 2011; Block and Jouhet, 2015). At least two groups of proteins were detected at the ER-chloroplast membrane contact sites (Tan et al., 2011). The first group includes several members of the trigalactosyldiacylglycerol (TGD) protein family, which form a bacterial-type ABC transporter for transporting lipids from the ER to the thylakoid membrane

(Xu et al., 2010; Wang et al., 2012; Fan et al., 2015). The second group includes lipid processing enzymes such as phosphatidylcholine (PC) synthase and CLIP1 lipase/acylhydrolase that directly act on lipids from the contacting ER-chloroplast membranes (Mehrshahi et al., 2013, 2014). In addition, a recent study indicated the presence of several lipid transfer proteins, including Azelaic Acid Induced 1 (AZI1), EARly *Arabidopsis* Aluminum Induced 1 (EARLI1), and Defective in Induced Resistance 1 (DIR1), at the ER-chloroplast contact site that facilitates the movement of a lipid-derived signal for systemic acquired resistance against pathogens (Cecchini et al., 2015).

Various abiotic stresses, such as high light exposure and wounding, can lead to accumulation of MEcPP in chloroplasts, which serves as a retrograde signaling metabolite that relays the chloroplast stress signal into the nucleus to alter gene expression (Xiao et al., 2012). Intriguingly, the chloroplast-synthesized MEcPP signal could activate the transcription of IRE1 and bZIP60, two key components of the ER stress-triggered UPR pathway via a Ca^{2+} -dependent transcription factor calmodulin-binding transcription activator3 (Walley et al., 2015; Benn et al., 2016). In addition, a loss-of-function mutation in an *Arabidopsis* gene encoding the chloroplast stearyl-acyl carrier protein desaturase, which introduces double bonds into FAs, constitutively activates the expression of a known ER-UPR marker gene *BIP3* (Iwata et al., 2018). A loss-of-function mutation in the *Arabidopsis* *SAL1* gene, which encodes a chloroplast/mitochondria-localized bifunctional enzyme with both 3'(2'),5'-biphosphate nucleotidase (converting PAP to AMP) and inositol polyphosphate 1-phosphatase activities, attenuated ER stress response and exhibited hyposensitivity to ER stress inducers (Xi et al., 2016). Together, these findings provide additional support for the involvement of the photosynthetic organelle in regulating the ER homeostasis.

THE ENDOPLASMIC RETICULUM-PEROXISOME COLLABORATION

Peroxisome is a semiautonomous single-membrane-bound organelle that participates in a wide range of biochemical processes, particularly the β -oxidation of fatty acids and metabolism of hydrogen peroxide (Smith and Aitchison, 2013). In plants, peroxisomes also perform other important functions such as the glycolate cycle and photorespiration, secondary metabolism, hormone (auxin and jasmonic acid) biosynthesis, metabolism of ROS and reactive nitrogen species (RNS) (Nyathi and Baker, 2006; Hu et al., 2012; Sandalio and Romero-Puertas, 2015). Notably, peroxisomes are highly dynamic organelles that alter their morphology, proliferation, and metabolic activities in response to environmental signals (Honsho et al., 2016; Kao et al., 2018). The membrane extensions of peroxisomes, termed as peroxules (Figure 1), are often observed when plants are exposed to exogenous H_2O_2 or high-intensity light (Sinclair et al., 2009; Barton et al., 2013; Jaipargas et al., 2016). Salt stress,

heavy metals, and herbicide application were known to increase the metabolic activity and proliferation rate of peroxisomes (Palma et al., 1987; McCarthy et al., 2001; Mitsuya et al., 2010; McCarthy-Suárez et al., 2011; Fahy et al., 2017).

It has been well known that peroxisome dynamics such as elongation, fission, and degradation as well as metabolic changes require their constant collaborations and communications with other intracellular organelles (Hu et al., 2012; Del Rio and Lopez-Huertas, 2016; Kao et al., 2018). The ER-peroxisome connection has been known for many years as peroxisomes are formed by budding from specialized ER regions and/or by growth and fission of preexisting peroxisomes in yeast and mammalian cells (Hu et al., 2012; Kao et al., 2018). Although there is no clear evidence to support the ER budding model for the plant peroxisomes (Mullen and Trelease, 2006; Trelease and Lingard, 2006), the ER is at least involved in the plant peroxisome biogenesis by providing membranes, lipids, and certain peroxisome membrane proteins (PMPs) to preexisting or fission-created nascent peroxisomes (Hu et al., 2012).

The plant peroxisomes were shown to be closely associated with the ER by early microscopic observation (Huang et al., 1983) and could be physically attached to the ER as suggested by live cell imaging of dynamic behaviors of peroxisomes (and peroxules) and the ER in *Arabidopsis* (Mathur, 2009; Sinclair et al., 2009; Barton et al., 2013). However, it remains unknown whether the observed ER-peroxisome contiguity in *Arabidopsis* is mediated by the peroxisome-ER physical tether that was first described in yeast. The yeast peroxisome-ER tethering complex consists of a peroxisome biogenic protein, peroxin 3 (PEX3), localized on the ER and peroxisome, and the peroxisome inheritance factor Inp1 that serves as a bridge to link the ER and peroxisome-localized PEX3 (Knoblach and Rachubinski, 2013). The PEX3-Inp1-PEX3 trimeric complex plays a key role in partitioning peroxisomes in dividing yeast cells and controlling the peroxisome population (Knoblach et al., 2013). The mammalian peroxisome-ER tether consists of the ER-localized VAPs and the PMPs with acyl-CoA binding domains (ACBDs) and is thought to regulate peroxisome proliferation and to facilitate the ER-peroxisome lipid exchange (Hua et al., 2017; Costello et al., 2017a,b). Despite microscopic observations of the ER-peroxule association (Sinclair et al., 2009; Barton et al., 2013), a plant peroxisome-ER tethering complex remains to be discovered. The identification of a peroxisome-ER tether is expected to shed light on the functional collaboration between the two dynamic organelles, especially the mechanisms of peroxisome biogenesis/maintenance and their dynamic responses to various environmental stresses.

It was recently suggested that peroxisomes, ER, and mitochondria could form a “redox triangle” that uses tethering complexes to assemble a hypothetical “redoxosome” that transmits intercompartmental redox signals to regulate ROS metabolism in response to cellular signals and environmental cues (Yoboue et al., 2018). A plant “redoxosome” should include protein tethering complexes of chloroplasts with the ER, mitochondria, and peroxisome. The chloroplast works together with mitochondria and peroxisomes in photorespiration involving inter-organellar metabolite exchanges while the chloroplast tubular extensions, stromules, are thought to interact with the

ER, mitochondria, and peroxisomes (Mathur et al., 2012; Hanson and Hines, 2018). Fluorescent microscopic studies and proteomic experiments with a plant genetic model system such as *Arabidopsis* could make a significant contribution to our understanding of such a “redoxosome” in plants. Dynamic physical associations of multiple organelles aided by organelle extensions and tethering complexes might be a common cellular mechanism that facilitates exchanges of ROS/RNS, Ca^{2+} , lipids, and other metabolites/signaling molecules to mount coordinated cellular responses to changing environment.

THE ENDOPLASMIC RETICULUM-VACUOLE ASSOCIATION

Vacuoles are single-membrane-bound organelles that are filled with a wide range of inorganic ions and organic molecules (Figure 1). In plants, at least two types of vacuoles have been identified, including protein storage vacuoles (PSVs) and lytic vacuoles (LVs) (Paris et al., 1996; Zhang et al., 2014). PSVs usually serve as a warehouse for seed storage proteins that are synthesized in the ER during seed maturation, while LVs occur in the vegetative tissues and contain acidic contents and degradative enzymes with lysosome-like properties (Shimada et al., 2018). It has been shown that the vacuoles play crucial roles in storage of nutrients and metabolites, detoxification, pH homeostasis, and stress tolerance (Muntz, 2007; Viotti, 2014). Maintaining proper turgor pressure in vacuoles is required for morphological alterations of cells during plant development, and the rapid vacuolar uptake or unloading of various ions and metabolites allows plants to efficiently cope with environmental stresses. For instance, AtNHX1 is an *Arabidopsis* tonoplast-localized Na^+/H^+ antiporter that moves excessive Na^+ from the cytosol into the vacuole, lowering the water potential of the vacuole and driving water flow into the cells to maintain plants' growth under high salinity condition (Apse et al., 1999). It is well known that stomatal opening or closure is associated with vacuole morphology changes in guard cells, highlighting the important roles of vacuole in plant response to abiotic stresses, such as high temperature and drought (Gao et al., 2005; Tanaka et al., 2007; Bak et al., 2013).

Many vacuolar proteins and metabolites are synthesized and processed in the ER and transported to the vacuoles. One well-established pathway for vacuolar transport is the COPII-mediated vesicle trafficking from the ER to the Golgi and the post-Golgi transport that involves the plant TGN and the pre-vacuolar compartment (PVC, also known as MVB for multi-vesicular body) (Xiang et al., 2013; Brillada and Rojas-Pierce, 2017). Recent studies indicated the presence of a direct Golgi-independent ER-vacuole trafficking route involving the machinery of autophagy (Viotti et al., 2013; Michaeli et al., 2014), which degrades and recycles damaged/misfolded/aggregated proteins and defective/excessive intracellular organelles (Wang et al., 2018b). More importantly, autophagy is an integral part of the ER stress-triggered UPR. Under the ER stress, ER components bud from the ER and form autophagosome with

the aid of appropriate cargo receptors, and the autophagosome subsequently fuses with the lytic vacuole to release the ER cargos for degradation via the classical macroautophagy pathway (Liu et al., 2012; Michaeli et al., 2014; Yang et al., 2016). A special process of autophagy, ER-phagy (Schuck et al., 2014) or reticulophagy (Liu et al., 2012), is activated to degrade damaged ER fragments when UPR fails to mitigate the ER stress. Further studies revealed that the ER stress-induced reticulophagy in *Arabidopsis* requires one of the ER-localized UPR sensor IRE1b but not bZIP60 (Liu et al., 2012).

Given the presence of a direct ER-vacuole trafficking route for transporting metabolites, proteins, and membranes in plant cells, it is quite possible that plant cells have multiple ER-vacuole contact sites that serve important cellular functions, especially when responding to environmental stresses. In yeast, the ER-vacuole contact site (Figure 1) [known as nuclear ER-vacuole junctions or NVJs (Pan et al., 2000)] has been well studied and is implicated in the biogenesis and transport of lipid droplets in response to metabolic stress (Hariri et al., 2018). The yeast NVJ is established by interaction between one of the two ER membrane proteins, Nvj1 and Ltc1 (lipid transfer at contact site1), and an armadillo repeat protein Vac8 that requires palmitoylation for its localization to the vacuolar membrane (Pan et al., 2000; Murley et al., 2015). The yeast NVJ tether also contains Nvj2, one of the seven SPM domain-containing proteins that are localized at MCSs, including three at ERMES and the remaining three (tricalbins) at EPCSs (Toulmay and Prinz, 2012). Despite essential roles of the vacuoles in plant growth, stress tolerance, and plant defense (Shimada et al., 2018), little is known about the plant ER-vacuole contact sites and their associated tethering complexes. *Arabidopsis* lacks a homolog of Nvj1 or Ltc1 but contains >100 armadillo repeat proteins (Sharma et al., 2014) and five tricalbin homologs known as AtSYTA-E or AtSYT1–5 (Craxton, 2004). Live cell imaging of fluorescently tagged ER/tonoplast-localized proteins coupled with optical tweezers (Sparkes, 2018) could reveal potential ER-vacuole contact sites and their dynamic changes in response to environmental stresses. Given the widespread occurrence of SMP-containing proteins at multiple MCSs in yeast and mammalian cells (Toulmay and Prinz, 2012), identification of a plant ER-vacuole tethering complex might be facilitated by confocal microscopic examination of fluorescently tagged AtSYT1–5 followed by biochemical studies of an AtSYT localized at the ER-vacuole contact sites.

CONCLUSION

Accumulating evidence supports important roles of the ER-organelle interactions in plant stress tolerance, which involves exchanges of metabolites and signaling molecules at specialized MCSs with unique tethering complexes. Further studies that combine live cell imaging, proteomics, and plant genetics are needed to fully understand the composition and dynamic regulation of these MCSs in response to environmental changes and their additional physiological functions.

AUTHOR CONTRIBUTIONS

LL and JL discussed the writing plan, LL drafted the manuscript, and JL edited the manuscript.

FUNDING

This work was partially supported by grants from National Natural Science Foundation of China (NSFC31600996 to LL and NSFC31730019 to JL). The open access publication fee

is provided by a startup fund from South China Agricultural University.

ACKNOWLEDGMENTS

We would like to thank Fen Su for her help in generating the figure and the handling editor and two reviewers for their constructive criticisms and helpful suggestions. We apologize to those colleagues whose works were not fully cited in this article.

REFERENCES

- Andersson, M. X., Goksör, M., and Sandelius, A. S. (2007). Optical manipulation reveals strong attracting forces at membrane contact sites between endoplasmic reticulum and chloroplasts. *J. Biol. Chem.* 282, 1170–1174. doi: 10.1074/jbc.M608124200
- Anelli, T., Bergamelli, L., Margittai, E., Rimessi, A., Fagioli, C., Malgaroli, A., et al. (2012). Ero1 α regulates Ca²⁺ fluxes at the endoplasmic reticulum-mitochondria interface (MAM). *Antioxid. Redox Signal.* 16, 1077–1087. doi: 10.1089/ars.2011.4004
- Angelos, E., and Brandizzi, F. (2018). NADPH oxidase activity is required for ER stress survival in plants. *Plant J.* 96, 1106–1120. doi: 10.1111/tjp.14091
- Angelos, E., Ruberti, C., Kim, S. J., and Brandizzi, F. (2017). Maintaining the factory: the roles of the unfolded protein response in cellular homeostasis in plants. *Plant J.* 90, 671–682. doi: 10.1111/tjp.13449
- Apse, M. P., Aharon, G. S., Snedden, W. A., and Blumwald, E. (1999). Salt tolerance conferred by overexpression of a vacuolar Na⁺/H⁺ antiporter in Arabidopsis. *Science* 285, 1256–1258. doi: 10.1126/science.285.5431.1256
- Arimura, S. I. (2018). Fission and fusion of plant mitochondria, and genome maintenance. *Plant Physiol.* 176, 152–161. doi: 10.1104/pp.17.01025
- Bak, G., Lee, E. J., Lee, Y., Kato, M., Segami, S., Sze, H., et al. (2013). Rapid structural changes and acidification of guard cell vacuoles during stomatal closure require phosphatidylinositol 3,5-bisphosphate. *Plant Cell* 25, 2202–2216. doi: 10.1105/tpc.113.110411
- Bao, Y., Pu, Y., Yu, X., Gregory, B. D., Srivastava, R., Howell, S. H., et al. (2018). IRE1B degrades RNAs encoding proteins that interfere with the induction of autophagy by ER stress in Arabidopsis thaliana. *Autophagy* 14, 1562–1573. doi: 10.1080/15548627.2018.1462426
- Barton, K., Mathur, N., and Mathur, J. (2013). Simultaneous live-imaging of peroxisomes and the ER in plant cells suggests contiguity but no luminal continuity between the two organelles. *Front. Physiol.* 4:196. doi: 10.3389/fphys.2013.00196
- Benn, G., Bjornson, M., Ke, H., De Souza, A., Balmond, E. I., Shaw, J. T., et al. (2016). Plastidial metabolite MECP induces a transcriptionally centered stress-response hub via the transcription factor CAMTA3. *Proc. Natl. Acad. Sci. USA* 113, 8855–8860. doi: 10.1073/pnas.1602582113
- Benning, C., and Ohta, H. (2005). Three enzyme systems for galactoglycerolipid biosynthesis are coordinately regulated in plants. *J. Biol. Chem.* 280, 2397–2400. doi: 10.1074/jbc.R400032200
- Bhandary, B., Marahatta, A., Kim, H.-R., and Chae, H.-J. (2012). An involvement of oxidative stress in endoplasmic reticulum stress and its associated diseases. *Int. J. Mol. Sci.* 14, 434–456. doi: 10.3390/ijms14010434
- Birk, J., Meyer, M., Aller, I., Hansen, H. G., Odermatt, A., Dick, T. P., et al. (2013). Endoplasmic reticulum: reduced and oxidized glutathione revisited. *J. Cell Sci.* 126, 1604–1617. doi: 10.1242/jcs.117218
- Block, M. A., and Jouhet, J. (2015). Lipid trafficking at endoplasmic reticulum-chloroplast membrane contact sites. *Curr. Opin. Cell Biol.* 35, 21–29. doi: 10.1016/j.ccb.2015.03.004
- Brandizzi, F., and Barlowe, C. (2013). Organization of the ER-Golgi interface for membrane traffic control. *Nat. Rev. Mol. Cell Biol.* 14, 382–392. doi: 10.1038/nrm3588
- Brillada, C., and Rojas-Pierce, M. (2017). Vacuolar trafficking and biogenesis: a maturation in the field. *Curr. Opin. Plant Biol.* 40, 77–81. doi: 10.1016/j.pbi.2017.08.005
- Caplan, J. L., Mamillapalli, P., Burch-Smith, T. M., Czymbek, K., and Dinesh-Kumar, S. P. (2008). Chloroplastic protein NRIP1 mediates innate immune receptor recognition of a viral effector. *Cell* 132, 449–462. doi: 10.1016/j.cell.2007.12.031
- Carraretto, L., Checchetto, V., De Bortoli, S., Formentin, E., Costa, A., Szabo, I., et al. (2016). Calcium flux across plant mitochondrial membranes: possible molecular players. *Front. Plant Sci.* 7:354. doi: 10.3389/fpls.2016.00354
- Cecchini, N. M., Steffes, K., Schlappi, M. R., Gifford, A. N., and Greenberg, J. T. (2015). Arabidopsis AZI1 family proteins mediate signal mobilization for systemic defence priming. *Nat. Commun.* 6:7658. doi: 10.1038/ncomms8658
- Chan, K. X., Mabbitt, P. D., Phua, S. Y., Mueller, J. W., Nisar, N., Gigolashvili, T., et al. (2016). Sensing and signaling of oxidative stress in chloroplasts by inactivation of the SAL1 phosphoadenosine phosphatase. *Proc. Natl. Acad. Sci. USA* 113, E4567–E4576. doi: 10.1073/pnas.1604936113
- Chung, W. Y., Jha, A., Ahuja, M., and Muallem, S. (2017). Ca²⁺ influx at the ER/PM junctions. *Cell Calcium* 63, 29–32. doi: 10.1016/j.ceca.2017.02.009
- Costello, J. L., Castro, I. G., Hacker, C., Schrader, T. A., Metz, J., Zeuschner, D., et al. (2017a). ACBD5 and VAPB mediate membrane associations between peroxisomes and the ER. *J. Cell Biol.* 216, 331–342. doi: 10.1083/jcb.201607055
- Costello, J. L., Castro, I. G., Schrader, T. A., Islinger, M., and Schrader, M. (2017b). Peroxisomal ACBD4 interacts with VAPB and promotes ER-peroxisome associations. *Cell Cycle* 16, 1039–1045. doi: 10.1080/15384101.2017.1314422
- Craxton, M. (2004). Synaptotagmin gene content of the sequenced genomes. *BMC Genomics* 5:43. doi: 10.1186/1471-2164-5-43
- Das, K., and Roychoudhury, A. (2014). Reactive oxygen species (ROS) and response of antioxidants as ROS-scavengers during environmental stress in plants. *Front. Environ. Sci.* 2:53. doi: 10.3389/fenvs.2014.00053
- Dasilva, L. L., Snapp, E. L., Denecke, J., Lippincott-Schwartz, J., Hawes, C., and Brandizzi, F. (2004). Endoplasmic reticulum export sites and Golgi bodies behave as single mobile secretory units in plant cells. *Plant Cell* 16, 1753–1771. doi: 10.1105/tpc.022673
- de Brito, O. M., and Scorrano, L. (2008). Mitofusin 2 tethers endoplasmic reticulum to mitochondria. *Nature* 456, 605–610. doi: 10.1038/nature07534
- De Clercq, I., Vermeirssen, V., Van Aken, O., Vandepoele, K., Murcha, M. W., Law, S. R., et al. (2013). The membrane-bound NAC transcription factor ANAC013 functions in mitochondrial retrograde regulation of the oxidative stress response in Arabidopsis. *Plant Cell* 25, 3472–3490. doi: 10.1105/tpc.113.117168
- Del Rio, L. A., and Lopez-Huertas, E. (2016). ROS generation in peroxisomes and its role in cell signaling. *Plant Cell Physiol.* 57, 1364–1376. doi: 10.1093/pcp/pcw076
- Deng, Y., Humbert, S., Liu, J. X., Srivastava, R., Rothstein, S. J., and Howell, S. H. (2011). Heat induces the splicing by IRE1 of a mRNA encoding a transcription factor involved in the unfolded protein response in Arabidopsis. *Proc. Natl. Acad. Sci. USA* 108, 7247–7252. doi: 10.1073/pnas.1102117108
- Detmer, S. A., and Chan, D. C. (2007). Functions and dysfunctions of mitochondrial dynamics. *Nat. Rev. Mol. Cell Biol.* 8, 870–879. doi: 10.1038/nrm2275
- Dickson, E. J., Jensen, J. B., Vivas, O., Kruse, M., Traynor-Kaplan, A. E., and Hille, B. (2016). Dynamic formation of ER-PM junctions presents a lipid

- phosphatase to regulate phosphoinositides. *J. Cell Biol.* 213, 33–48. doi: 10.1083/jcb.201508106
- Ding, B., Turgeon, R., and Parthasarathy, M. V. (1992). Substructure of freeze-substituted plasmodesmata. *Protoplasma* 169, 28–41. doi: 10.1007/BF01343367
- Dojcinovic, D., Krosting, J., Harris, A. J., Wagner, D. J., and Rhoads, D. M. (2005). Identification of a region of the Arabidopsis AtAOX1a promoter necessary for mitochondrial retrograde regulation of expression. *Plant Mol. Biol.* 58, 159–175. doi: 10.1007/s11103-005-5390-1
- Dormann, P., and Benning, C. (2002). Galactolipids rule in seed plants. *Trends Plant Sci.* 7, 112–118. doi: 10.1016/S1360-1385(01)02216-6
- Duncan, O., Murcha, M. W., and Whelan, J. (2013). Unique components of the plant mitochondrial protein import apparatus. *Biochim. Biophys. Acta* 1833, 304–313. doi: 10.1016/j.bbamcr.2012.02.015
- Dupree, P., and Sherrier, D. J. (1998). The plant Golgi apparatus. *Biochim. Biophys. Acta* 1404, 259–270. doi: 10.1016/S0167-4889(98)00061-5
- Fahy, D., Sanad, M. N., Duscha, K., Lyons, M., Liu, F., Bozhkov, P., et al. (2017). Impact of salt stress, cell death, and autophagy on peroxisomes: quantitative and morphological analyses using small fluorescent probe N-BODIPY. *Sci. Rep.* 7:39069. doi: 10.1038/srep46643
- Fan, J., Zhai, Z., Yan, C., and Xu, C. (2015). Arabidopsis TRIGALACTOSYLDIACYLGLYCEROL5 Interacts with TGD1, TGD2, and TGD4 to facilitate lipid transfer from the endoplasmic reticulum to plastids. *Plant Cell* 27, 2941–2955. doi: 10.1105/tpc.15.00394
- Foyer, C. H., Karpinska, B., and Krupinska, K. (2014). The functions of WHIRLY1 and REDOX-RESPONSIVE TRANSCRIPTION FACTOR 1 in cross tolerance responses in plants: a hypothesis. *Philos. Trans. R. Soc. Lond. B. Biol. Sci.* 369, 20130226. doi: 10.1098/rstb.2013.0226
- Fujita, M., Mizukado, S., Fujita, Y., Ichikawa, T., Nakazawa, M., Seki, M., et al. (2007). Identification of stress-tolerance-related transcription-factor genes via mini-scale full-length cDNA Over-eXpressor (FOX) gene hunting system. *Biochem. Biophys. Res. Commun.* 364, 250–257. doi: 10.1016/j.bbrc.2007.09.124
- Gao, H., Brandizzi, F., Benning, C., and Larkin, R. M. (2008). A membrane-tethered transcription factor defines a branch of the heat stress response in *Arabidopsis thaliana*. *Proc. Natl. Acad. Sci. USA* 105, 16398–16403. doi: 10.1073/pnas.0808463105
- Gao, X. Q., Li, C. G., Wei, P. C., Zhang, X. Y., Chen, J., and Wang, X. C. (2005). The dynamic changes of tonoplasts in guard cells are important for stomatal movement in *Vicia faba*. *Plant Physiol.* 139, 1207–1216. doi: 10.1104/pp.105.067520
- Gatta, A. T., Wong, L. H., Sere, Y. Y., Calderon-Norena, D. M., Cockcroft, S., Menon, A. K., et al. (2015). A new family of StART domain proteins at membrane contact sites has a role in ER-PM sterol transport. *elife* 4:e07253. doi: 10.7554/eLife.07253
- Giordano, F., Saheki, Y., Idevall-Hagren, O., Colombo, S. F., Pirruccello, M., Milosevic, I., et al. (2013). PI(4,5)P₂-dependent and Ca²⁺-regulated ER-PM interactions mediated by the extended synaptotagmins. *Cell* 153, 1494–1509. doi: 10.1016/j.cell.2013.05.026
- Grison, M. S., Brocard, L., Fouillen, L., Nicolas, W., Wewer, V., Dormann, P., et al. (2015). Specific membrane lipid composition is important for plasmodesmata function in Arabidopsis. *Plant Cell* 27, 1228–1250. doi: 10.1105/tpc.114.135731
- Hanson, M. R., and Hines, K. M. (2018). Stromules: probing formation and function. *Plant Physiol.* 176, 128–137. doi: 10.1104/pp.17.01287
- Hariri, H., Rogers, S., Ugrankar, R., Liu, Y. L., Feathers, J. R., and Henne, W. M. (2018). Lipid droplet biogenesis is spatially coordinated at ER-vacuole contacts under nutritional stress. *EMBO Rep.* 19, 57–72. doi: 10.15252/embr.201744815
- Hawes, C., Osterrieder, A., Hummel, E., and Sparkes, I. (2008). The plant ER-Golgi interface. *Traffic* 9, 1571–1580. doi: 10.1111/j.1600-0854.2008.00773.x
- Heilmann, I. (2008). Towards understanding the function of stress-inducible PtdIns(4,5)P₂ in plants. *Commun. Integr. Biol.* 1, 204–206. doi: 10.4161/cib.1.2.7226
- Hetz, C., Chevet, E., and Oakes, S. A. (2015). Proteostasis control by the unfolded protein response. *Nat. Cell Biol.* 17, 829–838. doi: 10.1038/ncb3184
- Higa, A., and Chevet, E. (2012). Redox signaling loops in the unfolded protein response. *Cell. Signal.* 24, 1548–1555. doi: 10.1016/j.cellsig.2012.03.011
- Ho, C. M., Paciorek, T., Abrash, E., and Bergmann, D. C. (2016). Modulators of stomatal lineage signal transduction alter membrane contact sites and reveal specialization among ERECTA kinases. *Dev. Cell* 38, 345–357. doi: 10.1016/j.devcel.2016.07.016
- Honsho, M., Yamashita, S.-I., and Fujiki, Y. (2016). Peroxisome homeostasis: mechanisms of division and selective degradation of peroxisomes in mammals. *Biochim. Biophys. Acta* 1863, 984–991. doi: 10.1016/j.bbamcr.2015.09.032
- Hou, Q., Ufer, G., and Bartels, D. (2016). Lipid signalling in plant responses to abiotic stress. *Plant Cell Environ.* 39, 1029–1048. doi: 10.1111/pce.12666
- Howell, S. H. (2013). Endoplasmic reticulum stress responses in plants. *Annu. Rev. Plant Biol.* 64, 477–499. doi: 10.1146/annurev-arplant-050312-120053
- Hu, J., Baker, A., Bartel, B., Linka, N., Mullen, R. T., Reumann, S., et al. (2012). Plant peroxisomes: biogenesis and function. *Plant Cell* 24, 2279–2303. doi: 10.1105/tpc.112.096586
- Hua, R., Cheng, D., Coyaude, E., Freeman, S., Di Pietro, E., Wang, Y., et al. (2017). VAPs and ACBD5 tether peroxisomes to the ER for peroxisome maintenance and lipid homeostasis. *J. Cell Biol.* 216, 367–377. doi: 10.1083/jcb.201608128
- Huang, A. H. C., Trelease, R. N., and Moore, T. S. (1983). *Plant peroxisomes. American society of plant physiologists monograph series.* (New York: Academic Press).
- Hurllock, A. K., Roston, R. L., Wang, K., and Benning, C. (2014). Lipid trafficking in plant cells. *Traffic* 15, 915–932. doi: 10.1111/tra.12187
- Ito, Y., Uemura, T., and Nakano, A. (2018). The Golgi entry core compartment functions as a COPII-independent scaffold for ER-to-Golgi transport in plant cells. *J. Cell Sci.* 131:jcs203893. doi: 10.1242/jcs.203893
- Ito, Y., Uemura, T., Shoda, K., Fujimoto, M., Ueda, T., and Nakano, A. (2012). *cis*-Golgi proteins accumulate near the ER exit sites and act as the scaffold for Golgi regeneration after brefeldin A treatment in tobacco BY-2 cells. *Mol. Biol. Cell* 23, 3203–3214. doi: 10.1091/mbc.E12-01-0034
- Iwata, Y., Ashida, M., Hasegawa, C., Tabara, K., Mishiba, K. I., and Koizumi, N. (2017). Activation of the Arabidopsis membrane-bound transcription factor bZIP28 is mediated by site-2 protease, but not site-1 protease. *Plant J.* 91, 408–415. doi: 10.1111/tpj.13572
- Iwata, Y., Iida, T., Matsunami, T., Yamada, Y., Mishiba, K. I., Ogawa, T., et al. (2018). Constitutive BiP protein accumulation in Arabidopsis mutants defective in a gene encoding chloroplast-resident stearyl-acyl carrier protein desaturase. *Genes Cells* 23, 456–465. doi: 10.1111/gtc.12585
- Iwata, Y., and Koizumi, N. (2012). Plant transducers of the endoplasmic reticulum unfolded protein response. *Trends Plant Sci.* 17, 720–727. doi: 10.1016/j.tplants.2012.06.014
- Jaipargas, E. A., Mathur, N., Bou Daher, F., Wasteneys, G. O., and Mathur, J. (2016). High light intensity leads to increased peroxisome-mitochondria interactions in plants. *Front. Cell Dev. Biol.* 4:6. doi: 10.3389/fcell.2016.00006
- Kao, Y. T., Gonzalez, K. L., and Bartel, B. (2018). Peroxisome function, biogenesis, and dynamics in plants. *Plant Physiol.* 176, 162–177. doi: 10.1104/pp.17.01050
- Kataoka, R., Takahashi, M., and Suzuki, N. (2017). Coordination between bZIP28 and HSF2 in the regulation of heat response signals in Arabidopsis. *Plant Signal. Behav.* 12:e1376159. doi: 10.1080/15592324.2017.1376159
- Knoblach, B., and Rachubinski, R. A. (2013). Doing the math: how yeast cells maintain their peroxisome populations. *Commun. Integr. Biol.* 6:e26901. doi: 10.4161/cib.26901
- Knoblach, B., Sun, X., Coquelle, N., Fagarasanu, A., Poirier, R. L., and Rachubinski, R. A. (2013). An ER-peroxisome tether exerts peroxisome population control in yeast. *EMBO J.* 32, 2439–2453. doi: 10.1038/emboj.2013.170
- Kohler, R. H., and Hanson, M. R. (2000). Plastid tubules of higher plants are tissue-specific and developmentally regulated. *J. Cell Sci.* 113, 81–89. https://www.researchgate.net/publication/12708981_Plastid_tubules_of_higher_plants_are_tissue-specific_and_developmentally_regulated
- Koizumi, N., Martinez, I. M., Kimata, Y., Kohno, K., Sano, H., and Chrispeels, M. J. (2001). Molecular characterization of two Arabidopsis Ire1 homologs, endoplasmic reticulum-located transmembrane protein kinases. *Plant Physiol.* 127, 949–962. doi: 10.1104/pp.010636
- Kurokawa, K., Okamoto, M., and Nakano, A. (2014). Contact of *cis*-Golgi with ER exit sites executes cargo capture and delivery from the ER. *Nat. Commun.* 5:3653. doi: 10.1038/ncomms4653
- Kwok, E. Y., and Hanson, M. R. (2004). Plastids and stromules interact with the nucleus and cell membrane in vascular plants. *Plant Cell Rep.* 23, 188–195. doi: 10.1007/s00299-004-0824-9

- Labbé, K., Murley, A., and Nunnari, J. (2014). Determinants and functions of mitochondrial behavior. *Annu. Rev. Cell Dev. Biol.* 30, 357–391. doi: 10.1146/annurev-cellbio-101011-155756
- Ladinsky, M. S., Mastronarde, D. N., McIntosh, J. R., Howell, K. E., and Staehelin, L. A. (1999). Golgi structure in three dimensions: functional insights from the normal rat kidney cell. *J. Cell Biol.* 144, 1135–1149. doi: 10.1083/jcb.144.6.1135
- Lahiri, S., Chao, J. T., Tavassoli, S., Wong, A. K., Choudhary, V., Young, B. P., et al. (2014). A conserved endoplasmic reticulum membrane protein complex (EMC) facilitates phospholipid transfer from the ER to mitochondria. *PLoS Biol.* 12:e1001969. doi: 10.1371/journal.pbio.1001969
- Lang, A., Peter, A. T. J., and Kornmann, B. (2015). ER-mitochondria contact sites in yeast: beyond the myths of ERMES. *Curr. Opin. Cell Biol.* 35, 7–12. doi: 10.1016/j.ceb.2015.03.002
- Lavell, A. A., and Benning, C. (2019). Cellular organization and regulation of plant glycerolipid metabolism. *Plant Cell Physiol.* pcz016. doi: 10.1093/pcp/pcz016
- Lee, S., and Min, K. T. (2018). The interface between er and mitochondria: molecular compositions and functions. *Mol. Cells* 41, 1000–1007. doi: 10.14348/molcells.2018.0438
- Lee, E., Vanneste, S., Perez-Sancho, J., Benitez-Fuente, F., Strelau, M., Macho, A. P., et al. (2019). Ionic stress enhances ER-PM connectivity via phosphoinositide-associated SYT1 contact site expansion in Arabidopsis. *Proc. Natl. Acad. Sci. USA* 116, 1420–1429. doi: 10.1073/pnas.1818099116
- Leijon, F., Melzer, M., Zhou, Q., Srivastava, V., and Bulone, V. (2018). Proteomic analysis of plasmodesmata from populus cell suspension cultures in relation with callose biosynthesis. *Front. Plant Sci.* 9:1681. doi: 10.3389/fpls.2018.01681
- Lev, S. (2012). Nonvesicular lipid transfer from the endoplasmic reticulum. *Cold Spring Harb. Perspect. Biol.* 4:a013300. doi: 10.1101/cshperspect.a013300
- Levy, A., Zheng, J. Y., and Lazarowitz, S. G. (2015). Synaptotagmin SYTA forms ER-plasma membrane junctions that are recruited to plasmodesmata for plant virus movement. *Curr. Biol.* 25, 2018–2025. doi: 10.1016/j.cub.2015.06.015
- Li-Beisson, Y., Neunzig, J., Lee, Y., and Philippar, K. (2017). Plant membrane-protein mediated intracellular traffic of fatty acids and acyl lipids. *Curr. Opin. Plant Biol.* 40, 138–146. doi: 10.1016/j.pbi.2017.09.006
- Liu, Y., Burgos, J. S., Deng, Y., Srivastava, R., Howell, S. H., and Bassham, D. C. (2012). Degradation of the endoplasmic reticulum by autophagy during endoplasmic reticulum stress in Arabidopsis. *Plant Cell* 24, 4635–4651. doi: 10.1105/tpc.112.101535
- Liu, J. X., and Howell, S. H. (2010). bZIP28 and NF-Y transcription factors are activated by ER stress and assemble into a transcriptional complex to regulate stress response genes in Arabidopsis. *Plant Cell* 22, 782–796. doi: 10.1105/tpc.109.072173
- Liu, J. X., and Howell, S. H. (2016). Managing the protein folding demands in the endoplasmic reticulum of plants. *New Phytol.* 211, 418–428. doi: 10.1111/nph.13915
- Liu, Y., and Li, J. (2014). Endoplasmic reticulum-mediated protein quality control in Arabidopsis. *Front. Plant Sci.* 5:162. doi: 10.3389/fpls.2014.00162
- Liu, J. X., Srivastava, R., Che, P., and Howell, S. H. (2007a). An endoplasmic reticulum stress response in Arabidopsis is mediated by proteolytic processing and nuclear relocation of a membrane-associated transcription factor, bZIP28. *Plant Cell* 19, 4111–4119. doi: 10.1105/tpc.106.050021
- Liu, J. X., Srivastava, R., Che, P., and Howell, S. H. (2007b). Salt stress responses in Arabidopsis utilize a signal transduction pathway related to endoplasmic reticulum stress signaling. *Plant J.* 51, 897–909. doi: 10.1111/j.1365-3113X.2007.03195.x
- Manford, A. G., Stefan, C. J., Yuan, H. L., Macgurn, J. A., and Emr, S. D. (2012). ER-to-plasma membrane tethering proteins regulate cell signaling and ER morphology. *Dev. Cell* 23, 1129–1140. doi: 10.1016/j.devcel.2012.11.004
- Marino, D., Dunand, C., Puppo, A., and Pauly, N. (2012). A burst of plant NADPH oxidases. *Trends Plant Sci.* 17, 9–15. doi: 10.1016/j.tplants.2011.10.001
- Mathur, J. (2009). Rapid peroxisomal responses to ROS suggest an alternative mechanistic model for post-biogenesis peroxisomal life cycle in plants. *Plant Signal. Behav.* 4, 787–789. doi: 10.4161/psb.4.8.9232
- Mathur, J., Mammone, A., and Barton, K. A. (2012). Organelle extensions in plant cells. *J. Integr. Plant Biol.* 54, 851–867. doi: 10.1111/j.1744-7909.2012.01175.x
- McCarthy, I., Romero-Puertas, M. C., Palma, J. M., Sandalio, L. M., Corpas, F. J., Gómez, M., et al. (2001). Cadmium induces senescence symptoms in leaf peroxisomes of pea plants. *Plant Cell Environ.* 24, 1065–1073. doi: 10.1046/j.1365-3040.2001.00750.x
- McCarthy-Suárez, I., Gómez, M., Del Río, L. A., and Palma, J. M. J. B. P. (2011). Role of peroxisomes in the oxidative injury induced by 2,4-dichlorophenoxyacetic acid in leaves of pea plants. *Biol. Plant.* 55, 485–492. doi: 10.1007/s10535-011-0114-7
- McFarlane, H. E., Lee, E. K., Van Bezouwen, L. S., Ross, B., Rosado, A., and Samuels, A. L. (2017). Multiscale structural analysis of plant ER-PM contact sites. *Plant Cell Physiol.* 58, 478–484. doi: 10.1093/pcp/pcw224
- Mehrshahi, P., Johnny, C., and Dellapenna, D. (2014). Redefining the metabolic continuity of chloroplasts and ER. *Trends Plant Sci.* 19, 501–507. doi: 10.1016/j.tplants.2014.02.013
- Mehrshahi, P., Stefano, G., Andaloro, J. M., Brandizzi, F., Froehlich, J. E., and Dellapenna, D. (2013). Transorganellar complementation redefines the biochemical continuity of endoplasmic reticulum and chloroplasts. *Proc. Natl. Acad. Sci. USA* 110, 12126–12131. doi: 10.1073/pnas.1306331110
- Mesmin, B., Kovacs, D., and D'angelo, G. (2019). Lipid exchange and signaling at ER-Golgi contact sites. *Curr. Opin. Cell Biol.* 57, 8–15. doi: 10.1016/j.ceb.2018.10.002
- Michaeli, S., Avin-Wittenberg, T., and Galili, G. (2014). Involvement of autophagy in the direct ER to vacuole protein trafficking route in plants. *Front. Plant Sci.* 5:134. doi: 10.3389/fpls.2014.00134
- Michaud, M., Gros, V., Tardif, M., Brugiere, S., Ferro, M., Prinz, W. A., et al. (2016). AtMic60 is involved in plant mitochondria lipid trafficking and is part of a large complex. *Curr. Biol.* 26, 627–639. doi: 10.1016/j.cub.2016.01.011
- Michaud, M., Prinz, W. A., and Jouhet, J. (2017). Glycerolipid synthesis and lipid trafficking in plant mitochondria. *FEBS J.* 284, 376–390. doi: 10.1111/febs.13812
- Michel, A. H., and Kornmann, B. (2012). The ERMES complex and ER-mitochondria connections. *Biochem. Soc. Trans.* 40, 445–450. doi: 10.1042/BST20110758
- Mishiba, K., Nagashima, Y., Suzuki, E., Hayashi, N., Ogata, Y., Shimada, Y., et al. (2013). Defects in IRE1 enhance cell death and fail to degrade mRNAs encoding secretory pathway proteins in the Arabidopsis unfolded protein response. *Proc. Natl. Acad. Sci. USA* 110, 5713–5718. doi: 10.1073/pnas.1219047110
- Mitsuya, S., El-Shami, M., Sparkes, I. A., Charlton, W. L., Lousa Cde, M., Johnson, B., et al. (2010). Salt stress causes peroxisome proliferation, but inducing peroxisome proliferation does not improve NaCl tolerance in Arabidopsis thaliana. *PLoS One* 5:e9408. doi: 10.1371/journal.pone.0009408
- Mueller, S. J., and Reski, R. (2015). Mitochondrial dynamics and the ER: the plant perspective. *Front. Cell Dev. Biol.* 3:78. doi: 10.3389/fcell.2015.00078
- Mullen, R. T., and Trelease, R. N. (2006). The ER-peroxisome connection in plants: development of the "ER semi-autonomous peroxisome maturation and replication" model for plant peroxisome biogenesis. *Biochim. Biophys. Acta* 1763, 1655–1668. doi: 10.1016/j.bbamcr.2006.09.011
- Muntz, K. (2007). Protein dynamics and proteolysis in plant vacuoles. *J. Exp. Bot.* 58, 2391–2407. doi: 10.1093/jxb/erm089
- Murley, A., Sarsam, R. D., Toulmay, A., Yamada, J., Prinz, W. A., and Nunnari, J. (2015). Ltc1 is an ER-localized sterol transporter and a component of ER-mitochondria and ER-vacuole contacts. *J. Cell Biol.* 209, 539–548. doi: 10.1083/jcb.201502033
- Murphy, M. P. (2013). Mitochondrial dysfunction indirectly elevates ROS production by the endoplasmic reticulum. *Cell Metab.* 18, 145–146. doi: 10.1016/j.cmet.2013.07.006
- Nagashima, Y., Mishiba, K., Suzuki, E., Shimada, Y., Iwata, Y., and Koizumi, N. (2011). Arabidopsis IRE1 catalyses unconventional splicing of bZIP60 mRNA to produce the active transcription factor. *Sci. Rep.* 1:29. doi: 10.1038/srep00029
- Nakashima, K., Ito, Y., and Yamaguchi-Shinozaki, K. (2009). Transcriptional regulatory networks in response to abiotic stresses in Arabidopsis and grasses. *Plant Physiol.* 149, 88–95. doi: 10.1104/pp.108.129791

- Nawkar, G. M., Kang, C. H., Maibam, P., Park, J. H., Jung, Y. J., Chae, H. B., et al. (2017). HY5, a positive regulator of light signaling, negatively controls the unfolded protein response in Arabidopsis. *Proc. Natl. Acad. Sci. USA* 114, 2084–2089. doi: 10.1073/pnas.1609844114
- Negi, J., Munemasa, S., Song, B., Tadakuma, R., Fujita, M., Azoulay-Shemer, T., et al. (2018). Eukaryotic lipid metabolic pathway is essential for functional chloroplasts and CO₂ and light responses in Arabidopsis guard cells. *Proc. Natl. Acad. Sci. USA* 115, 9038–9043. doi: 10.1073/pnas.1810458115
- Ng, S., Ivanova, A., Duncan, O., Law, S. R., Van Aken, O., De Clercq, I., et al. (2013). A membrane-bound NAC transcription factor, ANAC017, mediates mitochondrial retrograde signaling in Arabidopsis. *Plant Cell* 25, 3450–3471. doi: 10.1105/tpc.113.113985
- Nicolas, W. J., Grison, M. S., Trepout, S., Gaston, A., Fouche, M., Cordelieres, F. P., et al. (2017). Architecture and permeability of post-cytokinesis plasmodesmata lacking cytoplasmic sleeves. *Nat. Plants* 3:17082. doi: 10.1038/nplants.2017.82
- Nyathi, Y., and Baker, A. (2006). Plant peroxisomes as a source of signalling molecules. *Biochim. Biophys. Acta* 1763, 1478–1495. doi: 10.1016/j.bbamcr.2006.08.031
- Osakabe, Y., Yamaguchi-Shinozaki, K., Shinozaki, K., and Tran, L. S. (2013). Sensing the environment: key roles of membrane-localized kinases in plant perception and response to abiotic stress. *J. Exp. Bot.* 64, 445–458. doi: 10.1093/jxb/ers354
- Osterrieder, A., Sparkes, I. A., Botchway, S. W., Ward, A., Ketelaar, T., De Ruijter, N., et al. (2017). Stacks off tracks: a role for the golgin AtCASP in plant endoplasmic reticulum-Golgi apparatus tethering. *J. Exp. Bot.* 68, 3339–3350. doi: 10.1093/jxb/erx167
- Ozgun, R., Uzilday, B., Iwata, Y., Koizumi, N., and Turkan, I. (2018). Interplay between the unfolded protein response and reactive oxygen species: a dynamic duo. *J. Exp. Bot.* 69, 3333–3345. doi: 10.1093/jxb/ery040
- Ozgun, R., Uzilday, B., Sekmen, A. H., and Turkan, I. (2015). The effects of induced production of reactive oxygen species in organelles on endoplasmic reticulum stress and on the unfolded protein response in arabidopsis. *Ann. Bot.* 116, 541–553. doi: 10.1093/aob/mcv072
- Palma, J. M., Gomez, M., Yanez, J., and Del Rio, L. A. (1987). Increased levels of peroxisomal active oxygen-related enzymes in copper-tolerant pea plants. *Plant Physiol.* 85, 570–574. doi: 10.1104/pp.85.2.570
- Pan, X., Roberts, P., Chen, Y., Kvam, E., Shulga, N., Huang, K., et al. (2000). Nucleus-vacuole junctions in *Saccharomyces cerevisiae* are formed through the direct interaction of Vac8p with Nvj1p. *Mol. Biol. Cell* 11, 2445–2457. doi: 10.1091/mbc.11.7.2445
- Paris, N., Stanley, C. M., Jones, R. L., and Rogers, J. C. (1996). Plant cells contain two functionally distinct vacuolar compartments. *Cell* 85, 563–572. doi: 10.1016/S0092-8674(00)81256-8
- Pastor-Cantizano, N., Bernat-Silvestre, C., Marcote, M. J., and Aniento, F. (2018). Loss of Arabidopsis p24 function affects ERD2 trafficking and Golgi structure, and activates the unfolded protein response. *J. Cell Sci.* 131:jcs203802. doi: 10.1242/jcs.203802
- Perez-Sancho, J., Vanneste, S., Lee, E., Mcfarlane, H. E., Esteban Del Valle, A., Valpuesta, V., et al. (2015). The Arabidopsis synaptotagmin1 is enriched in endoplasmic reticulum-plasma membrane contact sites and confers cellular resistance to mechanical stresses. *Plant Physiol.* 168, 132–143. doi: 10.1104/pp.15.00260
- Pfanner, N., Van Der Laan, M., Amati, P., Capaldi, R. A., Caudy, A. A., Chacinska, A., et al. (2014). Uniform nomenclature for the mitochondrial contact site and cristae organizing system. *J. Cell Biol.* 204, 1083–1086. doi: 10.1083/jcb.201401006
- Prinz, W. A. (2014). Bridging the gap: membrane contact sites in signaling, metabolism, and organelle dynamics. *J. Cell Biol.* 205, 759–769. doi: 10.1083/jcb.201401126
- Quon, E., Sere, Y. Y., Chauhan, N., Johansen, J., Sullivan, D. P., Dittman, J. S., et al. (2018). Endoplasmic reticulum-plasma membrane contact sites integrate sterol and phospholipid regulation. *PLoS Biol.* 16:e2003864. doi: 10.1371/journal.pbio.2003864
- Ramming, T., Hansen, H. G., Nagata, K., Ellgaard, L., and Appenzeller-Herzog, C. (2014). GPx8 peroxidase prevents leakage of H₂O₂ from the endoplasmic reticulum. *Free Radic. Biol. Med.* 70, 106–116. doi: 10.1016/j.freeradbiomed.2014.01.018
- Ranty, B., Aldon, D., Cotelle, V., Galaud, J. P., Thuleau, P., and Mazars, C. (2016). Calcium sensors as key hubs in plant responses to biotic and abiotic stresses. *Front. Plant Sci.* 7:327. doi: 10.3389/fpls.2016.00327
- Robinson, D. G., Brandizzi, F., Hawes, C., and Nakano, A. (2015). Vesicles versus tubes: is endoplasmic reticulum-Golgi transport in plants fundamentally different from other eukaryotes? *Plant Physiol.* 168, 393–406. doi: 10.1104/pp.15.00124
- Ruberti, C., Lai, Y., and Brandizzi, F. (2018). Recovery from temporary endoplasmic reticulum stress in plants relies on the tissue-specific and largely independent roles of bZIP28 and bZIP60, as well as an antagonizing function of BAX-Inhibitor 1 upon the pro-adaptive signaling mediated by bZIP28. *Plant J.* 93, 155–165. doi: 10.1111/tjp.13768
- Saheki, Y., and De Camilli, P. (2017). Endoplasmic reticulum-plasma membrane contact sites. *Annu. Rev. Biochem.* 86, 659–684. doi: 10.1146/annurev-biochem-061516-044932
- Sandalio, L. M., and Romero-Puertas, M. C. (2015). Peroxisomes sense and respond to environmental cues by regulating ROS and RNS signalling networks. *Ann. Bot.* 116, 475–485. doi: 10.1093/aob/mcv074
- Santos, C. X., Tanaka, L. Y., Wosniak, J., and Laurindo, F. R. (2009). Mechanisms and implications of reactive oxygen species generation during the unfolded protein response: roles of endoplasmic reticulum oxidoreductases, mitochondrial electron transport, and NADPH oxidase. *Antioxid. Redox Signal.* 11, 2409–2427. doi: 10.1089/ars.2009.2625
- Saravanan, R. S., Slabaugh, E., Singh, V. R., Lapidus, L. J., Haas, T., and Brandizzi, F. (2009). The targeting of the oxysterol-binding protein ORP3a to the endoplasmic reticulum relies on the plant VAP33 homolog PVA12. *Plant J.* 58, 817–830. doi: 10.1111/j.1365-3113.2009.03815.x
- Schapiro, A. L., Voigt, B., Jasik, J., Rosado, A., Lopez-Cobollo, R., Menzel, D., et al. (2008). Arabidopsis synaptotagmin 1 is required for the maintenance of plasma membrane integrity and cell viability. *Plant Cell* 20, 3374–3388. doi: 10.1105/tpc.108.063859
- Schattat, M., Barton, K., Baudisch, B., Klosgen, R. B., and Mathur, J. (2011). Plastid stromule branching coincides with contiguous endoplasmic reticulum dynamics. *Plant Physiol.* 155, 1667–1677. doi: 10.1104/pp.110.170480
- Schauder, C. M., Wu, X., Saheki, Y., Narayanaswamy, P., Torta, F., Wenk, M. R., et al. (2014). Structure of a lipid-bound extended synaptotagmin indicates a role in lipid transfer. *Nature* 510, 552–555. doi: 10.1038/nature13269
- Schuck, S., Gallagher, C. M., and Walter, P. (2014). ER-phagy mediates selective degradation of endoplasmic reticulum independently of the core autophagy machinery. *J. Cell Sci.* 127, 4078–4088. doi: 10.1242/jcs.154716
- Scorrano, L., De Matteis, M. A., Emr, S., Giordano, F., Hajnoczky, G., Kornmann, B., et al. (2019). Coming together to define membrane contact sites. *Nat. Commun.* 10:1287. doi: 10.1038/s41467-019-09253-3
- Selitrannik, M., and Lev, S. (2016). The role of phosphatidylinositol-transfer proteins at membrane contact sites. *Biochem. Soc. Trans.* 44, 419–424. doi: 10.1042/BST20150182
- Seo, P. J., Kim, M. J., Song, J. S., Kim, Y. S., Kim, H. J., and Park, C. M. (2010). Proteolytic processing of an Arabidopsis membrane-bound NAC transcription factor is triggered by cold-induced changes in membrane fluidity. *Biochem. J.* 427, 359–367. doi: 10.1042/BJ20091762
- Shapiguzov, A., Vainonen, J. P., Hunter, K., Tossavainen, H., Tiwari, A., Jarvi, S., et al. (2019). Arabidopsis RCD1 coordinates chloroplast and mitochondrial functions through interaction with ANAC transcription factors. *Life* 8:e43284. doi: 10.7554/eLife.43284
- Sharma, M., Singh, A., Shankar, A., Pandey, A., Baranwal, V., Kapoor, S., et al. (2014). Comprehensive expression analysis of rice Armadillo gene family during abiotic stress and development. *DNA Res.* 21, 267–283. doi: 10.1093/dnares/dst056
- Shimada, T., Takagi, J., Ichino, T., Shirakawa, M., and Hara-Nishimura, I. (2018). Plant Vacuoles. *Annu. Rev. Plant Biol.* 69, 123–145. doi: 10.1146/annurev-plant-042817-040508
- Siao, W., Wang, P., Voigt, B., Hussey, P. J., and Baluska, F. (2016). Arabidopsis SYT1 maintains stability of cortical endoplasmic reticulum networks and VAP27-1-enriched endoplasmic reticulum-plasma membrane contact sites. *J. Exp. Bot.* 67, 6161–6171. doi: 10.1093/jxb/erw381
- Sinclair, A. M., Trobacher, C. P., Mathur, N., Greenwood, J. S., and Mathur, J. (2009). Peroxide extension over ER-defined paths constitutes a rapid subcellular

- response to hydroxyl stress. *Plant J.* 59, 231–242. doi: 10.1111/j.1365-313X.2009.03863.x
- Smith, J. J., and Aitchison, J. D. (2013). Peroxisomes take shape. *Nat. Rev. Mol. Cell Biol.* 14, 803–817. doi: 10.1038/nrm3700
- Sparkes, I. (2018). Lessons from optical tweezers: quantifying organelle interactions, dynamics and modelling subcellular events. *Curr. Opin. Plant Biol.* 46, 55–61. doi: 10.1016/j.pbi.2018.07.010
- Sparkes, I. A., Ketelaar, T., De Ruijter, N. C., and Hawes, C. (2009). Grab a Golgi: laser trapping of Golgi bodies reveals in vivo interactions with the endoplasmic reticulum. *Traffic* 10, 567–571. doi: 10.1111/j.1600-0854.2009.00891.x
- Srivastava, R., Chen, Y., Deng, Y., Brandizzi, F., and Howell, S. H. (2012). Elements proximal to and within the transmembrane domain mediate the organelle-to-organelle movement of bZIP28 under ER stress conditions. *Plant J.* 70, 1033–1042. doi: 10.1111/j.1365-313X.2012.04943.x
- Stael, S., Wurzing, B., Mair, A., Mehlmer, N., Vothknecht, U. C., and Teige, M. (2012). Plant organellar calcium signalling: an emerging field. *J. Exp. Bot.* 63, 1525–1542. doi: 10.1093/jxb/err394
- Stefan, C. J. (2018). Building ER-PM contacts: keeping calm and ready on alarm. *Curr. Opin. Cell Biol.* 53, 1–8. doi: 10.1016/j.ceb.2018.03.008
- Stefano, G., and Brandizzi, F. (2018). Advances in plant ER architecture and dynamics. *Plant Physiol.* 176, 178–186. doi: 10.1104/pp.17.01261
- Su, Z., Ma, X., Guo, H., Sukiran, N. L., Guo, B., Assmann, S. M., et al. (2013). Flower development under drought stress: morphological and transcriptomic analyses reveal acute responses and long-term acclimation in Arabidopsis. *Plant Cell* 25, 3785–3807. doi: 10.1105/tpc.113.115428
- Sun, X., Feng, P., Xu, X., Guo, H., Ma, J., Chi, W., et al. (2011). A chloroplast envelope-bound PHD transcription factor mediates chloroplast signals to the nucleus. *Nat. Commun.* 2, 477. doi: 10.1038/ncomms1486
- Sun, Y., Huang, D., and Chen, X. (2019). Dynamic regulation of plasmodesmata permeability and its application to horticultural research. *Hortic. Res.* 6:47. doi: 10.1038/s41438-019-0129-3
- Sun, L., Lu, S. J., Zhang, S. S., Zhou, S. F., Sun, L., and Liu, J. X. (2013). The lumen-facing domain is important for the biological function and organelle-to-organelle movement of bZIP28 during ER stress in Arabidopsis. *Mol. Plant* 6, 1605–1615. doi: 10.1093/mp/sst059
- Sutter, J. U., Campanoni, P., Blatt, M. R., and Paneque, M. (2006). Setting SNAREs in a different wood. *Traffic* 7, 627–638. doi: 10.1111/j.1600-0854.2006.00414.x
- Suzuki, N., Koussevitzky, S., Mittler, R., and Miller, G. (2012). ROS and redox signalling in the response of plants to abiotic stress. *Plant Cell Environ.* 35, 259–270. doi: 10.1111/j.1365-3040.2011.02336.x
- Tan, X. L., Wang, Q. Y., Tian, B. X., Zhang, H. A., Lu, D. L., and Zhou, J. (2011). A *Brassica napus* lipase locates at the membrane contact sites involved in chloroplast development. *PLoS One* 6:e26831. doi: 10.1371/journal.pone.0026831
- Tanaka, Y., Kutsuna, N., Kanazawa, Y., Kondo, N., Hasegawa, S., and Sano, T. (2007). Intra-vacuolar reserves of membranes during stomatal closure: the possible role of guard cell vacuoles estimated by 3-D reconstruction. *Plant Cell Physiol.* 48, 1159–1169. doi: 10.1093/pcp/pcm085
- Tian, L., Zhang, Y., Kang, E., Ma, H., Zhao, H., Yuan, M., et al. (2018). Basic-leucine zipper 17 and Hmg-CoA reductase degradation 3A are involved in salt acclimation memory in Arabidopsis. *J. Integr. Plant Biol.* doi: 10.1111/jipb.12744
- Tilsner, J., Nicolas, W., Rosado, A., and Bayer, E. M. (2016). Staying tight: plasmodesmal membrane contact sites and the control of cell-to-cell connectivity in plants. *Annu. Rev. Plant Biol.* 67, 337–364. doi: 10.1146/annurev-arplant-043015-111840
- Toulmay, A., and Prinz, W. A. (2012). A conserved membrane-binding domain targets proteins to organelle contact sites. *J. Cell Sci.* 125, 49–58. doi: 10.1242/jcs.085118
- Trelease, R. N., and Lingard, M. J. (2006). “Participation of the plant ER in peroxisome biogenesis” in *The plant endoplasmic reticulum*. ed. D. G. Robinson (Berlin, Heidelberg: Springer-Verlag), 205–232.
- Tu, B. P., and Weissman, J. S. (2002). The FAD- and O₂-dependent reaction cycle of Ero1-mediated oxidative protein folding in the endoplasmic reticulum. *Mol. Cell* 10, 983–994. doi: 10.1016/S1097-2765(02)00696-2
- Umate, P. (2011). Oysterol binding proteins (OSBPs) and their encoding genes in Arabidopsis and rice. *Steroids* 76, 524–529. doi: 10.1016/j.steroids.2011.01.007
- van Meer, G., Voelker, D. R., and Feigenson, G. W. (2008). Membrane lipids: where they are and how they behave. *Nat. Rev. Mol. Cell Biol.* 9, 112–124. doi: 10.1038/nrm2330
- Venditti, R., Masone, M. C., Rega, L. R., Di Tullio, G., Santoro, M., Polishchuk, E., et al. (2019a). The activity of Sac1 across ER-TGN contact sites requires the four-phosphate-adaptor-protein-1. *J. Cell Biol.* 218, 783–797. doi: 10.1083/jcb.201812021
- Venditti, R., Rega, L. R., Masone, M. C., Santoro, M., Polishchuk, E., Sarnataro, D., et al. (2019b). Molecular determinants of ER-Golgi contacts identified through a new FRET-FLIM system. *J. Cell Biol.* 218, 1055–1065. doi: 10.1083/jcb.201812020
- Viotti, C. (2014). ER and vacuoles: never been closer. *Front. Plant Sci.* 5:20. doi: 10.3389/fpls.2014.00020
- Viotti, C., Kruger, F., Krebs, M., Neubert, C., Fink, F., Lupanga, U., et al. (2013). The endoplasmic reticulum is the main membrane source for biogenesis of the lytic vacuole in Arabidopsis. *Plant Cell* 25, 3434–3449. doi: 10.1105/tpc.113.114827
- Walley, J., Xiao, Y., Wang, J. Z., Baidoo, E. E., Keasling, J. D., Shen, Z., et al. (2015). Plastid-produced interorganelle stress signal MEcPP potentiates induction of the unfolded protein response in endoplasmic reticulum. *Proc. Natl. Acad. Sci. USA* 112, 6212–6217. doi: 10.1073/pnas.1504828112
- Wang, Y., Berkowitz, O., Selinski, J., Xu, Y., Hartmann, A., and Whelan, J. (2018c). Stress responsive mitochondrial proteins in Arabidopsis thaliana. *Free Radic. Biol. Med.* 122, 28–39. doi: 10.1016/j.freeradbiomed.2018.03.031
- Wang, J. Z., and Dehesh, K. (2018). ER: the silk road of interorganellar communication. *Curr. Opin. Plant Biol.* 45, 171–177. doi: 10.1016/j.pbi.2018.07.012
- Wang, P., Hawes, C., and Hussey, P. J. (2017). Plant endoplasmic reticulum-plasma membrane contact sites. *Trends Plant Sci.* 22, 289–297. doi: 10.1016/j.tplants.2016.11.008
- Wang, P., Hawes, C., Richardson, C., and Hussey, P. J. (2018a). Characterization of proteins localized to plant ER-PM contact sites. *Methods Mol. Biol.* 1691, 23–31. doi: 10.1007/978-1-4939-7389-7_3
- Wang, P. W., Hawkins, T. J., Richardson, C., Cummins, I., Deeks, M. J., Sparkes, I., et al. (2014). The plant cytoskeleton, NET3C, and VAP27 mediate the link between the plasma membrane and endoplasmic reticulum. *Curr. Biol.* 24, 1397–1405. doi: 10.1016/j.cub.2014.05.003
- Wang, P., Mugume, Y., and Bassham, D. C. (2018b). New advances in autophagy in plants: regulation, selectivity and function. *Semin. Cell Dev. Biol.* 80, 113–122. doi: 10.1016/j.semcdb.2017.07.018
- Wang, P. W., Richardson, C., Hawkins, T. J., Sparkes, I., Hawes, C., and Hussey, P. J. (2016). Plant VAP27 proteins: domain characterization, intracellular localization and role in plant development. *New Phytol.* 210, 1311–1326. doi: 10.1111/nph.13857
- Wang, Z., Xu, C., and Benning, C. (2012). TGD4 involved in endoplasmic reticulum-to-chloroplast lipid trafficking is a phosphatidic acid binding protein. *Plant J.* 70, 614–623. doi: 10.1111/j.1365-313X.2012.04900.x
- Watson, S. J., Sowden, R. G., and Jarvis, P. (2018). Abiotic stress-induced chloroplast proteome remodelling: a mechanistic overview. *J. Exp. Bot.* 69, 2773–2781. doi: 10.1093/jxb/ery053
- Woodson, J. D., and Chory, J. (2012). Organelle signaling: how stressed chloroplasts communicate with the nucleus. *Curr. Biol.* 22, R690–R692. doi: 10.1016/j.cub.2012.07.028
- Wu, H., Carvalho, P., and Voeltz, G. K. (2018). Here, there, and everywhere: the importance of ER membrane contact sites. *Science* 361:466. doi: 10.1126/science.aan5835
- Xi, H., Xu, H., Xu, W., He, Z., Xu, W., and Ma, M. (2016). A SAL1 loss-of-function arabidopsis mutant exhibits enhanced cadmium tolerance in association with alleviation of endoplasmic reticulum stress. *Plant Cell Physiol.* 57, 1210–1219. doi: 10.1093/pcp/pcw069
- Xiang, L., Etcheberria, E., and Van Den Ende, W. (2013). Vacuolar protein sorting mechanisms in plants. *FEBS J.* 280, 979–993. doi: 10.1111/febs.12092
- Xiao, Y., Savchenko, T., Baidoo, E. E., Chehab, W. E., Hayden, D. M., Tolstikov, V., et al. (2012). Retrograde signaling by the plastidial metabolite MEcPP regulates expression of nuclear stress-response genes. *Cell* 149, 1525–1535. doi: 10.1016/j.cell.2012.04.038

- Xu, C., Moellering, E. R., Muthan, B., Fan, J., and Benning, C. (2010). Lipid transport mediated by Arabidopsis TGD proteins is unidirectional from the endoplasmic reticulum to the plastid. *Plant Cell Physiol.* 51, 1019–1028. doi: 10.1093/pcp/pcq053
- Yang, Z. T., Lu, S. J., Wang, M. J., Bi, D. L., Sun, L., Zhou, S. F., et al. (2014). A plasma membrane-tethered transcription factor, NAC062/ANAC062/NTL6, mediates the unfolded protein response in Arabidopsis. *Plant J.* 79, 1033–1043. doi: 10.1111/tpj.12604
- Yang, X., Srivastava, R., Howell, S. H., and Bassham, D. C. (2016). Activation of autophagy by unfolded proteins during endoplasmic reticulum stress. *Plant J.* 85, 83–95. doi: 10.1111/tpj.13091
- Yoboue, E. D., Sitia, R., and Simmen, T. (2018). Redox crosstalk at endoplasmic reticulum (ER) membrane contact sites (MCS) uses toxic waste to deliver messages. *Cell Death Dis.* 9:331. doi: 10.1038/s41419-017-0033-4
- Zeeshan, H. M., Lee, G. H., Kim, H. R., and Chae, H. J. (2016). Endoplasmic reticulum stress and associated ROS. *Int. J. Mol. Sci.* 17:327. doi: 10.3390/ijms17030327
- Zhang, C., Hicks, G. R., and Raikhel, N. V. (2014). Plant vacuole morphology and vacuolar trafficking. *Front. Plant Sci.* 5:476. doi: 10.3389/fpls.2014.00476
- Zhao, X., Guo, X., Tang, X., Zhang, H., Wang, M., Kong, Y., et al. (2018). Misregulation of ER-Golgi vesicle transport induces ER stress and affects seed vigor and stress response. *Front. Plant Sci.* 9:658. doi: 10.3389/fpls.2018.00658
- Zhao, P., Liu, F., Zhang, B., Liu, X., Wang, B., Gong, J., et al. (2013). MAIGO2 is involved in abscisic acid-mediated response to abiotic stresses and Golgi-to-ER retrograde transport. *Physiol. Plant.* 148, 246–260. doi: 10.1111/j.1399-3054.2012.01704.x
- Zhu, J. K. (2016). Abiotic stress signaling and responses in plants. *Cell* 167, 313–324. doi: 10.1016/j.cell.2016.08.029

Conflict of Interest Statement: The authors declare that the research was conducted in the absence of any commercial or financial relationships that could be construed as a potential conflict of interest.

Copyright © 2019 Liu and Li. This is an open-access article distributed under the terms of the Creative Commons Attribution License (CC BY). The use, distribution or reproduction in other forums is permitted, provided the original author(s) and the copyright owner(s) are credited and that the original publication in this journal is cited, in accordance with accepted academic practice. No use, distribution or reproduction is permitted which does not comply with these terms.

Advantages of publishing in Frontiers



OPEN ACCESS

Articles are free to read
for greatest visibility
and readership



FAST PUBLICATION

Around 90 days
from submission
to decision



HIGH QUALITY PEER-REVIEW

Rigorous, collaborative,
and constructive
peer-review



TRANSPARENT PEER-REVIEW

Editors and reviewers
acknowledged by name
on published articles

Frontiers

Avenue du Tribunal-Fédéral 34
1005 Lausanne | Switzerland

Visit us: www.frontiersin.org

Contact us: info@frontiersin.org | +41 21 510 17 00



REPRODUCIBILITY OF RESEARCH

Support open data
and methods to enhance
research reproducibility



DIGITAL PUBLISHING

Articles designed
for optimal readership
across devices



FOLLOW US

@frontiersin



IMPACT METRICS

Advanced article metrics
track visibility across
digital media



EXTENSIVE PROMOTION

Marketing
and promotion
of impactful research



LOOP RESEARCH NETWORK

Our network
increases your
article's readership



A Predominant Role of AtEDE1 in Catalyzing a Rate-Limiting Demannosylation Step of an Arabidopsis Endoplasmic Reticulum-Associated Degradation Process

OPEN ACCESS

Edited by:

Junxian He,
The Chinese University of Hong
Kong, Hong Kong SAR, China

Reviewed by:

Dawei Zhang,
Sichuan University, China
Jinbo Shen,
Zhejiang Agriculture and Forestry
University, China

*Correspondence:

Linchuan Liu
lciliu@scau.edu.cn
Jianming Li
lian@umich.edu

[†]Present address:

Yi-min She,
Center for Biologics Evaluation
Biologics and Genetic Therapies
Directorate, Health Canada, Ottawa,
ON, Canada

[†]These authors have contributed
equally to this work

Specialty section:

This article was submitted to
Plant Physiology,
a section of the journal
Frontiers in Plant Science

Received: 24 May 2022

Accepted: 10 June 2022

Published: 07 July 2022

Citation:

Zhang J, Xia Y, Wang D, Du Y,
Chen Y, Zhang C, Mao J, Wang M,
She Y-m, Peng X, Liu L, Voglmeir J,
He Z, Liu L and Li J (2022) A
Predominant Role of AtEDE1 in
Catalyzing a Rate-Limiting
Demannosylation Step of an
Arabidopsis Endoplasmic Reticulum-
Associated Degradation Process.
Front. Plant Sci. 13:952246.
doi: 10.3389/fpls.2022.952246

Jianjun Zhang^{1,2,3†}, Yang Xia^{3†}, Dinghe Wang^{4,5†}, Yamin Du⁶, Yongwu Chen^{4,5},
Congcong Zhang^{4,5}, Juan Mao^{1,2}, Muyang Wang⁵, Yi-Min She[†], Xinxiang Peng¹, Li Liu⁶,
Josef Voglmeir⁶, Zuhua He⁵, Linchuan Liu^{1,2*} and Jianming Li^{1,2,3*}

¹State Key Laboratory for Conservation and Utilization of Subtropical Agro-Bioresources, South China Agricultural University, Guangzhou, China, ²Guangdong Key Laboratory for Innovative Development and Utilization of Forest Plant Germplasm, College of Forestry and Landscape Architecture, South China Agricultural University, Guangzhou, China, ³Department of Molecular, Cellular, and Developmental Biology, University of Michigan, Ann Arbor, MI, United States, ⁴University of Chinese Academy of Sciences, Beijing, China, ⁵The Center of Excellence for Molecular Plant Sciences, Chinese Academy of Sciences, Shanghai, China, ⁶Glycomics and Glycan Bioengineering Research Center, College of Food Science and Technology, Nanjing Agricultural University, Nanjing, China

Endoplasmic reticulum-associated degradation (ERAD) is a key cellular process for degrading misfolded proteins. It was well known that an asparagine (N)-linked glycan containing a free α 1,6-mannose residue is a critical ERAD signal created by Homologous to α -mannosidase 1 (Htm1) in yeast and ER-Degradation Enhancing α -Mannosidase-like proteins (EDEMs) in mammals. An earlier study suggested that two Arabidopsis homologs of Htm1/EDEMs function redundantly in generating such a conserved N-glycan signal. Here we report that the Arabidopsis *irb1* (*reversal of bri1*) mutants accumulate brassinosteroid-insensitive 1–5 (*bri1*–5), an ER-retained mutant variant of the brassinosteroid receptor BRI1 and are defective in one of the Arabidopsis Htm1/EDEM homologs, AtEDE1. We show that the wild-type AtEDE1, but not its catalytically inactive mutant, rescues *irb1*–1. Importantly, an insertional mutation of the Arabidopsis Asparagine-Linked Glycosylation 3 (ALG3), which causes N-linked glycosylation with truncated glycans carrying a different free α 1,6-mannose residue, completely nullifies the inhibitory effect of *irb1*–1 on *bri1*–5 ERAD. Interestingly, an insertional mutation in AtEDE2, the other Htm1/EDEM homolog, has no detectable effect on *bri1*–5 ERAD; however, it enhances the inhibitory effect of *irb1*–1 on *bri1*–5 degradation. Moreover, AtEDE2 transgenes rescued the *irb1*–1 mutation with lower efficacy than AtEDE1. Simultaneous elimination of AtEDE1 and AtEDE2 completely blocks generation of α 1,6-mannose-exposed N-glycans on *bri1*–5, while overexpression of either AtEDE1 or AtEDE2 stimulates *bri1*–5 ERAD and enhances the *bri1*–5 dwarfism. We concluded that, despite its functional redundancy with AtEDE2, AtEDE1 plays a predominant role in promoting *bri1*–5 degradation.

Keywords: endoplasmic reticulum-associated degradation, N-glycan, protein degradation, BRASSINOSTEROID-INSENSITIVE 1, α 1,2-mannosidase, α 1,6-mannose residue

INTRODUCTION

Endoplasmic reticulum-associated degradation (ERAD) is an essential part of a highly conserved ER-localized protein quality control (ERQC) system for removing ER-retained nonnative or mis-assembled proteins, which involves retrotranslocation through the ER membrane, ubiquitination by a membrane-anchored ubiquitin ligase (E3), and eventual degradation *via* the cytosolic proteasome (Preston and Brodsky, 2017). A key event of this process is selection of terminally-misfolded proteins from repairable misfolded proteins and folding intermediates. However, little is known about how eukaryotic cells execute this selection step. Recent studies in yeast and mammalian cells have shown that an asparagine (Asn)-linked glycan (N-glycan) containing an exposed α 1,6-mannose (Man) residue on misfolded glycoproteins serves as a crucial ERAD signal that marks a terminally misfolded glycoprotein for degradation. Such a signal is generated through trimming a specific terminal α 1,2-Man residue from N-linked $\text{Man}_8\text{GlcNAc}_2$ (GlcNAc, N-acetylglucosamine) glycans by the Homologous to α -mannosidase 1 (Htm1) and mammalian ER-degradation enhancing α -mannosidase-like proteins (EDEMs; Quan et al., 2008; Clerc et al., 2009; Hosokawa et al., 2010). The exposed α 1,6-Man residue and its surrounding misfolded region are recognized by the yeast OS-9 (Yos9)/mammalian Osteosarcoma amplified 9 (OS-9) protein and the yeast HMG-CoA reductase degradation protein 3 (Hrd3)/mammalian Suppressor/enhancer of lin-12-like protein1 (Sel1L) protein, respectively (Xu and Ng, 2015). It is believed that Yos9/OS-9 and Hrd3/Sel1L work together to bring a committed ERAD client to the membrane-anchored E3 ligase Hrd1 (HRD1 in mammals) for ubiquitination and subsequent retrotranslocation into the cytosol for proteasomal degradation (Smith et al., 2011).

Although similar processes were known to exist in plants (Ceriotti and Roberts, 2006; Liu et al., 2011), our knowledge about a plant ERAD system still remains limited (Strasser, 2018). Recent discoveries of several Arabidopsis ERAD clients made Arabidopsis an attractive genetic model system to study the plant ERAD process (Jin et al., 2007; Hong et al., 2009, 2012; Li et al., 2009; Nekrasov et al., 2009; Baer et al., 2016). Among them are *bri1-5* and *bri1-9*, which are mutant variants of BRASSINOSTEROID-INSENSITIVE 1 (BRI1), a well-studied surface receptor for the plant steroid hormone brassinosteroids (BRs; Li and Chory, 1997; Kinoshita et al., 2005). A Cys⁶⁹-Tyr mutation in *bri1-5* and a Ser⁶⁶²-Phe mutation in *bri1-9* are thought to cause minor structural defects that are recognized by a highly conserved ER quality control (ERQC) mechanism in Arabidopsis. This ERQC consists of EMS-mutagenized *bri1* suppressor 1 (EBS1), the Arabidopsis homolog of the mammalian UDP-glucose:glycoprotein glucosyltransferase (UGGT) capable of differentiating misfolded glycoproteins from their native conformers, and EBS2 (also known as calreticulin 3 or CRT3), a plant-specific member of the CRT/calnexin (CNX) family capable of high-affinity binding to a monoglucosylated N-glycan (Jin et al., 2007, 2009; Hong et al., 2008). The EBS1-EBS2 system and other chaperone-mediated ERQC mechanisms retain the two mutant *bri1* proteins in the ER, leading to their eventual

degradation *via* ERAD and a severe BR-insensitive dwarf phenotype (Jin et al., 2007, 2009).

It was previously shown that the protein abundance of these Arabidopsis ERAD clients could be greatly increased by treatment with kifunensine (Kif; Hong et al., 2008, 2009; Nekrasov et al., 2009; Saijo et al., 2009), a widely used inhibitor of α 1,2-mannosidases including Htm1/EDEMs (Elbein et al., 1990), suggesting involvement of Man-trimming steps in the Arabidopsis ERAD process (Liu and Li, 2014). Further genetic and metabolic studies not only confirmed this pharmacological finding but also concluded that the N-glycan signal for tagging an Arabidopsis ERAD client is conserved to be a free α 1,6-Man residue-containing N-glycan (Hong et al., 2012). The Arabidopsis has two homologs of Htm1/EDEMs, AtEDE1, and AtEDE2 (known previously as MNS5 and MNS4 for α -mannosidase 5 and 4, respectively), and a previous reverse genetic investigation suggested that these two Htm1/EDEM homologs function redundantly in ERAD of *bri1-5* as single mutation of either protein fails to suppress the *bri1-5* phenotype (Huttner et al., 2014b). However, it remains unknown whether AtEDE1 and AtEDE2 are required to generate the conserved N-glycan code on a known ERAD client. Here, we report a forward genetic study showing that despite functional redundancy of AtEDE1/MNS5 and AtEDE2/MNS4, loss-of-function mutations in AtEDE1 alone could partially suppress the dwarf phenotype of *bri1-5* by weakly inhibiting *bri1-5* degradation. We have found that AtEDE2 could rescue the *irb1-1* mutation but with a lower efficacy than AtEDE1, likely due to its weaker promoter and a slightly weaker biochemical activity. More importantly, the mass spectrometry-based N-glycan analyses coupled with linkage-specific mannosidases demonstrated the functional redundancy of AtEDE1 and AtEDE2 in removing the C-branch terminal α 1,2-Man residue, thus exposing the ERAD-signaling α 1,6-Man residue. Furthermore, our transgenic experiments indicated that the AtEDE1/AtEDE2-catalyzed creation of the N-glycan ERAD signal constitutes a major rate-limiting step of the *bri1-5* ERAD pathway.

MATERIALS AND METHODS

Plant Materials and Growth Conditions

All Arabidopsis mutants and transgenic lines used in this study are in Wassilewskija-2 (Ws-2) or Columbia-0 (Col-0) ecotype. All 6 *irb1* mutants were isolated from two large-scale EMS-mutagenesis-based genetic screens for extragenic suppressors of the Arabidopsis *bri1-5* mutant (in Ws-2 ecotype; Noguchi et al., 1999). The T-DNA insertional mutant *edem2-t* (SALK_095857, Col-0) was obtained from the Arabidopsis Biological Resource Center (ABRC) at Ohio State University and crossed with *bri1-5* and *irb1-1 bri1-5*, while the T-DNA insertional mutant *alg3-t2* (SALK_046061; Col-0) was previously described (Hong et al., 2012). Methods for seed sterilization and conditions for plant growth were described previously (Li et al., 2001), and the hypocotyl elongation assays on BL-containing medium were carried out according to a previously described protocol (Neff et al., 1999).

Map-Based Cloning of the *IRB1* Gene

The *irb1 bri1-5* mutant (ecotype Ws-2) was crossed with a *bri1-9* mutant (ecotype Col-0; Jin et al., 2007), and the resulting F1 plants were allowed for self-fertilization to generate several F2 mapping populations. Genomic DNAs from segregating F2 seedlings exhibiting the *irb1 bri1-5*-like morphology were extracted as previously described (Li and Chory, 1998) and used for PCR-based mapping using previously published simple sequence length polymorphism markers (Pacurar et al., 2012), and oligonucleotides listed in **Supplementary Table S1**.

Construction of Plasmids and Generation of Transgenic Plants

A 5,279-bp genomic fragment of *At1g27520* containing 1,348-bp promoter and 591-bp 3'-untranscribed/untranslated region was PCR-amplified from the BAC T17H3 DNA obtained from ABRC using the *gAtEDEM1* primer set (**Supplementary Table S1**) and was cloned into BamHI/SalI-digested *pPZP212* vector (Hajdukiewicz et al., 1994). The resulting *gAtEDEM1* plasmid was subsequently used to perform a site-directed mutagenesis using the *AtEDEM1Mut* primer set (**Supplementary Table S1**) and the QuikChange II XL Site-Directed Mutagenesis kit (Agilent) to generate a *mgAtEDEM1* transgene that produced a glutamate(E)¹³⁴-glutamine(Q) mutated catalytically-inactive variant of AtEDEM1 by the manufacturer's recommended protocol. A 6,323-bp genomic fragment of *At5g43710* containing 1,586-bp promoter/5'-untranslated region and a 466-bp 3'-untranslated/untranscribed region was amplified from the BAC MQD19 DNA (also obtained from ABRC) using the *gAtEDEM2* primer set (**Supplementary Table S1**) and subsequently cloned into the XmaI/KpnI-digested *pPZP212* vector (Hajdukiewicz et al., 1994). A 1,811-bp coding sequence (CDS) fragment and a 1,872-bp CDS fragment containing the entire coding region of *AtEDEM1* and *AtEDEM2* were amplified from an *At1g27520* cDNA clone R19200 and an *At5g43710* cDNA clone G09215 (both were obtained from ABRC) using the primer sets, *cAtEDEM1GFP* and *cAtEDEM2GFP* (**Supplementary Table S1**), double digested with SpeI/XbaI and BamHI (depending on the introduced restriction sites on the primers), and subsequently cloned into the XbaI/BamHI-digested *pBRI1::BRI1-GFP* (Friedrichsen et al., 2000) to generate a *pBRI1::cAtEDEM1-GFP* plasmid and a *pBRI1::cAtEDEM2-GFP* plasmid, respectively. To generate non-tagged *pBRI1::cAtEDEM1/2* plasmids, the first cDNAs of the wild-type Arabidopsis seedlings and the *pBRI1cAtEDEM1* and *pBRI1cAtEDEM2* primer sets (see **Supplementary Table S1**) were used to amplify the CDS fragments of AtEDEM1/2, which were digested with BamHI/KpnI and subsequently cloned into the BamHI/KpnI-digested *pC1300pBRI1* plasmid, a modified *pCambial300* vector (Leclercq et al., 2015) that contains a 1.6-kb BRI1 promoter fragment. To create transgenes of *pBRI1::At1g30000-GFP*, *pBRI1::At1g51590-GFP*, and *pBRI1::Htm1-GFP*, the first strand cDNAs of the wild-type Arabidopsis plants and yeast genomic DNAs were used to amplify the open-reading frames of *At1g30000* (*MNS3*), *At1g51590* (*MNS1*), and the yeast Htm1 with the *1g30000GFP*, *1g51590GFP*, and *Htm1GFP* primer sets

(**Supplementary Table S1**), respectively. The PCR-amplified CDS fragments were digested with XbaI/SpeI and BamHI/BglII (depending on the introduced restriction sites of the primers) and subsequently cloned into the XbaI/BamHI-digested *pBRI1::BRI1-GFP* plasmid to generate *pBRI1::c1g30000-GFP*, *pBRI1::c1g51590-GFP*, and *pBRI1::Htm1-GFP* plasmids. A two-step cloning strategy was used to create the *pBRI1::bri1-5ED-GFP-HDEL* plasmid. The coding sequence of the BRI1's extracellular domain was amplified from a *pBRI1::bri1-5-GFP* plasmid (Hong et al., 2008) using the *BRI1ED* primer set (**Supplementary Table S1**), digested with SpeI and BamHI, and cloned into the XbaI/BamHI-cut *pBRI1::BRI1-GFP* plasmid (Hong et al., 2008) to generate the *pBRI1::bri1-5ED-GFP* plasmid. The resulting plasmid was used as the DNA template to amplify the coding sequence of GFP with the *GFPHdel* primer set [**Supplementary Table S1**, its reverse primer containing coding sequence of the HDEL (histidine-aspartate-glutamate-leucine) ER-retrieval motif], which was subsequently digested with BamHI and KpnI and cloned into the BamHI/KpnI-digested *pBRI1::bri1-5-GFP* plasmid to create the *pBRI1::BRI1ED-GFP-HDEL* plasmid. The created transgenes were fully sequenced to ensure no PCR-introduced error and were individually transformed into various Arabidopsis lines or used for transient expression in tobacco leaves.

Transient Expression and Confocal Microscopic Analysis of GFP-Tagged EDEM Fusion Proteins in Tobacco Leaves

The *pBRI1::cAtEDEM1-GFP*, *pBRI1::cAtEDEM2-GFP*, *pBRI1::At1g3000-GFP*, *pBRI1::At1g51590-GFP*, and *pSITE03-ER-RFP* (encoding a red fluorescent protein (RFP) tagged at its C-terminus with the ER-retrieval HDEL motif; Chakrabarty et al., 2007), and *p35S:p19* (encoding the p19 protein of tomato bushy stunt virus that was known for suppressing gene silencing; Voinnet et al., 2003) plasmids were cotransformed into leaves of 3-week-old tobacco (*Nicotiana benthamiana*) plants via an *Agrobacterium*-mediated infiltration method (Voinnet et al., 2003). Forty-eight hours after infiltration, the localization patterns of AtEDEM1-GFP or AtEDEM2-GFP and the ER-localized RFP-HDEL in the co-infiltrated tobacco leaf epidermal cells were examined using a Leica confocal laser-scanning microscope (TCS SP5 DM6000B) with an HCX PL APOCS 63X 1.30 glycerin lens and LAS AF software (Leica Microsystems). The GFP or RFP signal was excited by using the 488- or 543-nm laser light, respectively.

Yeast Complementation Assay

The yeast strain $\Delta htm1$ carrying the *pDN436* plasmid (Ng et al., 2000) that encodes a HA-tagged CPY* (the ER-retained misfolded variant of the vacuolar carboxypeptidase Y) was provided by Amy Chang (University of Michigan). The coding sequence of the yeast Htm1 and AtEDEM1 were individually amplified from the yeast genomic DNA and the first-strand Arabidopsis cDNAs, respectively, and the resulting PCR fragments were used to replace the yeast *ALG9* fragment from the *pYEp352-ScALG9* expression plasmid (Frank and Aebi, 2005) to create *pYEp352-Htm1* and *pYEp352-AtEDEM1* plasmids following a previously described cloning strategy (Hong et al., 2009). After sequencing to ensure

no PCR-introduced error, these two plasmids were individually transformed into the $\Delta htm1$ mutant yeast cells by a previously-published transformation protocol (Gietz and Woods, 2002). Yeast cells of the $\Delta htm1$ mutant strain and *pYEp352-Htm1/AtEDEMI*-transformed $\Delta htm1$ strains were grown to mid-log phase ($OD_{600} \sim 1.5$) and treated with 100 μ g/ml CHX (cycloheximide). Similar amounts of yeast cells were removed at 0, 1, 2, and 4 h after the CHX addition, collected by centrifugation on a bench-top microcentrifuge at room temperature, and resuspended in 1X yeast extraction buffer (0.3M sorbitol, 0.1M NaCl, 5mM MgCl₂, and 10mM Tris, pH 7.4). After cell lysis by vigorous vortexing with glass beads, the resuspended yeast cells were mixed with 2X SDS sample buffer [100mM Tris-HCl, pH 6.8, 4% (w/v) SDS; 0.2% (w/v) bromophenol blue, 20% (v/v) glycerol, and 200mM β -mercaptoethanol], boiled for 10 min, and centrifuged for 10 min to remove insoluble cellular debris. The resulting supernatants were separated on 10% SDS/PAGE and analyzed by immunoblotting with an anti-HA antibody (10A5; Invitrogen).

Protein Extraction and Immunoblot Analyses

Two or 4-week-old *Arabidopsis* seedlings treated with or without CHX (Sigma-Aldrich), Kif (Toronto Research Chemicals), or BL (brassinolide) (Chemicon, Inc. Canada), or 3 g of agro-infiltrated tobacco leaves, were ground into fine powder in liquid nitrogen, resuspended in 2X SDS sample buffer, and boiled for 10 min. After 10 min centrifugation in a bench-top Eppendorf microcentrifuge at the top speed at room temperature to remove insoluble cellular debris, the clear supernatants were used immediately for immunoblot analysis or incubated with or without 1,000 U Endo Hf in 1X G5 buffer (New England Biolabs) for 1 h at 37°C. These treated protein samples were subsequently separated by 7% or 10% SDS-PAGE and analyzed by Coomassie Blue staining or by immunoblot with antibody raised against BRI1, GFP (632381, Clontech), ACTIN (CW0264, Beijing CWBio), and BRI1-EMS-SUPPRESSOR1 (BES1) (Mora-García et al., 2004). Chemiluminescence immunoblot signals were visualized by X-ray films or by the Odyssey® Dlx Infrared Imaging System (LI-COR).

RNA Isolation and Reverse Transcription-PCR

Total RNAs were isolated from 2-week-old *Arabidopsis* seedlings grown on ½ MS medium containing 1% sucrose and 0.8% phytagel (Sigma) as described previously (Li et al., 2001). For each RT-PCR experiment, 2 μ g of total RNAs were reverse transcribed using the Invitrogen's SuperScript First-Strand Synthesis System for RT-PCR according to the manufacturer's recommended protocol. To analyze the transcripts of *IRB1/AtEDEMI* in *bri1-5* and *irb1-1 bri1-5* mutant backgrounds or the *AtEDEMI2* transcription in wild-type Col-0 and the *edem2-t* insertional mutants, 0.5 μ l of the first-strand cDNA reaction products was used as a template for PCR amplification with the primer sets shown in **Supplementary Table S1**. The *ACTIN2* transcript was amplified using the *ACTIN2* primer set (**Supplementary Table S1**) as a control. Amplified RT-PCR

products were separated by 1% agarose gel, visualized by ethidium bromide staining, and photographed with a Gel Doc™ XR+ Gel Documentation system (Bio-Rad).

Glycan Structure Analysis

Ten grams of 4-week-old soil-grown plants were collected, immediately ground in liquid nitrogen, and then dissolved in the protein extraction buffer [50mM Tris-HCl, pH 7.5, 150mM NaCl, 5mM EDTA, 0.2% (v/v) Triton X-100 (Sigma), 0.2% (v/v) Nonidet P-40 (Roche), 1mM phenylmethylsulfonyl fluoride (PMSF, Sigma-Aldrich), and a cOmplete™ protease inhibitor cocktail (Roche)]. After 15 min centrifugation at 10,000 \times g to remove insoluble cellular debris, the supernatants were used to immunoprecipitate the GFP-tagged bri1-5ED using anti-GFP monoclonal antibody-conjugated-agarose (D153-8, MBL International Corporation). The immunoprecipitated proteins were further separated by SDS-PAGE. The bri1-5ED-GFP-HDEL protein bands in the gel slices were digested by 50 ng of trypsin (Promega) followed by chymotrypsin (Sigma) in 25mM NH₄HCO₃, and the extracted peptides were subsequently analyzed by the data dependent LC-MS/MS on an Orbitrap Fusion Tribrid mass spectrometer (Thermo) coupled with ultraperformance nanoflow LC system (Waters) to identify the glycosylated BRI1 peptides following a previously published procedure (Ma et al., 2016). The identification of N-glycopeptides was achieved through parallel LC-MS/MS analyses of intact glycopeptides by the low-energy collision-induced dissociation (CID) and high-energy collision-induced dissociation (HCD) to determine both peptide sequences and their-associated glycan structures. To accurately validate the structures of N-glycans on bri1-5ED-GFP-HDEL, the immunoprecipitated bri1-5ED-GFP-HDEL was directly eluted from the beads in the glycine buffer (0.1M glycine HCl pH 3.0), and neutralized in the Tris-HCl buffer (pH 7.5). The purified protein samples were subsequently dried, dissolved with 23 μ l 500mM NaH₂PO₄, 12.5 μ l denaturing buffer [containing 1M β -mercaptoethanol and 2% (w/v) SDS]. Following the glycosidase digestion with PNGase F (Prozyme), samples were fluorescence labeled with 2AB and then separated by hydrophilic interaction liquid chromatography (HILIC). N-glycans of each single chromatographic fraction were collected, dried, subjected to further digestion by highly-specific α 1,3-(Qlyco, Nanjing, China), α 1,6-(Qlyco, Nanjing, China), and α 1,2/3/6-exomanno-sidases (Prozyme), and separated by ultra-performance liquid chromatography (UPLC) (Liu et al., 2016a).

Sequence and Phylogeny Analysis

Forty-one unique protein sequences were downloaded from NCBI and aligned using a MUSCLE program (Edgar, 2004) at <http://www.phylogeny.fr> (Dereeper et al., 2008). These sequences include IRB1/AtEDEMI/MNS5 (NP_564288); AtEDEMI2/MNS4 (NP_199184); XP_006307064.1 and XP_006282375.1 of *Capsella rubella*; XP_010322255.1 and XP_004236144.1 (*Solanum lycopersicum*); XP_003536208.1 and XP_003549640.1 (*Glycine max*); XP_002311656.2 and XP_024437663.1 (*Populus trichocarpa*); XP_008646239.1 and XP_008654408.1 (*Zea mays*); XP_015622855.1 and XP_015619333.1 (*Oryza sativa*); XP_003573

110.1 and XP_003569932.1 (*Brachypodium distachyon*); KMZ61171 and KMZ61126.1 (*Zostera marina*); XP_020518838.1 and XP_006838875.1 (*Amborella trichopoda*); XP_024536391.1 and XP_002969801.2 (*Selaginella moellendorffii*); XP_024401298.1 (*Physcomitrella patens*); PTQ27873.1 and PTQ31295.1 (*Marchantia polymorpha*); GBG76786.1 (*Chara braunii*); GAQ84904.1 and GAQ88520.1 (*Klebsormidium nitens*); XP_005643868.1 and XP_005647098.1 (*Coccomyxa subellipsoidea* C-169); XP_001420019.1 (*Ostreococcus lucimarinus* CCE9901), XP_003081735.3 (*Ostreococcus tauri*), XP_003059643.1 (*Micromonas pusilla* CCMP1545), XP_002504119.1 (*Micromonas commode*), XP_005845108.1 (a partial polypeptide from *Chlorella variabilis*); PRW45694.1 (*Chlorella sorokiniana*); and XP_007514253.1 (*Bathycoccus prasinos*). The two spruce EDEM sequences were obtained as translational products of sequenced mRNAs (GCHX01235049 and GCHX01346827) from *Picea glauca*. Yeast Htm1 (NP_012074) and the Arabidopsis At1g51590/MNS1 (OAP12316.1, one of the two Golgi-localized α 1,2-mannosidase; Liebminger et al., 2009), were used as the outgroups to root the phylogeny tree. The aligned sequences were used to construct a phylogeny tree by the PhyML program (Guindon et al., 2010) with the bootstrapping (number of bootstraps: 100) procedure at <http://www.phylogeny.fr>, and the derived consensus tree was visualized with the TreeDyn program.¹ The aligned amino acid sequences were used to obtain the conserved 430-amino-acid-long core domains of glycosylhydrolase family 47 (glyco_hydro_47), which were subsequently used to perform pairwise comparison to obtain their sequence identity and similarity. The glyco_hydro_47 domains of AtEDEM1/2, their homologs of rice, *Selaginella*, *Amborella*, and the liverwort, plus those of the three human EDEMs (EDEM1, NP_055489; EDEM2, NP_001341937; and EDEM3, NP_001306889) were aligned by the MUSCLE program at www.phylogeny.fr and the resulting aligned sequences were visualized by the BoxShade program at http://embnet.vital-it.ch/software/BOX_form.html.

RESULTS

Isolation and Characterization of *irb1* Mutants

The mutant *bri1-5* receptor, which carries the Cys⁶⁹-Tyr mutation in the extracellular domain of BRI1, is retained in the ER by at least three independent mechanisms and is degraded by a Kif-sensitive ERAD process (Hong et al., 2008). To identify components of its degradation machinery, we performed two large-scale ethyl methanesulfonate (EMS)-mutagenesis projects with the *bri1-5* mutant and isolated >60 *irb* mutants (*reversal of bri1-5*), several of which were found to be allelic to *ebd4*, *ebd5*, *ebd6*, and *ebd7* (Hong et al., 2009; Su et al., 2011, 2012; Liu et al., 2015). These screens also identified six allelic *irb1* mutants. As shown in **Figures 1A–C**, the *irb1-1* mutation nicely suppresses the growth defects of *bri1-5*. The *irb1-1 bri1-5* double mutant, compared to the parental *bri1-5* mutant, has a larger rosette with easily recognizable petioles (**Figure 1A**), a longer

hypocotyl when grown in the dark (**Figure 1B**), and taller inflorescence stems at maturity (**Figure 1C**). Interestingly, the difference in etiolated hypocotyl length between *bri1-5* and *irb1-1 bri1-5* disappeared when grown on medium containing brassinazole (BRZ; **Figures 1B,D**), a specific inhibitor of BR biosynthesis (Asami et al., 2000), suggesting that the phenotypic suppression of *bri1-5* by *irb1-1* likely depends on BR perception. Consistent with these phenotypic changes, a BR-induced hypocotyl elongation assay (Neff et al., 1999) showed that *irb1-1* partially restored the BR sensitivity of the BR-insensitive mutant *bri1-5* (**Figure 1E**). An immunoblot assay that examined the BR-induced change in the phosphorylation status of BES1, a robust biochemical marker of BR signaling (Mora-Garcia et al., 2004), further supported increased BR sensitivity of *bri1-5* by *irb1-1* (**Figure 1F**).

The *irb1-1* Mutation Inhibits the Degradation of *bri1-5*

Our previous studies showed that the restored BR sensitivity in suppressor mutants of two ER-retained BR receptors (*bri1-5* and *bri1-9*) are caused by defective ER quality control (ERQC) systems including ERAD (Jin et al., 2007, 2009; Hong et al., 2008, 2009, 2012; Su et al., 2011, 2012; Liu et al., 2015). To determine if the *irb1-1* mutation inhibits ER retention or ERAD of *bri1-5*, we performed an immunoblot assay using an anti-BRI1 antibody (Mora-Garcia et al., 2004) and discovered that the *irb1-1 bri1-5* mutant accumulated more *bri1-5* proteins than the parental *bri1-5* mutant (**Figure 2A**). However, the degree of the *bri1-5* abundance increase was somewhat lower than what was observed in the *ebd5 bri1-5* mutant (**Figure 2A**), which is defective in the Arabidopsis homolog of the yeast Hrd3 and mammalian Sel1L that function as a key recruitment factor to bring a committed ERAD client to the ER membrane anchored E3 ligase (Liu et al., 2011; Su et al., 2011). To eliminate the possibility that the increased *bri1-5* abundance in *irb1-1 bri1-5* is caused by increased *bri1-5* biosynthesis, we performed a cycloheximide (CHX)-chase experiment, which revealed increased stability of *bri1-5* in *irb1-1 bri1-5* compared to *bri1-5* (**Figure 2B**). Together, these experiments strongly suggested that *irb1-1* partially inhibits ERAD of *bri1-5*. Based on what were shown in other known Arabidopsis ERAD mutants (Hong et al., 2009, 2012; Su et al., 2011, 2012; Liu et al., 2015), we predicted that increased accumulation of *bri1-5* in *irb1-1 bri1-5* would saturate the *bri1-5*'s ER-retention systems, leading to escape of a small pool of *bri1-5* proteins from the ER to the plasma membrane (PM) where *bri1-5* could partially activate the BR signaling process. Indeed, a simple biochemical assay using endoglycosidase H (Endo H), an endoglycosidase that removes high-mannose (HM)-type N-glycans of ER-retained glycoproteins but not the complex-type (C-type) N-glycans on proteins that travel through the Golgi body (Faye and Chrispeels, 1985), revealed the presence of a very small pool of *bri1-5* proteins carrying the HM-type N-glycan suggestive of ER escape and PM localization (**Figure 2A**). Contrast to what were previously reported of other ERAD mutations, *irb1-1* was not able to suppress the *bri1-9* mutation (**Supplementary Figure 1A**).

¹www.treedyn.org

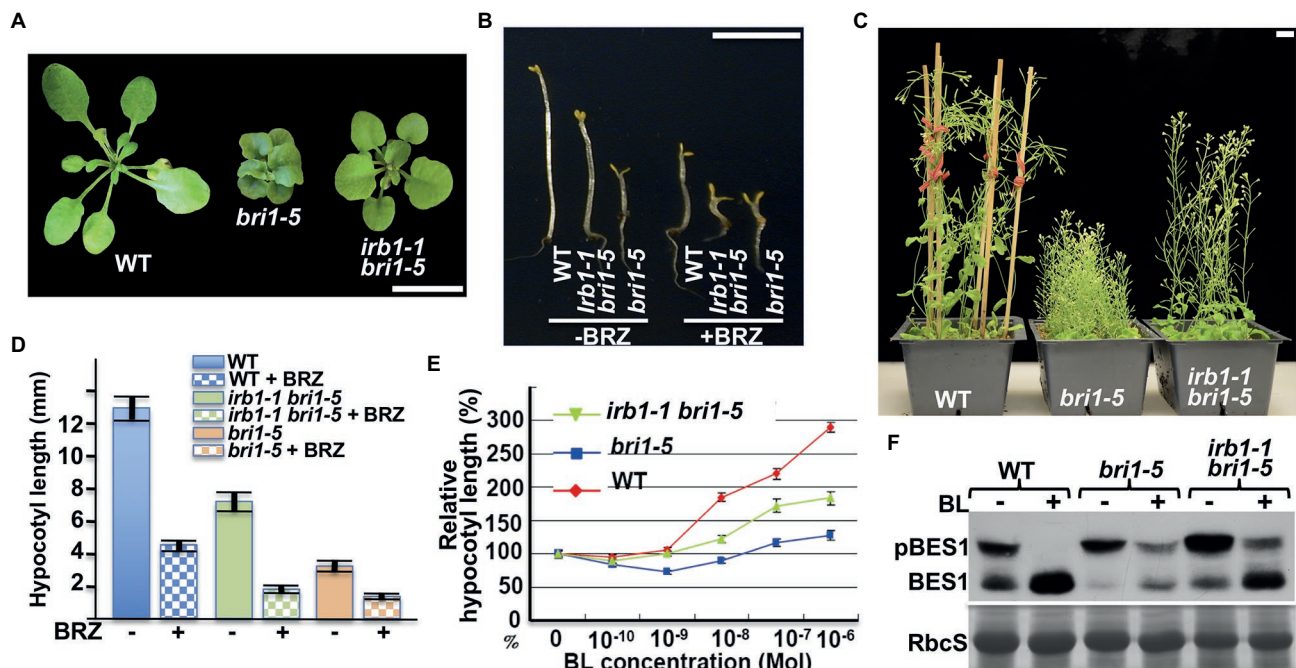


FIGURE 1 | *irb1-1* suppresses the *bri1-5* phenotypes and confers partial BR sensitivity to the *bri1-5* mutant. **(A)** Photographs of 4-week-old soil-grown plants of the wild-type (ecotype Ws-2), *bri1-5*, and the *irb1-1 bri1-5* double mutant. **(B)** Photographs of 5-day-old dark-grown seedlings of wild-type (Ws-2), *irb1-1 bri1-5*, and *bri1-5* grown on medium supplemented with or without 2 μ M brassinazole (BRZ). **(C)** Photographs of 2-month-old soil-grown mature plants of wild-type, *bri1-5*, and *irb1-1 bri1-5*. In **(A–C)**, scale bar = 1 cm. **(D)** Quantitative analysis of average hypocotyl lengths of 5-day-old dark-grown seedlings grown on $\frac{1}{2}$ MS medium supplemented with or without 2 μ M BRZ. A total of ~60 seedlings from two independent experiments were analyzed and the error bars indicate \pm SEs. **(E)** Quantitative analysis of hypocotyl elongation of 10-day-old light grown seedlings on $\frac{1}{2}$ MS medium containing varying concentrations of brassinolide (BL). A total of ~90 seedlings from three biological replicates were analyzed. Each data point represents the relative value of average hypocotyl length of BL-treated seedlings to that of mock-treated seedlings of the same genotype, and error bars represent \pm SEs. **(F)** Immunoblot analysis of BL-induced dephosphorylation of BES1. Equal amounts of total proteins extracted from 2-week-old light-grown seedlings treated with or without 1 μ M BL for 2 h were separated by 10% SDS-PAGE and analyzed by immunoblotting using an anti-BES1 antibody. The lower strip is Coomassie blue staining of the small subunit of ribulose-1,5-bisphosphate carboxylase/oxygenase (RbcS) on a duplicated gel, which was used as a loading control.

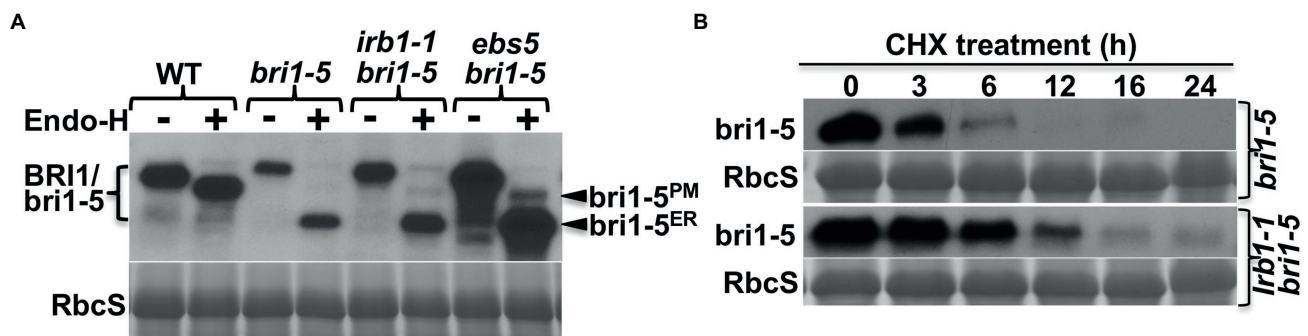


FIGURE 2 | *irb1-1* is a weak endoplasmic reticulum-associated degradation (ERAD) mutant with increased abundance of *bri1-5* **(A)**. Immunoblot analysis of the *bri1-5* abundance. Equal amounts of total proteins extracted from 2-week-old light-grown seedlings were treated with or without Endo H, separated by 8% SDS-PAGE, and analyzed by immunoblotting using an anti-BRI1 antibody. **(B)** Immunoblot analysis of the *bri1-5* stability in *bri1-5* and *irb1-1 bri1-5* mutants. Two-week-old seedlings were transferred into liquid $\frac{1}{2}$ MS medium containing 180 μ M cycloheximide (CHX). Equal amounts of seedlings were removed at indicated incubation times to extract total proteins in 2 X SDS sample buffer, which were subsequently analyzed by immunoblotting with the anti-BRI1 antibody. In both **(A,B)**, Coomassie blue staining of the RbcS band on duplicated gels was used as loading control.

This finding is consistent with the fact that no single *irb1* allele was identified in our previous genetic screens for *bri1-9* suppressors, which led to discoveries of multiple alleles of

EBS1-EBS7 genes (Jin et al., 2007, 2009; Hong et al., 2009, 2012; Su et al., 2011, 2012; Liu et al., 2015). This is likely caused by weak inhibition of *bri1-9* ERAD by the *irb1-1*

mutation (**Supplementary Figure 1B**) combined with a potential weaker receptor function of the surface-localized bri1-9 compared to the PM-localized bri1-5.

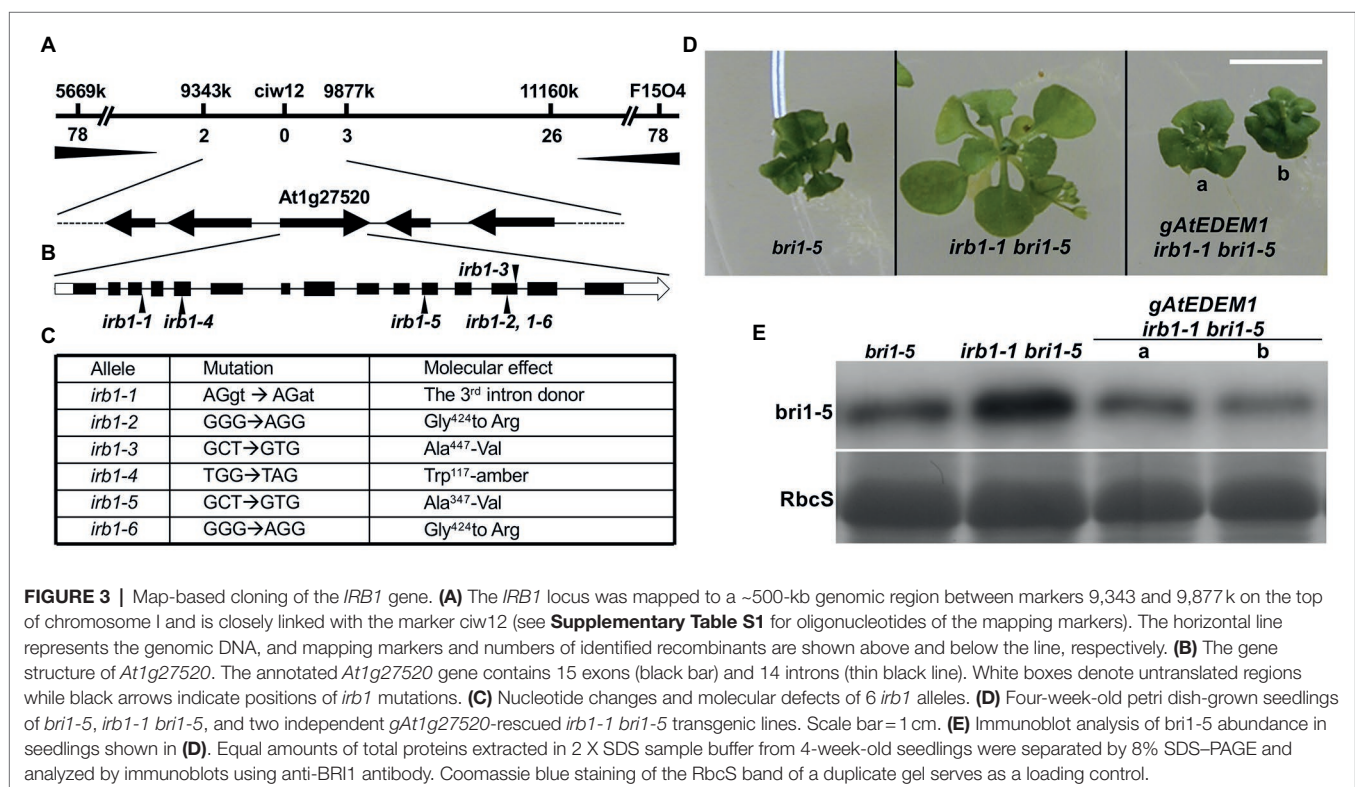
Molecular Cloning of the *IRB1* Gene

To understand how the *irb1-1* mutation inhibits ERAD of bri1-5, we cloned the *IRB1* gene using the map-based cloning strategy. The *irb1-1 bri1-5* mutant (in ecotype *Ws-2*) was crossed with a *bri1-9* mutant (in ecotype *Columbia-0* or *Col-0*) and the resulting F1 plants were allowed to self-fertilization to produce several mapping populations. Genomic DNAs of >1,000 *irb1-1 bri1-5*-like F2 seedlings from these mapping populations were used to determine a close linkage of the *IRB1* locus with an SSLP marker *ciw12* (9,621,357–9,621,484, see **Supplementary Table S1** for nucleotide sequences) on chromosome I (**Figure 3A**), which is located close to the *Arabidopsis* gene *At1g27520* [known previously as *MNS5* (Huttner et al., 2014a), 9,558,752–9,563,751] encoding a potential homolog of Htm1/EDEMs that play a key role in the yeast/mammalian ERAD processes (Clerc et al., 2009; Hosokawa et al., 2010; Huttner et al., 2014b). Consistent with the result of our phenotypic analysis of *irb1-1 bri1-9* double mutant, none of these partially suppressed F2 seedlings was homozygous for the *bri1-9* mutation. Sequence analysis of this gene amplified from *bri1-5* and *irb1-1 bri1-5* identified a G-A mutation in *irb1-1 bri1-5* at the third exon/intron junction (AGgt-AGat; **Figure 3C**), which was predicted to affect the correct splicing of its third intron. RT-PCR analysis of *At1g27520* transcripts with total RNAs isolated from the *irb1-1 bri1-5* and *bri1-5* seedlings identified several aberrantly-spliced *At1g27520*

transcripts in *irb1-1 bri1-5* but failed to detect the presence of the correctly-spliced *At1g27520* transcript that could be easily detected in *bri1-5* (**Supplementary Figure 2**), suggesting that *irb1-1* is likely a null allele of *At1g27520*. The identity of *At1g27520* as *IRB1* was supported by genetic mapping and sequence analysis of five other *irb1* mutants (*irb1-2–irb1-6*; **Supplementary Figure 3**), each carrying a single nucleotide G-A or C-T mutation in *At1g27520*, which changes Gly⁴²⁴ to Arg in *irb1-2* and *irb1-6* (identified in two independent screens), Ala⁴⁴⁷ to Val in *irb1-3*, Trp¹¹⁷ to the amber stop codon TAG in *irb1-4*, and Ala³⁴⁷ to Val in *irb1-5* (**Figure 3C**; **Supplementary Figure 4**). Further support for *At1g27520* being the *IRB1* gene came from a transgenic rescue experiment. As shown in **Figures 3C,D**, introduction of a 5.3-kb *gAt1g27520* genomic transgene into *irb1-1 bri1-5* not only suppressed its growth phenotype but also reduced its bri1-5 protein abundance.

IRB1 Is a Homolog of the Yeast Htm1/ Mammalian EDEMs and Is Highly Conserved in Land Plants

The *IRB1/At1g27520* gene (renamed hereinafter as *AtEDEMI* due to its conserved protein sequence and biochemical function with the mammalian EDEMs) consists of 15 exons and 14 introns (**Figure 3B**) and encodes a polypeptide of 574 amino acids with a weak signal peptide of 28 amino acids (AAs), which was annotated as one of the two *Arabidopsis* homologs of Htm1/EDEMs recently shown to be functionally redundant in the *Arabidopsis* ERAD process that degrades both bri1-5 and bri1-9 (Hirao et al., 2006; Quan et al., 2008; Clerc et al., 2009;



Hosokawa et al., 2010; Huttner et al., 2014b). IRB1/AtEDEMI displays 35/54% and 42–47/58–64%, sequence identity and similarity with the yeast Htm1 and three human EDEMs, respectively, within the conserved 430-AA domain of the glycosylhydrolase family 47 (**Supplementary Figure 4**). The second Arabidopsis Htm1/EDEM homolog, At5g43710 [624 AAs with a longer C-terminal domain, previously known as MNS4 (Huttner et al., 2014b) but was renamed hereinafter as AtEDEMI2], exhibits 38/53% and 43–48/61–66% sequence identity and similarity with Htm1 and three human EDEMs, respectively, within its conserved 430-AA domain (**Supplementary Figure 4**). It should be interesting to note that the sequence identity/similarity between AtEDEMI and AtEDEMI2 are only 47%/61%, which is very similar to the 47/64% and 45/63% sequence identity/similarity between AtEDEMI and human EDEM1 and between AtEDEMI2 and human EDEM2, respectively (**Supplementary Figure 4**). However, both AtEDEMI and AtEDEMI2 are quite conserved among land plants. AtEDEMI and AtEDEMI2 exhibit 74–98/86–99% and 78–99/87–99% sequence identity/similarity with AtEDEMI and AtEDEMI2 homologs from land plants (**Supplementary Figure 5**), respectively, including the liverwort *Marchantia Polymorpha* (Bowman et al., 2017), the moss *P. patens* (Rensing et al., 2008), and the spikemoss *Selaginella moellendorffii* (Banks et al., 2011). It is also interesting to note that almost all sequenced land plants contain two EDEM homologs except *Physcomitrella*, which lacks an AtEDEMI homolog (**Supplementary Figure 5**) likely due to a gene loss event during its long evolution history.

A direct support for the functional conservation between AtEDEMI and Htm1/EDEMs came from two reciprocal complementation experiments. A yeast complementation assay showed that the wild-type AtEDEMI could partially substitute for the yeast Htm1 to stimulate degradation of a yeast model ERAD substrate, an ER-retained mutant variant of the vacuolar carboxypeptidase Y (CPY*) (Ng et al., 2000; **Supplementary Figure 6A**). Consistently, the *BRI1* promoter-driven expression of the yeast *Htm1* gene could partially suppress the morphological and biochemical phenotype of the *irb1-3 bri1-5* mutant (**Supplementary Figure 6B**).

The Two Arabidopsis EDEM Homologs Are Localized in the ER

To investigate if the two Arabidopsis EDEM homologs localize in the ER, we generated C-terminal AtEDEMI/AtEDEMI2-GFP fusion transgenes driven by the *BRI1* promoter and transiently expressed the resulting *pBRI1::AtEDEMI/AtEDEMI2-GFP* transgene in tobacco (*Nicotiana benthamiana*) leaf epidermal cells along with a known transgene encoding a widely-used ER marker red fluorescent protein tagged with a widely-used ER marker RFP-HDEL (HDEL) ER retrieval motif at its C-terminus [RFP-HDEL; Chakrabarty et al., 2007]. Confocal microscopic examination of the fluorescent patterns of agro-infiltrated tobacco leaves revealed that the green fluorescent patterns of the two AtEDEMI-GFPs overlapped nicely with that of RFP-HDEL (**Supplementary Figure 7A**), indicating that both AtEDEMI and AtEDEMI2 are localized in the ER.

Consistent with our microscopic results, Endo H-analysis of the two transiently-expressed GFP-fusion proteins showed that both AtEDEMs were Endo-H sensitive (**Supplementary Figure 7B**) and were thus glycosylated with HM-type N-glycans indicative of ER-localization. By contrast, the GFP-tagged Atlg30000 (a predicted ER α 1,2-mannosidase I homolog, also known as MNS3; Liebminger et al., 2009) and GFP-tagged Atlg51590 (one of the two Golgi-type α 1,2-mannosidases, also known as MNS1; Liebminger et al., 2009) were found to be Endo-H resistant despite being predicted to carry 5 and 3 N-glycosylation sites, respectively (**Supplementary Figure 7B**). Our results on the cellular localization of Atlg30000/MNS3, Atlg51590/MNS1, and the two AtEDEMs are consistent with three published studies on the five Arabidopsis α 1,2-mannosidases (Liebminger et al., 2009; Huttner et al., 2014b; Schoberer et al., 2019).

The α 1,2-Mannosidase Activity Is Required for the Biological Function of AtEDEMI

Our previous study demonstrated that ERAD of both *bri1-5* and *bri1-9* requires the conserved α 1,6-Man-exposed N-glycan signal (Hong et al., 2012), which was known to be generated in yeast and mammals by the α 1,2-mannosidase activity of Htm1/EDEMs (**Figure 4A**; Quan et al., 2008; Clerc et al., 2009; Hosokawa et al., 2010). Interestingly, an earlier study suggested that the mannosidase activity of EDEM1 might not be important to promote ERAD in cultured mammalian cells as several catalytically-dead EDEM1 proteins could enhance degradation of known ERAD substrates (Cormier et al., 2009; Ninagawa et al., 2014). To investigate if AtEDEMI absolutely requires its predicted α 1,2-mannosidase activity for its role in ERAD or has an α 1,2-mannosidase-independent function in promoting *bri1-5* degradation, we performed a PCR-based site-directed mutagenesis experiment with the *irb1-1*-complementing *gAtEDEMI* genomic construct to mutate Glu¹³⁴ (corresponding to the human EDEM1's Glu²²⁰ known to be essential for its α 1,2 mannosidase activity; Hosokawa et al., 2010) to glutamine (Q), and transformed the resulting mutant transgene into the *irb1-1 bri1-5* double mutant. As shown in **Figure 4B**, the E¹³⁵-Q-mutated *gmAtEDEMI* (m indicating mutant) transgene failed to complement the *irb1-1* mutation in the *bri1-5* background, indicating that the function of AtEDEMI in promoting *bri1-5* ERAD absolutely requires its predicted α 1,2-mannosidase activity.

The *alg3* Mutation Could Nullify the Suppressive Effect of the *irb1* Mutation on *bri1-5* Dwarfism

Earlier studies indicated that the other α 1,6-Man residue on N-linked glycans of misfolded proteins (**Figure 4C**), when being exposed, could also function as an ERAD N-glycan signal that can be recognized and bound by the ERAD receptor Yos9/OS-9/EBS6 (Quan et al., 2008; Clerc et al., 2009; Hong et al., 2012). We reasoned that if the effect of the *irb1* mutations on ERAD of *bri1-5* was indeed caused by a failure or a reduced rate of generation of the conserved ERAD N-glycan signal carrying a free α 1,6-Man residue, the suppressive effects of the *irb1-1* mutation on the *bri1-5* dwarfism and *bri1-5* ERAD would

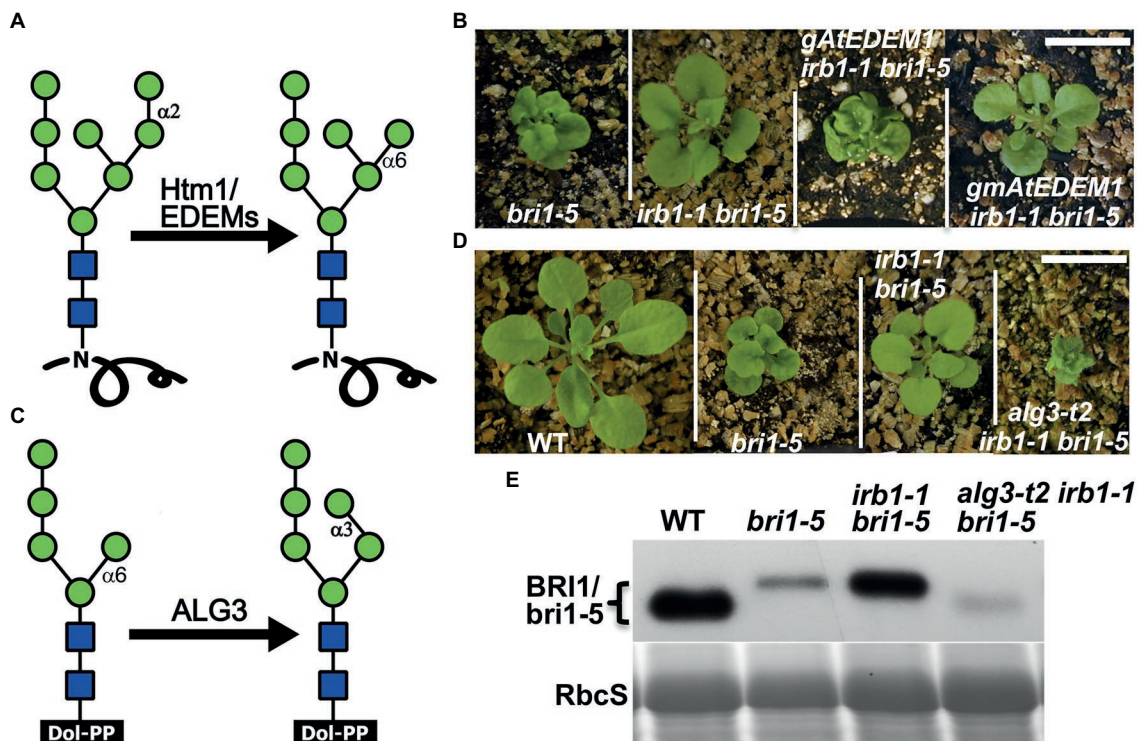


FIGURE 4 | AtEDEMI promotes *bri1-5* ERAD likely through its predicted α 1,2-mannosidase activity. **(A)** Schematic presentation of the α 1,2-mannosidase activity of Htm1/EDEMs. **(B)** Photographs of 4-week-old soil-grown plants of *bri1-5*, *irb1-1 bri1-5*, *gAtEDEMI irb1-1 bri1-5*, and *gmAtEDEMI irb1-1 bri1-5* transgenic lines. **(C)** A schematic presentation of the mannosyltransferase activity of Asparagine-Linked Glycosylation 3 (ALG3). **(D)** Photographs of 4-week-old soil-grown plants of WT, *bri1-5*, *irb1-1 bri1-5*, and *alg3-t2 irb1-1 bri1-5* mutants. In **(B,D)**, scale bar = 1 cm. **(E)** Immunoblotting analysis of the *bri1-5* abundance. Equal amounts of total proteins extracted in 2X SDS buffer from 4-week-old leaves were separated by 8% SDS-PAGE and analyzed by immunoblot with anti-BRI1 antibody. Coomassie blue staining of RbcS on a duplicated gel serves loading control.

be eliminated by a loss-of-function mutation of Asparagine-Linked Glycosylation 3 (ALG3), a highly-specific mannosyltransferase that adds an α 1,3-Man residue to the other α 1,6-Man residue (Henquet et al., 2008; Kajiura et al., 2010). Loss-of-function *alg3* mutations result in N-glycosylation of glycoproteins with a truncated $\text{Man}_5\text{GlcNAc}_2$ glycan carrying a different free α 1,6-Man residue (Figure 4C). Indeed, when crossed into the *irb1-1 bri1-5* double mutant, a T-DNA insertional *alg3* mutation, *alg3-t2* that was previously reported (Hong et al., 2012), nullified the suppressive effect of the *irb1-1* mutation on *bri1-5*. As shown in Figure 4D, the *alg3-t2 irb1-1 bri1-5* triple mutant is a much severe dwarf mutant than the *bri1-5* mutant. Consistent with the enhanced dwarfism phenotype, immunoblot assay showed that the *alg3-t2* mutation not only increased the mobility of the *bri1-5* band (due to smaller N-glycans) but also reduced the *bri1-5* protein level below that of the *bri1-5* single mutant (Figure 4E). We thus concluded that the inhibition of *bri1-5* degradation in the *irb1-1 bri1-5* double mutant is caused by inhibition of generating the α 1,6-Man-exposed N-glycans on the mutant BR receptor.

AtEDEMI and AtEDEMI2 Play a Redundant Role in ERAD of *bri1-5*

Our finding that the *irb1-1* mutant is a weak ERAD mutant of *bri1-5* coupled with the fact that the Arabidopsis genome

encodes two potential EDEM homologs (Huttner et al., 2014b) prompted us to test the possibility that AtEDEMI functions redundantly with AtEDEMI2 in degrading *bri1-5*. To test our hypothesis, we first transformed a genomic *gAtEDEMI2* transgene into the *irb1-1 bri1-5* mutant and found that while this transgene was able to rescue the *irb1-1* mutation, the percentage of rescued *irb1-1 bri1-5* plants among the resulting *gAtEDEMI2 irb1-1 bri1-5* transgenic lines (a total of 70 lines) was relatively low (~20%; Supplementary Figure 8A) compared to 90% of rescued *gAtEDEMI2 irb1-1 bri1-5* lines (out of 58 lines). This difference in the *irb1-1*-rescuing activity could be caused by the weaker promoter or weaker catalytic activity of AtEDEMI2. To differentiate these two possibilities, we created two additional transgenic constructs *pBRI1::cAtEDEMI* and *pBRI1::cAtEDEMI2* (c stands for cDNA) using the *BRI1* promoter (*pBRI1*) to drive the expression of AtEDEMI or AtEDEMI2, transformed each transgene into the *irb1-1 bri1-5* double mutant, and analyzed the resulting transgenic plants. The transgenic expression of each cDNA construct not only complemented the *irb1-1* mutation but also led to severe dwarfism compared to the parental *bri1-5* mutant, although the percentage of severely dwarfed transgenic lines is higher with the *pBRI1::cAtEDEMI* transgene than with the *pBRI1::cAtEDEMI2* transgene (Supplementary Figure 8B). Together, these results suggested that the weaker physiological

activity of AtEDEEM2 in *bri1-5* ERAD is likely contributed by its weaker promoter and its weaker biochemical activity.

The functional redundancy between AtEDEEM1 and AtEDEEM2 was further supported by our genetic study. We obtained a T-DNA insertional mutant for AtEDEEM2 (SALK_095857, named hereinafter as *edem2-t*) and crossed the mutation into *bri1-5*. RT-PCR analysis showed that the T-DNA insertion resulted in no detectable level of the *AtEDEEM2* transcript (Supplementary Figure 9) while phenotypic examination indicated that the *edem2-t* mutation was not able to suppress the dwarf phenotype of dark or light-grown *bri1-5* mutant or to inhibit the *bri1-5* ERAD (Figures 5A–C), explaining why several independent genetic screens for *bri1-5* suppressors failed to uncover a single *edem2* mutation. However, when the *edem2-t* mutation was crossed into the *irb1-1 bri1-5* double mutant, it enhanced the suppressive effect of the *irb1-1* mutation on *bri1-5*. As shown in Figures 5A,B, the triple *irb1-1 edem2-t bri1-5* mutant has a longer hypocotyl in the dark and is noticeably larger in the light than the *irb1-1 bri1-5* double mutant. Consistent with the morphological phenotypes, the abundance of *bri1-5* in *irb1-1 edem2-t bri1-5* is significantly higher than that of the *irb1-1 bri1-5* double mutant (Figure 5C). A CHX-chase experiment indicated that the increased abundance of *bri1-5* in the *irb1-1 edem2-t bri1-5* triple mutant was caused by near complete inhibition of *bri1-5* degradation rather than by increased protein synthesis (Figures 5D,E). More importantly, the amount of the Endo H-resistant form of *bri1-5*, which was thought to be localized on the PM (Hong et al., 2008), is also higher in the triple mutant than the *irb1-1 bri1-5* mutant (Figure 5C). Taken together, these results demonstrated that AtEDEEM1 and AtEDEEM2 function redundantly in the ERAD process that degrades *bri1-5*, which is consistent with an earlier study on the physiological functions

of AtEDEEM1 and AtEDEEM2 (Huttner et al., 2014b). More importantly, our study revealed that AtEDEEM1 exhibits a stronger physiological activity in promoting *bri1-5* degradation due to its stronger promoter and a stronger biochemical activity.

Simultaneous Elimination of AtEDEEM1 and AtEDEEM2 Results in Inhibition of the C-Branch Terminal α 1,2-Man-Residue Trimming

To directly examine the impact of simultaneous elimination of the two EDEM homologs on the α 1,2-Man residue-trimming activity on misfolded glycoproteins, we intended to analyze the N-glycans on *bri1-5* in Arabidopsis mutants. Due to the failure of the anti-BRI1 antibody to immunoprecipitate the endogenous BRI1/*bri1-5* protein, we generated a *pBRI1::bri1-5ED-GFP-HDEL* transgene, consisting of the 1.5-kb *BRI1* promoter, the coding sequences of the entire extracellular domain (ED) of *bri1-5* and green fluorescent protein tagged with the HDEL ER-retrieval motif (Supplementary Figure 10A), transformed it into the wild-type, an *irb1-1 edem2-t* double mutant, and an *eds5-1* mutant. The last mutant is defective in a key client-recruitment factor that recognizes and brings an ERAD substrate to the ER membrane anchored E3 ligase (Su et al., 2011) and was used to stabilize the *bri1-5ED-GFP-HDEL* fusion protein for easy detection of exposed α 1,6-Man residue. An Endo H-immunoblot assay with the total proteins of the resulting *pBRI1::bri1-5ED-GFP-HDEL* (in the wild-type background) transgenic lines showed that the engineered *bri1-5ED-GFP-HDEL* was indeed retained in the ER (Supplementary Figure 10B). As expected, a Kif treatment experiment revealed that *bri1-5ED-GFP-HDEL* was degraded *via* a glycan-dependent

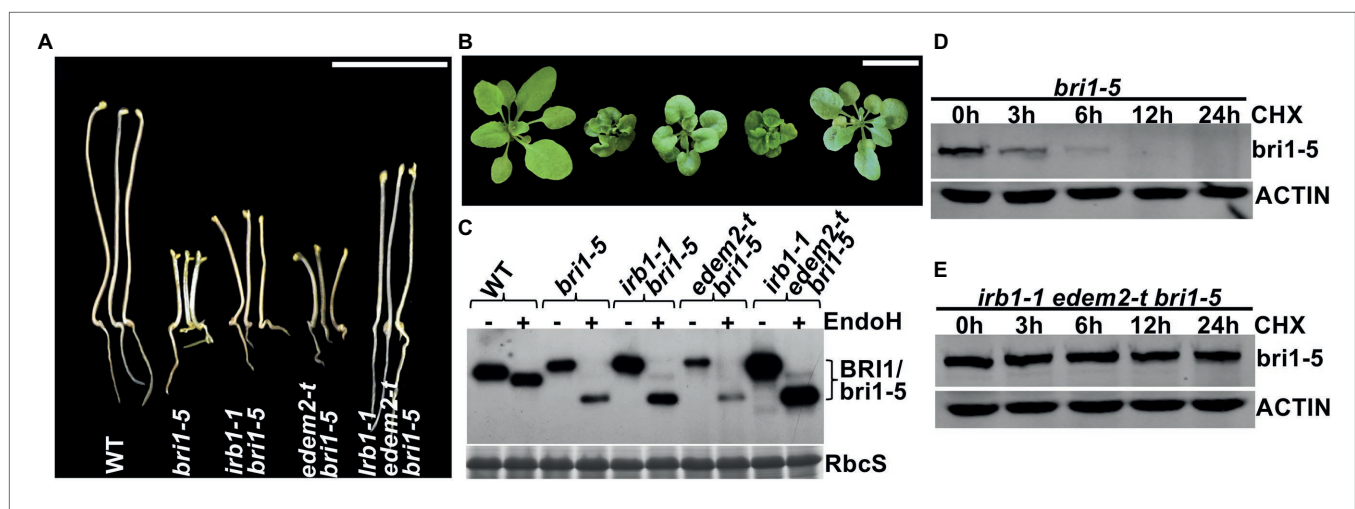


FIGURE 5 | AtEDEEM1 and AtEDEEM2 function redundantly in promoting *bri1-5* ERAD. **(A)** Pictures of 5-day-old dark-grown seedlings of WT, *bri1-5*, *irb1-1 bri1-5*, *edem2-t bri1-5*, and *irb1-1 edem2-t bri1-5*. **(B)** Photographs of 6-week-old soil-grown seedlings. In **(A,B)**, scale bar = 1 cm. **(C)** Immunoblot analysis of the *bri1-5* abundance. Equal amounts of total proteins extracted from 2-week-old light-grown seedlings were treated with or without Endo H, separated by 8% SDS-PAGE, and analyzed by immunoblotting using an anti-BRI1 antibody. The lower strip is Coomassie blue-stained RbcS bands of a duplicated gel as a loading control. **(D-E)** Immunoblotting analysis of the *bri1-5* stability in *bri1-5* and *irb1-1 edem2-t bri1-5* mutant seedlings. Two-week-old seedlings were carefully transferred into liquid $\frac{1}{2}$ MS medium containing 180 μ M CHX for continued growth. Equal amounts of seedlings were taken out at different time points and were immediately used to extract total proteins with 2 X SDS sample buffer. The proteins were subsequently separated by 8% SDS-PAGE and analyzed by western blot with anti-BRI1 antibody. The same filters were also probed with anti-ACTIN antibody to control for equal sample loading.

manner (**Supplementary Figure 10C**), indicating that bri1-5ED-GFP-HDEL could be used as a reporter to analyze the impact of the double mutation of AtEDEMI and AtEDEMI2 on the α 1,2-Man-trimming reactions of an ERAD client in Arabidopsis.

A representative transgenic line in each mutant background was used to immunoprecipitate bri1-5ED-GFP-HDEL, which was subsequently analyzed by high-resolution liquid chromatography tandem mass spectrometry (LC-MS/MS) to determine the N-glycan structures of the ER retained fusion protein. As shown in **Figures 6A,B**, two major N-glycans, Hex₇GlcNAc₂ (i.e., Man₇; Hex refers hexose) and Hex₈GlcNAc₂ (i.e., GlcMan₇; Glc refers glucose) were detected at the glycosylation site at residue Asn¹¹² position of the chymotrypsin-digested bri1-5ED-GFP-HDEL peptide LNSHIN¹¹²GSVSGF in the *eb5* mutant. In contrast, a different N-glycan profile was observed in the mass spectrum of the protein digest in the *irb1-1 edem2-t* double mutant, in which the two glycopeptide ions were identified to contain N-glycans of Hex₈GlcNAc₂ (i.e., Man₈) and Hex₉GlcNAc₂ (i.e., GluMan₈). Similar N-glycan distributions were also observed at other glycosylation sites, for example, the two distinct N-glycans were presented at residue Asn⁶³⁶ of peptide NPCN⁶³⁶TISR of the trypsin digest of the immunoprecipitated bri1-5ED-GFP-HDEL (**Supplementary Figure 11**). The observation of the difference of one Man residue in the N-glycan structures at residues Asn¹¹² and Asn⁶³⁶ of bri1-5ED-GFP-HDEL between *eb5* and the *irb1-1 edem2-t* double mutant is consistent with the functional conservation between AtEDEMI and Htm1, strongly suggesting that the *irb1-1 edem2-t* double mutations likely inhibit the Man-trimming activity essential for ERAD of bri1-5.

To validate the exact position of the AtEDEMI/AtEDEMI2-trimmed α 1,2-Man residue in the N-glycan structures, the immunoprecipitated bri1-5ED-GFP-HDEL fusion protein was treated with PNGase F, an amidase that cleaves the covalent bond between the innermost GlcNAc residue and the glycosylated Asn residue (Tarentino et al., 1985). The released N-glycans were fluorescently labeled with 2AB and subsequently separated by HILIC. Individual N-glycan fractions were collected, digested with specific α 1,3-, α 1,6-, or α 1,2/3/6-exomannosidases, and analyzed by UPLC. **Figure 6C**; **Supplementary Figure 12** show that Hex₇GlcNAc₂ and Hex₈GlcNAc₂ glycans accumulated in *eb5* were sensitive to both α 1,3- and α 1,6-mannosidases, indicating that Hex₇GlcNAc₂ is Man₇GlcNAc₂ with free α 1,3-Man and α 1,6-Man residues (**Figure 6A**). The same cleavage response of Hex₈GlcNAc₂ to both α -mannosidases (**Supplementary Figure 12**) indicated that this is a monoglucosylated GlcMan₇GlcNAc₂ glycan, which is consistent with our earlier conclusion that bri1-5 is retained in the ER by several independent retention mechanisms that include the UGGT-CRT/CNX system (Hong et al., 2008). Our α -mannosidase analysis of the PNGase F-cleaved N-glycans of the immunoprecipitated bri1-5ED-GFP-HDEL of the *irb1-1 edem2-t bri1-5* triple mutant showed that the Hex₈GlcNAc₂ glycan was sensitive only to the α 1,3-exomannosidase but could not be cleaved by the α 1,6-exomannosidase (**Figure 6C**),

indicating the presence of a terminal α 1,2-Man residue that protects the α 1,6-Man residue from its cleavage by the α 1,6-exomannosidase. Taken together, these biochemical analyses confirmed that the *irb1 edem2-t* double mutation blocks the removal of the C-branch α 1,2-Man residue.

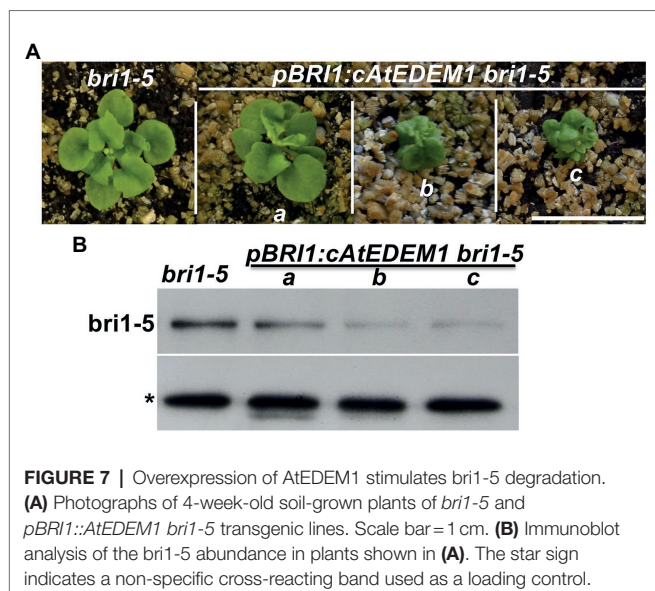
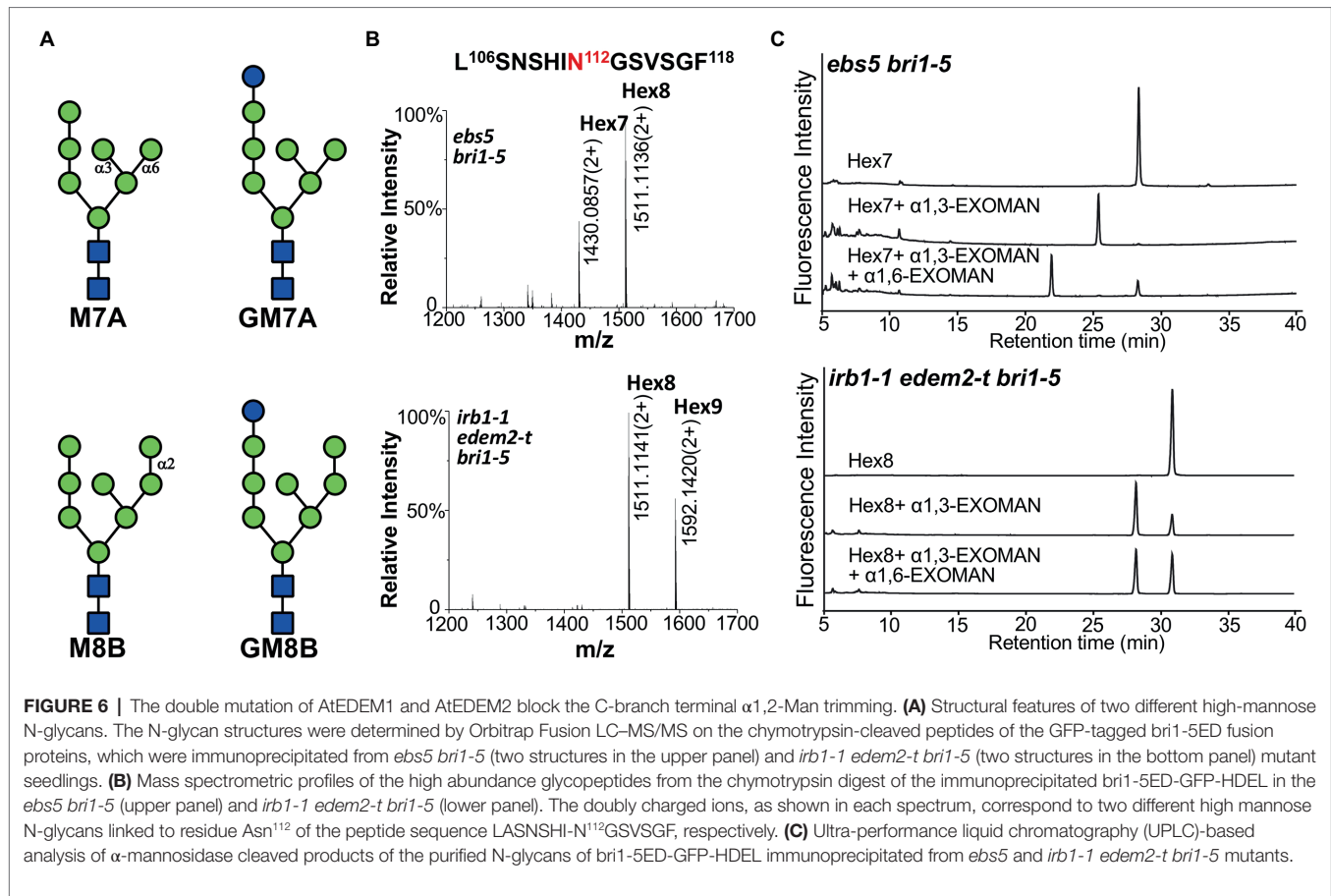
The Arabidopsis EDEMs Catalyze a Rate-Limiting Step of a Plant ERAD Pathway

While performing the transgenic rescue experiments, we noticed that some of the *gAtEDEMI* transgenic lines exhibited stronger dwarfism than the parental *bri1-5* strain (**Figure 3C**). Similar stronger dwarf phenotypes were not observed in our previous experiments that overexpressed *EBS5* or *EBS6* in the *bri1-5* mutant, whose protein products work together to bring a committed ERAD client to the membrane-anchored Hrd1 E3 ligase complex (Su et al., 2011, 2012), suggesting that recognition and recruitment of a marked bri1-5 to the ERAD machinery is not the rate-limiting step. By contrast, similar severe dwarfism phenotypes were observed in the *alg3 eb5 bri1-9* or *alg3 irb1-1 bri1-5* triple mutant containing mutant BR receptors glycosylated with α 1,6-Man-exposing N-glycans that mark a misfolded protein for ERAD (Hong et al., 2012; **Figure 4D**), indicating that generating the ERAD N-glycan signal is a major rate-limiting step of the Arabidopsis ERAD pathway. Consistent with the severe dwarfism phenotype, an immunoblot analysis showed that the abundance of bri1-5 in those severely-dwarfed *gAtEDEMI irb1-1 bri1-5* transgenic lines or *alg3 irb1-1 bri1-5* triple mutant was much lower than that of the parental *bri1-5* mutant (**Figures 3D, 4D**). Severely dwarfed transgenic *irb1-1 bri1-5* mutants were also observed when the *BRI1* promoter was used to drive overexpression of the cDNA transgene of *AtEDEMI* or *AtEDEMI2* in the *irb1-1 bri1-5* mutant (**Supplementary Figures 6B,C**). When transformed into the single *bri1-5* mutant, the *pBRI1::AtEDEMI* transgene also caused severe dwarfism in the resulting *pBRI1::AtEDEMI bri1-5* transgenic lines and immunoblot analysis showed that the severely-dwarfed transgenic lines accumulated less bri1-5 than the parental *bri1-5* mutant (**Figures 7A,B**). Taken together, our data strongly suggested that the AtEDEMI/AtEDEMI2-mediated cleavage of the C-branch terminal α 1,2-Man residue is a major rate-limiting step in the Arabidopsis ERAD pathway that degrades ER-retained mutant bri1-5 receptor.

DISCUSSION

A Predominant Role of AtEDEMI in the ERAD Pathway That Degrades bri1-5

While an earlier study using the reverse genetic approach showed that neither *edem1/mns5* nor *edem2/mns4* but an *mns4 mns5* double mutation had any visible impact on the dwarf phenotypes of *bri1-5* and *bri1-9* and concluded that the two Arabidopsis Htm1/EDEM homologs function redundantly in promoting degradation of bri1-5 and bri1-9



(Huttner et al., 2014b), our forward genetic study revealed that six EMS-introduced single nucleotide changes in AtEDEMI partially suppress the *bri1-5* dwarfism by weakly inhibiting bri1-5 degradation. Interestingly, the null *irb1-1* mutation (due to defective splicing-caused early translational

termination) failed to suppress the *bri1-9* mutation, which is likely attributed to its weak inhibition of the ERAD pathway that degrades bri1-5 and bri1-9 and a potentially weaker receptor function of the PM-localized bri1-9 compared to bri1-5. Consistent with the earlier study (Huttner et al., 2014b), a loss-of-function *edem2-t* mutation had no effect on bri1-5 degradation and no single EMS-introduced *edem2* mutation has so far been uncovered in several forward genetic screens for extragenic suppressors of *bri1-5* and *bri1-9* mutants, which discovered multiple alleles of *EBS1-EBS7* genes, revealing potential difference between the two Arabidopsis EDEM homologs in stimulating ERAD of bri1-5 and bri1-9. Consistently, while a genomic *gAtEDEMI* transgene could achieve >90% phenotypic complementation out of 83 *gAtEDEMI irb1-1 bri1-5* transgenic mutants, a similar genomic *gAtEDEMI2* transgene only led to ~20% of the *gAtEDEMI2 irb1-1 bri1-5* transgenic lines being phenotypically similar to or severer than *bri1-5*. Importantly, when driven by the same *pBRI1* promoter, AtEDEMI produced higher percentage of severely dwarfed transgenic mutant than AtEDEMI2 in the *irb1-1 bri1-5* mutant. As expected, a T-DNA insertional mutation in AtEDEMI2 (*edem2-t*) mutation significantly enhances the suppressive effect of *irb1-1* on the *bri1-5* dwarfism as simultaneous elimination of the two AtEDEMs completely blocks the ERAD of bri1-5, leading to markedly increased

amount of ER-escaping *bri1-5* carrying the C-type N-glycans. Thus, our study demonstrated that despite functional redundancy of AtEDEM1/MNS5 and AtEDEM2/MNS4, the former α 1,2-mannosidase plays a predominant role in an ERAD process that degrades *bri1-5*. Our conclusion is supported by a recent study revealing a non-redundant role of AtEDEM1/MNS5 in the Arabidopsis ERAD pathway (Sun et al., 2022).

Our study provided further genetic and biochemical support for the key role of the two AtEDEM2s in generating the conserved N-glycan signal to mark ERAD substrates. First, both AtEDEM2s exhibit significant sequence identity/similarity with Htm1/EDEM2s, and AtEDEM1 and Htm1 complemented each other's loss-of-function mutation (**Supplementary Figure 6**). Second, a catalytically-dead mutant of AtEDEM1 failed to rescue the *irb1-1* mutation while the wild-type copy of the transgene fully complemented the *irb1-1* mutation, implying that the predicted α 1,2-mannosidase activity is essential for its physiological function in degrading the mutant *bri1-5* receptor. Third, a T-DNA insertional *alg3-t* mutation, which causes N-glycosylation with truncated Man₅GlcNAc₂ glycans carrying a different free α 1,6-Man residue, could nullify the suppressive effect of the *irb1-1* mutation on the *bri1-5* dwarfism and its inhibitory effect on the ERAD of *bri1-5*, implying that the *irb1-1* mutant was compromised in the activity to generate α 1,6-Man-exposed N-glycans on misfolded glycoproteins. Finally, N-glycan analysis of GFP-tagged *bri1-5ED* proteins purified from *bri1-5* and *irb1-1 edem2 bri1-5* mutant provided a direct *in vivo* evidence for the two AtEDEM2s being the ER-localized C-branch-specific α 1,2-mannosidases. However, it remains a possibility that AtEDEM2s might function as the necessary cofactors for the suspected C-branch α 1,2-mannosidases. Therefore, *in vitro* enzyme assays using heterologously-expressed AtEDEM2s will be needed to definitively prove that AtEDEM1 and AtEDEM2 are indeed active α 1,2-mannosidases that catalyze the C-branch α 1,2-Man trimming reaction of the ER-retained misfolded glycoproteins.

In addition, our investigation revealed that the generation of the conserved N-glycan signal constitute a rate-limiting step in the Arabidopsis ERAD process that degrades *bri1-5*. Our earlier studies showed that overexpression of EBS5 or EBS6, which work together to recruit a committed ERAD client to the ER membrane-anchored Hrd1 E3 ligase, failed to enhance the dwarfism of *bri1-5* and/or *bri1-9* and to stimulate degradation of the corresponding mutant BR receptors (Su et al., 2011, 2012). In this study, we showed that overexpression of AtEDEM1 or AtEDEM2 could enhance the *bri1-5* dwarf phenotype and stimulate *bri1-5* degradation, which is consistent with the morphological and biochemical phenotypes of *alg3 irb1-1 bri1-5* or *alg3 ebs3 bri1-5/bri1-9* mutants that have their ER-localized glycoproteins to be decorated with N-glycans carrying another exposed α 1,6-Man residue (Hong et al., 2012). Our revelation is also consistent with studies in yeast and mammalian systems, which suggested that the α 1,2-Man-trimming reaction (that drives a misfolded glycoprotein into the ERAD pathway) is a slow process to favor refolding over removal.

The Two Arabidopsis EDEM2s Evolved Independently in the Green Lineage and May Participate in Different Physiological Processes

Although the two AtEDEM2s exhibit relatively low sequence homology (50% identity/64% similarity) with each other, each AtEDEM2 displays 71–99% identity/81–99% similarity with their respective orthologs from other land plant species, suggesting a very ancient gene duplication event that generated the two EDEM2 paralogs in the green lineage. It is interesting to note that at least three detected *irb1* mutations, *irb1-2/irb1-6* changing Gly⁴²⁴ to Arg and *irb1-5* mutating Ala³⁴⁷ to Val, alter amino acids that are only conserved in EDEM1 as Gly⁴²⁴ is replaced by Cys and Ala³⁴⁷ is replaced by Pro in EDEM2s (**Supplementary Figure 4**). BLAST searches against existing databases indicated that the genome of the earliest land plant *M. polymorpha* (Bowman et al., 2017) encodes homologs of both AtEDEM2s whereas the *Physcomitrella* genome only encodes an AtEDEM2 homolog (Rensing et al., 2008). Similarly, the sequenced genomes of two charophyte green algae whose ancestor was thought to give rise to land plants showed that while *Klebsormidium flaccidum* has homologs of both AtEDEM2s (Hori et al., 2014), *Chara braunii*, which is more closely-related to land plants, has only an AtEDEM2 homolog (Nishiyama et al., 2018; **Supplementary Figure 5**). We suspect that the *AtEDEM1* homologous gene might be lost in the genomes of the moss and the *Charophyceae* alga during their 400–500 million year-evolution history. It is interesting to note that a dozen of recently-sequenced *Chlorophyte* algae genomes encode no, one, or two homologs of the AtEDEM2s (**Supplementary Figure 5**). For example, *M. pusilla* RCC299, *M. pusilla* CCMP1545, and *Bathycoccus parasinos* (all in the Prasinophytes family) contain a potential AtEDEM1 homolog while the genomes of *Ostreococcus lucimarinus* CCE9901, *Ostreococcus tauri*, and *Chlorella variabilis* encode a potential AtEDEM2 homolog. Interestingly, the three fully-sequenced *Chlorophyte* green algae, *Chlamydomonas reinhardtii*, *Dunaliella salina* CCAP19/18 and *Volvox carterii*, lack any AtEDEM2 homolog, but *Coccomyxa subellipsoidea* C-169 (known previously as *Chlorella vulgaris* and a close relative of *Chlorella variabilis* NC64A), which belongs to the class *Trebouxiophyceae*, contains homologs of both AtEDEM2s (**Supplementary Figure 5**). These analyses strongly suggest that the gene duplication event that created the two EDEM2s in the green lineage occurred before the splitting of Streptophytes (consisting of the land plants and their closely-related green algae such as *K. flaccidum* and *C. braunii*) and Chlorophytes (containing most of the remaining green algae). Further phylogenetic studies are needed to know if the EDEM1/2 gene duplication predated the animal-plant split.

Both plant EDEM2s are highly conserved throughout the long evolution of the green lineage, implying that each EDEM2 plays distinct evolutionarily-conserved physiological functions despite shared biochemical activity. As discussed above, our transgenic experiments with *gAtEDEM1/2* genomic and *pBRI1::AtEDEM1/2* cDNA transgenes revealed that the two Arabidopsis EDEM2s exhibited a clear difference in rescuing

the null *irb1-1* mutation, which is likely due to different promoter activities and potential difference in biochemical activities of the two AtEDEMs. Gene expression analysis of the two AtEDEMs using the Arabidopsis eFP browser 2.0 (http://bar.utoronto.ca/efp2/Arabidopsis/Arabidopsis_eFPBrowser2.html; Winter et al., 2007) not only revealed a largely-overlapping expression pattern but also detected tissues where *IRB1/AtEDEM1* or *AtEDEM2* is expressed higher than the other (**Supplementary Figure 13**), suggesting their involvement in different developmental and physiological processes. Analysis of gene co-expression profiles using ATTED-II (Obayashi et al., 2009) seems to support our hypothesis. As shown in **Supplementary Figure 14**, it is *AtEDEM2* but not *AtEDEM1* that is co-expressed with known and/or predicted ER chaperones/folding catalysts. A similar finding was previously reported for three Arabidopsis CRTs (Jin et al., 2009). While the two highly conserved Arabidopsis CRTs, CRT1, and CRT2, were known to be co-expressed with ER chaperones/folding enzymes, the plant-specific CRT3, which was responsible for retaining *bril-9* in the ER, was shown to be coexpressed with genes implicated in plant stress tolerance (Jin et al., 2009). Detailed phenotypic analysis with the *irb1*, *edem2-t*, and *irb1 edem2-t* mutants or transgenic lines that overexpress *AtEDEM1* or *AtEDEM2* could be used to investigate if the two AtEDEMs have overlapping yet distinctive biological functions during plant growth and development or plant stress tolerance.

Is EDEM a Folding Sensor of the ERAD Pathway?

One of the remaining mysteries of the ERAD process is how the system determines if a nonnative glycoprotein is a folding intermediate, a repairable or irreparable misfolded protein and should thus be allowed to continue its folding/refolding process or be condemned into the ERAD process. It was previously suggested that the yeast MNS1, the ER-localized α 1,2-mannosidase that specifically cleaves the terminal α 1,2-Man residue from the middle branch of N-linked $\text{Man}_9\text{GlcNAc}_2$ glycan, serves as a timer, due to its slow enzymatic kinetics, to create a discrete time window for a given glycoprotein to attain its native conformation before being marked for degradation by ERAD (Su et al., 1993; Helenius et al., 1997). Although recent studies have convincingly shown that it is Htm1 and EDEMs that generate the conserved N-glycan ERAD signal, the MNS1/ERManI-mediated middle branch α 1,2-Man trimming remains a key event for ERAD because Htm1/EDEMs act only on B-branch trimmed $\text{Man}_8\text{GlcNAc}_2$ but not untrimmed $\text{Man}_9\text{GlcNAc}_2$ for removing the C-branch terminal α 1,2-Man residue (Quan et al., 2008; Clerc et al., 2009). Thus, MNS1/ERManI could still be functionally involved in differentiating a terminally-misfolded glycoprotein from repairable misfolded protein or a folding intermediate, especially when considering a recent *in vitro* assay showing that the human ERManI preferentially removes α 1,2-Man residues from unfolded/misfolded glycoproteins (Aikawa et al., 2012, 2014). However, recent

studies demonstrated that both animal and plant homologs of the yeast MNS1 are not localized in the ER but were instead found mainly in the Golgi body or the ER-Golgi intermediate compartment, making ERManI less likely to be the folding sensor of the ERAD pathway (Huttner et al., 2014b; Benyair et al., 2015; Schoberer et al., 2019). More importantly, a recent study showed that a T-DNA insertion of the Arabidopsis homolog of MNS1/ERManI fails to suppress the dwarf phenotype of *bril-9* and *bril-5*, suggesting that the generation of a conserved N-glycan ERAD in plants might not require the B-branch α 1,2-Man-trimming step (Huttner et al., 2014b). It is worthy to mention that a recent yeast study did uncover a Htm1-dependent but MNS1-independent ERAD pathway (Hosomi et al., 2010).

Given their crucial roles in generating the necessary ERAD N-glycan signal and their ER location, Htm1/EDEMs could be directly involved in differentiating terminally misfolded glycoproteins from repairable misfolded glycoproteins or folding intermediates (Shenkman et al., 2018). EDEMs were previously shown to function as molecular chaperones that can bind non-/misfolded proteins but not their native conformers (Hosokawa et al., 2006). However, this chaperone function alone will not qualify Htm1/EDEMs as the folding sensor capable of differentiating a terminally-misfolded protein from repairable misfolded proteins or folding intermediates because all these proteins have hydrophobic residue-exposing surfaces that would interact with a molecular chaperone. EDEMs might need a partner to function as an ERAD folding sensor. Indeed, several recent studies suggested that a protein disulfide isomerase (PDI) might be such a factor that works together with EDEMs to preferentially act on terminally-misfolded glycoproteins that are trapped into a non-native folding state (Gauss et al., 2011; Pfeiffer et al., 2016; Liu et al., 2016b). Similarly, three recent studies have shown that binding of ERdj5, ERp56, or TXNDC11 (thioredoxin domain containing 11), three members of the mammalian PDI family (Kozlov et al., 2010), was required to stimulate the redox-sensitive α 1,2-Man-trimming activity of EDEM1 and EDEM3 (Timms et al., 2016; Lamriben et al., 2018; Shenkman et al., 2018; Yu et al., 2018). Direct testing AtEDEMs-PDI interaction or identifying AtEDEMs-binding proteins could lead to a better understanding on how the two AtEDEMs select their substrates to initiate an Arabidopsis ERAD process.

DATA AVAILABILITY STATEMENT

The original contributions presented in the study are included in the article/**Supplementary Material**; further inquiries can be directed to the corresponding authors.

AUTHOR CONTRIBUTIONS

JL conceived the research plans. JL and LinL supervised the project, suggested experiments, and wrote the article

with supports from JM, JV, Y-MS, XP, and ZH. YX initiated, JZ continued, and DW completed the project with technical supports from YC, CZ, and MW. YD performed the exomannosidase digestion experiments with supervision from LiL and JV. Y-MS carried out the mass spectrometry assays. JZ, DW, YX, YD, JV, LinL, and JL analyzed the data and prepared figures. All authors contributed to the article and approved the submitted version.

FUNDING

This study was supported partly by grants from the National Natural Science Foundation of China (NSFC31730019 to JL and NSFC31600996 to LinL), a grant from the National Science Foundation (IOS1121496 to JL), and a grant from the Chinese Academy of Sciences (2012CSP004 to JL).

REFERENCES

- Aikawa, J., Matsuo, I., and Ito, Y. (2012). In vitro mannose trimming property of human ER α 1,2 mannosidase I. *Glycoconj. J.* 29, 35–45. doi: 10.1007/s10719-011-9362-1
- Aikawa, J., Takeda, Y., Matsuo, I., and Ito, Y. (2014). Trimming of glucosylated N-glycans by human ER α 1,2-mannosidase I. *J. Biochem.* 155, 375–384. doi: 10.1093/jb/mvu008
- Asami, T., Min, Y. K., Nagata, N., Yamagishi, K., Takatsuto, S., Fujioka, S., et al. (2000). Characterization of brassinazole, a triazole-type brassinosteroid biosynthesis inhibitor. *Plant Physiol.* 123, 93–100. doi: 10.1104/pp.123.1.93
- Baer, J., Taylor, I., and Walker, J. C. (2016). Disrupting ER-associated protein degradation suppresses the abscission defect of a weak hsl2 mutant in Arabidopsis. *J. Exp. Bot.* 67, 5473–5484. doi: 10.1093/jxb/erw313
- Banks, J. A., Nishiyama, T., Hasebe, M., Bowman, J. L., Gribskov, M., Depamphilis, C., et al. (2011). The Selaginella genome identifies genetic changes associated with the evolution of vascular plants. *Science* 332, 960–963. doi: 10.1126/science.1203810
- Benyair, R., Ogen-Shtern, N., Mazkereth, N., Shai, B., Ehrlich, M., and Lederkremer, G. Z. (2015). Mammalian ER mannosidase I resides in quality control vesicles, where it encounters its glycoprotein substrates. *Mol. Biol. Cell* 26, 172–184. doi: 10.1091/mbc.E14-06-1152
- Bowman, J. L., Kohchi, T., Yamato, K. T., Jenkins, J., Shu, S., Ishizaki, K., et al. (2017). Insights into land plant evolution garnered from the *Marchantia polymorpha* genome. *Cell* 171, 287–304.e15. doi: 10.1016/j.cell.2017.09.030
- Cerioti, A., and Roberts, L. M. (2006). “Endoplasmic reticulum-associated protein degradation in plant cells,” in *The Plant Endoplasmic Reticulum*. ed. D. G. Robinson (Berlin Heidelberg: Springer-Verlag), 75–98.
- Chakrabarty, R., Banerjee, R., Chung, S. M., Farman, M., Citovsky, V., Hogenhout, S. A., et al. (2007). PSITE vectors for stable integration or transient expression of autofluorescent protein fusions in plants: probing Nicotiana benthamiana-virus interactions. *Mol. Plant-Microbe Interact.* 20, 740–750. doi: 10.1094/MPMI-20-7-0740
- Clerc, S., Hirsch, C., Oggier, D. M., Deprez, P., Jakob, C., Sommer, T., et al. (2009). Htm1 protein generates the N-glycan signal for glycoprotein degradation in the endoplasmic reticulum. *J. Cell Biol.* 184, 159–172. doi: 10.1083/jcb.200809198
- Cormier, J. H., Tamura, T., Sunryd, J. C., and Hebert, D. N. (2009). EDEM1 recognition and delivery of misfolded proteins to the SEL1L-containing ERAD complex. *Mol. Cell* 34, 627–633. doi: 10.1016/j.molcel.2009.05.018
- Dereeper, A., Guignon, V., Blanc, G., Audic, S., Buffet, S., Chevenet, F., et al. (2008). Phylogeny.fr: robust phylogenetic analysis for the non-specialist. *Nucleic Acids Res.* 36, W465–W469. doi: 10.1093/nar/gkn180
- Edgar, R. C. (2004). MUSCLE: multiple sequence alignment with high accuracy and high throughput. *Nucleic Acids Res.* 32, 1792–1797. doi: 10.1093/nar/gkh340
- Elbein, A. D., Tropea, J. E., Mitchell, M., and Kaushal, G. P. (1990). Kifunensine, a potent inhibitor of the glycoprotein processing mannosidase I. *J. Biol. Chem.* 265, 15599–15605. doi: 10.1016/S0021-9258(18)55439-9
- Faye, L., and Chrispeels, M. J. (1985). Characterization of N-linked oligosaccharides by affinity blotting with concanavalin A-peroxidase and treatment of the blots with glycosidases. *Anal. Biochem.* 149, 218–224. doi: 10.1016/0003-2697(85)90498-1
- Frank, C. G., and Aebi, M. (2005). ALG9 mannosyltransferase is involved in two different steps of lipid-linked oligosaccharide biosynthesis. *Glycobiology* 15, 1156–1163. doi: 10.1093/glycob/cwj002
- Friedrichsen, D. M., Joazeiro, C. A., Li, J., Hunter, T., and Chory, J. (2000). Brassinosteroid-insensitive-1 is a ubiquitously expressed leucine-rich repeat receptor serine/threonine kinase. *Plant Physiol.* 123, 1247–1256. doi: 10.1104/pp.123.4.1247
- Gauss, R., Kanehara, K., Carvalho, P., Ng, D. T., and Aebi, M. (2011). A complex of Pdi1p and the mannosidase Htm1p initiates clearance of unfolded glycoproteins from the endoplasmic reticulum. *Mol. Cell* 42, 782–793. doi: 10.1016/j.molcel.2011.04.027
- Gietz, R. D., and Woods, R. A. (2002). Transformation of yeast by lithium acetate/single-stranded carrier DNA/polyethylene glycol method. *Methods Enzymol.* 350, 87–96. doi: 10.1016/S0076-6879(02)50957-5
- Guindon, S., Dufayard, J. F., Lefort, V., Anisimova, M., Hordijk, W., and Gascuel, O. (2010). New algorithms and methods to estimate maximum-likelihood phylogenies: assessing the performance of PhyML 3.0. *Syst. Biol.* 59, 307–321. doi: 10.1093/sysbio/syq010
- Hajdukiewicz, P., Svab, Z., and Maliga, P. (1994). The small, versatile pPZP family of Agrobacterium binary vectors for plant transformation. *Plant Mol. Biol.* 25, 989–994. doi: 10.1007/BF00014672
- Helenius, A., Trombetta, E. S., Hebert, D. N., and Simons, J. F. (1997). Calnexin, calreticulin and the folding of glycoproteins. *Trends Cell Biol.* 7, 193–200. doi: 10.1016/S0962-8924(97)01032-5
- Henquet, M., Lehle, L., Schreuder, M., Rouwendal, G., Molthoff, J., Helsper, J., et al. (2008). Identification of the gene encoding the α 1,3-mannosyl transferase (ALG3) in Arabidopsis and characterization of downstream n-glycan processing. *Plant Cell* 20, 1652–1664. doi: 10.1105/tpc.108.060731
- Hirao, K., Natsuka, Y., Tamura, T., Wada, I., Morito, D., Natsuka, S., et al. (2006). EDEM3, a soluble EDEM homolog, enhances glycoprotein endoplasmic reticulum-associated degradation and mannose trimming. *J. Biol. Chem.* 281, 9650–9658. doi: 10.1074/jbc.M512191200
- Hong, Z., Jin, H., Fitchette, A. C., Xia, Y., Monk, A. M., Faye, L., et al. (2009). Mutations of an α 1,6 mannosyltransferase inhibit endoplasmic reticulum-

ACKNOWLEDGMENTS

We are grateful to the proteomic core facility at the Center of Excellence for Molecular Plant Sciences, Chinese Academy of Science to perform the N-glycan analysis, the MCDB departmental shared imaging lab of University of Michigan for technical help, and the Arabidopsis Biological Resource Center at Ohio State University for supplying cDNA/BAC genomic clones and Arabidopsis T-DNA insertional mutants (*SALK_095857* and *SALK_046061*), Amy Chang for the yeast Δ htm1 mutant strain, Markus Aebi for the *YEp352-yALG9* plasmid, and Tzvi Tzfira for the *pSITE03-RFP-HDEL* plasmid.

SUPPLEMENTARY MATERIAL

The Supplementary Material for this article can be found online at: <https://www.frontiersin.org/articles/10.3389/fpls.2022.952246/full#supplementary-material>

- associated degradation of defective brassinosteroid receptors in Arabidopsis. *Plant Cell* 21, 3792–3802. doi: 10.1105/tpc.109.070284
- Hong, Z., Jin, H., Tzfira, T., and Li, J. (2008). Multiple mechanism-mediated retention of a defective brassinosteroid receptor in the endoplasmic reticulum of Arabidopsis. *Plant Cell* 20, 3418–3429. doi: 10.1105/tpc.108.061879
- Hong, Z., Kajiura, H., Su, W., Jin, H., Kimura, A., Fujiyama, K., et al. (2012). Evolutionarily conserved glycan signal to degrade aberrant brassinosteroid receptors in Arabidopsis. *Proc. Natl. Acad. Sci. U. S. A.* 109, 11437–11442. doi: 10.1073/pnas.1119173109
- Hori, K., Maruyama, F., Fujisawa, T., Togashi, T., Yamamoto, N., Seo, M., et al. (2014). *Klebsormidium flaccidum* genome reveals primary factors for plant terrestrial adaptation. *Nat. Commun.* 5:3978. doi: 10.1038/ncomms4978
- Hosokawa, N., Tremblay, L. O., Sleno, B., Kamiya, Y., Wada, I., Nagata, K., et al. (2010). EDEM1 accelerates the trimming of α 1,2-linked mannose on the C branch of N-glycans. *Glycobiology* 20, 567–575. doi: 10.1093/glycob/cwq001
- Hosokawa, N., Wada, I., Natsuka, Y., and Nagata, K. (2006). EDEM accelerates ERAD by preventing aberrant dimer formation of misfolded α 1-antitrypsin. *Genes Cells* 11, 465–476. doi: 10.1111/j.1365-2443.2006.00957.x
- Hosomi, A., Tanabe, K., Hirayama, H., Kim, I., Rao, H., and Suzuki, T. (2010). Identification of an Htm1 (EDEM)-dependent, Mns1-independent endoplasmic reticulum-associated degradation (ERAD) pathway in *Saccharomyces cerevisiae*: application of a novel assay for glycoprotein ERAD. *J. Biol. Chem.* 285, 24324–24334. doi: 10.1074/jbc.M109.095919
- Huttner, S., Veit, C., Vavra, U., Schoberer, J., Dicker, M., Maresch, D., et al. (2014a). A context-independent N-glycan signal targets the misfolded extracellular domain of Arabidopsis STRUBBELIG to endoplasmic-reticulum-associated degradation. *Biochem. J.* 464, 401–411. doi: 10.1042/BJ20141057
- Huttner, S., Veit, C., Vavra, U., Schoberer, J., Liebminger, E., Maresch, D., et al. (2014b). Arabidopsis class I α -mannosidases MNS4 and MNS5 are involved in endoplasmic reticulum-associated degradation of Misfolded glycoproteins. *Plant Cell* 26, 1712–1728. doi: 10.1105/tpc.114.123216
- Jin, H., Hong, Z., Su, W., and Li, J. (2009). A plant-specific calreticulin is a key retention factor for a defective brassinosteroid receptor in the endoplasmic reticulum. *Proc. Natl. Acad. Sci. U. S. A.* 106, 13612–13617. doi: 10.1073/pnas.0906144106
- Jin, H., Yan, Z., Nam, K. H., and Li, J. (2007). Allele-specific suppression of a defective brassinosteroid receptor reveals a physiological role of UGGT in ER quality control. *Mol. Cell* 26, 821–830. doi: 10.1016/j.molcel.2007.05.015
- Kajiura, H., Seki, T., and Fujiyama, K. (2010). Arabidopsis thaliana ALG3 mutant synthesizes immature oligosaccharides in the ER and accumulates unique N-glycans. *Glycobiology* 20, 736–751. doi: 10.1093/glycob/cwq028
- Kinoshita, T., Cano-Delgado, A., Seto, H., Hiranuma, S., Fujioka, S., Yoshida, S., et al. (2005). Binding of brassinosteroids to the extracellular domain of plant receptor kinase BRI1. *Nature* 433, 167–171. doi: 10.1038/nature03227
- Kozlov, G., Maattanen, P., Thomas, D. Y., and Gehring, K. (2010). A structural overview of the PDI family of proteins. *FEBS J.* 277, 3924–3936. doi: 10.1111/j.1742-4658.2010.07793.x
- Lamriben, L., Oster, M. E., Tamura, T., Tian, W., Yang, Z., Clausen, H., et al. (2018). EDEM1's mannosidase-like domain binds ERAD client proteins in a redox-sensitive manner and possesses catalytic activity. *J. Biol. Chem.* 293, 13932–13945. doi: 10.1074/jbc.RA118.004183
- Leclercq, J., Szabolcs, T., Martin, F., and Montoro, P. (2015). Development of a new pCambia binary vector using gateway technology. *Plasmid* 81, 50–54. doi: 10.1016/j.plasmid.2015.07.003
- Li, J., and Chory, J. (1997). A putative leucine-rich repeat receptor kinase involved in brassinosteroid signal transduction. *Cell* 90, 929–938. doi: 10.1016/S0092-8674(00)80357-8
- Li, J., and Chory, J. (1998). Preparation of DNA from Arabidopsis. *Methods Mol. Biol.* 82, 55–60. PMID: 9664412
- Li, J., Nam, K. H., Vafeados, D., and Chory, J. (2001). BIN2, a new brassinosteroid-insensitive locus in Arabidopsis. *Plant Physiol.* 127, 14–22. doi: 10.1104/pp.127.1.14
- Li, J., Zhao-Hui, C., Batoux, M., Nekrasov, V., Roux, M., Chinchilla, D., et al. (2009). Specific ER quality control components required for biogenesis of the plant innate immune receptor EFR. *Proc. Natl. Acad. Sci. U. S. A.* 106, 15973–15978. doi: 10.1073/pnas.0905532106
- Liebminger, E., Huttner, S., Vavra, U., Fischl, R., Schoberer, J., Grass, J., et al. (2009). Class I α -mannosidases are required for N-glycan processing and root development in Arabidopsis thaliana. *Plant Cell* 21, 3850–3867. doi: 10.1105/tpc.109.072363
- Liu, L., Cui, F., Li, Q., Yin, B., Zhang, H., Lin, B., et al. (2011). The endoplasmic reticulum-associated degradation is necessary for plant salt tolerance. *Cell Res.* 21, 957–969. doi: 10.1038/cr.2010.181
- Liu, Y. C., Fujimori, D. G., and Weissman, J. S. (2016b). Htm1p-Pdi1p is a folding-sensitive mannosidase that marks N-glycoproteins for ER-associated protein degradation. *Proc. Natl. Acad. Sci. U. S. A.* 113, E4015–E4024. doi: 10.1073/pnas.1608795113
- Liu, F. F., Kulnich, A., Du, Y. M., Liu, L., and Voglmeier, J. (2016a). Sequential processing of mannose-containing glycans by two α -mannosidases from *Solitealea canadensis*. *Glycoconj. J.* 33, 159–168. doi: 10.1007/s10719-016-9651-9
- Liu, Y., and Li, J. (2014). Endoplasmic reticulum-mediated protein quality control in Arabidopsis. *Front. Plant Sci.* 5:162. doi: 10.3389/fpls.2014.00162
- Liu, Y., Zhang, C., Wang, D., Su, W., Liu, L., Wang, M., et al. (2015). EBS7 is a plant-specific component of a highly conserved endoplasmic reticulum-associated degradation system in Arabidopsis. *Proc. Natl. Acad. Sci. U. S. A.* 112, 12205–12210. doi: 10.1073/pnas.1511724112
- Ma, J., Wang, D., She, J., Li, J., Zhu, J. K., and She, Y. M. (2016). Endoplasmic reticulum-associated N-glycan degradation of cold-upregulated glycoproteins in response to chilling stress in Arabidopsis. *New Phytol.* 212, 282–296. doi: 10.1111/nph.14014
- Mora-Garcia, S., Vert, G., Yin, Y., Cano-Delgado, A., Cheong, H., and Chory, J. (2004). Nuclear protein phosphatases with Kelch-repeat domains modulate the response to brassinosteroids in Arabidopsis. *Genes Dev.* 18, 448–460. doi: 10.1101/gad.1174204
- Neff, M. M., Nguyen, S. M., Malancharuvil, E. J., Fujioka, S., Noguchi, T., Seto, H., et al. (1999). BAS1: A gene regulating brassinosteroid levels and light responsiveness in Arabidopsis. *Proc. Natl. Acad. Sci. U. S. A.* 96, 15316–15323. doi: 10.1073/pnas.96.26.15316
- Nekrasov, V., Li, J., Batoux, M., Roux, M., Chu, Z. H., Lacombe, S., et al. (2009). Control of the pattern-recognition receptor EFR by an ER protein complex in plant immunity. *EMBO J.* 28, 3428–3438. doi: 10.1038/emboj.2009.262
- Ng, D. T., Spear, E. D., and Walter, P. (2000). The unfolded protein response regulates multiple aspects of secretory and membrane protein biogenesis and endoplasmic reticulum quality control. *J. Cell Biol.* 150, 77–88. doi: 10.1083/jcb.150.1.77
- Ninagawa, S., Okada, T., Sumitomo, Y., Kamiya, Y., Kato, K., Horimoto, S., et al. (2014). EDEM2 initiates mammalian glycoprotein ERAD by catalyzing the first mannose trimming step. *J. Cell Biol.* 206, 347–356. doi: 10.1083/jcb.201404075
- Nishiyama, T., Sakayama, H., De Vries, J., Buschmann, H., Saint-Marcoux, D., Ullrich, K. K., et al. (2018). The Chara genome: secondary complexity and implications for plant terrestrialization. *Cell* 174, 448–464.e24. doi: 10.1016/j.cell.2018.06.033
- Noguchi, T., Fujioka, S., Choe, S., Takatsuto, S., Yoshida, S., Yuan, H., et al. (1999). Brassinosteroid-insensitive dwarf mutants of Arabidopsis accumulate brassinosteroids. *Plant Physiol.* 121, 743–752. doi: 10.1104/pp.121.3.743
- Obayashi, T., Hayashi, S., Saeki, M., Ohta, H., and Kinoshita, K. (2009). ATTED-II provides coexpressed gene networks for Arabidopsis. *Nucleic Acids Res.* 37, D987–D991. doi: 10.1093/nar/gkn807
- Pacurar, D. I., Pacurar, M. L., Street, N., Bussell, J. D., Pop, T. I., Gutierrez, L., et al. (2012). A collection of INDEL markers for map-based cloning in seven Arabidopsis accessions. *J. Exp. Bot.* 63, 2491–2501. doi: 10.1093/jxb/err422
- Pfeiffer, A., Stephanowitz, H., Krause, E., Volkwein, C., Hirsch, C., Jarosch, E., et al. (2016). A complex of Htm1 and the oxidoreductase Pdi1 accelerates degradation of misfolded glycoproteins. *J. Biol. Chem.* 291, 12195–12207. doi: 10.1074/jbc.M115.703256
- Preston, G. M., and Brodsky, J. L. (2017). The evolving role of ubiquitin modification in endoplasmic reticulum-associated degradation. *Biochem. J.* 474, 445–469. doi: 10.1042/BCJ20160582
- Quan, E. M., Kamiya, Y., Kamiya, D., Denic, V., Weibezahn, J., Kato, K., et al. (2008). Defining the glycan destruction signal for endoplasmic reticulum-associated degradation. *Mol. Cell* 32, 870–877. doi: 10.1016/j.molcel.2008.11.017
- Rensing, S. A., Lang, D., Zimmer, A. D., Terry, A., Salamov, A., Shapiro, H., et al. (2008). The Physcomitrella genome reveals evolutionary insights into the conquest of land by plants. *Science* 319, 64–69. doi: 10.1126/science.1150646

- Saijo, Y., Tintor, N., Lu, X., Rauf, P., Pajeroska-Mukhtar, K., Haweker, H., et al. (2009). Receptor quality control in the endoplasmic reticulum for plant innate immunity. *EMBO J.* 28, 3439–3449. doi: 10.1038/emboj.2009.263
- Schoberer, J., König, J., Veit, C., Vavra, U., Liebminger, E., Botchway, S. W., et al. (2019). A signal motif retains Arabidopsis ER- α -mannosidase I in the cis-Golgi and prevents enhanced glycoprotein ERAD. *Nat. Commun.* 10:3701. doi: 10.1038/s41467-019-11686-9
- Shenkman, M., Ron, E., Yehuda, R., Benyair, R., Khalaila, I., and Lederkremer, G. Z. (2018). Mannosidase activity of EDEM1 and EDEM2 depends on an unfolded state of their glycoprotein substrates. *Commun. Biol.* 1:172. doi: 10.1038/s42003-018-0174-8
- Smith, M. H., Ploegh, H. L., and Weissman, J. S. (2011). Road to ruin: targeting proteins for degradation in the endoplasmic reticulum. *Science* 334, 1086–1090. doi: 10.1126/science.1209235
- Strasser, R. (2018). Protein quality control in the endoplasmic reticulum of plants. *Annu. Rev. Plant Biol.* 69, 147–172. doi: 10.1146/annurev-arplant-042817-040331
- Su, W., Liu, Y., Xia, Y., Hong, Z., and Li, J. (2011). Conserved endoplasmic reticulum-associated degradation system to eliminate mutated receptor-like kinases in Arabidopsis. *Proc. Natl. Acad. Sci. U. S. A.* 108, 870–875. doi: 10.1073/pnas.1013251108
- Su, W., Liu, Y., Xia, Y., Hong, Z., and Li, J. (2012). The Arabidopsis homolog of the mammalian OS-9 protein plays a key role in the endoplasmic reticulum-associated degradation of misfolded receptor-like kinases. *Mol. Plant* 5, 929–940. doi: 10.1093/mp/sss042
- Su, K., Stoller, T., Rocco, J., Zemsky, J., and Green, R. (1993). Pre-Golgi degradation of yeast prepro- α -factor expressed in a mammalian cell. Influence of cell type-specific oligosaccharide processing on intracellular fate. *J. Biol. Chem.* 268, 14301–14309. doi: 10.1016/S0021-9258(19)85241-9
- Sun, X., Guo, C., Ali, K., Zheng, Q., Wei, Q., Zhu, Y., et al. (2022). A non-redundant function of MNS5: a class I α -1, 2 Mannosidase, in the regulation of endoplasmic reticulum-associated degradation of misfolded glycoproteins. *Front. Plant Sci.* 13:873688. doi: 10.3389/fpls.2022.873688
- Tarentino, A. L., Gomez, C. M., and Plummer, T. H. Jr. (1985). Deglycosylation of asparagine-linked glycans by peptide:N-glycosidase F. *Biochemistry* 24, 4665–4671. doi: 10.1021/bi00338a028
- Timms, R. T., Menzies, S. A., Tchasovnikarova, I. A., Christensen, L. C., Williamson, J. C., Antrobus, R., et al. (2016). Genetic dissection of mammalian ERAD through comparative haploid and CRISPR forward genetic screens. *Nat. Commun.* 7:11786. doi: 10.1038/ncomms11786
- Voinnet, O., Rivas, S., Mestre, P., and Baulcombe, D. (2003). An enhanced transient expression system in plants based on suppression of gene silencing by the p19 protein of tomato bushy stunt virus. *Plant J.* 33, 949–956. doi: 10.1046/j.1365-3113X.2003.01676.x
- Winter, D., Vinegar, B., Nahal, H., Ammar, R., Wilson, G. V., and Provart, N. J. (2007). An "electronic fluorescent pictograph" browser for exploring and analyzing large-scale biological data sets. *PLoS One* 2:e718. doi: 10.1371/journal.pone.0000718
- Xu, C., and Ng, D. T. (2015). O-mannosylation: the other glycan player of ER quality control. *Semin. Cell Dev. Biol.* 41, 129–134. doi: 10.1016/j.semcdb.2015.01.014
- Yu, S., Ito, S., Wada, I., and Hosokawa, N. (2018). ER-resident protein 46 (ERp46) triggers the mannose-trimming activity of ER degradation-enhancing α -mannosidase-like protein 3 (EDEM3). *J. Biol. Chem.* 293, 10663–10674. doi: 10.1074/jbc.RA118.003129

Conflict of Interest: The authors declare that the research was conducted in the absence of any commercial or financial relationships that could be construed as a potential conflict of interest.

Publisher's Note: All claims expressed in this article are solely those of the authors and do not necessarily represent those of their affiliated organizations, or those of the publisher, the editors and the reviewers. Any product that may be evaluated in this article, or claim that may be made by its manufacturer, is not guaranteed or endorsed by the publisher.

Copyright © 2022 Zhang, Xia, Wang, Du, Chen, Zhang, Mao, Wang, She, Peng, Liu, Voglmeir, He, Liu and Li. This is an open-access article distributed under the terms of the Creative Commons Attribution License (CC BY). The use, distribution or reproduction in other forums is permitted, provided the original author(s) and the copyright owner(s) are credited and that the original publication in this journal is cited, in accordance with accepted academic practice. No use, distribution or reproduction is permitted which does not comply with these terms.



Review

Mechanisms of Endoplasmic Reticulum Protein Homeostasis in Plants

Zhihao Duan, Kai Chen, Tao Yang, Ronghui You, Binzhao Chen, Jianming Li and Linchuan Liu

Special Issue

Regulation of Plant Protein Homeostasis under Stress

Edited by

Dr. Borja Belda-Palazón and Dr. Alejandro Ferrando





Review

Mechanisms of Endoplasmic Reticulum Protein Homeostasis in Plants

Zhihao Duan ¹ , Kai Chen ¹, Tao Yang ¹, Ronghui You ¹, Binzhao Chen ¹, Jianming Li ^{1,2,*} and Linchuan Liu ^{1,*}

¹ State Key Laboratory for Conservation and Utilization of Subtropical Agro-Bioresources, Guangdong Key Laboratory for Innovative Development and Utilization of Forest Plant Germplasm, College of Forestry and Landscape Architecture, South China Agricultural University, Guangzhou 510642, China

² Department of Biology, Hong Kong Baptist University, Kowloon, Hong Kong

* Correspondence: li-jianming@hkbu.edu.hk (J.L.); lcliu@scau.edu.cn (L.L.)

Abstract: Maintenance of proteome integrity is essential for cell function and survival in changing cellular and environmental conditions. The endoplasmic reticulum (ER) is the major site for the synthesis of secretory and membrane proteins. However, the accumulation of unfolded or misfolded proteins can perturb ER protein homeostasis, leading to ER stress and compromising cellular function. Eukaryotic organisms have evolved sophisticated and conserved protein quality control systems to ensure protein folding fidelity via the unfolded protein response (UPR) and to eliminate potentially harmful proteins via ER-associated degradation (ERAD) and ER-phagy. In this review, we summarize recent advances in our understanding of the mechanisms of ER protein homeostasis in plants and discuss the crosstalk between different quality control systems. Finally, we will address unanswered questions in this field.

Keywords: ER homeostasis; unfolded protein response (UPR); ER-associated degradation (ERAD); ER-phagy; *Arabidopsis thaliana*



Citation: Duan, Z.; Chen, K.; Yang, T.; You, R.; Chen, B.; Li, J.; Liu, L. Mechanisms of Endoplasmic Reticulum Protein Homeostasis in Plants. *Int. J. Mol. Sci.* **2023**, *24*, 17599. <https://doi.org/10.3390/ijms242417599>

Academic Editors: Alejandro Ferrando and Borja Belda-Palazón

Received: 27 November 2023

Revised: 14 December 2023

Accepted: 15 December 2023

Published: 18 December 2023



Copyright: © 2023 by the authors. Licensee MDPI, Basel, Switzerland. This article is an open access article distributed under the terms and conditions of the Creative Commons Attribution (CC BY) license (<https://creativecommons.org/licenses/by/4.0/>).

1. Introduction

The endoplasmic reticulum (ER) is the largest intracellular organelle and plays essential roles in protein folding, lipid biosynthesis, detoxification, calcium storage, and carbohydrate metabolism [1,2]. In eukaryotic cells, nearly one-third of all proteins enter the secretory pathway via the ER. Only those proteins that are properly folded are allowed to leave the ER and be delivered to their final destinations. However, protein folding is a highly error-prone process that can be easily perturbed by a wide range of cellular and environmental stresses, leading to the accumulation of misfolded proteins and their aggregates in the ER, causing cellular dysfunctions or even cell death. To cope with this situation, eukaryotes have evolved many ER protein quality control (ERQC) systems to preserve ER proteostasis and to maintain cell survival [3]. In plants, ER stress usually occurs when they are subjected to unfavorable environmental conditions or at specific developmental stages. An evolutionarily conserved signal network, known as the unfolded protein response (UPR), is activated during ER stress to restore ER homeostasis [4]. In addition to transducing the ER stress signal to the nucleus to stimulate the expression of ER chaperones for ER-assisted protein folding/refolding (ERAF), the UPR also boosts the cellular capacity to degrade misfolded ER proteins through proteasomal and/or autophagic degradation [5,6]. ER-associated protein degradation (ERAD) is a well-characterized ER protein quality control mechanism that targets misfolded, improperly assembled, and even unwanted “correctly-folded” proteins for cytosolic proteasomal degradation. Genetic and biochemical studies on yeast and mammalian cells revealed sophisticated ERAD mechanisms and identified many ERAD components that are conserved from yeast to humans [7]. Recent genetic studies using the model plant *Arabidopsis thaliana* have also discovered a highly conserved ERAD complex [8,9]. *Arabidopsis* mutants with defects in

ERAD components often exhibit abnormal responses to biotic or abiotic stress [8], demonstrating the necessity of the ERAD function in maintaining ER protein homeostasis during plant–environment interactions. Additionally, multiple lines of evidence have revealed that some stress conditions not only induce the UPR, but also activate the autophagy pathway to ensure the timely clearance of ER portions containing misfolded/aggregated proteins or damaged ER [10]. This means that the UPR exquisitely cooperates with ERAD and ER-phagy to maintain ER homeostasis, ER morphology, and ER function (Figure 1). Here, we will focus on recent advances in understanding the regulatory mechanisms of ER protein homeostasis and review the recent findings on the UPR, ERAD, and ER-phagy, suggesting an integration of ER protein quality control mechanisms during plant growth and development.

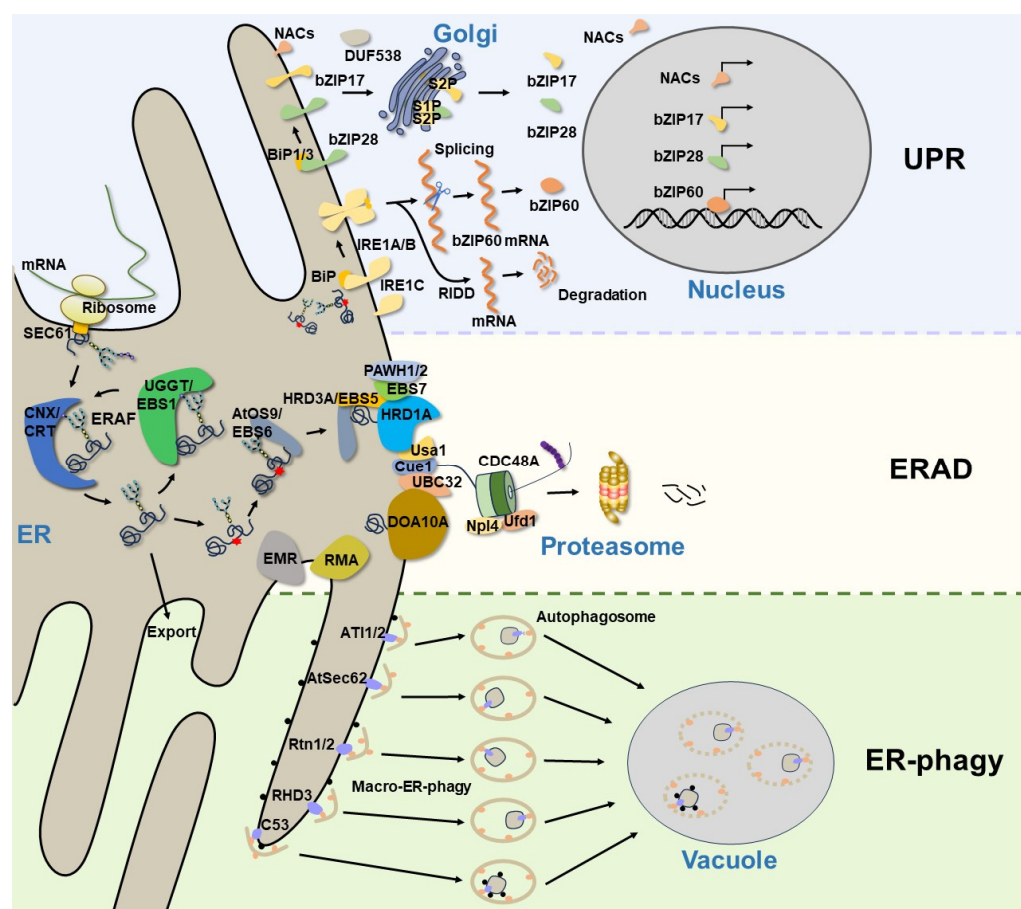


Figure 1. A current model of ER protein homeostasis in plants. The newly synthesized secretory and membrane proteins in the ER undergo folding and assembly, while those misfolded/unfolded proteins are handled by the ERAF mechanisms. The accumulation of misfolded proteins in the ER will trigger the UPR to relieve ER stress and restore ER homeostasis. In Arabidopsis, the UPR is modulated via the UPR sensor IRE1A/B, as well as via bZIP transcription factors (bZIP17, bZIP28, and bZIP60) and plant-specific NAC transcription factors. Terminally misfolded proteins are degraded by the ERAD system, which consists of many membrane-anchored E3 ligases and other conserved components. However, large protein aggregates or damaged ER segments that cannot be degraded by ERAD are eventually removed through ER-phagy. The ER-phagy receptors selectively recognize their cargoes and recruit them to the autophagosomes for autophagic degradation.

2. Activation of the UPR to Restore ER Homeostasis

The ER is the entry site for the secretory pathway. Newly synthesized secretory and integral transmembrane proteins enter the ER through the translocation channel in an unfolded state [11]. Upon entry into the ER, the luminal molecular chaperones and folding

enzymes facilitate protein folding and complex assembly to attain native conformations and properly assembled complexes [12], while incomplete or misfolded glycoproteins are handled by the ERAF system, which promotes protein refolding by the ER folding-sensor enzyme, UDP-glucose: glycoprotein glucosyltransferase (UGGT, known as EBS1 in Arabidopsis), and the lectin-like molecular chaperones, calnexin (CNX)/calreticulin (CRT) [13,14] (Figure 1). However, the ERAF is an error-prone process that often fails, especially when interfered with cellular and environment stresses, causing excessive accumulation of misfolded proteins and improperly assembled complexes in the ER. This leads to ER stress and activates an evolutionarily conserved UPR signaling cascade. The UPR was initially described in yeast, and it was later discovered in other eukaryotic organisms. In metazoans, three ER transmembrane proteins, inositol-requiring enzyme 1 (IRE1) [15,16], activating transcription factor 6 (ATF6) [17], and protein kinase R (PKR)-like ER kinase (PERK) [18], have been identified as UPR receptors that sense misfolded proteins in the ER and initiate distinctive signaling cascades to increase the ER folding capacity, reduce protein synthesis rates, and boost ERAD efficiency. While the UPR pathway is highly conserved across diverse eukaryotic organisms, only two UPR branches, which are mediated by homologs of IRE1 and ATF6, have been characterized in plants [19] (Table 1). The Arabidopsis genome encodes two IRE1 homologs: AtIRE1A and AtIRE1B [20,21]. Both of them have conserved functional modules consisting of an ER luminal N-terminal sensor domain, a single transmembrane domain, and the cytosolic catalytic domain possessing the kinase and endo-ribonucleotidase (RNase) activities [20]. During ER stress, AtIRE1A and AtIRE1B can homodimerize and autophosphorylate to catalyze the unconventional cytoplasmic splicing of *BASIC LEUCINE ZIPPER60* (*bZIP60*) mRNA, producing an active nuclear-localized bZIP60 transcription factor to regulate the expression of UPR target genes [22,23] (Figure 1). AtIRE1B is widely expressed in whole plants, while AtIRE1A is mainly expressed in embryos and seeds [20], and they display different responses to biotic and abiotic stress [24]. AtIRE1C is a recently discovered Brassicaceae-specific IRE1 isoform [25,26], which contains only a transmembrane domain and a cytosolic region with kinase and ribonucleotidase domains. Although AtIRE1C lacks the sensor domain that is essential in other IRE1 isoforms, it still participates in the physiological UPR, specifically during gametogenesis in Arabidopsis [26]. It remains to be investigated how AtIRE1C senses the disturbed ER protein homeostasis. In addition, IRE1 is able to cleave cellular mRNAs, leading to their degradation through a process known as regulated IRE-dependent decay (RIDD) [27,28] (Figure 1), which is considered an efficient way to reduce the influx of proteins into the ER. Evidence has demonstrated that Arabidopsis IRE1s participate in the degradation of a subset of mRNAs encoding the secretory pathway proteins [29]. The other branch of the UPR signaling network in plants is composed of bZIP membrane-associated transcription factors. In Arabidopsis, AtbZIP17 and AtbZIP28 are two functional homologs of the metazoan ATF6, featuring a N-terminal cytosol-facing bZIP domain, a single transmembrane segment, and a C-terminal lumen-facing UPR-sensing domain [30,31]. Upon ER stress, AtbZIP17 and AtbZIP28 are translocated from the ER to the Golgi. The Golgi membrane-localized site 1 protease (S1P) and site 2 protease (S2P) sequentially cleave the two AtbZIP proteins to release their N-terminal bZIP transcriptional domains that can translocate into the nucleus to upregulate the expression of many UPR genes encoding protein chaperones, folding catalysts, and components of the ERAD machinery and autophagy pathway [30,31] (Figure 1). Although it seems that bZIP60 and bZIP17/bZIP28 work on two independent, parallel pathways, they still coordinately regulate numerous overlapping genes to alleviate ER stress and to enhance plant stress tolerance [32,33]. In recent years, some plant-specific NAC [no apical meristem (NAM), Arabidopsis transcription activation factor (ATAF1/2) and cup-shaped cotyledon (CUC2)] type transcription factors and DUF538 family proteins have been reported to be involved in the plant UPR pathway [34–38], suggesting that plants have developed unique strategies to cope with ER stress in response to a wide variety of biotic and abiotic stresses.

Table 1. Plant components involved in maintaining ER protein homeostasis.

Pathways	Name	Type	Targets	Species	References
UPR	AtIRE1A, AtIRE1B, AtIRE1C	Sensor	--	<i>A. thaliana</i>	[20,25,26]
	AtbZIP60	Transcription factor	--	<i>A. thaliana</i>	[23]
	AtbZIP17	Transcription factor	--	<i>A. thaliana</i>	[31]
	AtbZIP28	Transcription factor	--	<i>A. thaliana</i>	[30]
	S1P, S2P	Proteases	--	<i>A. thaliana</i>	[30]
	NAC	Transcription factor	--	<i>A. thaliana</i>	[34–36]
	DUF538	--	--	<i>A. thaliana</i>	[37,38]
ERAD	EBS5/AtHRD3A	Adaptor	MLO1; bri1-5/1-9	<i>A. thaliana</i>	[39,40]
	EBS6/AtOS9	Adaptor	EFR *; bri1-5/1-9	<i>A. thaliana</i>	[41,42]
	EBS7	--	EFR *; bri1-5/1-9	<i>A. thaliana</i>	[43]
	PAWH1, PAWH2	--	EFR *; bri1-5/1-9	<i>A. thaliana</i>	[44]
	UBC32	E2	MLO12; bri1-5/1-9	<i>A. thaliana</i>	[45]
	OsUBC45	E2	--	<i>O. sativa</i>	[46]
	HRD1A	E3 ligase	bri1-5/1-9; UBC32	<i>A. thaliana</i>	[39,47]
	AtDOA10A/CER9/SUD1	E3 ligase	HMGR; SQE1	<i>A. thaliana</i>	[48,49]
	AtRMA1, AtRMA2, AtRMA3	E3 ligase	PIP2;1	<i>A. thaliana</i>	[50,51]
	CaRma1H1	E3 ligase	PIP2;1	<i>C. annuum</i>	[50]
	EMR	E3 ligase	MLO12; bri1-5	<i>A. thaliana</i>	[52]
	CDC48A	AAA ATPase	--	<i>A. thaliana</i>	[53]
ER-phagy	ATI1, ATI2	Receptor	AGO1; MSBP1	<i>A. thaliana</i>	[54–56]
	AtSec62	Receptor	--	<i>A. thaliana</i>	[57]
	Rtn1, Rtn2	Receptor	--	<i>Z. mays</i>	[58]
	RHD3	Receptor	--	<i>A. thaliana</i>	[59]
	C53	Receptor	--	<i>A. thaliana</i>	[60]

*: misfolded EFR; and --: unknown.

Although much is known about the downstream nuclear events of the UPR pathway [61,62], the mechanism through which plant UPR receptors sense the accumulation of misfolded proteins in the ER remains unclear. In *Saccharomyces cerevisiae*, a groove-like area was observed in the 3D structure of the yeast Ire1p luminal domain. It is generally believed that un/misfolded proteins directly bind the groove site formed by Ire1p oligomerization, leading to the activation of its cytosolic RNase activity [63]. However, a subsequent structural biology study with the human IRE1 α suggested that the groove in its luminal domain is too small to bind misfolded proteins [64], raising the question of whether there is a direct binding between misfolded proteins and IRE1 α in vivo. In mammalian cells, the chaperone protein BiP (binding immunoglobulin protein), an ER-localized member of the HSP70 family, can interact with the luminal domains of IRE1 α and PERK to prevent the dimerization or oligomerization needed for their activation, thus inhibiting the UPR. Such BiP-IRE1 α /PERK interaction also prevents BiP from binding its cochaperones [65]. Upon ER stress, BiP binds to un/misfolded proteins, leading to the liberation of IRE1 α and PERK. The two liberated UPR sensors can subsequently dimerize/oligomerize to activate their respective catalytic activities, thus activating the UPR signaling cascades [65–67]. In recent years, a variety of IRE1 α -binding proteins were discovered in mammals, some of which are involved in the posttranslational modifications of IRE1 α to regulate its activity or protein stability [6]. However, little is known about the interacting proteins and the regulatory mechanisms of plant IRE1s. It was known that the mammalian BiP binds to ATF6 and prevents the ER-Golgi trafficking of ATF6 and that the titration of BiP by un/misfolded proteins under ER stress conditions allows ATF6 translocation into the Golgi where ATF6 is cleaved by S1P and S2P [68]. Similarly, two Arabidopsis BiP homologs, BiP1 and BiP3, were found to interact with the C-terminal intrinsically disordered regions of bZIP28 to retain it on the ER membrane [69]. The competitive binding of the BiPs with un/misfolded proteins release bZIP28 that can be translocated to the Golgi for the S1P-/S2P-catalyzed cleavage. Thus, BiPs plays important roles in the ER protein homeostasis, not only in ERAF but

also in the recognition of misfolded proteins and the regulation of the UPR pathways. In addition to BiPs, recent studies also discovered interactions of the UPR sensors with protein disulfide isomerases (PDIs) [70–72], but how such bindings regulate the UPR mechanism to restore ER protein homeostasis remains to be explored.

3. Removal of Misfolded Proteins through ERAD

ERAD is a highly conserved protein quality control system responsible for sending terminally misfolded proteins for cytosolic degradation, thereby maintaining the ER protein homeostasis. Extensive genetic and biochemical studies in yeast and mammals have revealed that an elaborate ERAD process involves at least four interdependent steps: substrate recognition, retrotranslocation across the ER membrane, ubiquitination at the cytosolic side, and degradation by 26S proteasomes [7]. One of the best-studied ERAD mechanisms deals with misfolded glycoproteins, because a majority of secretory or transmembrane proteins are modified by asparagine (N)-linked glycosylation. It was believed that this ERAD machinery recognizes a unique N-glycan structure on the terminally misfolded glycoproteins. If a misfolded glycoprotein stays in the ER for too long engaging repeatedly futile folding attempts, its N-linked glycans are trimmed by folding-sensitive ER-localized α -1,2-mannosidase, known as homologous to α -mannosidase 1 (Htm1) in yeast and ER-degradation enhancing α -mannosidase-like proteins (EDEMs) in mammals [73,74], to expose the α -1,6 mannose residue on N-glycans. This special N-glycan is recognized by a unique lectin chaperone, known as OS9 (osteosarcoma amplified 9) in mammals and Yos9 (yeast homolog of OS9) in yeast, while the hydrophobic amino acid residues exposed on the surface of misfolded glycoproteins are captured by Sel1L (suppressor enhancer of Lin12 1-like) in mammals and Hrd3 (HMG-CoA reductase degradation protein 3) in yeast [75]. Yos9/OS9 works together with Hrd3/Sel1L to bring a terminally misfolded glycoprotein to the ER membrane-anchored ERAD machinery that builds around a multi-transmembrane ubiquitin E3 ligase. In yeast, Hrd1 (HMG-CoA reductase degradation protein 1) and Doa10 (degradation of alpha2) are two major ERAD E3 ligases. It is generally believed that misfolded proteins with folding lesions in their luminal domains (ERAD-L) or membrane-spanning domains (ERAD-M) are degraded by Hrd1, and those defective in the cytoplasmic domains (ERAD-C) are mediated by Doa10 [76]. In fact, the ERAD systems that dispose a wide variety of substrates are more complicated in mammals that have many different E3 ubiquitin ligases implicated in ERAD [77]. It is worth mentioning that the yeast ERAD E3 ubiquitin ligases not only catalyze the polyubiquitin conjugation on their clients but also serve as retrotranslocons to extract ERAD substrates into the cytosol [78–80]. The ERAD retrotranslocons could also include several other transmembrane proteins, such as Der1 (degradation in the endoplasmic reticulum protein 1) [81] and its homolog DFM1 (DER1-like family member protein 1) [82]. Both the Hrd1- and Doa10-based ERAD machinery contain other conserved components, such as the AAA+-type ATPase, Cdc48 (cell division cycle protein 48, p97 in mammals) and its cofactors Npl4 (nuclear protein localization protein 4) and Ufd1 (ubiquitin fusion degradation protein 1) for escorting the extracted ERAD substrates to the proteasome, Cue1 (coupling of ubiquitin conjugation to ER degradation protein 1) for recruiting E2 and several ubiquitin-conjugating E2 enzymes [83] (Figure 1). Notably, while the α -1,6-mannose-exposed N-glycan structure serves as the ERAD signal for degrading misfolded glycoproteins, the recognition and targeting of nonglycosylated misfolded proteins for degradation remain unclear.

Previous studies have revealed that ERAD is important for plant growth and development [84,85], but the exact mechanisms were not well-understood until some endogenous ERAD substrates were discovered in plants. Most of the published plant ERAD studies were focused on mutant plant proteins known to be important for plant growth and stress tolerance. For example, several mutant variants of the barley mildew resistance Locus O (MLO) carrying single amino acid substitution in the cytosolic loops were discovered as plant ERAD clients degraded through the Hrd1-containing ERAD pathway involving the ubiquitin-conjugating enzyme UBC32 [45,86]. In Arabidopsis, two mutant variants of the

brassinosteroid receptor BRI1 (BRASSINOSTEROID-INSENSITIVE 1), *bri1-5* and *bri1-9*, are also degraded by the Hrd1 ERAD complex, producing the BR-insensitive dwarfism phenotype [87]. Forward and reverse genetic studies using the corresponding Arabidopsis *bri1-5* and *bri1-9* have discovered not only conserved but also plant-specific components of the Arabidopsis Hrd1-containing ERAD machinery (Table 1). The conserved components include EBS5 for EMS-mutagenized *bri1* suppressor 5 (also known as AtHRD3A or AtSel1L for its sequence homology to Hrd3/Sel1L) [39,40], EBS6 (also known as AtOS9 for being the Arabidopsis homolog of Yos9/OS9) [41,42], Hrd1A and Hrd1B (two Arabidopsis homologs of the yeast Hrd1) [39], and ubiquitin conjugase UBC32 [45]. The plant-specific components include EBS7, an ER membrane protein that is highly conserved in land plants, and two highly homologous proteins known as PAWH1/2 for protein associated with Hrd1. EBS7 is predicted to contain three transmembrane segments, while PAWHs have an AIM24 (altered inheritance of mitochondria protein 24) domain that is thought to be conserved in land plants and plays important roles in ER stress tolerance and the UPR and a C-terminal membrane anchor [88]. Interestingly, loss-of-function mutations in EBS7 cause rapid degradation of the two PAWHs and Hrd1. The simultaneous elimination of PAWH1 and PAWH2 also leads to rapid disappearance of EBS7 and Hrd1, suggesting important regulatory functions of the two plant-specific components of the Hrd1 ERAD complex [43]. Further studies are needed to fully understand how EBS7 and PAWHs coordinately regulate the protein stability and E3 ligase activity of the Hrd1. Mass spectrometry-based proteomic approaches coupled with reverse genetics of Arabidopsis could identify additional components, regulators, and, more importantly, endogenous substrates of the plant Hrd1-containing ERAD system.

Compared to the HRD1 complex, little is known about the roles of other E3 ligases in the plant ERAD system. The Arabidopsis genome encodes two homologs of DOA10 (AtDOA10A and AtDOA10B). It has been reported that AtDOA10A (SUD1 for SUPPRESSOR OF DRY2 DEFECTS1 or CER9 for ECERIFERUM9) is involved in the cuticle lipid biosynthesis, plant drought response, and ABA metabolism [48,89], but the precise mechanisms and corresponding substrates remain unknown. A recent study demonstrated that degradation of a GFP fusion protein with the Arabidopsis SQUALENE EPOXIDASE (AtSQE1), a rate-limiting sterol synthetic enzyme that converts squalene into 2,3-epoxysqualene, is mediated by AtDOA10A [49]. However, AtSQE1 is a correctly folded ER transmembrane protein and little is known how such a correctly folded ERAD substrate is recognized by the ERAD system. It also remains to be investigated whether or not AtDOA10A-facilitated AtSQE1 degradation requires additional components of the AtDOA10A system. Unlike AtDOA10A, AtDOA10B could be induced by ER stress and interacted with UBC32 when coexpressed in tobacco leaves. Interestingly, DOA10B only exists in the Brassicaceae species and was unable to complement the yeast *doa10* mutant, suggesting that AtDOA10B might have a more distinctive function than AtDOA10A in the ER [49]. In contrast to yeast that has two ER membrane-anchored E3 ligases, plants have additional ER membrane-anchored/associated E3 ligases implicated in ERAD, such as RMA1 (RING membrane-anchored 1) and the Arabidopsis cytosolic E3 ligase EMR (ERAD-mediating RING finger protein). The Rma1H1 (RING membrane-anchor 1 homolog 1) from hot pepper (*Capsicum annuum*) and three homologs of RMA1 (AtRMA1, AtRMA2 and AtRMA3) from Arabidopsis are involved in regulating the trafficking and protein abundance of aquaporin PIP2;1 (plasma membrane intrinsic protein 2;1) [50,51]. EMR that is induced by ER stress colocalizes with the ER membrane-anchored UBC32 and exhibits the ubiquitin ligase activity in vitro [52]. Although EMR knockdown partially rescued the *bri1-5* dwarfism phenotype, it remains to be investigated whether EMR is involved in the ERAD of *bri1-5* and other endogenous ERAD substrates.

Maintaining protein homeostasis in a changing environment is vital for cell function and organismal viability. In recent years, the physiological functions of ERAD have been extensively studied in mammals and proven to be closely related to health and disease [90]. In plants, ERAD is thought to play an essential role in plant adaptation to biotic and abiotic

stress. ERAD components, such as HRD1A/1B, EBS6/AtOS9, EBS7, and PAWH1/2, are involved in the degradation of misfolded EFR (elongation factor thermo-unstable/EF-Tu receptor), a plasma membrane-localized immune receptor that recognizes and binds the bacterial translation elongation factor EF-Tu [42–44]. A recent study also revealed that OsUBC45, a rice homolog of the Arabidopsis UBC32, functions as an ERAD component that regulates rice resistance against blast disease and bacterial blight [46]. Salt treatment leads to the accumulation of ubiquitinated proteins and induces the ER stress response [40]. Arabidopsis mutants of the Hrd1 ERAD complex exhibit activated UPR and altered tolerance to salt stress [39,42–45]. Furthermore, UBC32 was also implicated in drought and oxidative stress responses [91], and a *hrd1a hrd1b* double mutant exhibits reduced sensitivity to heat stress [92]. Of note, some ERAD components, such as AtOS9 and UBC32, were themselves degraded via a self-regulatory mechanism known as “the ER turning” to influence plant growth and stress adaptation [42,45,47,93].

4. Removal of ER Portions through ER-Phagy

As the largest intracellular organelle, the ER undergoes dynamic remodeling during the cell cycle to maintain its structural integrity and metabolic functions. The aggregates of misfolded proteins and/or excess/damaged ER segments, which cannot be degraded by the ERAD pathway, are eventually removed through ER-phagy or reticulophagy, a selective autophagy by which parts of the ER network are removed through lysosomal degradation [94]. Depending on how the substrates are delivered to the lysosomes/vacuoles, ER-phagy can be classified into two categories: macro-ER-phagy and micro-ER-phagy. In macro-ER-phagy, a precursor cisterna called phagophore elongates, expands, and finally closes to form a sealed double membrane structure, known as the autophagosome. Autophagosomes then bind and deliver their ER cargos to lysosomes/vacuoles for degradation. In contrast, micro-ER-phagy involves the direct piecemeal engulfment of abnormal ER fragments by endosomal and/or lysosomal/vacuolar invagination [10,95].

The ER-phagy connects the excessive/damaged ER fragments with autophagosomes through the ER-phagy receptors that interact with the ubiquitin-like ATG8 (autophagy-related protein 8), permitting continued incorporation of damaged ER segments into the ATG8-decorated phagophores. To date, a number of membrane and soluble ER-phagy receptors have been identified in *Saccharomyces cerevisiae* and mammalian cells [95,96]. Their differential distribution throughout the ER sheets, tubes, and perinuclear ER facilitates targeting various regions of the ER network to the autophagosome. In plants, only a few ER-phagy receptors have been discovered, such as ATI1 (ATG8-Interacting protein 1)/ATI2 (ATG8-Interacting protein 2), Sec62 (translocation protein Sec62), Rtn1 (Reticulon-1)/Rtn2 (Reticulon-2), C53, and RHD3 (Root Hair Defective 3) proteins [97] (Figure 1). ATI1 and ATI2 are two plant-specific ER-phagy receptors that interact with ATG8 [54]. They have a single transmembrane domain and long N-terminal intrinsically disordered regions (IDRs) containing functional AIMs. It has been reported that ATI1 and ATI2 are located in the ER membrane. However, upon being exposed to darkness (carbon starvation), ATI1 and ATI2 associate with starvation-induced spherical compartments that are subsequently delivered to the vacuole, suggesting that both ATI1 and ATI2 are involved in the selective degradation of certain proteins [54]. AGO1 (Argonaute1) is the key component of the RNA silencing pathway and plays an important role in host innate antiviral immunity [98], but plant viruses have evolved suppressors of RNA silencing to hijack the host AGO1 for their transmission [99]. In Arabidopsis, AGO1 interacts with ATI1 and ATI2 on the ER and is targeted to the vacuole by the induction of the polerovirus F-box P0 protein [55,100]. In addition, MSBP1 (Membrane Steroid Binding Protein 1) has also been identified as an ER-phagy cargo. MSBP1 is localized in the ER and interacts with both ATI1 and ATI2. Following carbon starvation and the application of concanamycin A, a V-ATPase inhibitor that stabilizes autophagic bodies, MSBP1 colocalizes with ATI1 and travels through the ER network to reach the vacuole for autophagic degradation [56]. It is worth noting that the

ATI1-mediated ER-phagy pathway is not induced by ER stress [56], which appears to be a distinct mechanism from other plant ER-phagy pathways.

As discussed above, the ER stress that triggers the UPR stimulates the production of many protein chaperones and folding catalysts, which is often accompanied with ER expansion to increase the protein folding capacity. Upon relief of the ER stress, eukaryotic cells need to reduce not only the abundance of those UPR-induced proteins but also the size of the ER network. In mammals, the translocon component Sec62 plays a crucial role in the recovER-phagy, a specific ER-phagy mechanism that re-establishes the ER homeostasis [101]. AtSec62, the Arabidopsis homolog of the mammalian Sec62, contains three transmembrane domains (TMDs) and a C-terminus luminal domain [57]. Loss-of-function mutations in AtSec62 lead to ER stress, impair vegetative growth, cause defective pollen development, and reduce fertility. Importantly, AtSec62 interacts with the Arabidopsis ATG8e through its AIMs upon ER stress induction [57]. Moreover, the overexpression of *AtSec62* in Arabidopsis enhances recovery from ER stress, a function similar to the mammalian Sec62 [57,101]. Thus, AtSec62 most likely functions as a plant ER-phagy receptor regulating the ER protein homeostasis and plays an important role in plant tolerance to environmental stresses.

It was known that maintaining the ER homeostasis requires dynamic changes in the ER structure consisting of interconnected branching tubules and flatten sacs/sheets throughout the entire cytoplasm [102]. Reticulons (Rtns) are a highly conserved eukaryotic protein family that mainly promotes the ER curvature [103]. Maize Rtn1 and Rtn2 are two ER-localized reticulon proteins that promote ER homeostasis in the aleurone cells of the corn endosperm. Rtn1/Rtn2 interact with the maize ATG8a, and their interactions were known to be enhanced upon treatment with the ER stress-inducing chemicals [58]. Importantly, the aleurone vacuoles of the maize *rtn1* and *rtn2* mutants accumulate many cytoplasmic fragments, suggesting that maize Rtn1 and Rtn2 could function as potential receptors for autophagy-mediated ER turnover [58]. In Arabidopsis, RTNLB3 (RTN-like B protein 3) and RTNLB13 were reported to physically interact with RHD3, a well-studied ER membrane-anchored atlastin-related GTPase important for the root hair development on the ER tubules that maintain the ER shape [104,105]. A recent study suggested that RHD3 might function as an ER-phagy receptor for selective ER protein degradation under ER stress based on its physical interaction with an Arabidopsis ATG8 and the reduced ER stress sensitivity and defective ER-phagy of the *rh3* mutant [59].

Arabidopsis C53 is a highly conserved soluble ER-phagy receptor discovered through an ATG8-based proteomic study [60]. Intriguingly, C53 localizes to the ER by forming a ternary receptor complex with the two key components of the ufmylation system known to be important for ER-phagy: UFL1 (ufmylation E3 ligase) and its substrate-recruitment adapter DDRGK1 (DDRGK domain-containing protein 1) [106]. Under normal conditions, C53 is kept in its inactive form by binding with another ubiquitin-like protein UFM1 (ufmylation modifier 1). However, certain ER stress-induced ribosome stalling transfers UFM1 to the translocon-associated ribosome via the UFL1-catalyzed ufmylation, thus freeing C53 for its binding to the phagophore-decorating ATG8 and activating the highly selective C53-mediated ER-phagy. Thus, the competitive binding of C53 with UFM1 and ATG8 plays a crucial role in coordinating the ribosome-associated protein quality control and selective autophagy [60]. Further investigation is necessary to fully understand the biochemical mechanism that links the UFL1-mediated ufmylation of ribosomal proteins with the C53-mediated ER-phagy.

5. Integrating ER Protein Homeostasis Strategies

The UPR and ERAD are two distinct but functionally connected cellular pathways that regulate ER homeostasis in response to cellular and environmental stress. Misfolded proteins accumulated in the ER are sensed via the UPR sensors, which activate several interdependent signaling cascades that reduce the influx of proteins into the ER and boost protein folding/refolding capacity [107]. Most genes encoding components and regulators

of the ERAD machinery are also induced by the UPR [108,109], thus promoting the ERAD and ER-phagy activity to dispose of misfolded proteins, improperly assembled protein complexes, large protein aggregates, and/or damaged ER fragments. Mutants with defective ERAD components often exhibit constitutive UPR activation and are hypersensitive to ER stress due to the over-accumulation of misfolded proteins in the ER [43,44,110]. The UPR can also be activated by various environmental stresses that interfere with protein folding or reduce ERAD efficiency or certain physiological conditions that demand much higher folding capacity. A short-term UPR is beneficial for cell survival by restoring ER homeostasis, but sustained overactivation of the UPR might trigger cellular dysfunction or even cell death [111]. In mammals, IRE1 α and ATF6 were found to be targeted for ERAD via the SEL1L-HRD1 protein complex, providing an effective autoregulatory strategy to restrain UPR hyperactivation [112,113], yet it remains unclear whether the protein stability of IRE1 homologs in yeast and plants is also regulated by the ERAD system. Recent studies have revealed that plant IRE1 plays an important role in coordinating the UPR and ER-phagy. In Arabidopsis, ER-phagy can be induced by ER stress-inducing chemicals, causing portions of the ER to be targeted to the vacuole [114]. Such a process likely involves AtIRE1B, because the loss-of-function *ire1b* mutation contained fewer ER stress-induced autophagosomes, compared to its wild-type control [114]. A recent study suggested that the RIDD but not the kinase activity of AtIRE1B is necessary for ER stress-induced autophagy via the degradation of the mRNAs of yet to be defined ER-phagy inhibitors [115]. In addition, many ER-phagy receptors are induced by UPR [101,116], suggesting that ER-phagy not only accelerates the turnover of the ER under stress conditions but also helps to restore the ER size and functions during the ER stress recovery period.

ERAD and ER-phagy are the two major intracellular proteolytic pathways that selectively degrade target proteins to maintain ER homeostasis. It has been suggested that ERAD mainly degrades detergent-soluble misfolded proteins in a substrate-specific manner, but ER-phagy is responsible for the degradation of detergent-insoluble protein aggregates and damaged/excess ER fragments [117]. How cells coordinate the two different degradation pathways remains a major question. The Z variant of human α -1 proteinase inhibitor (A1PiZ) is a misfolded protein that can be recognized and degraded by the ERAD system in yeast and humans [118,119]. However, excessive accumulation of A1PiZ, which aggregates in the ER, is targeted to the vacuole via an autophagy pathway [118], suggesting that cells could resort to distinct strategies to degrade misfolded proteins depending on the abundance of substrates. Similarly, it was found that the deficiency of SEL1L-HRD1 ERAD in β cells resulted in the accumulation of proinsulin in the ER as high molecular weight conformers, which activate the ER-phagy pathway to eliminate these misfolded proinsulin proteins and their aggregates. However, when both SEL1L and autophagy are absent in β cells, mice develop diabetes shortly after weaning and die prematurely [120], suggesting that the induction of ER-phagy in the absence of ERAD might be a beneficial adaptation for cells to cope with the abnormal accumulation of misfolded proteins in the ER. Furthermore, it was revealed that SEL1L-HRD1 ERAD may have an impact on ER-phagy activity by limiting the availability of its substrate (ER fragments). It is only when SEL1L-HRD1 ERAD is compromised that the ER will be fragmented and then eliminated through ER-phagy [121]. CDC48 plays a vital role in many cellular processes that are essential for cell viability [53,122]. In ERAD, CDC48 is required for extracting ubiquitinated substrates from ER membranes for proteasomal degradation [83]. Interestingly, CDC48 is shown to be involved in the autophagy pathway, with CDC48 and its cofactor Shp1/Ubx1 being identified as essential components for the biogenesis of autophagosomes [123]. A recent study has found that non-functional CDC48 complexes can be eliminated through UIM-directed autophagy, which relies on the ubiquitin-interacting motif (UIM) sequences to bind to ATG8 [124,125]. In Arabidopsis, plant UBX domain-containing (PUX) protein PUX7, 8, 9, and 13 bind to ATG8 with their UIM motifs, thus allowing for the autophagic degradation of the inactive CDC48 [125]. Given the essential role of CDC48 in ERAD,

further study is necessary to ascertain whether the ERAD pathway is regulated through autophagy via the CDC48 protein.

6. Concluding Remarks

Eukaryotes have evolved diverse ER quality control systems to maintain ER homeostasis. In recent years, despite the rapid progress made in understanding the processes and functions of the UPR, ERAD, and ER-phagy in yeast and mammalian cells, there are still many unanswered questions about these processes and functions in plants. Firstly, plants have developed conserved but different mechanisms to confront ER stress in response to changing environments. Further studies are needed to understand the molecular mechanisms of plant-specific proteins in the UPR pathway and to explore both their roles in controlling the expression of multiple UPR genes and their impact on cellular functions. In particular, the integration of the UPR with multiple plant physiological signals needs to be investigated. Secondly, the UPR and ERAD are interconnected processes that work together to maintain proteome integrity in the ER, and the crosstalk between the UPR and ERAD involves multiple regulatory mechanisms that require further investigation. In addition, it remains unclear when a misfolded protein terminates its futile repair process and enters into the ERAD pathway. Thirdly, plants have specific ERAD components that play essential roles in maintaining the stability of the Hrd1 complex, and elucidating the biological function and mechanistic details of these plant-specific components will help us to better understand the plant ERAD system. Meanwhile, recent advances in cryo-EM and proximity labeling proteomics offer the potential to explore the mechanisms underlying substrate recognition, retrotranslocation, and ubiquitin processing. In addition to the degradation of misfolded proteins, the ERAD system is also responsible for the quantity control of folding-competent proteins. Therefore, the plant endogenous substrates that are mediated by ERAD should be identified in future studies. Finally, the specific interplay and regulatory mechanisms between ERAD and ER-phagy in plants are not yet fully understood. Further research is needed to elucidate how ERAD may influence or be influenced by ER-phagy and to determine the molecular components and signaling pathways involved in this crosstalk.

Author Contributions: Writing—original draft preparation, Z.D., K.C., T.Y., R.Y. and B.C.; figure and table organization—Z.D. and T.Y.; writing—review and editing, J.L. and L.L.; funding acquisition, J.L. and L.L. All authors have read and agreed to the published version of the manuscript.

Funding: This work was partially funded by grants from the National Natural Science Foundation of China (No. 31970187, 31600996 to L.L. and No. 31730019 to J.L.) and the Guangdong Basic and Applied Basic Research Foundation (No. 2022A1515010803 to L.L.).

Institutional Review Board Statement: Not applicable.

Informed Consent Statement: Not applicable.

Data Availability Statement: No new data were created or analyzed in this study. Data sharing is not applicable to this article.

Acknowledgments: We greatly acknowledge all the authors in the field whose primary research could not be cited in this review due to space limitations.

Conflicts of Interest: The authors declare no conflict of interest.

References

1. Chen, S.; Novick, P.; Ferro-Novick, S. ER structure and function. *Curr. Opin. Cell Biol.* **2013**, *25*, 428–433. [[CrossRef](#)] [[PubMed](#)]
2. Schwarz, D.S.; Blower, M.D. The endoplasmic reticulum: Structure, function and response to cellular signaling. *Cell Mol. Life Sci.* **2016**, *73*, 79–94. [[CrossRef](#)] [[PubMed](#)]
3. Sun, Z.; Brodsky, J.L. Protein quality control in the secretory pathway. *J. Cell Biol.* **2019**, *218*, 3171–3187. [[CrossRef](#)] [[PubMed](#)]
4. Howell, S.H. Endoplasmic reticulum stress responses in plants. *Annu. Rev. Plant Biol.* **2013**, *64*, 477–499. [[CrossRef](#)] [[PubMed](#)]
5. Braakman, I.; Bulleid, N.J. Protein folding and modification in the mammalian endoplasmic reticulum. *Annu. Rev. Biochem.* **2011**, *80*, 71–99. [[CrossRef](#)] [[PubMed](#)]

6. Hetz, C.; Zhang, K.; Kaufman, R.J. Mechanisms, regulation and functions of the unfolded protein response. *Nat. Rev. Mol. Cell Biol.* **2020**, *21*, 421–438. [\[CrossRef\]](#)
7. Krshnan, L.; van de Weijer, M.L.; Carvalho, P. Endoplasmic Reticulum-Associated Protein Degradation. *Cold Spring Harb. Perspect. Biol.* **2022**, *14*, a041247. [\[CrossRef\]](#)
8. Chen, Q.; Yu, F.; Xie, Q. Insights into endoplasmic reticulum-associated degradation in plants. *New Phytol.* **2020**, *226*, 345–350. [\[CrossRef\]](#)
9. Liu, Y.; Li, J. Endoplasmic reticulum-mediated protein quality control in Arabidopsis. *Front. Plant Sci.* **2014**, *5*, 162. [\[CrossRef\]](#)
10. Chino, H.; Mizushima, N. ER-Phagy: Quality Control and Turnover of Endoplasmic Reticulum. *Trends Cell Biol.* **2020**, *30*, 384–398. [\[CrossRef\]](#)
11. Rapoport, T.A.; Li, L.; Park, E. Structural and Mechanistic Insights into Protein Translocation. *Annu. Rev. Cell Dev. Biol.* **2017**, *33*, 369–390. [\[CrossRef\]](#) [\[PubMed\]](#)
12. Balchin, D.; Hayer-Hartl, M.; Hartl, F.U. In vivo aspects of protein folding and quality control. *Science* **2016**, *353*, aac4354. [\[CrossRef\]](#) [\[PubMed\]](#)
13. Jin, H.; Yan, Z.; Nam, K.H.; Li, J. Allele-specific suppression of a defective brassinosteroid receptor reveals a physiological role of UGGT in ER quality control. *Mol. Cell* **2007**, *26*, 821–830. [\[CrossRef\]](#) [\[PubMed\]](#)
14. Jin, H.; Hong, Z.; Su, W.; Li, J. A plant-specific calreticulin is a key retention factor for a defective brassinosteroid receptor in the endoplasmic reticulum. *Proc. Natl. Acad. Sci. USA* **2009**, *106*, 13612–13617. [\[CrossRef\]](#) [\[PubMed\]](#)
15. Tirasophon, W.; Welihinda, A.A.; Kaufman, R.J. A stress response pathway from the endoplasmic reticulum to the nucleus requires a novel bifunctional protein kinase/endoribonuclease (Ire1p) in mammalian cells. *Genes Dev.* **1998**, *12*, 1812–1824. [\[CrossRef\]](#) [\[PubMed\]](#)
16. Wang, X.Z.; Harding, H.P.; Zhang, Y.; Jolicoeur, E.M.; Kuroda, M.; Ron, D. Cloning of mammalian Ire1 reveals diversity in the ER stress responses. *EMBO J.* **1998**, *17*, 5708–5717. [\[CrossRef\]](#) [\[PubMed\]](#)
17. Haze, K.; Yoshida, H.; Yanagi, H.; Yura, T.; Mori, K. Mammalian transcription factor ATF6 is synthesized as a transmembrane protein and activated by proteolysis in response to endoplasmic reticulum stress. *Mol. Biol. Cell* **1999**, *10*, 3787–3799. [\[CrossRef\]](#)
18. Harding, H.P.; Zhang, Y.; Ron, D. Protein translation and folding are coupled by an endoplasmic-reticulum-resident kinase. *Nature* **1999**, *397*, 271–274. [\[CrossRef\]](#)
19. Howell, S.H. Evolution of the unfolded protein response in plants. *Plant Cell Environ.* **2021**, *44*, 2625–2635. [\[CrossRef\]](#)
20. Koizumi, N.; Martinez, I.M.; Kimata, Y.; Kohno, K.; Sano, H.; Chrispeels, M.J. Molecular characterization of two Arabidopsis Ire1 homologs, endoplasmic reticulum-located transmembrane protein kinases. *Plant Physiol.* **2001**, *127*, 949–962. [\[CrossRef\]](#)
21. Noh, S.J.; Kwon, C.S.; Chung, W.I. Characterization of two homologs of Ire1p, a kinase/endoribonuclease in yeast, in *Arabidopsis thaliana*. *Biochim. Biophys. Acta* **2002**, *1575*, 130–134. [\[CrossRef\]](#) [\[PubMed\]](#)
22. Nagashima, Y.; Mishiba, K.; Suzuki, E.; Shimada, Y.; Iwata, Y.; Koizumi, N. Arabidopsis IRE1 catalyses unconventional splicing of bZIP60 mRNA to produce the active transcription factor. *Sci. Rep.* **2011**, *1*, 29. [\[CrossRef\]](#) [\[PubMed\]](#)
23. Deng, Y.; Humbert, S.; Liu, J.X.; Srivastava, R.; Rothstein, S.J.; Howell, S.H. Heat induces the splicing by IRE1 of a mRNA encoding a transcription factor involved in the unfolded protein response in Arabidopsis. *Proc. Natl. Acad. Sci. USA* **2011**, *108*, 7247–7252. [\[CrossRef\]](#) [\[PubMed\]](#)
24. Afrin, T.; Seok, M.; Terry, B.C.; Pajerowska-Mukhtar, K.M. Probing natural variation of IRE1 expression and endoplasmic reticulum stress responses in Arabidopsis accessions. *Sci. Rep.* **2020**, *10*, 19154. [\[CrossRef\]](#) [\[PubMed\]](#)
25. Mishiba, K.I.; Iwata, Y.; Mochizuki, T.; Matsumura, A.; Nishioka, N.; Hirata, R.; Koizumi, N. Unfolded protein-independent IRE1 activation contributes to multifaceted developmental processes in Arabidopsis. *Life Sci. Alliance* **2019**, *2*, e201900459. [\[CrossRef\]](#) [\[PubMed\]](#)
26. Pu, Y.; Ruberti, C.; Angelos, E.R.; Brandizzi, F. AtIRE1C, an unconventional isoform of the UPR master regulator AtIRE1, is functionally associated with AtIRE1B in Arabidopsis gametogenesis. *Plant Direct* **2019**, *3*, e00187. [\[CrossRef\]](#) [\[PubMed\]](#)
27. Hollien, J.; Weissman, J.S. Decay of endoplasmic reticulum-localized mRNAs during the unfolded protein response. *Science* **2006**, *313*, 104–107. [\[CrossRef\]](#)
28. Kimmig, P.; Diaz, M.; Zheng, J.; Williams, C.C.; Lang, A.; Aragon, T.; Li, H.; Walter, P. The unfolded protein response in fission yeast modulates stability of select mRNAs to maintain protein homeostasis. *Elife* **2012**, *1*, e00048. [\[CrossRef\]](#)
29. Mishiba, K.; Nagashima, Y.; Suzuki, E.; Hayashi, N.; Ogata, Y.; Shimada, Y.; Koizumi, N. Defects in IRE1 enhance cell death and fail to degrade mRNAs encoding secretory pathway proteins in the Arabidopsis unfolded protein response. *Proc. Natl. Acad. Sci. USA* **2013**, *110*, 5713–5718. [\[CrossRef\]](#)
30. Liu, J.X.; Srivastava, R.; Che, P.; Howell, S.H. An endoplasmic reticulum stress response in Arabidopsis is mediated by proteolytic processing and nuclear relocation of a membrane-associated transcription factor, bZIP28. *Plant Cell* **2007**, *19*, 4111–4119. [\[CrossRef\]](#)
31. Liu, J.X.; Srivastava, R.; Che, P.; Howell, S.H. Salt stress responses in Arabidopsis utilize a signal transduction pathway related to endoplasmic reticulum stress signaling. *Plant J.* **2007**, *51*, 897–909. [\[CrossRef\]](#) [\[PubMed\]](#)
32. Ko, D.K.; Kim, J.Y.; Thibault, E.A.; Brandizzi, F. An IRE1-proteasome system signalling cohort controls cell fate determination in unresolved proteotoxic stress of the plant endoplasmic reticulum. *Nat. Plants* **2023**, *9*, 1333–1346. [\[CrossRef\]](#) [\[PubMed\]](#)
33. Ko, D.K.; Brandizzi, F. Advanced genomics identifies growth effectors for proteotoxic ER stress recovery in *Arabidopsis thaliana*. *Commun. Biol.* **2022**, *5*, 16. [\[CrossRef\]](#) [\[PubMed\]](#)

34. Sun, L.; Yang, Z.T.; Song, Z.T.; Wang, M.J.; Sun, L.; Lu, S.J.; Liu, J.X. The plant-specific transcription factor gene NAC103 is induced by bZIP60 through a new cis-regulatory element to modulate the unfolded protein response in Arabidopsis. *Plant J.* **2013**, *76*, 274–286. [[CrossRef](#)] [[PubMed](#)]
35. Yang, Z.T.; Lu, S.J.; Wang, M.J.; Bi, D.L.; Sun, L.; Zhou, S.F.; Song, Z.T.; Liu, J.X. A plasma membrane-tethered transcription factor, NAC062/ANAC062/NTL6, mediates the unfolded protein response in Arabidopsis. *Plant J.* **2014**, *79*, 1033–1043. [[CrossRef](#)] [[PubMed](#)]
36. Yang, Z.T.; Wang, M.J.; Sun, L.; Lu, S.J.; Bi, D.L.; Sun, L.; Song, Z.T.; Zhang, S.S.; Zhou, S.F.; Liu, J.X. The membrane-associated transcription factor NAC089 controls ER-stress-induced programmed cell death in plants. *PLoS Genet.* **2014**, *10*, e1004243. [[CrossRef](#)] [[PubMed](#)]
37. Yu, C.Y.; Kanehara, K. The Unfolded Protein Response Modulates a Phosphoinositide-Binding Protein through the IRE1-bZIP60 Pathway. *Plant Physiol.* **2020**, *183*, 221–235. [[CrossRef](#)]
38. Yu, C.Y.; Sharma, O.; Nguyen, P.H.T.; Hartono, C.D.; Kanehara, K. A pair of DUF538 domain-containing proteins modulates plant growth and trichome development through the transcriptional regulation of GLABRA1 in *Arabidopsis thaliana*. *Plant J.* **2021**, *108*, 992–1004. [[CrossRef](#)]
39. Su, W.; Liu, Y.; Xia, Y.; Hong, Z.; Li, J. Conserved endoplasmic reticulum-associated degradation system to eliminate mutated receptor-like kinases in Arabidopsis. *Proc. Natl. Acad. Sci. USA* **2011**, *108*, 870–875. [[CrossRef](#)]
40. Liu, L.; Cui, F.; Li, Q.; Yin, B.; Zhang, H.; Lin, B.; Wu, Y.; Xia, R.; Tang, S.; Xie, Q. The endoplasmic reticulum-associated degradation is necessary for plant salt tolerance. *Cell Res.* **2011**, *21*, 957–969. [[CrossRef](#)]
41. Hüttner, S.; Veit, C.; Schoberer, J.; Grass, J.; Strasser, R. Unraveling the function of *Arabidopsis thaliana* OS9 in the endoplasmic reticulum-associated degradation of glycoproteins. *Plant Mol. Biol.* **2012**, *79*, 21–33. [[CrossRef](#)] [[PubMed](#)]
42. Su, W.; Liu, Y.; Xia, Y.; Hong, Z.; Li, J. The Arabidopsis homolog of the mammalian OS-9 protein plays a key role in the endoplasmic reticulum-associated degradation of misfolded receptor-like kinases. *Mol. Plant* **2012**, *5*, 929–940. [[CrossRef](#)] [[PubMed](#)]
43. Liu, Y.; Zhang, C.; Wang, D.; Su, W.; Liu, L.; Wang, M.; Li, J. EBS7 is a plant-specific component of a highly conserved endoplasmic reticulum-associated degradation system in Arabidopsis. *Proc. Natl. Acad. Sci. USA* **2015**, *112*, 12205–12210. [[CrossRef](#)] [[PubMed](#)]
44. Lin, L.; Zhang, C.; Chen, Y.; Wang, Y.; Wang, D.; Liu, X.; Wang, M.; Mao, J.; Zhang, J.; Xing, W.; et al. PAWH1 and PAWH2 are plant-specific components of an Arabidopsis endoplasmic reticulum-associated degradation complex. *Nat. Commun.* **2019**, *10*, 3492. [[CrossRef](#)] [[PubMed](#)]
45. Cui, F.; Liu, L.; Zhao, Q.; Zhang, Z.; Li, Q.; Lin, B.; Wu, Y.; Tang, S.; Xie, Q. Arabidopsis ubiquitin conjugase UBC32 is an ERAD component that functions in brassinosteroid-mediated salt stress tolerance. *Plant Cell* **2012**, *24*, 233–244. [[CrossRef](#)] [[PubMed](#)]
46. Wang, Y.; Yue, J.; Yang, N.; Zheng, C.; Zheng, Y.; Wu, X.; Yang, J.; Zhang, H.; Liu, L.; Ning, Y.; et al. An ERAD-related ubiquitin-conjugating enzyme boosts broad-spectrum disease resistance and yield in rice. *Nat. Food* **2023**, *4*, 774–787. [[CrossRef](#)] [[PubMed](#)]
47. Chen, Q.; Zhong, Y.; Wu, Y.; Liu, L.; Wang, P.; Liu, R.; Cui, F.; Li, Q.; Yang, X.; Fang, S.; et al. HRD1-mediated ERAD tuning of ER-bound E2 is conserved between plants and mammals. *Nat. Plants* **2016**, *2*, 16094. [[CrossRef](#)]
48. Doblas, V.G.; Amorim-Silva, V.; Pose, D.; Rosado, A.; Esteban, A.; Arro, M.; Azevedo, H.; Bombarely, A.; Borsani, O.; Valpuesta, V.; et al. The SUD1 gene encodes a putative E3 ubiquitin ligase and is a positive regulator of 3-hydroxy-3-methylglutaryl coenzyme a reductase activity in Arabidopsis. *Plant Cell* **2013**, *25*, 728–743. [[CrossRef](#)]
49. Etherington, R.D.; Bailey, M.; Boyer, J.B.; Armbruster, L.; Cao, X.; Coates, J.C.; Meinnel, T.; Wirtz, M.; Giglione, C.; Gibbs, D.J. Nt-acetylation-independent turnover of SQUALENE EPOXIDASE 1 by Arabidopsis DOA10-like E3 ligases. *Plant Physiol.* **2023**, *193*, 2086–2104. [[CrossRef](#)]
50. Lee, H.K.; Cho, S.K.; Son, O.; Xu, Z.; Hwang, I.; Kim, W.T. Drought stress-induced Rma1H1, a RING membrane-anchor E3 ubiquitin ligase homolog, regulates aquaporin levels via ubiquitination in transgenic Arabidopsis plants. *Plant Cell* **2009**, *21*, 622–641. [[CrossRef](#)]
51. Chen, Q.; Liu, R.; Wu, Y.; Wei, S.; Wang, Q.; Zheng, Y.; Xia, R.; Shang, X.; Yu, F.; Yang, X.; et al. ERAD-related E2 and E3 enzymes modulate the drought response by regulating the stability of PIP2 aquaporins. *Plant Cell* **2021**, *33*, 2883–2898. [[CrossRef](#)] [[PubMed](#)]
52. Park, J.H.; Kang, C.H.; Nawkar, G.M.; Lee, E.S.; Paeng, S.K.; Chae, H.B.; Chi, Y.H.; Kim, W.Y.; Yun, D.J.; Lee, S.Y. EMR, a cytosolic-abundant ring finger E3 ligase, mediates ER-associated protein degradation in Arabidopsis. *New Phytol.* **2018**, *220*, 163–177. [[CrossRef](#)] [[PubMed](#)]
53. Stolz, A.; Hilt, W.; Buchberger, A.; Wolf, D.H. Cdc48: A power machine in protein degradation. *Trends Biochem. Sci.* **2011**, *36*, 515–523. [[CrossRef](#)] [[PubMed](#)]
54. Honig, A.; Avin-Wittenberg, T.; Ufaz, S.; Galili, G. A new type of compartment, defined by plant-specific Atg8-interacting proteins, is induced upon exposure of Arabidopsis plants to carbon starvation. *Plant Cell* **2012**, *24*, 288–303. [[CrossRef](#)] [[PubMed](#)]
55. Michaeli, S.; Clavel, M.; Lechner, E.; Viotti, C.; Wu, J.; Dubois, M.; Hacquard, T.; Derrien, B.; Izquierdo, E.; Lecorbeiller, M.; et al. The viral F-box protein P0 induces an ER-derived autophagy degradation pathway for the clearance of membrane-bound AGO1. *Proc. Natl. Acad. Sci. USA* **2019**, *116*, 22872–22883. [[CrossRef](#)] [[PubMed](#)]
56. Wu, J.; Michaeli, S.; Picchianti, L.; Dagdas, Y.; Galili, G.; Peled-Zehavi, H. ATI1 (ATG8-interacting protein 1) and ATI2 define a plant starvation-induced reticulophagy pathway and serve as MSBP1/MAPR5 cargo receptors. *Autophagy* **2021**, *17*, 3375–3388. [[CrossRef](#)]

57. Hu, S.; Ye, H.; Cui, Y.; Jiang, L. AtSec62 is critical for plant development and is involved in ER-phagy in *Arabidopsis thaliana*. *J. Integr. Plant Biol.* **2020**, *62*, 181–200. [[CrossRef](#)]
58. Zhang, X.; Ding, X.; Marshall, R.S.; Paez-Valencia, J.; Lacey, P.; Vierstra, R.D.; Otegui, M.S. Reticulon proteins modulate autophagy of the endoplasmic reticulum in maize endosperm. *Elife* **2020**, *9*, e51918. [[CrossRef](#)]
59. Sun, J.; Wang, W.; Zheng, H. ROOT HAIR DEFECTIVE3 Is a Receptor for Selective Autophagy of the Endoplasmic Reticulum in Arabidopsis. *Front. Plant Sci.* **2022**, *13*, 817251. [[CrossRef](#)]
60. Stephani, M.; Picchianti, L.; Gajic, A.; Beveridge, R.; Skarwan, E.; Sanchez de Medina Hernandez, V.; Mohseni, A.; Clavel, M.; Zeng, Y.; Naumann, C.; et al. A cross-kingdom conserved ER-phagy receptor maintains endoplasmic reticulum homeostasis during stress. *Elife* **2020**, *9*, e58396. [[CrossRef](#)]
61. Ko, D.K.; Brandizzi, F. Transcriptional competition shapes proteotoxic ER stress resolution. *Nat. Plants* **2022**, *8*, 481–490. [[CrossRef](#)] [[PubMed](#)]
62. Ko, D.K.; Brandizzi, F. Coexpression Network Construction and Visualization from Transcriptomes Underlying ER Stress Responses. *Methods Mol. Biol.* **2023**, *2581*, 385–401. [[CrossRef](#)] [[PubMed](#)]
63. Credle, J.J.; Finer-Moore, J.S.; Papa, F.R.; Stroud, R.M.; Walter, P. On the mechanism of sensing unfolded protein in the endoplasmic reticulum. *Proc. Natl. Acad. Sci. USA* **2005**, *102*, 18773–18784. [[CrossRef](#)] [[PubMed](#)]
64. Zhou, J.; Liu, C.Y.; Back, S.H.; Clark, R.L.; Peisach, D.; Xu, Z.; Kaufman, R.J. The crystal structure of human IRE1 luminal domain reveals a conserved dimerization interface required for activation of the unfolded protein response. *Proc. Natl. Acad. Sci. USA* **2006**, *103*, 14343–14348. [[CrossRef](#)] [[PubMed](#)]
65. Kopp, M.C.; Larburu, N.; Durairaj, V.; Adams, C.J.; Ali, M.M.U. UPR proteins IRE1 and PERK switch BiP from chaperone to ER stress sensor. *Nat. Struct. Mol. Biol.* **2019**, *26*, 1053–1062. [[CrossRef](#)] [[PubMed](#)]
66. Carrara, M.; Prisci, F.; Nowak, P.R.; Kopp, M.C.; Ali, M.M. Noncanonical binding of BiP ATPase domain to Ire1 and Perk is dissociated by unfolded protein CH1 to initiate ER stress signaling. *Elife* **2015**, *4*, e03522. [[CrossRef](#)] [[PubMed](#)]
67. Kopp, M.C.; Nowak, P.R.; Larburu, N.; Adams, C.J.; Ali, M.M. In vitro FRET analysis of IRE1 and BiP association and dissociation upon endoplasmic reticulum stress. *Elife* **2018**, *7*, e30257. [[CrossRef](#)]
68. Shen, J.; Chen, X.; Hendershot, L.; Prywes, R. ER stress regulation of ATF6 localization by dissociation of BiP/GRP78 binding and unmasking of Golgi localization signals. *Dev. Cell* **2002**, *3*, 99–111. [[CrossRef](#)]
69. Srivastava, R.; Deng, Y.; Shah, S.; Rao, A.G.; Howell, S.H. BINDING PROTEIN is a master regulator of the endoplasmic reticulum stress sensor/transducer bZIP28 in Arabidopsis. *Plant Cell* **2013**, *25*, 1416–1429. [[CrossRef](#)]
70. Eletto, D.; Eletto, D.; Dersh, D.; Gidalevitz, T.; Argon, Y. Protein disulfide isomerase A6 controls the decay of IRE1alpha signaling via disulfide-dependent association. *Mol. Cell* **2014**, *53*, 562–576. [[CrossRef](#)]
71. Oka, O.B.; van Lith, M.; Rudolf, J.; Tungsum, W.; Pringle, M.A.; Bulleid, N.J. ERp18 regulates activation of ATF6alpha during unfolded protein response. *EMBO J.* **2019**, *38*, e100990. [[CrossRef](#)] [[PubMed](#)]
72. Higa, A.; Taouji, S.; Lhomond, S.; Jensen, D.; Fernandez-Zapico, M.E.; Simpson, J.C.; Pasquet, J.M.; Schekman, R.; Chevet, E. Endoplasmic reticulum stress-activated transcription factor ATF6alpha requires the disulfide isomerase PDIA5 to modulate chemoresistance. *Mol. Cell Biol.* **2014**, *34*, 1839–1849. [[CrossRef](#)] [[PubMed](#)]
73. Quan, E.M.; Kamiya, Y.; Kamiya, D.; Denic, V.; Weibezahn, J.; Kato, K.; Weissman, J.S. Defining the glycan destruction signal for endoplasmic reticulum-associated degradation. *Mol. Cell* **2008**, *32*, 870–877. [[CrossRef](#)] [[PubMed](#)]
74. Clerc, S.; Hirsch, C.; Oggier, D.M.; Deprez, P.; Jakob, C.; Sommer, T.; Aebi, M. Htm1 protein generates the N-glycan signal for glycoprotein degradation in the endoplasmic reticulum. *J. Cell Biol.* **2009**, *184*, 159–172. [[CrossRef](#)] [[PubMed](#)]
75. Hanna, J.; Schutz, A.; Zimmermann, F.; Behlke, J.; Sommer, T.; Heinemann, U. Structural and biochemical basis of Yos9 protein dimerization and possible contribution to self-association of 3-hydroxy-3-methylglutaryl-coenzyme A reductase degradation ubiquitin-ligase complex. *J. Biol. Chem.* **2012**, *287*, 8633–8640. [[CrossRef](#)] [[PubMed](#)]
76. Carvalho, P.; Goder, V.; Rapoport, T.A. Distinct ubiquitin-ligase complexes define convergent pathways for the degradation of ER proteins. *Cell* **2006**, *126*, 361–373. [[CrossRef](#)] [[PubMed](#)]
77. Christianson, J.C.; Carvalho, P. Order through destruction: How ER-associated protein degradation contributes to organelle homeostasis. *EMBO J.* **2022**, *41*, e109845. [[CrossRef](#)]
78. Vasic, V.; Denkert, N.; Schmidt, C.C.; Riedel, D.; Stein, A.; Meinecke, M. Hrd1 forms the retrotranslocation pore regulated by auto-ubiquitination and binding of misfolded proteins. *Nat. Cell Biol.* **2020**, *22*, 274–281. [[CrossRef](#)]
79. Schmidt, C.C.; Vasic, V.; Stein, A. Doa10 is a membrane protein retrotranslocase in ER-associated protein degradation. *Elife* **2020**, *9*, e56945. [[CrossRef](#)]
80. Schoebel, S.; Mi, W.; Stein, A.; Ovchinnikov, S.; Pavlovicz, R.; DiMaio, F.; Baker, D.; Chambers, M.G.; Su, H.; Li, D.; et al. Cryo-EM structure of the protein-conducting ERAD channel Hrd1 in complex with Hrd3. *Nature* **2017**, *548*, 352–355. [[CrossRef](#)]
81. Neal, S.; Jaeger, P.A.; Duttke, S.H.; Benner, C.; Glass, C.K.; Ideker, T.; Hampton, R.Y. The Dfm1 Derlin Is Required for ERAD Retrotranslocation of Integral Membrane Proteins. *Mol. Cell* **2018**, *69*, 915. [[CrossRef](#)] [[PubMed](#)]
82. Mehnert, M.; Sommer, T.; Jarosch, E. Der1 promotes movement of misfolded proteins through the endoplasmic reticulum membrane. *Nat. Cell Biol.* **2014**, *16*, 77–86. [[CrossRef](#)] [[PubMed](#)]
83. Christianson, J.C.; Jarosch, E.; Sommer, T. Mechanisms of substrate processing during ER-associated protein degradation. *Nat. Rev. Mol. Cell Biol.* **2023**, *24*, 777–796. [[CrossRef](#)] [[PubMed](#)]

84. Vitale, A.; Boston, R.S. Endoplasmic reticulum quality control and the unfolded protein response: Insights from plants. *Traffic* **2008**, *9*, 1581–1588. [[CrossRef](#)] [[PubMed](#)]
85. Saijo, Y.; Tintor, N.; Lu, X.; Rauf, P.; Pajeroska-Mukhtar, K.; Haweker, H.; Dong, X.; Robatzek, S.; Schulze-Lefert, P. Receptor quality control in the endoplasmic reticulum for plant innate immunity. *EMBO J.* **2009**, *28*, 3439–3449. [[CrossRef](#)] [[PubMed](#)]
86. Müller, J.; Piffanelli, P.; Devoto, A.; Miklis, M.; Elliott, C.; Ortmann, B.; Schulze-Lefert, P.; Panstruga, R. Conserved ERAD-like quality control of a plant polytopic membrane protein. *Plant Cell* **2005**, *17*, 149–163. [[CrossRef](#)] [[PubMed](#)]
87. Hong, Z.; Jin, H.; Tzfira, T.; Li, J. Multiple mechanism-mediated retention of a defective brassinosteroid receptor in the endoplasmic reticulum of Arabidopsis. *Plant Cell* **2008**, *20*, 3418–3429. [[CrossRef](#)]
88. Guan, Y.; Chang, G.; Zhao, J.; Wang, Q.; Qin, J.; Tang, M.; Wang, S.; Ma, L.; Ma, J.; Sun, G.; et al. Parallel evolution of two AIM24 protein subfamilies and their conserved functions in ER stress tolerance in land plants. *Plant Commun.* **2023**, *4*, 100513. [[CrossRef](#)]
89. Lu, S.; Zhao, H.; Des Marais, D.L.; Parsons, E.P.; Wen, X.; Xu, X.; Bangarusamy, D.K.; Wang, G.; Rowland, O.; Juenger, T.; et al. Arabidopsis ECERIFERUM9 involvement in cuticle formation and maintenance of plant water status. *Plant Physiol.* **2012**, *159*, 930–944. [[CrossRef](#)]
90. Bhattacharya, A.; Qi, L. ER-associated degradation in health and disease—From substrate to organism. *J. Cell Sci.* **2019**, *132*, jcs232850. [[CrossRef](#)]
91. Cui, F.; Liu, L.; Li, Q.; Yang, C.; Xie, Q. UBC32 mediated oxidative tolerance in Arabidopsis. *J. Genet. Genom.* **2012**, *39*, 415–417. [[CrossRef](#)] [[PubMed](#)]
92. Li, L.M.; Lü, S.Y.; Li, R.J. The Arabidopsis endoplasmic reticulum associated degradation pathways are involved in the regulation of heat stress response. *Biochem. Biophys. Res. Commun.* **2017**, *487*, 362–367. [[CrossRef](#)] [[PubMed](#)]
93. Chen, Q.; Liu, R.; Wang, Q.; Xie, Q. ERAD Tuning of the HRD1 Complex Component AtOS9 Is Modulated by an ER-Bound E2, UBC32. *Mol. Plant* **2017**, *10*, 891–894. [[CrossRef](#)] [[PubMed](#)]
94. Mochida, K.; Nakatogawa, H. ER-phagy: Selective autophagy of the endoplasmic reticulum. *EMBO Rep.* **2022**, *23*, e55192. [[CrossRef](#)] [[PubMed](#)]
95. Molinari, M. ER-phagy responses in yeast, plants, and mammalian cells and their crosstalk with UPR and ERAD. *Dev. Cell* **2021**, *56*, 949–966. [[CrossRef](#)] [[PubMed](#)]
96. Ferro-Novick, S.; Reggiori, F.; Brodsky, J.L. ER-Phagy, ER Homeostasis, and ER Quality Control: Implications for Disease. *Trends Biochem. Sci.* **2021**, *46*, 630–639. [[CrossRef](#)]
97. Bao, Y.; Bassham, D.C. ER-Phagy and Its Role in ER Homeostasis in Plants. *Plants* **2020**, *9*, 1771. [[CrossRef](#)]
98. Qu, F.; Ye, X.; Morris, T.J. Arabidopsis DRB4, AGO1, AGO7, and RDR6 participate in a DCL4-initiated antiviral RNA silencing pathway negatively regulated by DCL1. *Proc. Natl. Acad. Sci. USA* **2008**, *105*, 14732–14737. [[CrossRef](#)]
99. Derrien, B.; Clavel, M.; Baumberger, N.; Iki, T.; Sarazin, A.; Hacquard, T.; Ponce, M.R.; Ziegler-Graff, V.; Vaucheret, H.; Micol, J.L.; et al. A Suppressor Screen for AGO1 Degradation by the Viral F-Box P0 Protein Uncovers a Role for AGO DUF1785 in sRNA Duplex Unwinding. *Plant Cell* **2018**, *30*, 1353–1374. [[CrossRef](#)]
100. Derrien, B.; Baumberger, N.; Schepetilnikov, M.; Viotti, C.; De Cillia, J.; Ziegler-Graff, V.; Isono, E.; Schumacher, K.; Genschik, P. Degradation of the antiviral component ARGONAUTE1 by the autophagy pathway. *Proc. Natl. Acad. Sci. USA* **2012**, *109*, 15942–15946. [[CrossRef](#)]
101. Fumagalli, F.; Noack, J.; Bergmann, T.J.; Cebollero, E.; Pisoni, G.B.; Fasana, E.; Fregno, I.; Galli, C.; Loi, M.; Soldà, T.; et al. Translocon component Sec62 acts in endoplasmic reticulum turnover during stress recovery. *Nat. Cell Biol.* **2016**, *18*, 1173–1184. [[CrossRef](#)] [[PubMed](#)]
102. Brandizzi, F. Maintaining the structural and functional homeostasis of the plant endoplasmic reticulum. *Dev. Cell* **2021**, *56*, 919–932. [[CrossRef](#)] [[PubMed](#)]
103. Wang, N.; Clark, L.D.; Gao, Y.; Kozlov, M.M.; Shemesh, T.; Rapoport, T.A. Mechanism of membrane-curvature generation by ER-tubule shaping proteins. *Nat. Commun.* **2021**, *12*, 568. [[CrossRef](#)] [[PubMed](#)]
104. Wang, H.; Lockwood, S.K.; Hoeltzel, M.F.; Schiefelbein, J.W. The ROOT HAIR DEFECTIVE3 gene encodes an evolutionarily conserved protein with GTP-binding motifs and is required for regulated cell enlargement in Arabidopsis. *Genes. Dev.* **1997**, *11*, 799–811. [[CrossRef](#)] [[PubMed](#)]
105. Wang, W.; Zheng, H. Arabidopsis reticulons inhibit ROOT HAIR DEFECTIVE3 to form a stable tubular endoplasmic reticulum network. *Plant Physiol.* **2023**. [[CrossRef](#)] [[PubMed](#)]
106. Gerakis, Y.; Quintero, M.; Li, H.; Hetz, C. The UFMylation System in Proteostasis and Beyond. *Trends Cell Biol.* **2019**, *29*, 974–986. [[CrossRef](#)]
107. Hwang, J.; Qi, L. Quality Control in the Endoplasmic Reticulum: Crosstalk between ERAD and UPR pathways. *Trends Biochem. Sci.* **2018**, *43*, 593–605. [[CrossRef](#)]
108. Kamauchi, S.; Nakatani, H.; Nakano, C.; Urade, R. Gene expression in response to endoplasmic reticulum stress in *Arabidopsis thaliana*. *FEBS J.* **2005**, *272*, 3461–3476. [[CrossRef](#)]
109. Martinez, I.M.; Chrispeels, M.J. Genomic analysis of the unfolded protein response in Arabidopsis shows its connection to important cellular processes. *Plant Cell* **2003**, *15*, 561–576. [[CrossRef](#)]
110. Hüttner, S.; Veit, C.; Vavra, U.; Schoberer, J.; Liebminger, E.; Maresch, D.; Grass, J.; Altmann, F.; Mach, L.; Strasser, R. Arabidopsis Class I α -Mannosidases MNS4 and MNS5 Are Involved in Endoplasmic Reticulum-Associated Degradation of Misfolded Glycoproteins. *Plant Cell* **2014**, *26*, 1712–1728. [[CrossRef](#)]

111. Hetz, C.; Papa, F.R. The Unfolded Protein Response and Cell Fate Control. *Mol. Cell* **2018**, *69*, 169–181. [[CrossRef](#)] [[PubMed](#)]
112. Horimoto, S.; Ninagawa, S.; Okada, T.; Koba, H.; Sugimoto, T.; Kamiya, Y.; Kato, K.; Takeda, S.; Mori, K. The unfolded protein response transducer ATF6 represents a novel transmembrane-type endoplasmic reticulum-associated degradation substrate requiring both mannose trimming and SEL1L protein. *J. Biol. Chem.* **2013**, *288*, 31517–31527. [[CrossRef](#)] [[PubMed](#)]
113. Sun, S.; Shi, G.; Sha, H.; Ji, Y.; Han, X.; Shu, X.; Ma, H.; Inoue, T.; Gao, B.; Kim, H.; et al. IRE1alpha is an endogenous substrate of endoplasmic-reticulum-associated degradation. *Nat. Cell Biol.* **2015**, *17*, 1546–1555. [[CrossRef](#)] [[PubMed](#)]
114. Liu, Y.; Burgos, J.S.; Deng, Y.; Srivastava, R.; Howell, S.H.; Bassham, D.C. Degradation of the endoplasmic reticulum by autophagy during endoplasmic reticulum stress in Arabidopsis. *Plant Cell* **2012**, *24*, 4635–4651. [[CrossRef](#)] [[PubMed](#)]
115. Bao, Y.; Pu, Y.; Yu, X.; Gregory, B.D.; Srivastava, R.; Howell, S.H.; Bassham, D.C. IRE1B degrades RNAs encoding proteins that interfere with the induction of autophagy by ER stress in *Arabidopsis thaliana*. *Autophagy* **2018**, *14*, 1562–1573. [[CrossRef](#)] [[PubMed](#)]
116. Zielke, S.; Kardo, S.; Zein, L.; Mari, M.; Covarrubias-Pinto, A.; Kinzler, M.N.; Meyer, N.; Stolz, A.; Fulda, S.; Reggiori, F.; et al. ATF4 links ER stress with reticulophagy in glioblastoma cells. *Autophagy* **2021**, *17*, 2432–2448. [[CrossRef](#)] [[PubMed](#)]
117. Houck, S.A.; Ren, H.Y.; Madden, V.J.; Bonner, J.N.; Conlin, M.P.; Janovick, J.A.; Conn, P.M.; Cyr, D.M. Quality control autophagy degrades soluble ERAD-resistant conformers of the misfolded membrane protein GnRHR. *Mol. Cell* **2014**, *54*, 166–179. [[CrossRef](#)]
118. Kruse, K.B.; Brodsky, J.L.; McCracken, A.A. Characterization of an ERAD gene as VPS30/ATG6 reveals two alternative and functionally distinct protein quality control pathways: One for soluble Z variant of human alpha-1 proteinase inhibitor (A1PiZ) and another for aggregates of A1PiZ. *Mol. Biol. Cell* **2006**, *17*, 203–212. [[CrossRef](#)]
119. Teckman, J.H.; Gilmore, R.; Perlmutter, D.H. Role of ubiquitin in proteasomal degradation of mutant alpha(1)-antitrypsin Z in the endoplasmic reticulum. *Am. J. Physiol. Gastrointest. Liver Physiol.* **2000**, *278*, G39–G48. [[CrossRef](#)]
120. Shrestha, N.; Torres, M.; Zhang, J.; Lu, Y.; Haataja, L.; Reinert, R.B.; Knupp, J.; Chen, Y.J.; Parlakgul, G.; Arruda, A.P.; et al. Integration of ER protein quality control mechanisms defines β cell function and ER architecture. *J. Clin. Investig.* **2023**, *133*, e163584. [[CrossRef](#)]
121. Wu, S.A.; Shen, C.; Wei, X.; Zhang, X.; Wang, S.; Chen, X.; Torres, M.; Lu, Y.; Lin, L.L.; Wang, H.H.; et al. The mechanisms to dispose of misfolded proteins in the endoplasmic reticulum of adipocytes. *Nat. Commun.* **2023**, *14*, 3132. [[CrossRef](#)] [[PubMed](#)]
122. Rancour, D.M.; Dickey, C.E.; Park, S.; Bednarek, S.Y. Characterization of AtCDC48. Evidence for multiple membrane fusion mechanisms at the plane of cell division in plants. *Plant Physiol.* **2002**, *130*, 1241–1253. [[CrossRef](#)] [[PubMed](#)]
123. Krick, R.; Bremer, S.; Welter, E.; Schlotterhose, P.; Muehe, Y.; Eskelinen, E.L.; Thumm, M. Cdc48/p97 and Shp1/p47 regulate autophagosome biogenesis in concert with ubiquitin-like Atg8. *J. Cell Biol.* **2010**, *190*, 965–973. [[CrossRef](#)] [[PubMed](#)]
124. Lei, Y.; Klionsky, D.J. UIM-UDS: A new interface between ATG8 and its interactors. *Cell Res.* **2019**, *29*, 507–508. [[CrossRef](#)]
125. Marshall, R.S.; Hua, Z.; Mali, S.; McLoughlin, F.; Vierstra, R.D. ATG8-Binding UIM Proteins Define a New Class of Autophagy Adaptors and Receptors. *Cell* **2019**, *177*, 766–781. [[CrossRef](#)]

Disclaimer/Publisher’s Note: The statements, opinions and data contained in all publications are solely those of the individual author(s) and contributor(s) and not of MDPI and/or the editor(s). MDPI and/or the editor(s) disclaim responsibility for any injury to people or property resulting from any ideas, methods, instructions or products referred to in the content.

PCP

PLANT & CELL PHYSIOLOGY



Downloaded from <https://academic.oup.com/pcp/issue/65/10> by guest on 24 July 2025

Special Issue

**Brassinosteroids: From Biosynthesis and
Signalling to Crop Improvement**

10

**2024 Vol. 65
October**

On the cover: Brassinosteroids (BRs) are a group of phytohormones required for the regulation of growth, development and response to environmental stresses. Since their discovery in the 1970s, significant advances have been made in understanding the mechanisms of BR biosynthesis and their intricate signalling pathways and crosstalk with other plant hormones. This special issue, organized by [Brigitte Poppenberger](#), [Eugenia \(Jenny\) Russinova](#) and [Sigal Savaldi-Goldstein](#), brings together the latest research on BRs and their modes of action in a range of plants, from basic models to crops. The cover image shows an *Arabidopsis thaliana* wild-type (right) and mutant plant (left) defective in brassinosteroid hormone perception. Photo credit: Dr. Eun-Ji Kim, courtesy of the Russinova lab, VIB-UGent, Belgium.

Post-translational Regulation of BRI1-EMS Suppressor 1 and Brassinazole-Resistant 1

Juan Mao¹, Biaodi Shen¹, Wenxin Li¹, Linchuan Liu^{1,*} and Jianming Li^{1,2,*}

¹State Key Laboratory for Conservation and Utilization of Subtropical Agro-Bioresources, Guangdong Key Laboratory for Innovative Development and Utilization of Forest Plant Germplasm, College of Forestry and Landscape Architecture, South China Agricultural University, 483 Wusan Road, Tianhe District, Guangzhou 510642, China

²Department of Biology, Hong Kong Baptist University, Kowloon, Hong Kong

*Corresponding authors: Linchuan Liu, E-mail, lliu@scau.edu.cn; Jianming Li, E-mail, li-jianming@hkbu.edu.hk

(Received 6 November 2023; Accepted 15 June 2024)

Brassinosteroid-insensitive 1 (BRI1)-EMS suppressor 1 (BES1) and Brassinazole-resistant 1 (BZR1) are two highly similar master transcription factors of the brassinosteroid (BR) signaling pathway that regulates a variety of plant growth and development processes as well as stress responses. Previous genetic and biochemical analyses have established a complex regulatory network to control the two transcription factors. This network includes coordination with other transcription factors and interactors, multiple post-translational modifications (PTMs) and differential subcellular localizations. In this review, we systematically detail the functions and regulatory mechanisms of various PTMs: phosphorylation/dephosphorylation, ubiquitination/deubiquitination, SUMOylation/deSUMOylation and oxidation/reduction, in regulating the subcellular localization, protein stability and the transcriptional activity of BES1/BZR1. We also discuss the current knowledge about the BES1/BZR1 interactors mediating the dynamic nucleocytoplasmic shuttling of BES1 and BZR1.

Keywords: BES1 • Brassinosteroids • BZR1 • Post-translational regulation

Introduction

Brassinosteroids (BRs) are essential phytohormones that regulate a wide range of physiological processes during plant growth and development and responses to pathogens and environmental stresses. In the past two and a half decades, extensive and intensive studies using *Arabidopsis* have greatly expanded our understanding of the BR signaling pathway. In *Arabidopsis*, BRs are perceived by several plasma membrane-localized receptors, including Brassinosteroid-insensitive 1 (BRI1) (Li and Chory 1997, Wang et al. 2001, Kinoshita et al. 2005) and its vascular tissue-specific homologs BRI1-like 1 (BRL1) and BRL3 (Cano-Delgado et al. 2004, Zhou et al. 2004). BR binding to the extracellular domain of BRI1 allows association with its coreceptor, BRI1-associated receptor kinase1 (BAK1) (Li et al. 2002, Nam and Li 2002, Hothorn et al. 2011, She et al. 2011,

Santiago et al. 2013), resulting in the dissociation of BRI1 kinase inhibitor 1, a negative regulator of BR signaling (Wang et al. 2011). The activated BRI1–BAK1 complex triggers intracellular phosphorylation events that lead to the inhibition of the key negative regulator, glycogen synthase kinase 3 (GSK3)-like kinase BRASSINOSTEROID-INSENSITIVE 2 (BIN2) (Li and Nam 2002). Upon BIN2 inhibition, the dephosphorylated and newly synthesized non-phosphorylated forms of BRI1-EMS suppressor 1 (BES1, also named BZR2) and Brassinazole-resistant 1 (BZR1), two master transcription factors in BR signaling, accumulate in the nucleus (Wang et al. 2002, Yin et al. 2002). The nuclear-localized BES1/BZR1 directly or indirectly regulate the transcription of thousands of BR-responsive genes to influence plant growth, development and stress response (Sun et al. 2010, Yu et al. 2011, Lv and Li 2020, Nolan et al. 2020). In the absence of BR, BIN2 phosphorylates BES1 and BZR1 to inhibit their nuclear localization, promote their degradation and reduce their DNA binding and transcriptional activities (Nam and Li 2002, Kim et al. 2009). Additionally, BES1 and BZR1 can integrate a wide range of internal and external signals to modulate plant growth and stress tolerance in a BR-independent manner (Albertos et al. 2022).

BES1 and BZR1 belong to the plant-specific BZR1 transcription factor family, which contains four other members in *Arabidopsis*, known as BEH1–4 for BES1/BZR1 homologs 1–4 (Yin et al. 2005). As the central transcription factors in the BR signaling pathway, BES1/BZR1 contain a basic helix–loop–helix DNA-binding domain (DBD) with β -hairpins to bind specific DNA sequences to regulate gene expression (Yin et al. 2005, Nosaki et al. 2018). They also contain additional conserved motifs to regulate their protein stability or transcriptional activity. The 14-3-3 binding motif (Bai et al. 2007, Gampala et al. 2007) and the Pro-Glu-Ser-Thr (PEST) motif (enriched with Pro, Glu, Ser and Thr residues) are responsible for protein stability (Wang et al. 2002, Yin et al. 2002). The BIN2-docking motif (DM) is required for their direct binding with BIN2 (Peng et al. 2010), and an Ethylene Response Factor-associated amphiphilic repression domain mediates BES1/BZR1 binding to the transcriptional

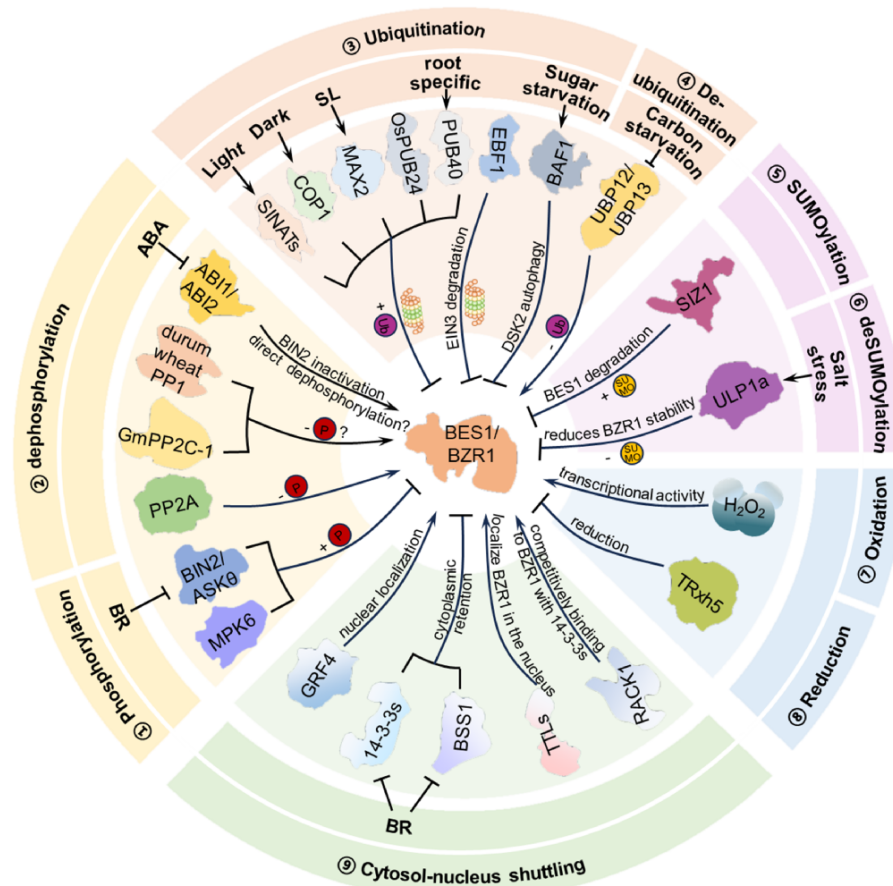


Fig. 1 The PTMs of BES1/BZR1. Colored arrows and T-ended lines indicate positive and negative regulation on the stability, activity or nuclear localization of BES1/BZR1. Parts 1 and 2 (light yellow background) illustrate the phosphorylation and dephosphorylation of BES1 and BZR1. BIN2, suppressed by BR, phosphorylates and inactivates BES1 and BZR1. PP2A dephosphorylates and activates BES1 and BZR1. In *Arabidopsis*, ABI1/ABI2 activates BES1 through inactivating BIN2 or through other uncertain mechanisms. Other phosphatases, GmPP2C-1 in soybean and PP1 in durum wheat, can also activate BZR1 or BES1. Parts 3 and 4 (light orange background) depict the ubiquitination and deubiquitination of BES1 and BZR1. Several families of E3 ubiquitin ligases target BZR1 or BES1 for degradation by the proteasome or autophagy, while UBP12 and UBP13 deubiquitinate BES1 under carbon starvation. Parts 5 and 6 (light pink background) show SUMOylation and deSUMOylation of BES1 and BZR1. SIZ1 mediates the SUMOylation and degradation of BES1, whereas ULP1a deSUMOylates BZR1 in the cytoplasm and reduces BZR1 stability. Parts 7 and 8 (light blue background) display the oxidation and reduction of BES1 and BZR1. H_2O_2 activates BES1 and BZR1 through oxidation, while TRXh5 reduces BZR1. Part 9 (light green background) describes the cytosol–nucleus shuttling of BES1 and BZR1. Cytoplasmic sequestration by 14-3-3s and BSS1 can inactivate BES1 and BZR1, whereas nuclear retention by GRF4, TTLs and RACK1 can activate them.

co-repressor TOPLESS-histone deacetylase 19 (Oh et al. 2014, Ryu et al. 2014). BES1 and BZR1 directly bind to E-box (CANNTG) elements and the BRRE (CGTGT/CG) motifs in the promoters of their target genes through their DBDs, respectively, to activate or repress the expression of many BR-responsive genes (He et al. 2005, Yin et al. 2005, Sun et al. 2010, Yu et al. 2011). Recent studies have shown that their subcellular localization, protein stability and transcriptional activities are regulated by many types of post-translational modifications (PTMs), including reversible phosphorylation/dephosphorylation, ubiquitination and SUMOylation, thus allowing them to function as important signaling hubs to link BR signaling with other plant signaling processes. In addition, the transcriptional activities of BES1 and BZR1 are also regulated by their interactions with many signaling proteins in plant cells. In this review, we discuss our current knowledge concerning the post-translational regulation of BES1 and BZR1 (Fig. 1).

PTMs of BES1/BZR1

The phosphorylation and dephosphorylation of BES1/BZR1

Reversible phosphorylation and dephosphorylation are important and dynamic modifications for BES1/BZR1's stability and activity. In the absence of BR, BIN2 phosphorylates BES1/BZR1 at serine (S) and threonine (T) residues in the central region, which includes 25 repeats of a consensus site (S/TXXXS/T, where S/T stands for serine or threonine and X stands for any amino acid) (Wang et al. 2002, Yin et al. 2002). Unlike the mammalian GSK3 kinase that relies on a priming phosphorylation event by another kinase to generate a substrate-binding pocket or an adapter protein that binds both GSK3 and its substrate for the GSK3-catalyzed substrate phosphorylation (Beurel et al. 2015), the BIN2-catalyzed BES1/BZR1 phosphorylation requires

a direct BIN2-substrate binding mediated by the BIN2 DM near the C-termini of the two transcription factors (He et al. 2002, Zhao et al. 2002, Yan et al. 2009, Peng et al. 2010). Interestingly, such a BIN2-binding motif is not present in the liverwort (*Marchantia polymorpha*) homolog of BES1, MpBES1, which exhibited no binding with MpBIN2, the liverwort homolog of *Arabidopsis* BIN2. As a result, MpBIN2 only weakly phosphorylated MpBES1 when coexpressed in tobacco leaves, and MpBES1 exhibited a much stronger BR signaling activity than BES1 in transgenic *Arabidopsis* plants (Mecchia et al. 2021), confirming the important role of the BIN2 DM in facilitating the BIN2-catalyzed BES1/BZR1 phosphorylation. Consistent with the *Arabidopsis* studies, the rice homolog of BZR1, OsBZR1, was shown to be phosphorylated by OsGSK2, one of the rice homologs of BIN2 (Bai et al. 2007, Min et al. 2019). The BIN2-catalyzed phosphorylation of BES1/BZR1 regulates protein stability, subcellular location and transcriptional activity (Gampala et al. 2007, Ryu et al. 2010, Wang et al. 2021b). ASK0, another member of the GSK3 family in *Arabidopsis*, is able to phosphorylate BES1/BZR1, and whether their activity is regulated by BIN2 through a similar mechanism is yet to be investigated (Rozhon et al. 2010). Phosphorylation at Ser173 of BZR1 and that at Ser171 and Thr175 of BES1 are critical for their interaction with 14-3-3 proteins, leading to function inhibition of BZR1/BES1 by promoting their cytoplasmic localization (Gampala et al. 2007, Ryu et al. 2010). Recent in vitro and in vivo assays have confirmed that Ser179 and Ser180 of BES1 are phosphorylation sites for BIN2. The phosphorylation of these two sites has a negative role in regulating BES1 function (Clark et al. 2021).

The Mitogen-activated Protein Kinase (MAPK, MPK) cascade is a widespread signaling module in plants, which is known to regulate the biosynthesis, transport and signaling of different hormones and the integration and amplification of plant immune signals (Zhang et al. 2018). MPK6, a component of the MAPK cascade, was reported to interact with and phosphorylate BES1 to maintain a balance between growth and defense in *Arabidopsis* (Kang et al. 2015). However, it remains unknown how MPK6-facilitated BES1 phosphorylation influences plant immunity.

The de/unphosphorylated BES1/BZR1 represent the active forms. In the current BR-signaling working model, when BIN2 is inactivated, the nuclear-localized type 2A protein phosphatase (PP2A) dephosphorylates phosphorylated BZR1 via a direct physical interaction between its B'-subunit and the PEST domain of BZR1, resulting in the accumulation of dephosphorylated BZR1 (Tang et al. 2011). However, the PEST motif is not conserved in the *Arabidopsis* BES1/BZR1 family, implying that the PEST-mediated dephosphorylation by PP2A is likely specific for BES1 and BZR1. Given that all six members are involved in BR signaling (Chen et al. 2019a, 2019b), it is reasonable to speculate that other phosphatases might be involved in dephosphorylating the other four BEH proteins. Indeed, two PP2C-type phosphatases in the core ABA-signaling pathway, ABI1 and ABI2, have been shown to indirectly influence the

phosphorylation status of BES1 (Wang et al. 2018, Albertos et al. 2022). Under normal growth conditions, ABI1 and ABI2 can dephosphorylate BIN2 through their direct interaction, leading to reduced phosphorylation of BES1 and enhanced BR signaling (Wang et al. 2018). A recent study found that heat stress triggers the dephosphorylation and activation of BES1 independently of the canonical BR signaling, mediated by ABA-controlled PP2C phosphatases like ABI1. Activated BES1 can then interact with a class A1 heat shock factor to enhance plant heat stress resistance by regulating the expression of heat-shock proteins (Albertos et al. 2022). However, the regulatory mechanism, which is not primarily dependent on BIN2, requires further investigation. Additionally, the dark/light transitions have been shown to affect the BES1 and BZR1 phosphorylation (Martinez et al. 2018). A recent study on the soybean homolog of BZR1 (GmBZR1) showed that the protein phosphatase PP2C-1, which contains a Leguminosae-specific N-terminal domain, interacts with and stimulates the accumulation of unphosphorylated GmBZR1 in the nucleus (Lu et al. 2017). However, it is unknown whether PP2C-1 directly dephosphorylates GmBZR1 or inhibits GmBIN2 to cause the increased accumulation of the unphosphorylated form of GmBZR1. Furthermore, whether the PP2C1-caused accumulation of un/dephosphorylated GmBZR1 is involved in BR-mediated plant growth is yet to be investigated. In durum wheat, another phosphatase family, type 1 protein phosphatase (PP1), could also regulate the phosphorylation status of BES1 to influence BR signaling, but the precise mechanism remains to be studied (Bradai et al. 2021). Together, these studies indicate that various types of protein phosphatases might be directly or indirectly involved in dephosphorylating members of the BES1/BZR1 family in plants.

Where the phosphorylation/dephosphorylation of BES1/BZR1 by BIN2 or their phosphatases occurs remains controversial but is a critical step in transmitting the extracellular BR signals into the nucleus. Several studies conclude that both phosphorylation and dephosphorylation of BES1/BZR1 take place in both the cytoplasm and the nucleus (Tang et al. 2011, Wang et al. 2012, Belkhadir and Jaillais 2015). However, other investigations propose that the phosphorylation/dephosphorylation of BES1/BZR1 could also occur at the plasma membrane, as evidenced by interactions between BR signaling components observed at the plasma membrane (Wang et al. 2013a, Amorim-Silva et al. 2019). A recent study, using confocal microscopy and immunoblot analysis, indicated that both BIN2-catalyzed phosphorylation and PP2A(B')-mediated dephosphorylation of BZR1 occur in the nucleus (Wang et al. 2021b), raising a question on how the extracellular BR signals reach the nucleus. Discrepancies in conclusions could stem from variations in analytical methods and different epitope tags used in different studies. Furthermore, variable cellular and environmental conditions could cause dynamic changes in the phosphorylation and dephosphorylation status of BES1/BZR1, thus complicating the interpretation of experimental results. Future studies should employ a combination of genetic, cell biology and biochemical approaches to pinpoint the precise locations

where BIN2-catalyzed phosphorylation of BES1/BZR1 and their dephosphorylation occur.

The ubiquitination-mediated stability regulation of BES1/BZR1

In the absence of BR, BIN2-mediated phosphorylation of BES1/BZR1 leads to their 26S proteasome-dependent degradation. BRs are generally considered to stabilize and activate BZR1 protein (He et al. 2002). However, a completely different mechanism for regulating BZR1 stability is recently proposed: BR promotes BZR1 degradation via the 26S proteasome pathway, probably to constantly supply newly synthesized BZR1 with high transcription activity (Wang et al. 2021b). Similar to the controversial issue of the subcellular locations of BES1/BZR1 phosphorylation and dephosphorylation, the protein stability of BZR1 could also be influenced by the experimental conditions and the biochemical reagents used to measure the protein levels of BES1/BZR1. Clearly, further investigations using highly specific antibodies are necessary to determine the protein stability of phosphorylated and non-/dephosphorylated forms of the endogenous BES1 and BZR1 proteins.

Ubiquitin E3 ligase is a required component of the ubiquitin–proteasome system. Several E3 ubiquitin ligases implicated in light signaling and hormone signaling have been identified to target BZR1 and BES1 for ubiquitination and degradation, thus regulating the signaling output of plant steroids and plant development. Seven-IN-Absentia of *Arabidopsis thaliana* (SINATs) and Constitutive Photomorphogenic 1 (COP1), two RING-type E3 ubiquitin ligases in *Arabidopsis*, play roles in promoting the degradation of BES1 and BZR1 to regulate hypocotyl elongation in light and dark, respectively (Kim et al. 2014, Yang et al. 2017). SINATs specifically promote the degradation of dephosphorylated BES1 and BZR1 under light to inhibit hypocotyl elongation (Yang et al. 2017), while COP1 facilitates the degradation of phosphorylated BZR1, thus increasing the ratio of dephosphorylated to phosphorylated BZR1 forms. This increases homodimerization of dephosphorylated BZR1 proteins to promote hypocotyl elongation in the dark (Kim et al. 2014). Organ-specific regulatory networks seem to be involved in the COP1-dependent regulation of the BES1 protein stability under adverse conditions. Under shade or warmer temperatures, COP1 physically interacts with BES1, reducing the abundance of nuclear-localized BES1 and cell expansion in the cotyledons (Costigliolo Rojas et al. 2022). However, in the hypocotyl, COP1 has the opposite effect on the nuclear BES1 levels, likely through reducing the abundance or activity of a negative regulator of BES1 stability under shade or warmer conditions (Costigliolo Rojas et al. 2022).

At least two F-box proteins, which are substrate-binding subunits of the multisubunit RING-type E3 ligases, are involved in regulating the stability of BES1/BZR1. The F-box protein More Axillary Growth Locus 2 (MAX2), a central component of the signaling pathways of strigolactone (SL) and the smoke-derived

karrikins (Nelson et al. 2011), was found to bind and ubiquitinate both phosphorylated and dephosphorylated forms of BES1 to suppress shoot branching (Wang et al. 2013b). Interestingly, the BES1–MAX2 interaction also inhibits the expression of the transcription factor BRANCHED1 (BRC1), which specifically induces the transcriptional network of the SL-regulated shoot branching (Hu et al. 2020). Together, these findings reveal an interesting interaction between two plant hormones: the MAX2-mediated degradation of BES1 and the inhibitory effect of the BES1–MAX2 interaction on the BRC1-regulated shoot branching transcriptional network. The other F-box protein recently implicated in regulating BZR1 stability is the nuclear-localized EIN3-binding F BOX protein1 (EBF1), a known negative regulator of the ethylene pathway (Potuschak et al. 2003). EBF1 directly and indirectly regulates the stability and activity of BZR1 to impact apical hook development and hypocotyl elongation. First, EBF1 and its homolog EBF2 promote the degradation of ethylene-insensitive 3 (EIN3), which is known to interact with BZR1 to stimulate the apical hook development (Wang et al. 2023). Second, EBF1 directly interacts with BZR1 and promotes BZR1 degradation via the 26S proteasome (Zhao et al. 2022).

Among the reported E3 ligases implicated in ubiquitinating BES1/BZR1 to control their stability, plant U-box 40 (PUB40) is regulated by BR and could therefore be involved in BR-regulated degradation of BZR1. It was found that PUB40 mediates the root-specific degradation of BZR1 to regulate root growth in response to inorganic phosphate deprivation in *Arabidopsis* (Kim et al. 2019). It remains to be investigated why PUB40-induced degradation of BZR1 only occurs in the root because the PUB40-YFP fusion protein, which was used to study the PUB40–BZR1 interaction, was driven by the constitutively active 35S promoter and should be present in the shoots as well. It should be worthy to note that OsPUB24, a rice U-Box E3 ligase, also ubiquitinates OsBZR1 and promotes proteasome-dependent degradation of OsBZR1 in response to BR (Min et al. 2019).

In addition to proteasome-mediated degradation, BES1/BZR1 could also be degraded by autophagy. Shifting light-grown *Arabidopsis* seedlings into darkness causes sugar starvation and induces the inactivation of the Target of Rapamycin (TOR) kinase and subsequent autophagy activation (Liu et al. 2010, Perez-Perez et al. 2010). It was found that the suppressed TOR induces BZR1 degradation through autophagy to inhibit plant growth (Zhang et al. 2016). Sugar starvation was recently shown to induce the expression of BES1-ASSOCIATED F-BOX1 (BAF1), an *Arabidopsis* F-box protein that interacts directly with BES1 to catalyze BES1 ubiquitination. Ubiquitinated BES1 then binds with DOMINANT SUPPRESSOR OF KAR2 (DSK2) for autophagy-mediated degradation (Wang et al. 2021a). DSK2, a well-studied ubiquitin receptor, is known to interact with the autophagy protein ATG8 (Floyd et al. 2012, Nolan et al. 2017), thus bringing the ubiquitinated BES1 into the autophagy degradation pathway (Nolan et al. 2017). Interestingly, BIN2 was shown to phosphorylate DSK2 to promote DSK2-ATG8 binding

to promote BES1 degradation (Nolan et al. 2017). The stability of BES1/BZR1 is tightly regulated by various ubiquitin ligases, likely ensuring the rapid and precise modulation of plant growth under different growth conditions.

It is no surprise that deubiquitination plays an important role in maintaining the stability of BES1/BZR1. A recent study showed that Ub-Specific Protease 12 (UBP12) and UB13, two important deubiquitinating enzymes that are strongly induced during the recovery of carbon starvation, directly interacted with BES1 to remove its covalently attached ubiquitins, thus stabilizing both phosphorylated and dephosphorylated BES1 for quick recovery after carbon starvation (Park et al. 2022, Xiong et al. 2022). Therefore, the ubiquitination and deubiquitination of BES1/BZR1 represent an important molecular mechanism by which plants adapt their growth patterns in response to changing internal and external conditions.

The other post-translational regulations

Reversible protein SUMOylation is another important PTM that could regulate protein activity. Similar to ubiquitination, SUMOylation involves the covalent conjugation of SUMO (small ubiquitin-like modifier) to certain lysine residues of target proteins by a similar E1 (activation)–E2 (conjugation)–E3 (ligation) enzymatic cascade. The *Arabidopsis* SIZ1, a SUMO E3 ligase, physically interacts with BES1 and mediates its SUMOylation at Lys302 independently of BR, promoting BES1 degradation (Zhang et al. 2019). Interestingly, SUMOylation of BZR1 at Lys280 and Lys320 promotes its stability by suppressing its interaction with BIN2 and reducing the BIN2-catalyzed BZR1 phosphorylation known to be linked with BZR1 instability, thus promoting plant growth under normal growth conditions (Srivastava et al. 2020). These findings reveal that the same PTM on two highly similar transcriptional factors can have opposing effects on their protein stability via distinct biochemical mechanisms. Salt stress induces the accumulation of the SUMO protease Ubiquitin-like specific Protease 1a (ULP1a), which deSUMOylates BZR1 in the cytoplasm and reduces BZR1 stability, thus attenuating BR-stimulated growth (Srivastava et al. 2020). It is noteworthy that the two SUMO conjugation sites, Lys280 and Lys320, are specific to BZR1 homologs in dicot plant species (Srivastava et al. 2020) and not present in monocot and bryophyte (*M. polymorpha*) plants. This suggests that SUMOylation/deSUMOylation of BZR1 at these two residues may be unique to dicot plants, or other Lys residues of BZR1 homologs in different plant species may undergo SUMOylation/deSUMOylation to regulate plant growth in response to environmental challenges.

BZR1, like other transcriptional factors (He et al. 2018), is also subject to redox regulation that affects its transcriptional activity (Tian et al. 2018). Hydrogen peroxide (H_2O_2), as an important signaling molecule, induces the oxidation of BZR1 at the conserved Cys63 residue situated in the connecting loop between two α -helices involved in DNA binding (Nosaki et al. 2018). The H_2O_2 -induced oxidative modification is believed to enhance the transcriptional activity of BZR1 by

strengthening the interactions with Phytochrome Interacting Factor 4 (PIF4) and Auxin Response Factor 6 (ARF6), which are key regulators in light and auxin signaling pathways, respectively (Tian et al. 2018). The increased interactions between BZR1 and PIF4 and ARF6 contribute to cell elongation and root stem cell maintenance, which can be reversed by *Arabidopsis* cytosolic thioredoxin-h5 (TRXh5) binding to BZR1 to reduce the oxidized Cys63 residue (Tian et al. 2018). Additionally, oxidized BZR1 interacts with the basic leucine zipper transcription factor G-BOX Binding Factor 2 (GBF2) to promote the expression of β -Amylase 1 (BAM1), important for starch degradation in guard cells, causing the stomatal opening (Li et al. 2020). Future investigations are needed to explore whether the oxidized Cys63 residue affects BR signaling and the mechanism for the increased binding of oxidized BZR1 with other transcriptional factors.

The Cytosol–Nuclear Shuttling of BES1/BZR1

The nucleocytoplasmic trafficking of BES1/BZR1 and their phosphorylation/dephosphorylation status is closely related, but the exact mechanisms remain controversial. When BR is low, the phosphorylated BES1/BZR1 is either trapped in the cytoplasm by 14-3-3 proteins (Gampala et al. 2007) or exported from the nucleus to the cytosol by 14-3-3 proteins (Wang et al. 2021b). When BR signaling is active, dephosphorylated BES1/BZR1 accumulates in the nucleus to regulate the transcription of BR-responsive genes (He et al. 2005). But when and how BES1/BZR1 traffics into the nucleus is currently uncertain. A new mechanism to regulate the nucleocytoplasmic trafficking of BZR1 is proposed. It is reported that the newly synthesized BZR1 in the cytoplasm is initially imported into the nucleus, where it is phosphorylated by BIN2. Subsequently, the nucleus-localized 14-3-3 proteins interact with the phosphorylated BZR1 to promote its entrance into the cytoplasm (Wang et al. 2021b). Despite the apparent energy cost for plants, the cytoplasmic phosphorylated BZR1 probably plays crucial roles in plant development, necessitating precise regulation of its abundance and phosphorylation status. Or, as a central transcription factor, the precise and rapid control of phosphorylation/dephosphorylation dynamics of nuclear-localized BZR1 is essential. A recent study revealed a role of GRF4 (General Regulatory Factor 4, a member of the 14-3-3 protein family) in retaining BZR1 in the cytoplasm (Yu et al. 2023). The auxin-activated MPK3/MPK6 phosphorylate GRF4 to reduce its protein stability, thus enhancing the accumulation of BZR1 in the nucleus to promote hypocotyl elongation (Yu et al. 2023). These findings provide a new insight into the interplay between auxin and BR signaling pathways in regulating plant development.

In addition to 14-3-3 proteins, various other proteins play a role in the differential localizations of BES1/BZR1. BRZ-SENSITIVE-SHORT HYPOCOTYL1 (BSS1), also known as BLADE ON PETIOLE1, interacts physically with BZR1 to retain BZR1 in the cytosol, thus suppressing BR signaling (Shimada et al. 2015). The *Arabidopsis* TETRATRICOPEPTIDE THIOREDOXIN-LIKE3

(TTL3) protein serves as a scaffolding protein to localize BZR1 in the nucleus and other key components of BR signaling at the plasma membrane (Amorim-Silva et al. 2019), but the physiological significance of such a BR signaling complex requires further investigation. In contrast, another scaffold protein, Receptor for Activated C Kinase 1 (RACK1), can promote the nuclear localization of BZR1 through competitively binding to BZR1 with 14-3-3 proteins (Li et al. 2023). Apart from the protein factors involved in the regulation of BES1/BZR1 localization, it has been observed that high temperature leads to the nuclear enrichment of BES1 (Albertos et al. 2022).

Conclusions and Future Research

BES1 and BZR1 function as central hubs that connect various signal pathways to regulate plant growth and development as well as stress adaptations. Numerous studies have greatly deepened our understanding of how their activities and stabilities are influenced by multiple PTMs, including reversible phosphorylation and dephosphorylation, degradation, SUMOylation and oxidation. Furthermore, it is likely that BES1 and BZR1 undergo additional modifications like nitrosylation, acetylation and methylation, which could be uncovered in the future through diverse research methodologies. Further investigation is required to understand how these complex regulatory networks cooperatively manage the activity and function of BES1 and BZR1 in different growth stages and environments. Many questions remain to be answered. Since BES1/BZR1 control the expression of their target genes in both a BR-dependent and BR-independent manner, the functions of their PTMs in BR-independent pathways need exploration. It is also interesting to note that while BES1 and BZR1 are ubiquitously expressed, some of their PTMs exhibit tissue, organ and/or developmental stage specificity. Further studies are needed to fully understand these specific regulatory mechanisms. Our current knowledge about the post-translational regulation of BES1/BZR1 primarily stems mostly from studies conducted on the model plant *Arabidopsis*, and it is thus important to determine whether similar PTMs also occur in other plant species, especially in important crop plants. These future studies will likely lead to better understanding of the roles of the PTMs of BES1/BZR1 in enhancing the yield and stress tolerance of major crops that are threatened by climate change.

Data Availability

No new data sets were generated or analyzed in this study.

Funding

National Natural Science Foundation of China (31900176 to J.M., 31870253 to J.L., 31970187 to L.L.); Guangdong Basic and Applied Research Foundation (2020A1515011387 to J.M., 2022A1515010803 to L.L.).

Disclosures

The authors have no conflicts of interest to declare.

References

- Albertos, P., Dundar, G., Schenk, P., Carrera, S., Cavalius, P., Sieberer, T., et al. (2022) Transcription factor BES1 interacts with HSFA1 to promote heat stress resistance of plants. *EMBO J.* 41: e108664.
- Amorim-Silva, V., Garcia-Moreno, A., Castillo, A.G., Lakhssassi, N., Esteban Del Valle, A., Perez-Sancho, J., et al. (2019) TTL proteins scaffold brassinosteroid signaling components at the plasma membrane to optimize signal transduction in *Arabidopsis*. *Plant Cell* 31: 1807–1828.
- Bai, M.Y., Zhang, L.Y., Gampala, S.S., Zhu, S.W., Song, W.Y., Chong, K., et al. (2007) Functions of OsBZR1 and 14-3-3 proteins in brassinosteroid signaling in rice. *Proc. Natl. Acad. Sci. U. S. A.* 104: 13839–13844.
- Belkhadir, Y. and Jaillais, Y. (2015) The molecular circuitry of brassinosteroid signaling. *New Phytol.* 206: 522–540.
- Beurel, E., Grieco, S.F. and Jope, R.S. (2015) Glycogen synthase kinase-3 (GSK3): regulation, actions, and diseases. *Pharmacol. Ther.* 148: 114–131.
- Bradai, M., Amorim-Silva, V., Belgaroui, N., Esteban Del Valle, A., Chaboute, M.E., Schmit, A.C., et al. (2021) Wheat type one protein phosphatase participates in the brassinosteroid control of root growth via activation of BES1. *Int. J. Mol. Sci.* 22: 10424.
- Cano-Delgado, A., Yin, Y., Yu, C., Vafeados, D., Mora-Garcia, S., Cheng, J.C., et al. (2004) BRL1 and BRL3 are novel brassinosteroid receptors that function in vascular differentiation in *Arabidopsis*. *Development* 131: 5341–5351.
- Chen, L.G., Gao, Z., Zhao, Z., Liu, X., Li, Y., Zhang, Y., et al. (2019a) BZR1 family transcription factors function redundantly and indispensably in BR signaling but exhibit BRI1-independent function in regulating anther development in *Arabidopsis*. *Mol. Plant* 12: 1408–1415.
- Chen, W., Lv, M., Wang, Y., Wang, P.A., Cui, Y., Li, M., et al. (2019b) BES1 is activated by EMS1-TPD1-SERK1/2-mediated signaling to control tapetum development in *Arabidopsis thaliana*. *Nat. Commun.* 10: 4164.
- Clark, N.M., Nolan, T.M., Wang, P., Song, G., Montes, C., Valentine, C.T., et al. (2021) Integrated omics networks reveal the temporal signaling events of brassinosteroid response in *Arabidopsis*. *Nat. Commun.* 12: 5858.
- Costigliolo Rojas, C., Bianchimano, L., Oh, J., Romero Montepaone, S., Tarkowska, D., Minguet, E.G. et al. (2022) Organ-specific COP1 control of BES1 stability adjusts plant growth patterns under shade or warmth. *Dev. Cell* 57: 2009–2025.e6.
- Floyd, B.E., Morris, S.C., Macintosh, G.C. and Bassham, D.C. (2012) What to eat: evidence for selective autophagy in plants. *J. Integr. Plant Biol.* 54: 907–920.
- Gampala, S.S., Kim, T.W., He, J.X., Tang, W., Deng, Z., Bai, M.Y., et al. (2007) An essential role for 14-3-3 proteins in brassinosteroid signal transduction in *Arabidopsis*. *Dev. Cell* 13: 177–189.
- He, H., Van Breusegem, F. and Mhamdi, A. (2018) Redox-dependent control of nuclear transcription in plants. *J. Exp. Bot.* 69: 3359–3372.
- He, J.X., Gendron, J.M., Sun, Y., Gampala, S.S., Gendron, N., Sun, C.Q., et al. (2005) BZR1 is a transcriptional repressor with dual roles in brassinosteroid homeostasis and growth responses. *Science* 307: 1634–1638.
- He, J.X., Gendron, J.M., Yang, Y., Li, J. and Wang, Z.Y. (2002) The GSK3-like kinase BIN2 phosphorylates and destabilizes BZR1, a positive regulator of the brassinosteroid signaling pathway in *Arabidopsis*. *Proc. Natl. Acad. Sci. U. S. A.* 99: 10185–10190.
- Hothorn, M., Belkhadir, Y., Dreux, M., Dabi, T., Noel, J.P., Wilson, I.A., et al. (2011) Structural basis of steroid hormone perception by the receptor kinase BRI1. *Nature* 474: 467–471.
- Hu, J., Sun, S. and Wang, X. (2020) Regulation of shoot branching by strigolactones and brassinosteroids: conserved and specific functions of *Arabidopsis* BES1 and rice BZR1. *Mol. Plant* 13: 808–810.

- Kang, S., Yang, F., Li, L., Chen, H., Chen, S. and Zhang, J. (2015) The *Arabidopsis* transcription factor BRASSINOSTEROID INSENSITIVE1-ETHYL METHANESULFONATE-SUPPRESSOR1 is a direct substrate of MITOGEN-ACTIVATED PROTEIN KINASE6 and regulates immunity. *Plant Physiol.* 167: 1076–1086.
- Kim, B., Jeong, Y.J., Corvalan, C., Fujioka, S., Cho, S., Park, T., et al. (2014) Darkness and gulliver2/phyB mutation decrease the abundance of phosphorylated BZR1 to activate brassinosteroid signaling in *Arabidopsis*. *Plant J.* 77: 737–747.
- Kim, E.J., Lee, S.H., Park, C.H., Kim, S.H., Hsu, C.C., Xu, S., et al. (2019) Plant U-Box40 mediates degradation of the brassinosteroid-responsive transcription factor BZR1 in *Arabidopsis* roots. *Plant Cell* 31: 791–808.
- Kim, T.W., Guan, S., Sun, Y., Deng, Z., Tang, W., Shang, J.X., et al. (2009) Brassinosteroid signal transduction from cell-surface receptor kinases to nuclear transcription factors. *Nat. Cell Biol.* 11: 1254–1260.
- Kinoshita, T., Cano-Delgado, A., Seto, H., Hiranuma, S., Fujioka, S., Yoshida, S., et al. (2005) Binding of brassinosteroids to the extracellular domain of plant receptor kinase BRI1. *Nature* 433: 167–171.
- Li, J. and Chory, J. (1997) A putative leucine-rich repeat receptor kinase involved in brassinosteroid signal transduction. *Cell* 90: 929–938.
- Li, J., Wen, J., Lease, K.A., Doke, J.T., Tax, F.E. and Walker, J.C. (2002) BAK1, an *Arabidopsis* LRR receptor-like protein kinase, interacts with BRI1 and modulates brassinosteroid signaling. *Cell* 110: 213–222.
- Li, J.G., Fan, M., Hua, W., Tian, Y., Chen, L.G., Sun, Y., et al. (2020) Brassinosteroid and hydrogen peroxide interdependently induce stomatal opening by promoting guard cell starch degradation. *Plant Cell* 32: 984–999.
- Li, J.M. and Nam, K.H. (2002) Regulation of brassinosteroid signaling by a GSK3/SHAGGY-like kinase. *Science* 295: 1299–1301.
- Li, Z., Fu, Y., Wang, Y. and Liang, J. (2023) Scaffold protein RACK1 regulates BR signaling by modulating the nuclear localization of BZR1. *New Phytol.* 239: 1804–1818.
- Liu, Y., Bassham, D.C. and Schumacher, K. (2010) TOR is a negative regulator of autophagy in *Arabidopsis thaliana*. *PLoS ONE* 5: e11883.
- Lu, X., Xiong, Q., Cheng, T., Li, Q.T., Liu, X.L., Bi, Y.D., et al. (2017) A PP2C-1 allele underlying a quantitative trait locus enhances soybean 100-seed weight. *Mol. Plant* 10: 670–684.
- Lv, M. and Li, J. (2020) Molecular mechanisms of brassinosteroid-mediated responses to changing environments in *Arabidopsis*. *Int. J. Mol. Sci.* 21: 2737.
- Martinez, C., Espinosa-Ruiz, A., de Lucas, M., Bernardo-Garcia, S., Franco-Zorrilla, J.M. and Prat, S. (2018) PIF4-induced BR biosynthesis is critical to diurnal and thermomorphogenic growth. *EMBO J.* 37: e99552.
- Mecchia, M.A., Garcia-Hourquet, M., Lozano-Elena, F., Planas-Riverola, A., Blasco-Escamez, D., Marques-Bueno, M., et al. (2021) The BES1/BZR1-family transcription factor MpBES1 regulates cell division and differentiation in *Marchantia polymorpha*. *Curr. Biol.* 31: 4860–4869.e8.
- Min, H.J., Cui, L.H., Oh, T.R., Kim, J.H., Kim, T.W. and Kim, W.T. (2019) OsBZR1 turnover mediated by OsSK22-regulated U-box E3 ligase OsPUB24 in rice BR response. *Plant J.* 99: 426–438.
- Nam, K.H. and Li, J. (2002) BRI1/BAK1, a receptor kinase pair mediating brassinosteroid signaling. *Cell* 110: 203–212.
- Nelson, D.C., Scaffidi, A., Dun, E.A., Waters, M.T., Flematti, G.R., Dixon, K.W., et al. (2011) F-box protein MAX2 has dual roles in karrikin and strigolactone signaling in *Arabidopsis thaliana*. *Proc. Natl. Acad. Sci. U. S. A.* 108: 8897–8902.
- Nolan, T.M., Brennan, B., Yang, M., Chen, J., Zhang, M., Li, Z., et al. (2017) Selective autophagy of BES1 mediated by DSK2 balances plant growth and survival. *Dev. Cell* 41: 33–46.e7.
- Nolan, T.M., Vukasinovic, N., Liu, D., Russinova, E. and Yin, Y. (2020) Brassinosteroids: multidimensional regulators of plant growth, development, and stress responses. *Plant Cell* 32: 295–318.
- Nosaki, S., Miyakawa, T., Xu, Y., Nakamura, A., Hirabayashi, K., Asami, T., et al. (2018) Structural basis for brassinosteroid response by BIL1/BZR1. *Nat. Plants* 4: 771–776.
- Oh, E., Zhu, J.Y., Ryu, H., Hwang, I. and Wang, Z.Y. (2014) TOPLESS mediates brassinosteroid-induced transcriptional repression through interaction with BZR1. *Nat. Commun.* 5: 4140.
- Park, S.H., Jeong, J.S., Zhou, Y., Binte Mustafa, N.F. and Chua, N.H. (2022) Deubiquitination of BES1 by UBP12/UBP13 promotes brassinosteroid signaling and plant growth. *Plant Commun.* 3: 100348.
- Peng, P., Zhao, J., Zhu, Y., Asami, T. and Li, J. (2010) A direct docking mechanism for a plant GSK3-like kinase to phosphorylate its substrates. *J. Biol. Chem.* 285: 24646–24653.
- Perez-Perez, M.E., Florencio, F.J. and Crespo, J.L. (2010) Inhibition of target of rapamycin signaling and stress activate autophagy in *Chlamydomonas reinhardtii*. *Plant Physiol.* 152: 1874–1888.
- Potuschak, T., Lechner, E., Parmentier, Y., Yanagisawa, S., Grava, S., Koncz, C., et al. (2003) EIN3-dependent regulation of plant ethylene hormone signaling by two *Arabidopsis* F box proteins: EBF1 and EBF2. *Cell* 115: 679–689.
- Rozhon, W., Mayerhofer, J., Petutschnig, E., Fujioka, S. and Jonak, C. (2010) ASKtheta, a group-III *Arabidopsis* GSK3, functions in the brassinosteroid signalling pathway. *Plant J.* 62: 215–223.
- Ryu, H., Cho, H., Bae, W. and Hwang, I. (2014) Control of early seedling development by BES1/TPL/HDA19-mediated epigenetic regulation of ABI3. *Nat. Commun.* 5: 4138.
- Ryu, H., Cho, H., Kim, K. and Hwang, I. (2010) Phosphorylation dependent nucleocytoplasmic shuttling of BES1 is a key regulatory event in brassinosteroid signaling. *Mol. Cells* 29: 283–290.
- Santiago, J., Henzler, C. and Hothorn, M. (2013) Molecular mechanism for plant steroid receptor activation by somatic embryogenesis co-receptor kinases. *Science* 341: 889–892.
- She, J., Han, Z., Kim, T.W., Wang, J., Cheng, W., Chang, J., et al. (2011) Structural insight into brassinosteroid perception by BRI1. *Nature* 474: 472–476.
- Shimada, S., Komatsu, T., Yamagami, A., Nakazawa, M., Matsui, M., Kawaide, H., et al. (2015) Formation and dissociation of the BSS1 protein complex regulates plant development via brassinosteroid signaling. *Plant Cell* 27: 375–390.
- Srivastava, M., Srivastava, A.K., Orosa-Puente, B., Campanaro, A., Zhang, C. and Sadanandom, A. (2020) SUMO conjugation to BZR1 enables brassinosteroid signaling to integrate environmental cues to shape plant growth. *Curr. Biol.* 30: 1410–1423.e3.
- Sun, Y., Fan, X.Y., Cao, D.M., Tang, W., He, K., Zhu, J.Y., et al. (2010) Integration of brassinosteroid signal transduction with the transcription network for plant growth regulation in *Arabidopsis*. *Dev. Cell* 19: 765–777.
- Tang, W., Yuan, M., Wang, R., Yang, Y., Wang, C., Osés-Prieto, J.A., et al. (2011) PP2A activates brassinosteroid-responsive gene expression and plant growth by dephosphorylating BZR1. *Nat. Cell Biol.* 13: 124–131.
- Tian, Y., Fan, M., Qin, Z., Lv, H., Wang, M., Zhang, Z., et al. (2018) Hydrogen peroxide positively regulates brassinosteroid signaling through oxidation of the BRASSINAZOLE-RESISTANT1 transcription factor. *Nat. Commun.* 9: 1063.
- Wang, C., Shang, J.X., Chen, Q.X., Osés-Prieto, J.A., Bai, M.Y., Yang, Y., et al. (2013a) Identification of BZR1-interacting proteins as potential components of the brassinosteroid signaling pathway in *Arabidopsis* through tandem affinity purification. *Mol. Cell. Proteom.* 12: 3653–3665.
- Wang, H., Tang, J., Liu, J., Hu, J., Liu, J., Chen, Y., et al. (2018) Abscisic acid signaling inhibits brassinosteroid signaling through dampening the dephosphorylation of BIN2 by ABI1 and ABI2. *Mol. Plant* 11: 315–325.

- Wang, H., Yang, C., Zhang, C., Wang, N., Lu, D., Wang, J., et al. (2011) Dual role of BK11 and 14-3-3s in brassinosteroid signaling to link receptor with transcription factors. *Dev. Cell* 21: 825–834.
- Wang, J., Sun, N., Zheng, L., Zhang, F., Xiang, M., Chen, H., et al. (2023) Brassinosteroids promote etiolated apical structures in darkness by amplifying the ethylene response via the EBF-EIN3/PIF3 circuit. *Plant Cell* 35: 390–408.
- Wang, P., Nolan, T.M., Clark, N.M., Jiang, H., Montes-Serey, C., Guo, H., et al. (2021a) The F-box E3 ubiquitin ligase BAF1 mediates the degradation of the brassinosteroid-activated transcription factor BES1 through selective autophagy in *Arabidopsis*. *Plant Cell* 33: 3532–3554.
- Wang, R., Wang, R., Liu, M., Yuan, W., Zhao, Z., Liu, X., et al. (2021b) Nucleocytoplasmic trafficking and turnover mechanisms of BRASSINAZOLE RESISTANT1 in *Arabidopsis thaliana*. *Proc. Natl. Acad. Sci. U. S. A.* 118: e2101838118.
- Wang, Y., Sun, S., Zhu, W., Jia, K., Yang, H. and Wang, X. (2013b) Strigolactone/MAX2-induced degradation of brassinosteroid transcriptional effector BES1 regulates shoot branching. *Dev. Cell* 27: 681–688.
- Wang, Z.Y., Bai, M.Y., Oh, E. and Zhu, J.Y. (2012) Brassinosteroid signaling network and regulation of photomorphogenesis. *Annu. Rev. Genet.* 46: 701–724.
- Wang, Z.Y., Nakano, T., Gendron, J., He, J., Chen, M., Vafeados, D., et al. (2002) Nuclear-localized BZR1 mediates brassinosteroid-induced growth and feedback suppression of brassinosteroid biosynthesis. *Dev. Cell* 2: 505–513.
- Wang, Z.Y., Seto, H., Fujioka, S., Yoshida, S. and Chory, J. (2001) BRI1 is a critical component of a plasma-membrane receptor for plant steroids. *Nature* 410: 380–383.
- Xiong, J., Yang, F., Yao, X., Zhao, Y., Wen, Y., Lin, H., et al. (2022) The deubiquitinating enzymes UBP12 and UBP13 positively regulate recovery after carbon starvation by modulating BES1 stability in *Arabidopsis thaliana*. *Plant Cell* 34: 4516–4530.
- Yan, Z., Zhao, J., Peng, P., Chihara, R.K. and Li, J. (2009) BIN2 functions redundantly with other *Arabidopsis* GSK3-like kinases to regulate brassinosteroid signaling. *Plant Physiol.* 150: 710–721.
- Yang, M., Li, C., Cai, Z., Hu, Y., Nolan, T., Yu, F., et al. (2017) SINAT E3 ligases control the light-mediated stability of the brassinosteroid-activated transcription factor BES1 in *Arabidopsis*. *Dev. Cell* 41: 47–58.e4.
- Yin, Y., Vafeados, D., Tao, Y., Yoshida, S., Asami, T. and Chory, J. (2005) A new class of transcription factors mediates brassinosteroid-regulated gene expression in *Arabidopsis*. *Cell* 120: 249–259.
- Yin, Y., Wang, Z.Y., Mora-Garcia, S., Li, J., Yoshida, S., Asami, T., et al. (2002) BES1 accumulates in the nucleus in response to brassinosteroids to regulate gene expression and promote stem elongation. *Cell* 109: 181–191.
- Yu, X., Li, L., Zola, J., Aluru, M., Ye, H., Foudree, A., et al. (2011) A brassinosteroid transcriptional network revealed by genome-wide identification of BES1 target genes in *Arabidopsis thaliana*. *Plant J.* 65: 634–646.
- Yu, Z., Ma, J., Zhang, M., Li, X., Sun, Y., Zhang, M., et al. (2023) Auxin promotes hypocotyl elongation by enhancing BZR1 nuclear accumulation in *Arabidopsis*. *Sci. Adv.* 9: eade2493.
- Zhang, L., Han, Q., Xiong, J., Zheng, T., Han, J., Zhou, H., et al. (2019) Sumoylation of BRI1-EMS-SUPPRESSOR 1 (BES1) by the SUMO E3 ligase SIZ1 negatively regulates brassinosteroids signaling in *Arabidopsis thaliana*. *Plant Cell Physiol.* 60: 2282–2292.
- Zhang, M., Su, J., Zhang, Y., Xu, J. and Zhang, S. (2018) Conveying endogenous and exogenous signals: MAPK cascades in plant growth and defense. *Curr. Opin. Plant Biol.* 45: 1–10.
- Zhang, Z., Zhu, J.Y., Roh, J., Marchive, C., Kim, S.K., Meyer, C., et al. (2016) TOR signaling promotes accumulation of BZR1 to balance growth with carbon availability in *Arabidopsis*. *Curr. Biol.* 26: 1854–1860.
- Zhao, J., Peng, P., Schmitz, R.J., Decker, A.D., Tax, F.E. and Li, J. (2002) Two putative BIN2 substrates are nuclear components of brassinosteroid signaling. *Plant Physiol.* 130: 1221–1229.
- Zhao, N., Zhao, M., Wang, L., Han, C., Bai, M. and Fan, M. (2022) EBF1 negatively regulates brassinosteroid-induced apical hook development and cell elongation through promoting BZR1 degradation. *Int. J. Mol. Sci.* 23: 15889.
- Zhou, A., Wang, H., Walker, J.C. and Li, J. (2004) BRL1, a leucine-rich repeat receptor-like protein kinase, is functionally redundant with BRI1 in regulating *Arabidopsis* brassinosteroid signaling. *Plant J.* 40: 399–409.

学校概况 机构设置 师资队伍 人才培养 科学研究 校园文化
对外交流 思政在线 服务社会 招生就业 信息公开 来访预约



关于我校2023年度大学生创新创业训练计划项目拟立项名单的公示

来源单位及审核人： 编辑： 审核发布：党委学生工作部（党委研究生工作部） 发布时间：2023-06-07 浏览次数： 4354

各单位、各位同学：

根据《广东省教育厅关于开展2023年国家级、省级大学生创新创业训练计划立项和结题验收工作的通知》《华南农业大学大学生创新创业训练计划管理办法》的相关规定，我校在4月份启动了本年度大学生创新创业的立项工作。经学生申报、学院评审、学校复审等程序，拟对《ZIFs衍生多孔碳基S/Co-CoSe2@NC复合正极材料与性能研究》等529个项目进行立项，现予以公示，具体名单详见附件。

公示期：2023年6月7日至6月9日

如有异议，请在公示期内通过书面形式向党委学生工作部（党委研究生工作部）反映。反映情况时要签名，不签署真实姓名，一律不予受理。

受理单位：党委学生工作部（党委研究生工作部）

联系人：萧润正

办公地址：泰山区创客空间313

联系电话：020-85287520

邮箱：453244662@qq.com

附件：2023年华南农业大学大学生创新创业训练计划拟立项名单

党委学生工作部（党委研究生工作部）

2023年6月7日

序号	所属学院	项目名称	资助类别	项目级别	项目负责人（第一主持人）		项目其它成员	指导教师信息			
					姓名	学号		指导教师	指导教师职称	教师工号	指导教师所属学院
189	经济管理学院	智能手机应用与农民工寻职渠道变迁研究	创新训练项目	校级	彭文仪	202123120120	苏琬琪/202123120122, 李欣奕/202123120311, 魏茵/202223320127, 郑静仪/202125610129, 甘欣可/202125610206	谢琳	副教授	30003742	经济管理学院
190	经济管理学院	农大特产店——打造高等农林院校特色农产品拼多多专卖店	创业训练项目	校级	梁煜培	202223210117	黄尉萍/202019110607, 何楷雯/202014610204, 李依璇/202223110214, 高艺庭/202223110208, 江尔琦/202223120311	龚毅, 张光辉	待完善, 教授	30004615, 30001394	校长办公室, 经济管理学院
191	经济管理学院	余生有鲤——观赏鱼和微景观亲子市场分析	创业训练项目	校级	陈小敏	202023910101	李敏萍/202023910308, 郑冬丽/202023910729, 董文玉/202129210503, 马懿桐/202223330117, 郑壹朵/202218320128	贾莉, 史锐	副教授, 待完善	30001414, 30003735	经济管理学院, 材料与能源学院
192	经济管理学院	补贴政策对农户高效利用耕地的影响研究	创新训练项目	校级	张振庭	202023910529	罗宁锋/202223910219, 宋紫姚/202223510123, 谢宝怡/202123210224, 黄浩民/202023910608, 李航/201929210110	梁耀明	副教授	30003581	经济管理学院
193	经济管理学院	保险素养对农户政策性水稻保险购买的影响	创新训练项目	校级	蔡东润	202123510201	叶函宇/202223210323, 陈思恩/202223320102, 吴子楷/202123510127	蔡健	副教授	30003967	经济管理学院
194	经济管理学院	风险偏好对于国家公园特许经营参与行为的影响研究——以大熊猫国家公园为例	创新训练项目	校级	徐思淇	202123610224	黄子珊/202123610208, 黄德林/202214110208, 蔡淇隆/202123610201, 赖冠英/202123610211, 赵润曦/202123610131	张奕婧	讲师	30003955	经济管理学院
195	经济管理学院	城市化对居民主观福祉的影响机制	创新训练项目	校级	赵炜琳	202123210331	赖凤娟/202123510208, 陈泽妍/202223210302, 周慧娟/202123220232	申津羽	讲师	30003966	经济管理学院
196	经济管理学院	金融创投对促进广东省“预制菜”发展的效用研究——基于乡村振兴战略深度实施的背景	创新训练项目	校级	王浩嘉	202033110221	李慧晴/202123210109, 徐煜柔/202123210325, 魏培佰/202123910223, 张丽莉/202123110130, 林丹童/202225710117	文晓巍	教授	30002844	经济管理学院
197	经济管理学院	我国公益金融产品投资偏好研究	创新训练项目	校级	陈瑞祺	202023210302	刘泓甫/202023210214, 张桢/202023210129, 郑晓鑫/202223210328, 欧阳伟杰/202239010118, 麦欣祺/202238190118	梁耀明	副教授	30003581	经济管理学院
198	经济管理学院	端稳农田生态“金饭碗”：广东农户秸秆还田驱动力的调查研究	创新训练项目	校级	叶宏	202123320127	刘家琪/202123320115, 黄嘉恩/202123110307, 龚欣玥/202123220305, 陈杨/202223120107	陈风波	副教授	30002558	经济管理学院
199	经济管理学院	信息不对称视角下大学生学科竞赛组队现状及存在问题的影响研究——以广东高校为例	创新训练项目	校级	吴欣梦	202123510221	陈倩怡/202023910504, 张嘉玲/202123610129, 张诗韵/202123610130, 周厚泰/202223910329, 李幸欣/202223910312	崔朝鸽	助教	30004642	经济管理学院
200	经济管理学院	广东省农村地区新能源汽车市场推广潜力与提升机制研究	创新训练项目	校级	曾雨欣	202123910429	骆顺珍/202123610120, 黄璇/202123110309, 蔡苏珊/202123320101, 陈燕/202138130203, 高嘉怡/202223320108	伍敬文	副教授	30004825	经济管理学院
201	经济管理学院	农村集体经济发展对土地复垦的影响研究——以广东地区为例	创新训练项目	校级	钟原	202223610234	梁萌慧/202223910616, 林渭其/202223220317, 岑雨萱/202223610201, 陈伟瑜/202223610204	李琴	教授	30002286	经济管理学院
202	林学与风景园林学院	珍贵树种红椿原生质体瞬时转化体系构建及应用	创新训练项目	国家级	柯嘉豪	202118110209	缪雨杰/202118110215, 庄诺/202118110226, 王鑫林/202118110218, 田梓煜/202218130224	李培	讲师	30004620	林学与风景园林学院
203	林学与风景园林学院	循香入梦——基于《红楼梦》系列场景的现代香品研制	创业训练项目	国家级	王烨含	202218710221	林乐毅/202123120315, 黄榆桐/202118710311, 肖子轩/202123310120, 陈汝恩/202218220102, 卢嘉敏/202033210119	陈意微	讲师	30004618	林学与风景园林学院
204	林学与风景园林学院	白蚁肠道中木质素降解真菌筛选及其在秸秆发酵中的应用	创新训练项目	国家级	杨伟涛	202118410124	方明曦/202118410106, 陈嘉怡/202218410101, 李惜妍/202218410106	张庆	副教授	30004272	林学与风景园林学院
205	林学与风景园林学院	基于城市生物多样性的广州城市公园动物景观特征及其对公众心理健康影响研究	创新训练项目	国家级	吴玉婷	202118710221	温淑宇/202018210122, 彭晓琪/202018210118, 郭熙雯/202118710105, 唐梓珊/202218710218, 莫菲/202218710421	汤辉	副教授	30002607	林学与风景园林学院
206	林学与风景园林学院	基于人工智能技术的社区绿地夜间活力评估及设计优化策略研究	创新训练项目	省级	黄文冉	202218220209	马心愉/202118710323, 林锦虹/202218210112, 詹祺晔/202118310125, 张正染/202118310127, 李嘉浩/202218220213	陈崇贤	副教授	30004635	林学与风景园林学院
207	林学与风景园林学院	利用植物ERQC关键组分构建酵母内质网蛋白折叠监控系统	创新训练项目	省级	张馨	202118110322	梁敏艳/202015140312, 关胜鸿/202015140405, 巫凤英/202118110317, 韩卓鑫/202218130109	刘林川	教授	30004624	林学与风景园林学院
208	林学与风景园林学院	基于多种典型人工智能算法的长时序广州城市土地利用演变研究	创新训练项目	省级	刘易桦	202018510218	冯子东/202118220105, 刘佛森/202118220219, 何佩莹/202118210207, 莫达松/202218210127, 陈佳/202218210104	李梦然, 王琦	讲师, 研究员	30004509, 300011666	林学与风景园林学院, 校外企业组
209	林学与风景园林学院	基于景观基因图谱的岭南水乡传统村落保护与发展策略研究	创新训练项目	省级	潘绮微	202118710114	黎可妍/202026410314, 刘幸妮/202118210117, 关海楹/202118710408, 陈心怡/202218510205	刘小蓓	副教授	30002325	林学与风景园林学院
210	林学与风景园林学院	基于自然教育理念的校园文创开发与应用研究——以华南农业大学为例	创业训练项目	省级	何嘉丽	202118710106	肖东芮/202118710123, 王嘉琪/202218210221, 郑曦君/202218710328, 徐唯卿/202218710126	李静, 程晓山	讲师, 副教授	30003511, 30003512	林学与风景园林学院, 林学与风景园林学院

荣誉证书

刘林川同志：

被评为华南农业大学“优秀共产党员”。

特发此证，以资鼓励。

中共华南农业大学委员会

二〇一九年六月

荣誉证书

刘林川 同志：

被评为华南农业大学庆祝建党100周年优秀
共产党员。

特发此证，以资鼓励。

中共华南农业大学委员会

2021年6月

荣誉证书

刘林川：

被评为2020-2021学年华南农业大学林学与风景园林学院"优秀班主任"。

特发此证，以资鼓励。

华南农业大学林学与风景园林学院
二〇二一年十二月三十日

林学与风景园林学院



Highly Cited Researcher 2023

In recognition of exceptional research performance,
demonstrating significant and broad influence in the field of
Cross-Field.

LINCHUAN LIU

has authored multiple Highly Cited Papers™ which rank in the top 1% by citations
for field and publication year in the Web of Science™ over the past decade.



Jonathan Gear
CEO, Clarivate

November 15, 2023

聘 书

植聘字(2020)第038号

兹 聘 请

刘林川 教授

任《植物生理学报》

第十二届编辑委员会委员

任 期 五 年

主 编



第12届《植物生理学报》编辑委员会名单

主 编 何祖华 中国科学院分子植物科学卓越创新中心

副主编 (以姓名汉语拼音排序)

蒋跃明 中国科学院华南植物园

李 殷(专职) 中国科学院分子植物科学卓越创新中心

编 委 (以姓名汉语拼音排序)

白 洋 中国科学院遗传与发育生物学研究所

晁代印 中国科学院分子植物科学卓越创新中心

陈惠萍 海南大学生命科学与药学院

程建峰 江西农业大学农学院

董金皋 河北农业大学生命科学学院

冯献忠 中国科学院东北地理与农业生态研究所

冯玉龙 沈阳农业大学生物科学技术学院

付爱根 西北大学生命科学学院

龚继明 中国科学院分子植物科学卓越创新中心

郭 岩 中国农业大学生物学院

郝广友 中国科学院沈阳应用生态研究所

何龙飞 广西大学农学院

洪 治 南京大学生命科学学院

侯宏伟 中国科学院水生生物研究所

胡红红 华中农业大学生命科学技术学院

黄继荣 上海师范大学生命科学学院

黄荣峰 中国农业科学院生物技术研究所

黄善金 清华大学生命科学学院

焦雨铃 中国科学院遗传与发育生物学研究所

蒯本科 复旦大学生命科学学院

郎翌博 中国科学院分子植物科学卓越创新中心

李 超 华东师范大学生命科学学院

李来庚 中国科学院分子植物科学卓越创新中心

李玉花 东北林业大学生命科学学院

李正国 重庆大学生命科学学院

林宏辉 四川大学生命科学学院

林荣呈 中国科学院植物研究所

刘长军 Biology Department, Brookhaven National Laboratory, USA

刘 栋 清华大学生命科学学院

刘军钟 云南大学生命科学学院

刘林川 华南农业大学林学与风景园林学院

刘晓东 新疆农业大学农学院

卢 山 南京大学生命科学学院

吕 华 Department of Biological Sciences, University of Maryland, Baltimore County, USA

孟庆伟 山东农业大学生命科学学院

米华玲 中国科学院植物分子科学卓越创新中心

裴雁曦 山西大学生命科学学院

戎均康 浙江农林大学农业与食品科学学院

沈振国 南京农业大学生命科学学院

施 慧 首都师范大学生命科学学院

施卫明 中国科学院南京土壤研究所

寿惠霞 浙江大学生命科学学院

夏光敏 山东大学生命科学学院

赵德刚 贵州省农业科学院/贵州大学生命科学学院

唐威华 中国科学院分子植物科学卓越创新中心

田长恩 广州大学生命科学学院

汪松虎 安徽农业大学园艺学院

王邦俊 西南大学生命科学学院

王宝山 山东师范大学生命科学学院

王 存 西北农林科技大学生命科技学院

王 东 南昌大学生命科学学院

王二涛 中国科学院分子植物科学卓越创新中心

王国栋 陕西师范大学生命科学学院

王宁宁 南开大学生命科学学院

王鹏程 中国科学院分子植物科学卓越创新中心

王文明 四川农业大学水稻研究所病虫害研究中心

王 勇 中国科学院分子植物科学卓越研究中心

王源超 南京农业大学植物保护学院

夏亦莽 香港浸会大学理学院

萧浪涛 湖南农业大学生物科学技术学院

谢卡斌 华中农业大学植物科学技术学院

徐 麟 中国科学院分子植物科学卓越创新中心

徐通达 福建农林大学海峡联合研究院

徐小冬 河南大学生命科学学院

闫大伟 河南大学生命科学学院

杨路明 河南农业大学园艺学院

杨万年 华中师范大学生命科学学院

杨兴洪 山东农业大学生命科学学院

姚 楠 中山大学生命科学学院

姚泉洪 上海市农业科学院生物技术研究所

于 峰 湖南大学生物学院

余迪求 云南大学生命科学学院/中国科学院西双版纳热带植物园

袁 政 上海交通大学生命科学技术学院

张怀刚 中国科学院西北高原生物研究所

张建华 香港浸会大学理学院

张劲松 中国科学院遗传与发育生物学研究所

张立军 沈阳农业大学生物科学技术学院

张立新 河南大学生命科学学院

张 林 扬州大学农业科技发展研究院

张 鹏 中国科学院分子植物科学卓越创新中心

张 群 南京农业大学生命科学学院

张少英 内蒙古农业大学农学院

张钟徽 华南师范大学生命科学学院

赵 洁 武汉大学生命科学学院

郑绍建 浙江大学生命科学学院

周传恩 山东大学生命科学学院

朱祝军 浙江农林大学农业与食品科学学院

编 辑 樊 培(编辑部主任) 冯丽丽 李 洁 李 殷 吴 佳

植物生理学报(原刊名《植物生理学通讯》)(月刊, 1951年创刊)

第56卷 第1期

2020年1月20日出版

编 辑 《植物生理学报》编辑部

地址: 上海市岳阳路319号31B楼; 邮政编码: 200031

电话: 021-54922836; 电子邮箱: zstx@sibs.ac.cn

网址: <http://www.plant-physiology.com>

主 编 何祖华

主 管 中国科学技术协会

主 办 中国植物生理与植物分子生物学学会

上海市岳阳路319号31A楼; 邮政编码: 200031

中国科学院上海生命科学研究院植物生理生态研究所

上海市枫林路300号; 邮政编码: 200032

出 版 科 学 出 版 社

北京市东黄城根北街16号; 邮政编码: 100717

印 刷 上海盛通时代印刷有限公司

上海市金山区广业路568号; 邮政编码: 201506

发行范围 公开

国内发行 上海市邮政局报刊发行局

订 阅 全国各地邮政局

国外发行 中国国际图书贸易总公司

北京市399信箱; 邮政编码: 100044

广告经营许可证号 3100420080068

ISSN 2095-1108

国内邮发代号: 4-267

定价: 120.00元

CN 31-2055/Q

国外发行代号: M-1364

编号：GLJCZK_0069

聘 书

刘林川 同志：

兹聘请您为国家林业和草原局院校教材建设
专家库专家，任期为2020年1月1日至2024年12月31日。

国家林业和草原局院校教材建设办公室

二〇二〇年四月二十日

